US Army Corps
of Engineers
Construction Engineering
Research Laboratories

USACERL Technical Report 98/86
June 1998

Masonry Bearing and Shear Walls Retrofitted With Overlay Composite Material

Seismic Evaluation and Dynamic Testing

by Ghassan Al-Chaar and Husein A. Hasan

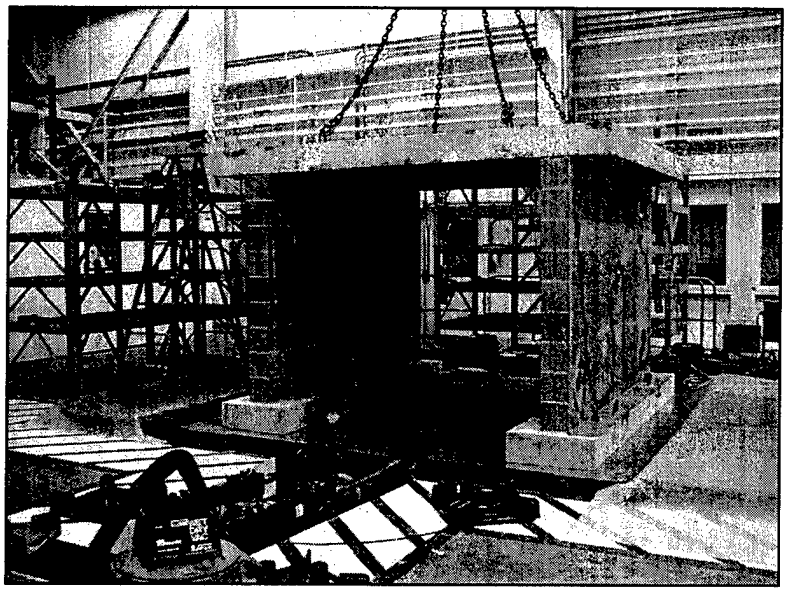

Unreinforced masonry bearing and shear walls common in the Tennessee Valley Authority's (TVA's) switchhouse structures have been found to be vulnerable to earthquakes. One technique to reduce the seismic vulnerability of these structures is to retrofit the masonry walls using the Hexcel-Fyfe TYFO™ system. This system consists of a glass fiber fabric combined with special epoxies to create a high strength, lightweight structural laminate. Hexcel-Fyfe TYFO™ can be designed to work in conjunction with existing walls to increase both the in-plane and out-of-plane seismic strength of the unreinforced masonry walls.

To ensure that this technique will perform its intended purpose, the U.S. Army Construction Engineering Research Laboratories (USACERL) and TVA conducted seismic analysis and shake-table seismic testing using USACERL's Triaxial Earthquake and Shock Simulator. The results of seismic testing documented in this report show that applying the overlay material to one side of the unreinforced masonry wall will enhance its seismic resistance.

USER EVALUATION OF REPORT

REFERENCE: USACERL Technical Report 98/86, *Masonry Bearing and Shear Walls Retrofitted With Overlay Composite Material: Seismic Evaluation and Dynamic Testing*

Please take a few minutes to answer the questions below, tear out this sheet, and return it to USACERL. As user of this report, your customer comments will provide USACERL with information essential for improving future reports.

1. Does this report satisfy a need? (Comment on purpose, related project, or other area of interest for which report will be used.)

_____

_____

_____

2. How, specifically, is the report being used? (Information source, design data or procedure, management procedure, source of ideas, etc.)

_____

_____

3. Has the information in this report led to any quantitative savings as far as manhours/contract dollars saved, operating costs avoided, efficiencies achieved, etc.? If so, please elaborate.

_____

_____

4. What is your evaluation of this report in the following areas?

   a. Presentation: _____

   b. Completeness: _____

   c. Easy to Understand: _____

   d. Easy to Implement: _____

   e. Adequate Reference Material: _____

   f. Relates to Area of Interest: _____

   g. Did the report meet your expectations? _____

   h. Does the report raise unanswered questions? _____

i. General Comments. (Indicate what you think should be changed to make this report and future reports of this type more responsive to your needs, more usable, improve readability, etc.)

_____

_____

_____

_____

_____

_____

5. If you would like to be contacted by the personnel who prepared this report to raise specific questions or discuss the topic, please fill in the following information.

Name: _____

Telephone Number: _____

Organization Address: _____

_____

_____

6. Please mail the completed form to:

Department of the Army
CONSTRUCTION ENGINEERING RESEARCH LABORATORIES
ATTN: CECER-TR-I
P.O. Box 9005
Champaign, IL 61826-9005

REPORT DOCUMENTATION PAGE

Form Approved
OMB No. 0704-0188

1. AGENCY USE ONLY *(Leave Blank)*	2. REPORT DATE	3. REPORT TYPE AND DATES COVERED
	June 1998	Final

4. TITLE AND SUBTITLE
Masonry Bearing and Shear Walls Retrofitted With Overlay Composite Material: Seismic Evaluation and Dynamic Testing

5. FUNDING NUMBERS
Reimbursable Order No.
TVA Contract 98KW-22043
WU G48

6. AUTHOR(S)
Ghassan Al-Chaar and Husein A. Hasan

7. PERFORMING ORGANIZATION NAME(S) AND ADDRESS(ES)
U.S. Army Construction Engineering Research Laboratories (USACERL)
P.O. Box 9005
Champaign, IL 61826-9005

8. PERFORMING ORGANIZATION REPORT NUMBER
TR 98/86

9. SPONSORING / MONITORING AGENCY NAME(S) AND ADDRESS(ES)
Tennessee Valley Authority
400 W. Summit Hill Drive WT9D-K
Knoxville, TN 37902-1499

10. SPONSORING / MONITORING AGENCY REPORT NUMBER

11. SUPPLEMENTARY NOTES
Copies are available from the National Technical Information Service, 5285 Port Royal Road, Springfield, VA 22161.

12a. DISTRIBUTION / AVAILABILITY STATEMENT
Approved for public release; distribution is unlimited.

12b. DISTRIBUTION CODE

13. ABSTRACT (Maximum 200 words)
Unreinforced masonry bearing and shear walls common in the Tennessee Valley Authority's (TVA's) switch-house structures have been found to be vulnerable to earthquakes. One technique to reduce the seismic vulnerability of these structures is to retrofit the masonry walls using the Hexcel-Fyfe TYFO™ system. This system consists of a glass fiber fabric combined with special epoxies to create a high strength, lightweight structural laminate. Hexcel-Fyfe TYFO™ can be designed to work in conjunction with existing walls to increase both the in-plane and out-of-plane seismic strength of the unreinforced masonry walls.

To ensure that this technique will perform its intended purpose, the U.S. Army Construction Engineering Research Laboratories (USACERL) and TVA conducted seismic analysis and shake-table seismic testing using USACERL's Triaxial Earthquake and Shock Simulator. The results of seismic testing documented in this report show that applying the overlay material to one side of the unreinforced masonry wall will enhance its seismic resistance.

14. SUBJECT TERMS		15. NUMBER OF PAGES
seismic vulnerability masonry walls retrofit	Triaxial Earthquake and Shock Simulator	200
		16. PRICE CODE

17. SECURITY CLASSIFICATION OF REPORT	18. SECURITY CLASSIFICATION OF THIS PAGE	19. SECURITY CLASSIFICATION OF ABSTRACT	20. LIMITATION OF ABSTRACT
Unclassified	Unclassified	Unclassified	SAR

Foreword

This project was a joint effort between the U.S. Army Corps of Engineers and the Tennessee Valley Authority (TVA) under TVA Contract Number 98KW-22043 "Military Facilities Engineering Technology"; Work Unit G48, "Dynamic Testing of Masonry Structures Retrofitted with Overlay Composite Material." The technical monitor was Charles Gutberlet, CEMP-ET.

The work was performed by the Engineering Division (FL-E) of the Facilities Technology Laboratory (FL), U.S. Army Construction Engineering Research Laboratories (USACERL) and the Synterprise Group of the Tennessee Valley Authority. The Principal Investigators were Ghassan Al-Chaar of USACERL and Husein A. Hasan of TVA. Larry M. Windingland is Division Chief, FL-E, and Michael Golish is acting Laboratory Operations Chief, FL. The USACERL technical editor was Linda L. Wheatley, Technical Information Team.

The authors acknowledge the work of James B. Gambill, who operates USACERL's Triaxial Earthquake and Shock Simulator (TESS). Mr. Gambill and William Gordon installed instrumentation and assisted in setting up the tests. The authors also acknowledge Joe Graziano, Joe Peyton, and Der Wang Jan of TVA for their technical support and contribution to this project, and Sean Marzano, Research Assistant, for acquiring data. Thanks and acknowledgement also go to Lee Norman of Structures Maintenance Inc. (SMI), Atlanta, GA. SMI provided the overlay material and personnel to install the overlay on the walls.

COL James A. Walter is the Commander of USACERL, and Dr. Michael J. O'Connor is Director.

Contents

List of Figures and Tables

Figures

Tables

1 Introduction

Background

Unreinforced masonry bearing and shear walls common in the Tennessee Valley Authority's (TVA's) switch house structures have been found to be vulnerable to earthquakes. One technique to reduce the seismic vulnerability of these structures is to retrofit the masonry walls using the Hexcel-Fyfe TYFO™ system.* This system consists of a glass fiber fabric combined with special epoxies to create a high strength, lightweight structural laminate. Hexcel-Fyfe TYFO™ can be designed to work in conjunction with existing walls to increase both the in-plane and out-of-plane seismic strength of the unreinforced masonry walls. To ensure that this technique will perform its intended purpose, the U.S. Army Construction Engineering Research Laboratories (USACERL) and TVA conducted seismic analysis and shake-table seismic testing using USACERL's Triaxial Earthquake and Shock Simulator (TESS) located in Champaign, IL. The tested model represents typical unreinforced masonry bearing and shear walls described in Chapter 2.

Objective

The objective of this project was to test the effectiveness of the Hexcel-Fyfe TYFO™ fiber composite system where it is applied to only one side of the unreinforced concrete masonry unit (CMU) bearing and shear walls to resist seismic excitation. Structural evaluation and a comparison of the dynamic performance of the repaired and unrepaired masonry walls were performed.

* The TYFO™ system is marketed by Hexcel Fyfe Co., 6044 Cornerstone Court West, Suite C, San Diego, CA 92121-4730.

Approach

Analytical Investigation on the Structural/Dynamic Behavior of the Wall

Analytical investigations were performed to determine the strength, stiffness, and dynamic characteristics of the unreinforced masonry walls. Test parameters, including the earthquake ground motion, model test setup, and instrumentation, were studied and determined. Predictive analyses of the repaired wall were also performed.

Seismic Testing on the Triaxial Earthquake and Shock Simulator

A model specimen was constructed that consisted of two unreinforced bearing walls with a reinforced concrete (R/C) slab spanning them. One wall was a typical as-built panel and the other was retrofitted with the Hexcel-Fyfe TYFO™ system. In this report, the wall with overlay is referred to as "protected" and the wall without overlay composite is referred to as "unprotected." Seismic testing performed at the USACERL testing facilities consisted of triaxial and uniaxial time histories. Accelerations, displacements, and strain data were recorded at several locations on the walls.

a. Resonant frequency measurement test: Before and after each seismic test, a low-level random white noise test in each primary axis of the test specimen was conducted to determine the basic resonant frequencies of the structure. The tests were performed by applying a random white noise signal to one primary axis of the shake table and slowly raising the amplitude of the signal manually while monitoring the vibration levels at critical locations on the model. Transfer functions were then computed and plotted for selected locations on the test structure to determine the resonant frequencies. All resonant frequencies below 100 Hz were determined.

b. Using time histories generated from site-specific response spectra, a series of triaxial tests was first performed on the model with one wall protected and the other unprotected. The model was tested until the unprotected wall exhibited crack formation. At this stage, testing was stopped to prepare the model for another series of tests. The damaged wall was reinforced with a layer of the Hexcel-Fyfe TYPO™ system, and the model was tested again.

c. Additional series of uniaxial in-plane tests of increasing magnitude were also performed until failure was reached in the model. At this stage of testing, the model consisted of a wall protected before the triaxial tests and another wall protected after damage had been observed from the triaxial tests.

This report describes the earthquake analysis and the shake-table testing program. Discussion on the dynamic behavior of the models, the performance of the Hexcel-Fyfe TYFO™ system, and recommendations regarding the use of this system for seismic retrofit of switch house structures are provided.

Scope

This work was limited to the study of the dynamic behavior of the model when the Hexcel-Fyfe TYFO™ system is applied to one side of wall. Additional studies should be done to assess the durability, fire resistance, long-term structural behavior, and other issues related to the Hexcel-Fyfe TYFO™ system overlay material. These issues were beyond the scope of this investigation.

Units of Weight and Measure

U.S. standard units of measure are used throughout this report. A table of conversion factors for Standard International (SI) units is provided below.

SI conversion factors		
1 in.	=	25.4 cm
1 ft	=	0.305 m
1 sq in.	=	6.452 cm^2
1 lb	=	0.453 kg
1 psi	=	6.89 kPa

2 Experimental Program

Description of Specimens and Test Setup

Two unreinforced concrete masonry walls were constructed on two reinforced concrete base beams. Each wall was 6 ft high, 9 ft-3 ½ in. long, and 8 in. thick, and was built from standard CMUs 8 in. by 8 in. by 16 in. Each R/C base beam was 8 in. high, 10 ft long, and 2 ft wide. Every base beam had four holes to anchor the model to the shake table. The walls were spaced 8 ft-½ in. apart (center-to-center) with a reinforced concrete slab 8 in. thick, 9 ft-3 ¾ in. by 10 ft-10 in. simply supported on the two walls. A typical connection detail between the masonry walls and their base beams is shown in Figure 1. Each connection consisted of three #3 bars, one bar near the center of the wall and one near each wall edge. The bars were cast in the base beams and extended 8 in. into one grouted cell in the bottom course of the wall. Similarly, a typical connection between the walls and the slab consisted of three #3 bars extending 8 in. into grouted cells of the top course of the wall. The poor connection details resembled old construction that marginally satisfied the minimum connection requirements of the current code. Researchers used type N mortar that was one part lime, one part cement, and six parts sand by volume. Appendix A figures show the specimens as prepared for testing. Figure A1 shows CMU walls and one racking specimen, Figure A2 shows the edge distance between an anchor hole and the nearest edge of the wall, Figure A3 shows bars connecting the slab to each wall, and Figure A4 shows the testing specimen assembled on the shake table.

Instrumentation and Data Acquisition

Three types of instrumentation were used during the testing program to measure the response of the model: electrical resistance strain gages, accelerometers, and linear resistive displacement transducers. The accelerations and displacements of the shake table were also measured in the X, Y, and Z axes. Table 1 describes and Figure 2 shows the placement of the instrumentation on the model.

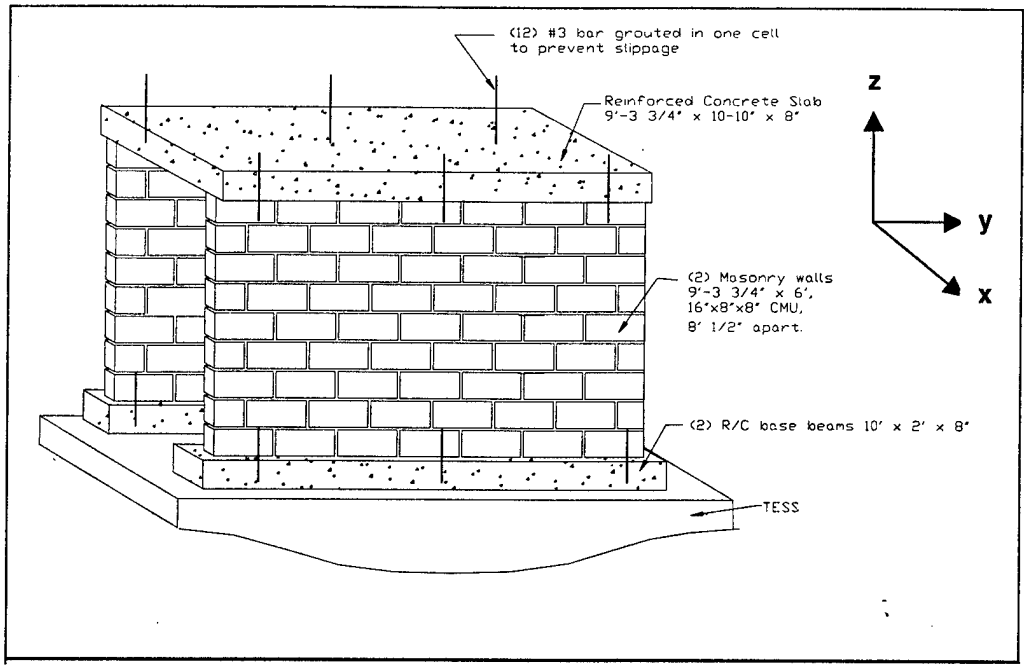

Figure 1. Connection details of the walls to the slab and their base beams.

Strain Gages

Electrical resistance strain gages were installed at several locations on the masonry blocks and on the surface of the Hexcel-Fyfe TYFO™ system. The strain gages were Tokyo Sokki Kenkyujo Co.* model number PFLR-30-11 rosette gages. Each rosette consisted of three strain gages oriented at 0°, 45°, and 90°. Each gage had a metal-foil sensing grid with complete polyamide encapsulation, a thermal expansion coefficient of 11.8x10-6/°C, and a gage factor thermal sensitivity of +0.15±0.05%/10°C. Each sensing grid was 30 mm by 2 mm. Each strain gage was connected to a Vishay model 2120 signal conditioner to provide power, balancing, and signal amplification.

* Tokyo Sokki Kenkyujo Co., Tokyo, Japan; distributor: College Station, TX.

Table 1. Instrumentation details.

Designation: A: Accelerometer
D: Relative displacement
S: Strain gage
X: Out-of-plan direction
Y: In-plane direction
Z: Vertical direction

Sensor No.	Record Channel No.	Scale Factor	Units	Positive Sense Direct	Location
ATX	1	0.400	g/volt	+X	TESS shake table
ATY	5	0.400	g/volt	+Y	TESS shake table
ATZ	7	0.400	g/volt	+Z	TESS shake table
A1X	9	0.487	g/volt	+X	North wall, center of bottom row of blocks
A1Y	10	0.498	g/volt	+Y	"
A1Z	11	0.496	g/volt	+Z	"
A2X	12	0.502	g/volt	+X	North wall, center of middle row of blocks
A2Y	13	0.500	g/volt	+Y	"
A2Z	14	0.501	g/volt	+Z	"
A3X	15	0.499	g/volt	+X	North wall, center of top row of blocks
A3Y	16	0.492	g/volt	+Y	"
A3Z	17	0.491	g/volt	+Z	"
A4X	18	0.505	g/volt	+X	South wall, center of bottom row of blocks
A4Y	19	0.503	g/volt	+Y	"
A4Z	20	0.497	g/volt	+Z	"
A5X	21	0.501	g/volt	+X	South wall, center of middle row of blocks
A5Y	22	0.506	g/volt	+Y	"
A5Z	23	0.500	g/volt	+Z	"
A6X	24	0.502	g/volt	+X	South wall, center of top row of blocks
A6Y	25	0.499	g/volt	+Y	"
A6Z	26	0.492	g/volt	+Z	"
A7X	27	0.487	g/volt	+X	Slab, center of the top surface
A7Y	28	0.489	g/volt	+Y	"
A7Z	29	0.488	g/volt	+Z	"
DTX	78	0.500	in/volt	+X	TESS shake table
DTY	79	1.000	in/volt	+Y	TESS shake table
DTZ	80	2.500	in/volt	+Z	TESS shake table
D1Y	33	2.498	in/volt	+Y	Centerline of North wall
D1X	34	2.500	in/volt	+X	"
D2Y	35	2.499	in/volt	+Y	Top of North wall
D2X	36	2.499	in/volt	+X	"
D3Y	37	2.504	in/volt	+Y	Centerline of South wall
D3X	38	2.500	in/volt	-X	"
D4Y	39	2.500	in/volt	+Y	Top of South wall

Table 1. Instrumentation details (continued).

Sensor No.	Record Channel No.	Scale Factor	Units	Positive Sense Direct	Location
D4X	40	2.501	in/volt	-X	"
D5Y	41	2.497	in/volt	+Y	Slab
D5X	42	2.499	in/volt	-X	"
S1D	44	0.0002	in/in/volt	Polar Dia.	North wall (12",12") from bottom East corner on FIBRWRAP™
S1H	45	0.0002	in/in/volt	Polar Horiz.	"
S2V	46	0.0002	in/in/volt	Polar Vert.	North wall (12",12") from bottom West corner on FIBRWRAP™
S2D	47	0.0002	in/in/volt	Polar Dia.	"
S2H	48	0.0002	in/in/volt	Polar Horiz.	"
S3V	49	0.0002	in/in/volt	Polar Vert.	North wall Center on FIBRWRAP™
S3D	50	0.0002	in/in/volt	Polar Dia.	"
S3H	51	0.0002	in/in/volt	Polar Horiz.	"
S4V	52	0.0002	in/in/volt	Polar Vert.	North wall (12",12") from top East corner on FIBRWRAP™
S4D	53	0.0002	in/in/volt	Polar Dia.	"
S4H	54	0.0002	in/in/volt	Polar Horiz.	"
S5V	55	0.0002	in/in/volt	Polar Vert.	North wall (12",12") from top West corner on FIBRWRAP™
S5D	56	0.0002	in/in/volt	Polar Dia.	"
S5H	57	0.0002	in/in/volt	Polar Horiz.	"
S6V	58	0.0002	in/in/volt	Polar Vert.	North wall center on CMU, inside face of the wall
S6D	59	0.0002	in/in/volt	Polar Dia.	"
S6H	60	0.0002	in/in/volt	Polar Horiz.	"
S7V	61	0.0002	in/in/volt	Polar Vert.	South wall (12",12") from bottom East corner inside face
S7D	62	0.0002	in/in/volt	Polar Dia.	"
S7H	63	0.0002	in/in/volt	Polar Horiz.	"
S8V	64	0.0002	in/in/volt	Polar Vert.	South wall center inside face
S8D	65	0.0002	in/in/volt	Polar Dia.	"
S8H	66	0.0002	in/in/volt	Polar Horiz.	"
S9V	67	0.0002	in/in/volt	Polar Vert.	South wall (12",12") from top East corner inside face
S9D	68	0.0002	in/in/volt	Polar Dia.	"
S9H	69	0.0002	in/in/volt	Polar Horiz.	"
S10V	70	0.0002	in/in/volt	Polar Vert.	South wall (12",12") from bottom East corner on FIBRWRAP™
S10D	71	0.0002	in/in/volt	Polar Dia.	"
S10H	72	0.0002	in/in/volt	Polar Horiz.	"
S11V	73	0.0002	in/in/volt	Polar Vert.	South wall center on FIBRWRAP™
S11D	74	0.0002	in/in/volt	Polar Dia.	"
S11H	75	0.0002	in/in/volt	Polar Horiz.	"
S12V	76	0.0002	in/in/volt	Polar Vert.	South wall (12",12") from top East corner on FIBRWRAP™
S12D	77	0.0002	in/in/volt	Polar Dia.	"
S12H	78	0.0002	in/in/volt	Polar Horiz.	"

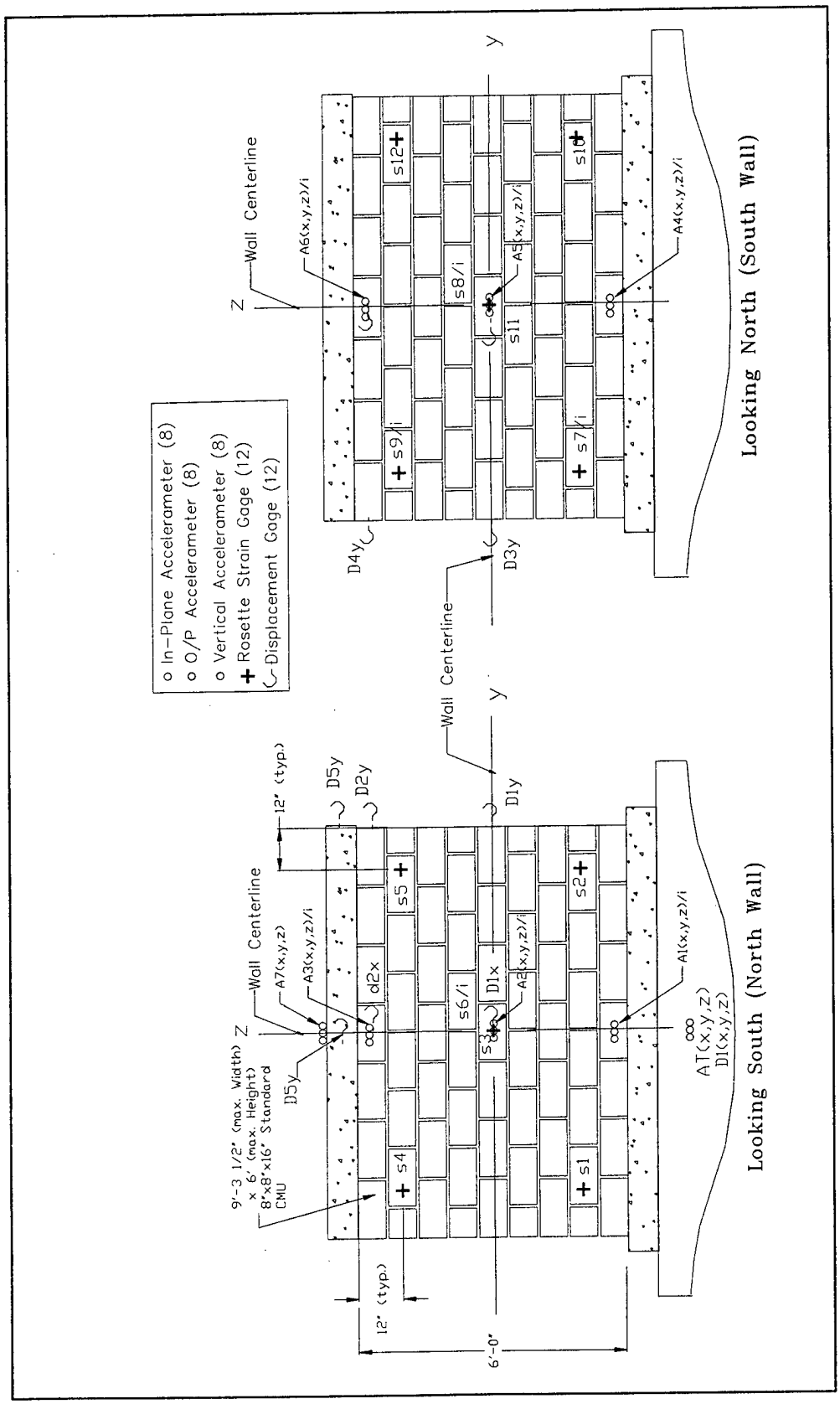

Figure 2. Instrumentation location on the model.

Accelerometers

Endevco* model 7290-10 and 7290-30 accelerometers were used to measure acceleration at various locations on the model, as shown in Figure 2. These accelerometers used a variable capacitance microsensor, which provided a frequency response down to zero frequency. The accelerometers were connected to Endevco model 4476.2 and 4476.2A signal conditioners to provide power, balancing, and signal amplification.

Absolute Displacement Transducers

Celesco† model PT101-10, PT101-20, and PT101-60A variable resistance displacement transducers were used to measure the absolute displacements of the shake table and the model walls and slab at various locations. These units used a spring-loaded precision rotary potentiometer with a flexible steel cable wrapped around the potentiometer shaft. The other end of the cable was attached to the point where the displacement was to be measured. When displacement occurred, the cable motion rotated the shaft of the potentiometer, causing a change in resistance. These transducers were mounted on a large steel reference frame connected to the foundation, and their sensing elements were attached to the model and the shake table using steel extension wires. Figure 2 shows the measurement locations. These transducers were connected to Endevco model 4471.3 signal conditioners, which provided direct current (DC) power and electrical balancing but no amplification.

Data Acquisition

Figure 3 is a schematic block diagram of the instrumentation, data acquisition, and test control systems. A total of 72 transducer channels were recorded using an MTS‡ model 468.20 digital data acquisition system. The DEC§ model VAX-4000-105A computer program was used to generate the shake-table control time history waveforms for each of the three axes, control the execution of the seismic tests, and record the response signal from the measurement transducers. The DEC program was also used to perform various analysis functions such as plotting and performing shock response spectra and transfer function calculations.

---

* Endevco Corporation, San Juan Capistrano, CA.

† Celesco Corporation, Canoga Park, CA.

‡ MTS Systems Corporation, Minneapolis, MN.

§ Digital Equipment Corporation, Maynard, MA.

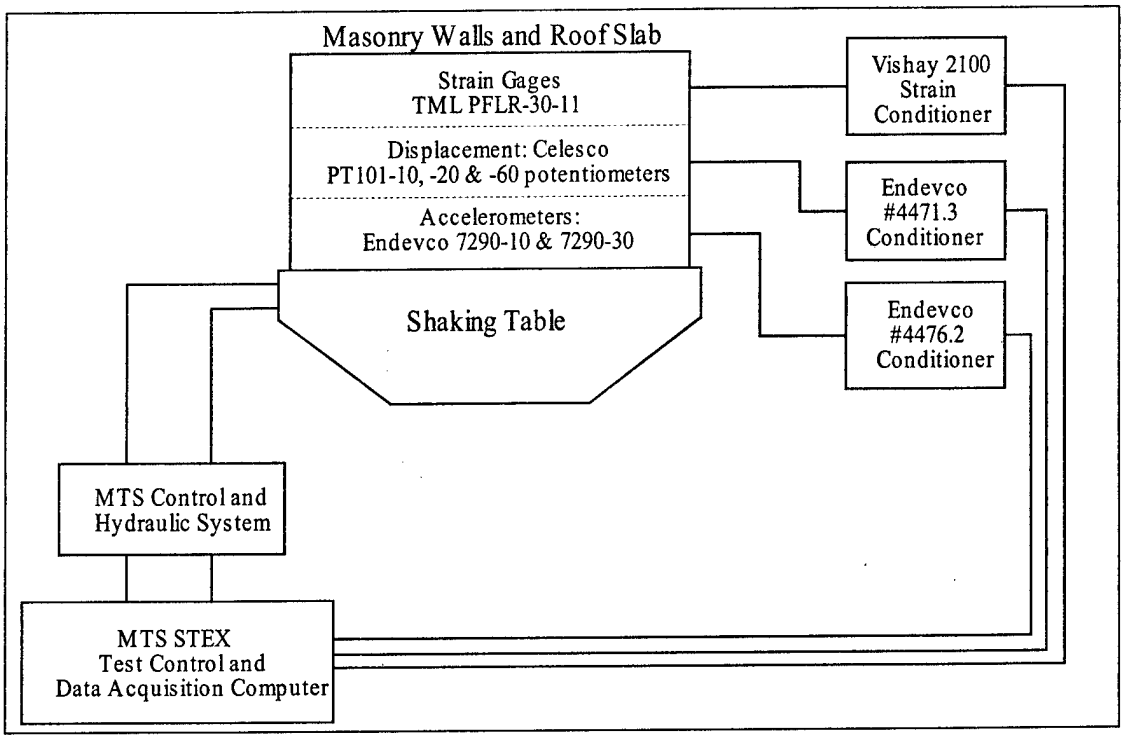

Figure 3. Schematic diagram of the data acquisition and test control systems.

Test Procedure

Tennessee Valley-wide design response spectra were used as the test response spectra for the X, Y, and Z axes of the TESS. These spectra were used to generate time history acceleration waveforms that were used to control the shake-table motion in the three axes. TVA supplied a required envelope function to control the acceleration amplitude and duration for each axis. The envelope consisted of 15 seconds (s) of strong motion with a 5 s ramp up period at the beginning and a 10 s period of ramp down at the end for a total duration of 30 s. The reference shock response spectra and the envelope function were input to a time history synthesis procedure in the DEC computer program. This procedure used an iterative process to generate a time history that would produce a shock response spectrum matching the reference shock spectrum within a specified error tolerance band.

When the time history generation procedure was performed on the original test response spectra supplied by TVA, the resulting acceleration time histories exceeded the displacement limits of the TESS at very low frequencies (i.e., below 1.0 Hertz [Hz]). USACERL and TVA mutually agreed to reduce the frequency components in the reference shock spectra between 0.3 and 1.0 Hz to bring the displacement requirements within the limits of the TESS. It was determined that these frequencies would have no significant impact on the response of the

masonry walls and slab system because the system under consideration would not have a frequency in this range. The three modified reference shock spectra were used to generate three acceleration time histories that were used as the shake-table inputs for all subsequent seismic tests. The test response spectra, the modified time histories, and the modified test response spectra are shown in Figures 4, 5, and 6.

To obtain a closer match between the shake-table response and the required reference input, the DEC computer program used a frequency domain transfer function model of the shake-table system to account for variations in the performance of the TESS across the frequency range of interest. In the modeling process, a wide band random signal was applied to each of the X, Y, and Z axes of the TESS, and the response was recorded. The transfer function was then computed for each axis using a matrix approach, which accounts for cross coupling between axes. During a seismic test, the input time history waveforms were modified by the inverse of the transfer function model before they were input to the shake-table control system.

When a seismic test was initiated, the following parameters were put into the test execution process to define the test: three acceleration time histories, the TESS random transfer function model, and a test definition file that specified the input and response data acquisition channels to be recorded for the test. At the completion of each test, the input and test response data were loaded into the

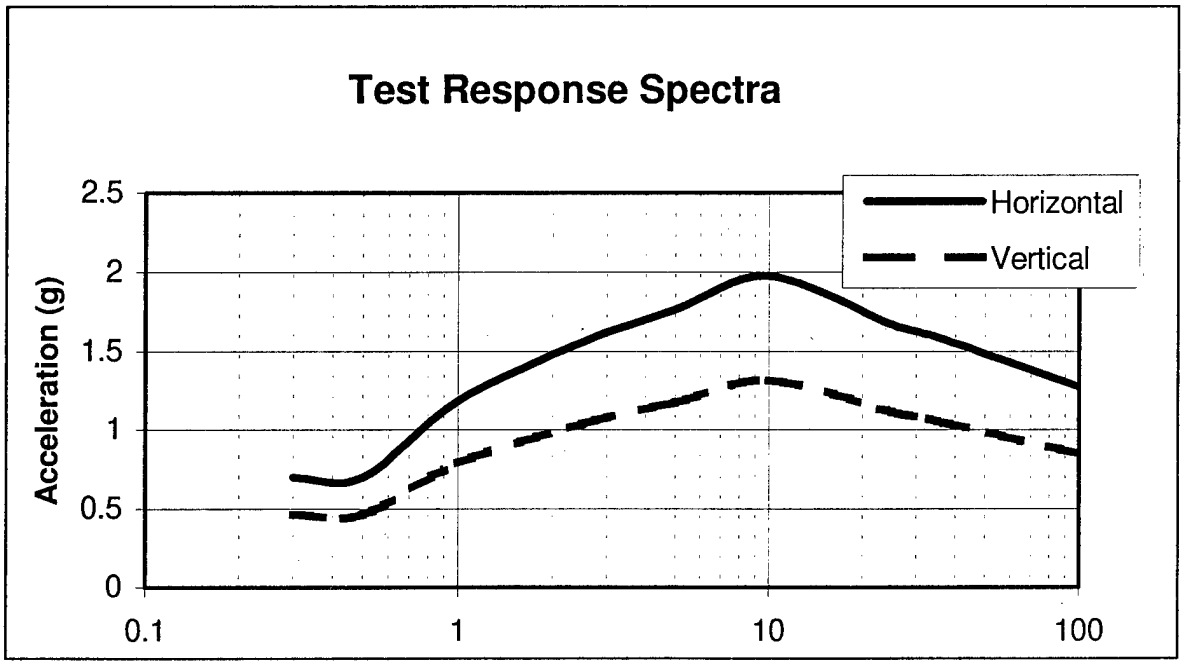

Figure 4. Horizontal and vertical ground spectra, 5% damping.

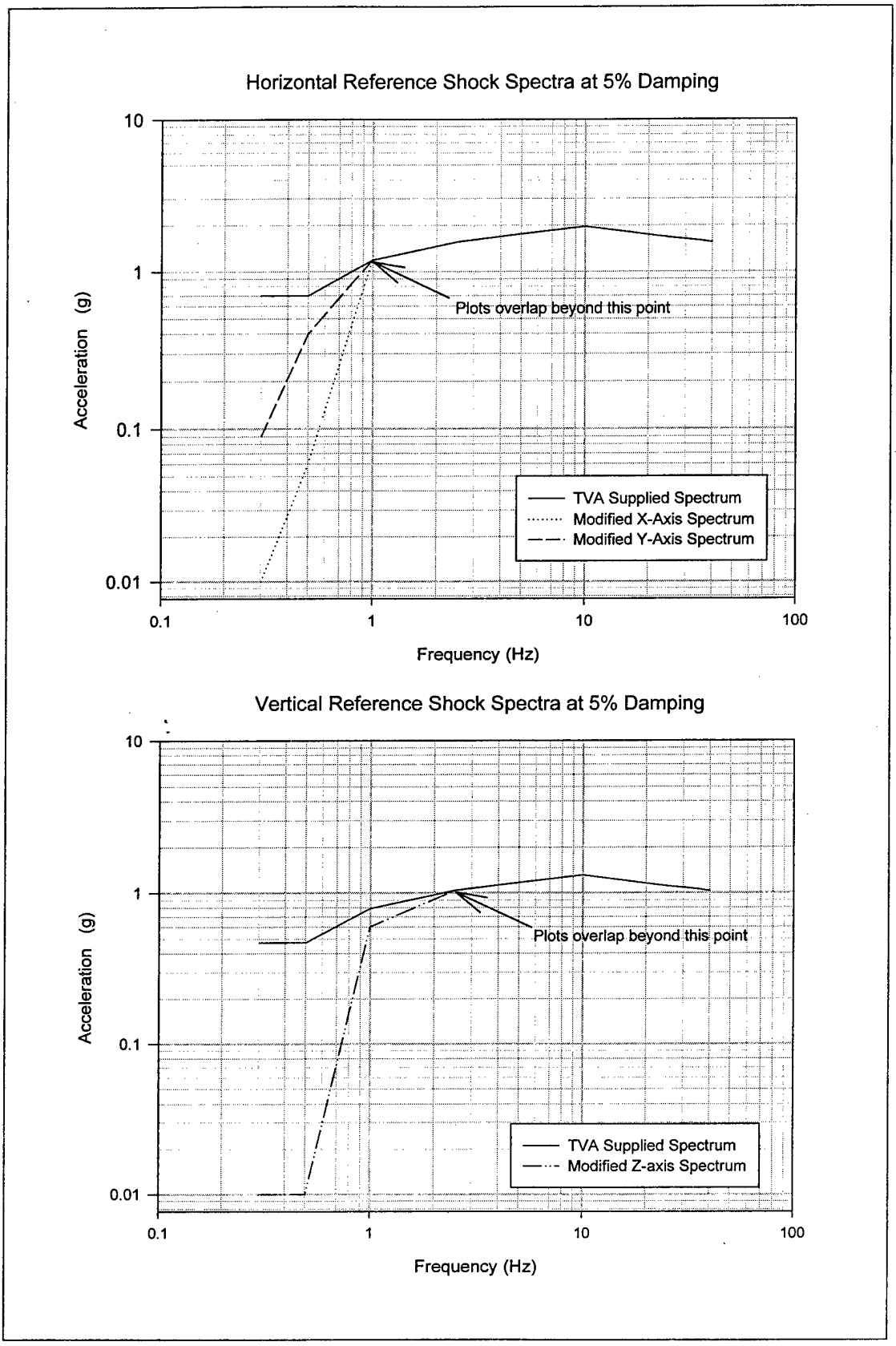

Figure 5. Horizontal and vertical references shock spectra at 5% damping.

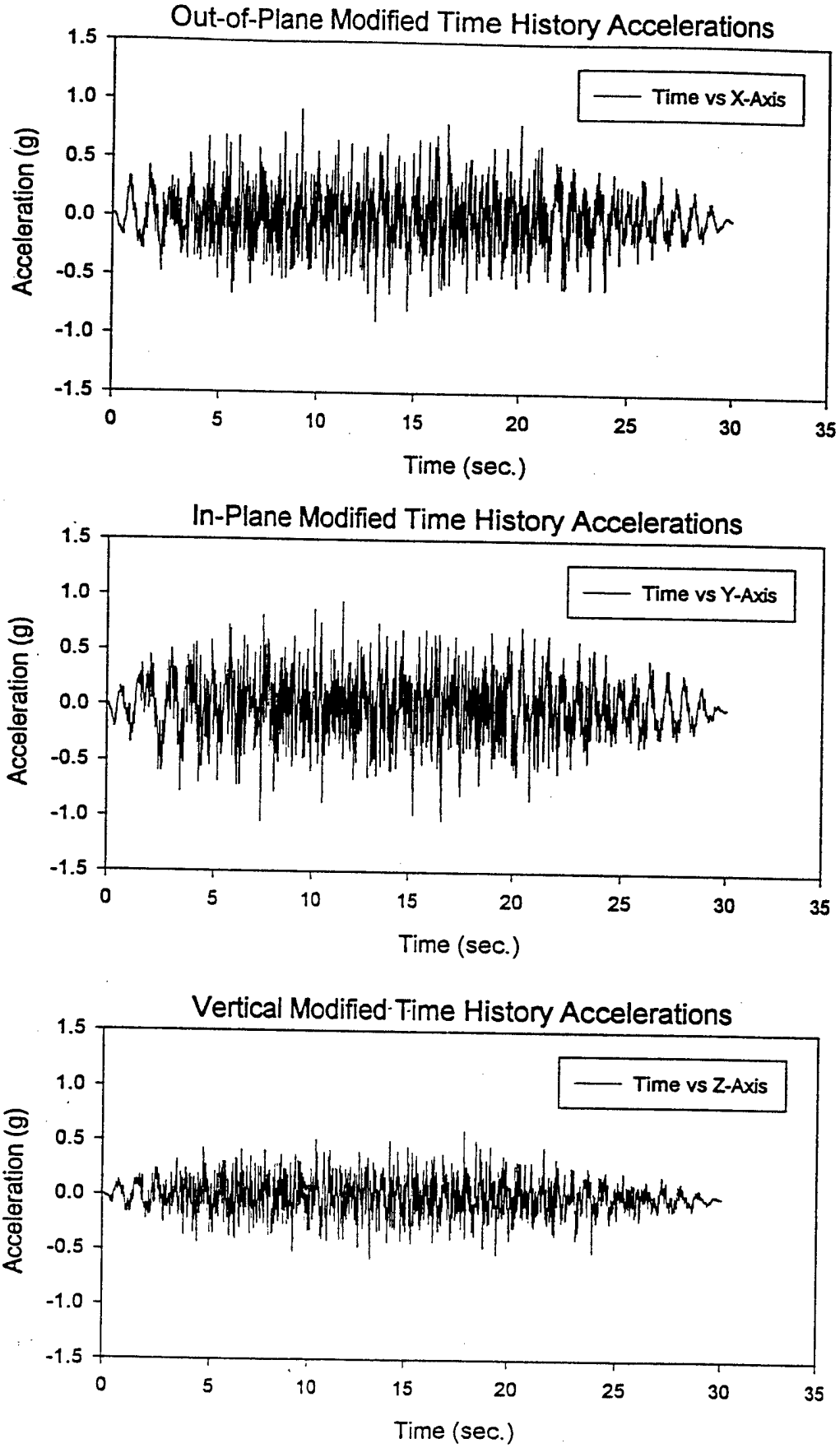

Figure 6. Modified time history acceleration used in seismic tests.

DEC data analysis module for plotting and frequency domain analysis. All of the reference spectra, input and test response data, model information, and analysis results were stored in a test database as a permanent record of the test.

The white noise and sine decay tests were performed using a process almost identical to the seismic tests, except that the inputs for these tests consisted of wide band random noise or a sinusoidal signal at a predetermined frequency, respectively, instead of the seismic acceleration time histories. These tests did not use the frequency domain transfer function model of the TESS described previously.

Material Properties

Mechanical Properties of Masonry Walls

Researchers tested 2 in. by 2 in. mortar cubes per American Society for Testing and Materials (ASTM) Designation C109-90, which yielded an average strength of 1,100 psi. The CMU tests were performed per ASTM C140 (Standard Methods for Sampling and Testing Concrete Masonry Units), which resulted in an average unit masonry strength of 4,690 psi. Prism strength tests were carried out per ASTM Designation E447-84 and resulted in an average strength of 3,920 psi uncorrected for the sample slenderness ratio. A net area correction factor of 1.07 was used to account for the prism height-to-thickness ratio. A racking test was carried out on one 4 ft by 4 ft specimen per ASTM E519 and resulted in a shear strength equal to 209 psi. Figures A5 through A9 in Appendix A show material testing. The racking test specimen mounted in the MTS machine before testing is shown in Figure A5, mode of failure of racking test is shown in Figure A6, compressive test of a CMU is shown in Figure A8, and prism strength and the mode of failure are shown in Figures A8 and A9.

Description of the Composite High Strength FIBRWRAP™ System

The FIBRWRAP™ composite is composed of TYFO S™ epoxy, which is 100 part A and 34.5 part B by weight mixed, applied on TYFO S™ plain unidirectional weave fabric SHE 51. The resin is mixed on site, applied to the structure, and poured on the fabric roll for saturation. The saturated roll is then applied to the structure in sections, from top to bottom. The resin cures at ambient temperature to form a continuous fiber confinement jacket.

The system is designed to increase the strength and ductility of R/C structures by providing a confining jacket of high strength composite around the structure.

The amount of coverage and the thickness of the composite jacket and level of confinement can be designed to meet the ductility demand. After standard curing at 70 to 75 °F for 5 days, the tensile strengths of the composite system are 6,900 psi in the normal direction and 6,700 psi at 90 degrees to the normal. In the normal direction, the tensile modulus is 3,500 ksi, and the tensile modulus in the direction 90 degrees to the normal is 1,400 ksi. Figures A4, A10, and A11 show the Hexcel-Fyfe TYFO™ as applied on the walls.

Test Response Spectra and Time Histories

The test response spectra used in the testing program are shown in Figures 4 and 5. The response spectra represent the design spectra for the Tennessee Valley Region. The vertical component of the ground response spectra was defined as two-thirds of the horizontal component as shown in Table 2. The spectra were based on a probabilistically derived rock motion with a 2,500-yr return period. The development of the Tennessee Valley Region ground response spectra is described in detail in the TVA report, *Earthquake Evaluation of the Switch House Structures at Cordova and Weakley Electric Substations*.

Table 2. Design response spectra.

Frequency (hz)	Horizontal Acceleration (g)	Vertical Acceleration (g)	Vert/Horiz Acceleration Ratio
0.3	0.70	0.47	0.67
0.5	0.70	0.47	0.67
1.0	1.19	0.79	0.67
2.5	1.56	1.04	0.67
5.0	1.76	1.18	0.67
10.0	1.98	1.32	0.67
25.0	1.67	1.11	0.67
35.0	1.59	1.06	0.67
100.0	1.28	0.85	0.67
400.0	1.28	0.85	0.67

The test response spectra shown in Figure 5 were used to generate three statistically independent time histories (two horizontal and one vertical) for use in the testing program. Each time history had a duration of 30 s with 15 s of strong motion, 5 s of buildup, and 10 s of decay. The three time histories are shown in Figure 6. Due to the displacement limits in the shake table in the low frequency range, the test response spectra were reduced in the frequency range of 0.30 to 1.0 Hz for the horizontal axis and 0.3 to 2.5 Hz in the vertical axis. The modified test response spectra were used to generate new time histories for use in the testing program, numerical comparison of the original and modified test response spectra are shown in Table 3. The modified test response spectra and the corresponding time histories are shown in Figures 4 and 6. Note that the reduction of the test response spectra in the low frequency range had no impact on the test results because the unreinforced masonry walls and concrete slab system used in the seismic testing program had no mode of vibrations in the low frequency range.

Table 3. Comparison of the original TVA test response spectra and modified spectra used for testing.

	Horizontal Shock Spectra				Vertical Shock Spectra	
Frequency (Hz)	TVA-Supplied Shock Spectrum (g)	Modified Shock Spectrum X-Axis (g)	Modified Shock Spectrum Y-Axis (g)	Frequency (Hz)	TVA-Supplied Shock Spectrum (g)	Modified Shock Spectrum X-Axis (g)
0.30	0.70	0.01	0.09	0.30	0.47	0.01
0.50	0.70	0.06	0.40	0.50	0.47	0.01
1.00	1.19	1.19	1.19	1.00	0.79	0.60
2.50	1.56	1.56	1.56	2.50	1.04	1.04
5.00	1.76	1.76	1.76	5.00	1.17	1.17
10.00	1.97	1.97	1.97	10.00	1.31	1.31
25.00	1.67	1.67	1.67	25.00	1.11	1.11
35.00	1.59	1.59	1.59	35.00	1.06	1.06
40.00	1.55	1.55	1.55	40.00	1.03	1.03

Note: All shock spectra are computed at 5 percent damping.

Seismic and Resonant Frequency Testing Program

A total of 16 seismic tests were conducted during a 2-wk period: four in-plane uniaxial tests, three triaxial tests, and nine resonant frequency tests. One in-plane uniaxial test and one triaxial test had to be aborted because of technical difficulties. The remaining three in-plane uniaxial tests were conducted with increasing magnitudes of 125, 150, and 200 percent of the original test responses spectra. One triaxial test was conducted with a magnitude of 50 percent of the original test response spectrum in the out-of-plane direction, combined with 100 percent of the original response spectra in the other two directions. The other triaxial test was conducted with a magnitude of 100 percent of the test response spectra in all directions. Each uniaxial and triaxial test was preceded and followed by a resonant frequency search test to determine the major modes of vibration of the model and the corresponding damping values. Table 4 lists all seismic tests conducted.

As stated in the previous section, the time histories used in all tests were modified below 1 Hz due to the displacement limits of the shake table. These modified time histories were used in the testing program.

Table 4. List of seismic and resonant frequency search tests performed on the TESS.

Test ID	North Wall	South Wall	Slab Connected?	Out-of-Plane Span	In-Plane Test Span	Vertical Span	Remarks
Freq1	Protected*	Unprotected	No	N/A	N/A	N/A	
Freq 2	Protected	Unprotected	Yes	N/A	N/A	N/A	
→ EQ 1	Protected	Unprotected	Yes	50%	100%	100%	
Freq 3	Protected	Protected	Yes	N/A	N/A	N/A	
EQ 2	Protected	Protected	Yes	100%	100%	100%	Bad Records
Freq 4	Protected	Protected	Yes	N/A	N/A	N/A	
EQ 3	Protected	Protected	Yes	0%	125% (Unfiltered)	0%	Aborted
Freq 5	Protected	Protected	Yes	N/A	N/A	N/A	
EQ 4	Protected	Protected	Yes	0%	125% (Unfiltered)	N/A	
Freq 6	Protected	Protected	Yes	N/A	N/A	N/A	
EQ 5	Protected	Protected	Yes	0%	150% (Filtered)	0%	
Freq 7	Protected	Protected	Yes	N/A	N/A	N/A	
→ EQ 6	Protected	Protected	Yes	0%	200% (Filtered)	0%	
Freq 7	Protected	Protected	Yes	N/A	N/A	N/A	
→ EQ 7	Protected	Protected	Yes	100%	100%	100%	Repeat EQ 2
Freq 8	Protected	Protected	Yes	N/A	N/A	N/A	

→ Seismic tests studied in this report.
* Protected = wall with overlay material;
Unprotected = wall without overlay material.

3 Structural Analysis

Introduction

Two sets of analyses were performed for the model. The first was a static analysis to determine the capacity of the models and compare the results with allowable stresses as adopted by the Uniform Building Code (UBC). The second was a dynamic response spectra model analysis to determine the seismic response of the model due to the Tennessee Valley-wide design response spectra.

Static Analysis

As shown in Appendix B, static analysis was performed to determine the allowable and acting stresses in accordance with the UBC requirements. The model was analyzed using two load combinations. The first combination consisted of applying lateral load in the out-of-plane direction combined with the gravity load of the model applied in the vertical direction. The magnitude of the load is equal to the tributary gravity weight of the model. The second load combination is similar to the first load combination except the lateral load was applied in the in-plane direction.

The analysis resulted in capacity-to-demand ratios of 36.9, 0.16, and 0.68 for pure compression, axial compression plus lateral out-of-plane loads, and axial compression plus lateral in-plane load respectively. As shown from the calculated capacity and demand ratios, the model has negligible out-of-plane capacity; however, it should be noted that the capacity of the model was calculated based on the UBC requirements, which have a built in safety factor. In addition, a racking test was performed to determine the actual shear capacity of the masonry blocks. The test showed that the actual shear capacity is much higher than allowable; specifically, the actual capacity to allowable ratio was 11.5.

Dynamic Analysis

As shown in Appendix C, dynamic and response spectrum modal analyses were prepared for the unreinforced masonry wall model used in the seismic testing program. The purpose of the analysis was to determine how accurate the dynamic analysis could predict the fundamental modes of vibration of the walls and to determine the maximum seismic forces that the walls would be subjected to as a result of the seismic input motion. This section describes the dynamic analysis.

Description of GT STRUDL Models

The unreinforced masonry was analyzed using GT STRUDL.* Three separate GT STRUDL models were developed. The basic masonry wall and base beam were the same in each of the three models. The basic wall was 9 ft-3 ¾ in. long and 6 ft high. The wall was constructed on a reinforced concrete base beam that was 10 ft long, 2 ft wide, and 8 in. high. For Model 3, two walls were parallel and supported a top slab that was 9 ft-3 ¾ in. by 10 ft-10 in.

The basic wall was modeled using the six degrees of freedom GT STRUDL element "SBHQ6." Each wall consisted of 32 elements and 45 joints. The top slab of Model 3 was modeled using 64 "SBHQ6" elements.

For the finite element analysis using GT STRUDL, the element property input data are element thickness and density. Since GT STRUDL assumes the elements are solid when performing the analysis, and the actual concrete masonry blocks are hollow, effective element thicknesses and densities were calculated for the concrete masonry block walls for model input. The model element thickness and density for the actual masonry wall thickness are as shown in Table 5. The GT STRUDL element thicknesses and densities for the concrete masonry were determined by the following equations using the concrete block properties listed in Table 5:

$$t_{GTSTRUDL} = \left(\frac{12I}{b}\right)^{1/3} = I^{1/3} \qquad \text{[Eq 1]}$$

* GT STRUDL is a computer program used worldwide. It is owned by Georgia Tech Research Corp., Georgia Institute of Technology, Atlanta, GA.

$$\rho_{GTSTRUDL} = w / t_{GTSTRUDL} \quad \text{[Eq 2]}$$

where,

$t_{GT\ STRUDL}$= effective thickness of masonry wall used in the model, in inches

I = moment of inertia of concrete masonry wall, in in.^{4}/linear ft of wall

b = width of section of wall, 12 in.

$\rho_{GT\ STRUDL}$= effective density of masonry used in the model, in lb/cu ft

w = weight of complete concrete masonry wall, in lb/sq ft of wall surface

Table 6 shows the material properties used for the models. The modulus of elasticity used for the concrete masonry is from the "Building Code Requirements for Masonry Structures," American Concrete Institute (ACI) 530-92 for CMUs with a net compressive strength of 1,500 psi and type N mortar.

The three GT STRUDL models were (1) a single basic wall model, (2) a single basic wall model with additional mass included at the top as joint loads, and (3) two basic walls modeled parallel approximately 8 ft apart, supporting a reinforced concrete slab 9 ft-3 ¾ in. long, 10 ft-10 in. wide and 8 in. thick. The additional mass included in Model 2 was equal to one-half of the weight of the 9 ft-3 ¾ in. long, 10 ft-10 in. wide and 8-in. thick concrete slab included in Model 3. The purpose of the concrete slab was to create compressive loads in the walls. Figures C1, C2, and C3 show these models. The attributes of the three GT STRUDL models are summarized in Table 7.

Eigenvalue (Frequency) Analysis

The eigenvalues and eigenvectors were calculated using the tridiagonalization method. The significant modes of vibration for the three models are summarized in Table 8. Further discussion of the results of the frequency analysis is contained in **Evaluation of Edge Conditions at Base of Walls** in Chapter 4.

Table 5. The CMU actual and GT STRUDL properties.

	Actual Block Properties (per ft of wall width)			GT STRUDL Model Properties	
Item	Moment of Inertia (in.)	Area (sq in.)	Weight (lb/sq ft)	Element Thickness (in.)	Element Density (lb/cu ft)
8 in. Hollow Block	308.7	30	44.5	6.76	78.97

Table 6. Material properties used for the GT STRUDL models.

Property	Concrete	Concrete Masonry
Modulus of Elasticity	3.6×10^6 psi	1.5×10^6 psi
Shear Modulus	1.44×10^6 psi	1.44×10^6 psi
Poisson's Ratio	0.17	0.17
Density	150 lb/cu ft (0.0868 pci)	44.5 psf of wall

Table 7. GT STRUDL model attributes.

No.	Wall Size (ft)	Number of Walls	Element Thickness (in.)	Top of Slab	Support Conditions		
					Sides	Top	Base
1	9.31' x 6'	1	6.76"	No	Free	Free	Fixed
2	9.31' x 6'	1	6.76"	No	Free	Free with top slab mass included	Fixed
3	9.31' x 6'	2	6.76"	Yes	Free	Supported by top slab	Fixed

Table 8. Significant modes of vibration for the three models.

Model	Freq (Hz) / Mass Part (%) X-Direct (In plane)			Freq (Hz) / Mass Part (%) Y-Direct (Vertical)			Freq (Hz) / Mass Part (%) Z-Direct (Out of plane)		
	Model 1	Model 2	Model 3	Model 1	Model 2	Model 3	Model 1	Model 2	Model 3
1	183.7	71.2	70.5	369.2	138.1	55.8	20.9	7.2	14.0
	71.6 %	81.2 %	65.5 %	86.4 %	4.7 %	28.8 %	66.3 %	86.7 %	90.5 %
2	407.9	190.2	89.0	448.3	158.0	138.8	122.8	93.1	126.3
	18.7 %	8.3 %	19.7 %	0.5 %	87.4 %	19.1 %	20.4 %	0.8 %	4.3 %
3	612.1	209.8	154.8	558.6		191.6	328.0	97.1	202.8
	2.3 %	3.0 %	1.2 %	1.5 %		36.1 %	6.8 %	7.9 %	1.8 %
4	785.4		228.9			202.0	553.5	305.4	
	3.8 %		4.5 %			1.7 %	4.2 %	2.7 %	

Response Spectra Modal Analysis

The structural models described earlier in this chapter were used to perform linear response spectra modal analysis. The design response spectra used in the analysis are shown in Figure 4.

All significant modes of vibration for the structures were used to calculate the total response of the structures to the seismic excitation. The modes included in the analysis were selected to ensure that at least 90 percent of the mass was considered in the analyses.

The complete-quadratic-combination (CQC) method was used to combine the modal responses. Using the CQC method ensured that the cross correlation between all modes was taken into account. It should be noted that the CQC method will degenerate to the square root of the sum of the squares (SRSS) method if no correlation exists between modes.

The total seismic response was created by combining the responses for the three directions by the root mean square (RMS) method. The total seismic response and the dead load were combined absolutely. Figures C4 through C22 show the defected shapes of the significant modes of vibration for each direction.

The combined axial compression and flexure stresses at the intersection of the masonry wall and the base beam were calculated using the results from the response spectra modal analysis, and assume the wall was uncracked and linearly elastic. The calculated tensile stress significantly exceeded the flexural tension allowed by "Building Code Requirements for Masonry Structures," ACI 530-95.

4 Experimental Results

All channels used in the seismic tests are plotted as shown in Appendix D. Table 9 summarizes the absolute maximum time history acceleration, Table 10 summarizes the absolute maximum time history displacement, and Table 11 summarizes the absolute maximum strain.

Observed Modes of Failure

During seismic test EQ-1, a tension crack formed on the top mortar joint of the south wall's bottom course. This crack can be seen around the unprotected south wall shown in Figures A12 and A13. Also during seismic test EQ-1, a spall was observed on the west edge of the south wall as shown in Figure A14.

The model survived the motion from seismic test EQ-2 without any failure. In tests EQ-3 through EQ-6, no failures were observed except that an uplift motion of the walls and lateral motion of the slab at the connections occurred without any misalignment in the model. Seismic test EQ-7 resulted in the out-of-plane slippage at the inside face of the north wall, between the two bottom courses, near the west and central anchors of the footing. This mode of failure is shown in Figure A15.

The in-plane test EQ-3 was a uniaxial in-plane seismic test equal to 125 percent of the time history record selected, as discussed previously. Since EQ-3 exhibited poor response, it was necessary to filter frequencies lower than 1 Hz from the seismic record. The filtered frequencies were used for subsequent seismic tests EQ-5 and EQ-6. The model response during seismic tests EQ-5 and EQ-6 was significant and indicated the high in-plane capacity of the walls. An uplift motion was observed during these tests, which clearly indicated that the weakest link in these walls was their connection to the foundation and the roof.

Triaxial tests EQ-1, EQ-6, and EQ-7 showed much more out-of-plane strength than was anticipated. Nearly negligible out-of-plane strength was expected, but significant strength was observed.

Table 9. Absolute maximum time history acceleration.

Channel	EQ1 (g)	EQ6 (g)	EQ7 (g)
A1x	0.66	0.70	1.47
A1y	1.00	2.21	1.05
A1z	1.50	3.23	1.51
A2x	0.90	1.25	1.00
A2y	1.14	2.16	1.19
A2z	0.21	3.73	2.03
A3x	0.38	1.28	0.54
A3y	1.37	3.16	1.52
A3z	1.18	3.99	2.10
A4x	0.66	1.13	1.55
A4y	1.18	2.78	1.60
A4z	0.80	2.78	1.55
A5x	0.58	1.00	1.40
A5y	1.80	2.77	1.55
A5z	1.06	3.67	2.19
A6x	0.34	1.16	0.52
A6y	1.38	2.74	1.54
A6z	1.96	4.77	3.10
A7x	0.30	0.43	0.40
A7y	1.15	2.34	1.64
A7z	2.40	4.88	4.16
Atx	0.53	0.13	0.96
Aty	1.05	2.29	0.92
Atz	0.55	0.41	0.56

Table 10. Absolute maximum time history displacement.

Channel	EQ1 (in.)	EQ6 (in.)	EQ7 (in.)
D1x-scaled	1.40	0.46	3.96
D1y-scaled	0.07	0.62	0.61
D2x-scaled	2.82	0.50	8.16
D2y-scaled	0.16	0.99	0.58
D3x-scaled	2.28	0.21	5.84
D3y-scaled	0.12	0.48	0.26
D4x-scaled	2.50	0.55	7.95
D4y-scaled	0.13	0.91	0.48
D5x-scaled	2.56	0.58	8.03
D5y-scaled	0.33	1.52	0.91
Dtx	1.23	0.05	2.54
Dty	4.23	4.06	4.33
Dtz	1.14	0.17	1.15

Table 11. Absolute maximum strain.

Channel	EQ1 (•in/in)	EQ6 (•in/in)	EQ7 (•in/in)
S1d	47.9	24.2	NA
S1h	21.5	39.8	NA
S2d	62.5	70.9	NA
S2h	14.7	18.6	NA
S2v	65.4	80.1	NA
S3d	23.4	28.1	24.8
S3h	21.5	12.7	14.3
S3v	16.6	15.8	18.8
S4d	NA	111.9	NA
S4h	16.6	13.1	NA
S4v	13.7	37.1	NA
S5d	12.7	17.0	NA
S5h	7.8	8.0	NA
S5v	16.6	20.1	NA
S6d	19.5	27.5	24.6
S6h	10.7	12.3	15.0
S6v	NA	0.2	0.4
S7d	18.6	25.2	NA
S7h	15.6	10.9	NA
S7v	30.3	34.6	NA
S8d	17.6	36.9	52.3
S8h	14.7	16.2	24.2
S8v	17.6	21.9	19.1
S9d	5.9	10.6	30.9
S9h	2.9	9.4	19.0
S9v	5.9	38.7	23.8

Resonant Frequency Tests

Before the testing program began, a series of uniaxial low-level random white noise tests was conducted to determine the major modes of vibration of the wall and wall/slab system. Additional white noise tests were also performed before and after each series of seismic testing. Plots of white noise tests are shown in Appendix E, and Table 12 summarizes the results of each resonant frequency test. As Table 12 shows, the major modes of vibration of the protected wall (north wall) are 13, 37.5, and 47.7 Hz in the out-of-plane, in-plane, and vertical directions respectively. Meanwhile, the major modes of vibration of the unprotected wall (south wall) are 10.4, 26.6, and 26.4 Hz in the out-of-plane, in-plane, and vertical directions, respectively. The protected wall has a higher frequency than that of the unprotected wall. The variation in frequency between the protected and unprotected walls is a result of the applied overlay on the north wall.

Table 12. Modal frequencies and damping from random data transfer functions.

North Wall

Test Condition	Out-of-Plane				In-Plane				Vertical			
	1st Freq (Hz)	Damping (%)	2nd Freq (Hz)	3rd Freq (Hz)	1st Freq (Hz)	Damping (%)	2nd Freq (Hz)	3rd Freq (Hz)	1st Freq (Hz)	Damping (%)	2nd Freq (Hz)	3rd Freq (Hz)
Before EQ1	13.05	3.03	48.83	72.27	37.50	9.34	44.73	82.23	47.66	4.93	>100	N/A
Before EQ1	4.02	4.75	32.81	73.24	31.45	3.80	43.36	86.72	36.72	7.45	85.16	N/A
After EQ1*	3.52	5.54	N/A	69.73	27.73	8.51	48.83	74.41	42.97	2.49	71.88	88.50
After EQ1**	6.39	3.03	N/A	71.29	29.49	6.90	59.77	85.35	45.12	2.37	72.07	92.97
After EQ2	2.34	8.29	50.59	68.95	25.98	6.25	47.85	75.20	39.26	2.74	52.54	86.33
After EQ6	4.80	2.04	46.09	77.93	26.37	10.81	34.96	72.85	47.27	5.95	60.16	95.12
After EQ6	4.54	4.34	36.52	74.80	18.55	6.71	51.37	71.68	37.31	2.60	52.15	82.23
After EQ7	2.86	6.64	32.42	62.70	17.58	7.15	37.31	N/A	32.42	3.88	38.09	79.88

South Wall

Test Condition	Out-of-Plane				In-Plane				Vertical			
	1st Freq (Hz)	Damping (%)	2nd Freq (Hz)	3rd Freq (Hz)	1st Freq (Hz)	Damping (%)	2nd Freq (Hz)	3rd Freq (Hz)	1st Freq (Hz)	Damping (%)	2nd Freq (Hz)	3rd Freq (Hz)
Before EQ1	10.35	1.96	22.27	71.29	26.56	8.95	N/A	N/A	26.37	8.51	***NOTE	
Before EQ1	4.03	4.75	45.12	73.63	14.06	7.54	60.74	74.81	36.91	7.13		
After EQ1	3.52	5.54	43.16	69.73	18.75	8.92	47.07	78.00	42.97	2.49		
After EQ1	6.39	3.03	44.92	71.00	26.95	6.50	50.78	85.35	45.51	2.99		
After EQ2	2.34	8.29	40.23	69.53	21.09	6.94	47.07	74.41	39.45	2.74		
After EQ6	6.25	6.23	36.33	90.43	25.98	4.57	34.57	64.80	16.60	12.04		
After EQ6	4.55	4.34	36.52	74.22	18.60	8.11	50.78	71.48	37.50	2.60		
After EQ7	2.86	6.64	32.42	39.45	17.58	6.43	35.55	N/A	32.42	3.03		

NOTES:

N/A = Frequency not measurable, * Damaged, ** Repaired

***: The frequency for the vertical axis of the South wall was very inconsistent.

Highlighted tests are with no slab on walls; the remaining tests with slab in place.

In addition, as shown in Table 12, the major modes of vibration of the wall and slab system are 4.0, 31.4, and 36.7 Hz in the out-of-plane, in-plane, and vertical directions respectively. The subsequent resonant frequency tests showed that the major modes of vibration of the wall and slab system ranged from 2.3 to 6.4 Hz, 17.5 to 27.7 Hz, and 32.4 to 45.5 Hz in the out-of-plane, in-plane, and vertical directions, respectively.

The associated damping ratio values were calculated for the walls and the wall/slab system. The damping values were calculated using the following equations:

$$\xi = 100\left(\frac{1}{2Q}\right) \qquad \text{[Eq 3]}$$

$$Q = \frac{\left(f_1/f_2\right)^2 + 1}{\left(f_1/f_2\right)^2 - 1} \qquad \text{[Eq 4]}$$

where

f_1 = 1st mode frequency

f_2 = 2nd mode frequency

Table 12 summarizes the damping values.

Researchers observed from the several resonant frequency tests performed on the model, that the system became more flexible when it was repeatedly subjected to an input motion.

Evaluation of Edge Conditions at Base of Walls

In the frequency analysis and the response spectra analysis, the base of the wall was assumed to be fixed for both translation and rotation. However, there was a significant difference in the frequencies calculated with the GT STRUDL fixed model and the frequencies determined by testing. The difference in the frequencies was most likely due to the analysis assumptions that the wall was linearly elastic and had a fixed edge at the base of the wall.

To evaluate the effect of the edge conditions on the predicted wall frequencies, the spring constants in Model 1 at the base of the wall were varied in several computer runs. The edge conditions considered ranged from fixed to spring constants of 100 kips per foot (k/ft) and 100 foot-kips (ft-k)per radian for translation and rotation, respectively. Various ratios of magnitude for the spring constants were considered between the three directions and between the translational and rotational values. Good agreement between the experimental results and the analysis results occurred when the transnational spring constants were taken as 1,000 k/ft and the rotational spring constants were 1,000 ft-k/ft. Table 13 summarizes the results of the evaluation.

Acceleration Response Spectra

Plots of acceleration response spectra measured at various locations are shown in Appendix F. Table 14 summarizes the maximum acceleration response spectra at the bottom, center, and top of each wall. A review of the accelerations in Table 14 shows that some of the recorded accelerations are not consistent. Recognizing this fact, the authors will continue to review all recorded acceleration data to ensure that no errors were introduced during the testing program.

Experimental Results of Stresses Based on Measured Accelerations

Table 16 summarizes the absolute maximum acceleration displacements and the corresponding shear stresses based on stress-displacement response plots in Appendix G. The shear stresses were computed based on a tributary weight of the structure equal to 12,592 lb. The net area of the wall-resisting loads is equal to the total of the CMU facial widths (two walls, two faces per wall, 1.25 in. facial width) multiplied by the length of the walls.

Seismic Test EQ-1

As Table 15 shows, the out-of-plane shear stresses were 8.2 psi and 6.7 psi for the north and south walls, respectively. The difference between these values was a result of the application of the Hexcel-Fyfe TYFO™ system to the north wall, which increased the wall stiffness. The in-plane shear stress of both walls was approximately the same with a value of about 31 psi.

Table 13. GT STRUDL analysis of test walls, seismic test of unreinforced masonry bearing and shear walls, and comparison of frequency results for various spring constants at base of wall.

Spring Constants						Frequency (Hz)								
						X-Direction (In-plane) Mode			Y-Direction (Vertical) Mode			Z-Direction (Out-of-plane) Mode		
KFX (k/ft)	KFY (k/ft)	KFZ (k/ft)	KMX (ft-k/rad)	KMY (ft-k/rad)	KMZ (ft-k/rad)	1	2	3	1	2	3	1	2	3
Shake table test frequencies before EQ1*						26.6	N/A	N/A	26.4	N/A		10.35	22.3	71.3
Fixed	Fixed	Fixed	Fixed	Fixed	Fixed	183.7	407.9	612.1	369.2	448.3	558.6	20.9	122.8	328.0
10,000	10,000	10,000	10,000	10,000	10,000	83	162.8		124.9			18.9	107.3	229.5
1,000	1,000	1,000	1,000	1,000	1,000	28.5	50.8		40.3			11.6	55.2	
100	100	100	100	100	100	9.1	16		12.8			4.3	17.5	
5,000	5,000	1,000	1,000	Fixed	Fixed	82.5	172.9		89.5			11.6	55.2	
5,000	5,000	1,000	1,000	1,000	Fixed	82.5	172.9		89.5			11.6	55.2	
5,000	5,000	1,000	1,000	1,000	1,000	59.7	113.7		89.4			11.6	55.2	
1,000	1,000	1,000	Fixed	Fixed	Fixed	39.8			40.3			19.8	53.0	

* South Wall (Unprotected).

Table 14. Maximum acceleration response with 5 percent damping.

Direction	Location	EQ1		EQ6		EQ7	
		Acceleration (g)	Frequency (Hz)	Acceleration (g)	Frequency (Hz)	Acceleration (g)	Frequency (Hz)
Out-of-Plane	Reference	2.18	9.90	No Input	- -	2.18	9.90
	Table	1.21	12.50	No Input	- -	2.41	9.90
North Wall	Bottom	2.71	26.62	3.65	40.00	5.53	28.22
	Center	2.78	26.62	4.62	40.00	3.99	353.61
	Top	1.25	1.02	6.21	37.74	1.94	37.74
South Wall	Bottom	2.23	29.91	3.70	33.59	3.36	35.61
	Center	2.71	29.91	3.41	40.00	4.22	35.61
	Top	1.27	1.02	3.52	35.61	1.88	40.00
In-Plane	Reference	2.27	9.90	2.43	9.90	2.27	9.90
	Table	2.44	11.79	5.12	8.82	2.46	15.77
North Wall	Bottom	2.56	33.59	5.00	8.82	2.71	35.61
	Center	2.75	6.22	5.31	37.74	2.89	14.04
	Top	3.84	40.00	8.64	33.59	4.49	40.00
South Wall	Bottom	2.71	11.79	7.68	25.12	3.77	28.22
	Center	3.50	14.88	7.25	25.12	3.66	19.90
	Top	4.08	12.50	9.13	35.61	4.08	19.90
Vertical	Reference	1.48	11.12	No Input	- -	1.48	11.12
	Table	1.50	11.12	No Input	- -	1.50	11.79
North Wall	Bottom	6.79	7.08	7.08	33.59	5.92	33.59
	Center	3.47	7.66	7.66	40.00	4.56	21.09
	Top	3.86	8.37	8.37	37.74	4.77	19.90
South Wall	Bottom	3.85	7.50	7.95	37.74	6.61	25.61
	Center	3.28	9.18	9.18	40.00	4.86	40.00
	Top	3.52	9.96	9.96	40.00	4.79	40.00

Furthermore, a review of Table 15 shows the maximum in-plane displacement of the south wall is greater than that of the north wall. However, the maximum acceleration recorded on both walls was about the same.

Seismic Test EQ-6

Out-of-plane accelerations were recorded from the pure in-plane seismic test, EQ-6. The out-of-plane measured accelerations corresponded to maximum shear stresses of 28.7 and 24.0 psi for the north and south walls, respectively. The out-of-plane displacements were small, but the corresponding stresses were significant.

Table 15. Maximum time history accelerations, base shears, and displacements.

Test Name	Wall and Direction	Time (s)	Maximum Time History Acceleration (g)	Maximum Time History Base Shear (psi)	Corresponding Time History Displacement (in.)	Time (s)	Maximum Time History Displacement (in.)	Corresponding Time History Acceleration (g)
EQ1	North Wall Out-of-Plane	8.99	0.38	8.2	1.32	24.01	2.82	0.11
EQ1	North Wall In-Plane	7.44	1.37	31.1	0.01	7.39	0.16	0.28
EQ1	South Wall Out-of-Plane	7.46	0.34	6.7	0.73	1.31	2.50	0.01
EQ1	South Wall In-Plane	7.45	1.38	31.7	0.08	14.35	0.13	0.48
EQ6	North Wall Out-of-Plane	17.79	1.28	28.7	0.19	20.07	0.50	0.17
EQ6	North Wall In-Plane	19.99	3.16	71.1	0.08	20.53	0.99	0.20
EQ6	South Wall Out-of-Plane	16.52	1.16	24.0	0.04	20.15	0.55	0.03
EQ6	South Wall In-Plane	17.80	2.74	66.2	0.08	20.52	0.91	0.19
EQ7	North Wall Out-of-Plane	17.71	0.54	12.0	0.68	1.32	8.16	0.17
EQ7	North Wall In-Plane	9.38	1.52	33.9	0.03	1.30	0.58	0.22
EQ7	South Wall Out-of-Plane	9.36	0.52	11.3	0.52	1.75	7.95	0.10
EQ7	South Wall In-Plane	9.33	1.54	35.4	0.02	1.60	0.48	0.14

The maximum out-of-plane displacement of the north wall was 0.50 in., which is slightly less than the maximum out-of-plane displacement of the south wall of 0.55 in. This difference was due, in part, to a tension crack that had appeared during EQ-1 within the mortar atop the bottom course of the south wall.

The EQ-6 test produced the largest in-plane stresses. These values were 71.1 psi for the north wall and 66.2 psi for the south wall. Again, the north wall had a slightly higher stiffness than the south wall, with the north wall exhibiting higher stresses and lower displacements.

Resultant stresses can be obtained by combining the stresses from the in-plane, out-of-plane, and vertical directions using any appropriate combination method such as CQC or SRSS.

Seismic Test EQ-7

The out-of-plane maximum displacement of the north wall was 8.16 in., while that of the south wall was 7.95 in. These values were very high, but the model did not collapse. The heavy slab and the Hexcel-Fyfe TYFO™ system had significantly contributed to the stability of the model. The out-of-plane displacements measured during seismic test EQ-7 were much higher than the displacements measured during test EQ-1. The difference in stresses does not reflect the difference in displacements in seismic tests EQ-1 and EQ-7 for the following reasons:

- Between the two tests, the specimen was subjected to a series of tests that resulted in degradation of stiffness.

- The lateral displacements of the south wall resulted from rotations around the tension crack at the top of the bottom course, while the lateral displacement of the north wall resulted from rotation about the top of its base beam. Thus, high out-of-plane displacements and low stresses were observed.

The maximum in-plane and out-of-plane stresses resulting from test EQ-7 were slightly higher than those of test EQ-1. In EQ-7, the in-plane seismic motions used were the same as EQ-1. However, the out-of-plane seismic excitation was twice that of EQ-1. Both the maximum out-of-plane and in-plane stresses resulting from EQ-7 were higher than those of EQ-1.

Experimental Results of Stresses Based on Measured Strains

To determine the stress distribution in the model from strain measurements, several 45° rosette strain gages were used. Using the basic relation between stress and strain in Mohr's circle, the measured strains were used to calculate corresponding stresses. Each rosette strain gage measured the strain in three directions 45° apart: the horizontal (ε_a), the vertical (ε_c), and the diagonal (ε_b). Thus,

$$\tau_{max} = \frac{E}{2(1+\nu)}\sqrt{(\varepsilon_a + \varepsilon_c)^2 + [2\varepsilon_b - (\varepsilon_a + \varepsilon_c)]^2} \qquad \text{[Eq 5]}$$

where

E = modulus of elasticity of the CMUs

ν = Poisson's ratio of the CMUs.

This equation was used to convert the recorded strain data into absolute shear stress values. The time histories of shear stresses are shown in Appendix H, and the maximum values are listed in Table 16. It is important to note that strain was not measured in the out-of-plane direction.

The measured absolute maximum shear stress values were 105.6 psi and 110.8 psi. These values were recorded by gages S1 and S2 located at the top of the north wall's protected side. These values were almost the same and occurred at about the same time.

The absolute maximum shear stress values were 44.8 psi for S4 and 25.2 psi for S5. The absolute maximum stresses had been reached about 3 s apart. The variation in S4 and S5 values was due to the instability of the slab as observed during testing.

The S3 strain gage was at the center of the protected side of the north wall, whereas S6 was at the center of the unprotected side of the north wall. The absolute maximum shear stress values were 76.6 psi for S3 and 70.7 psi for S6. The variation in S3 and S6 values was a result of the effect of the overlay being on one side, which made it more rigid than the opposite side. The rigid side received higher load, and higher stresses were achieved.

The absolute maximum strains calculated at the bottom, center, and top of the north wall decreased from bottom to top. The bottom of the wall was significantly more stressed than the center and top, but no failure was observed in EQ-1.

Strain gages S7, S8, and S9 were attached to the unprotected south wall. These gages yielded maximum absolute values that decreased from bottom to top. This wall failed during seismic test EQ-1. Failure was characterized by the formation of a tension crack in the mortar along the top of the bottom course. By comparison between the absolute maximum values of S1 of the protected north wall and S7 of the unprotected south wall, it was observed that the south wall failed under lower stresses, whereas the protected north wall remained intact. This difference was a result of the Hexcel-Fyfe TYFO™ system overlay on the north wall.

The absolute maximum shear stresses calculated from EQ-6 are listed in Table 16. The maximum value of all calculated stresses was 262.4 psi. This shear stress, measured from strain gage S4, had exceeded the shear stress of 209 psi, which was measured from the racking test. It is evident that the north wall did not fail because of the contribution of the Hexcel-Fyfe TYFO ™ system.

Seismic test EQ-6 was conducted with a magnitude of 200 percent of the original test response spectra, and no failures were observed. However, an uplift motion was observed during this test. This uplift was due to poor connections between the walls and the base beams.

Failure on the north wall was only observed during EQ-7, where the unprotected inside face of the bottom course (located between the center bar and the west bar) popped out of the wall, as Figure A15 shows.

The computed stresses for the north wall per seismic test EQ-7 were relatively lower than those computed from seismic tests EQ-1 and EQ-6. The maximum stresses at the centers of both sides of the north wall were almost the same, but they occurred about 14 s apart.

Table 16. Maximum shear stresses per rosette strain gages.

	EQ1		EQ2		EQ7	
Gage	Stress (psi)	Time (sec)	Stress (psi)	Time (sec)	Stress (psi)	Time (sec)
S1	105.6	19.18	110.3	20.62	N/A	N/A
S2	110.8	19.22	134.1	17.71	N/A	N/A
S3	53.8	7.44	76.6	16.51	60.6	23.59
S4	44.8	6.00	262.4	17.61	N/A	N/A
S5	25.2	6.29	38.5	7.48	N/A	N/A
S6	46.1	1.11	70.7	22.42	61.0	9.38
S7	98.1	4.06	108.4	21.72	N/A	N/A
S8	42.6	7.39	58.1	17.81	133.9	6.35
S9	10.8	19.85	74.4	20.62	N/A	N/A
S11	N/A	N/A	N/A	N/A	89.5	6.35

Comparisons of the shear stresses of the unprotected and protected sides of the north and south walls revealed the following observations:

- The repaired and damaged south wall received higher stresses than the undamaged and retrofitted (protected) north wall.

- The stress on the unprotected side of the damaged, then repaired, south wall was higher than on the protected side of the undamaged, retrofitted north wall.

- The south wall stiffness may have been reduced after the unprotected wall was damaged in the EQ-1 test.

Note that the above stresses were calculated from strain gages located on the CMUs. Since the measured strains did not account for the strain in the mortar, the calculation shown in Equation 5 represents the lower bound stresses (i.e., the actual stresses should be higher).

5 Conclusion

The effectiveness of the Hexcel-Fyfe TYFO™ system applied to one side of the wall has been received with skepticism, especially when out-of-plane loading is considered. The tests have shown that applying the overlay material to one side of the unreinforced masonry wall will enhance its seismic resistance. This enhanced resistance is due, in part, to the Hexcel-Fyfe TYFO™ system resisting slippage in the cracks and increasing arching action where cracks have formed.

The connection of the walls to roof and foundations are the weak links in the existing structures. Enhancing the performance of the walls will not be achieved without the application of an appropriate connection anchoring system that satisfies current codes or would be qualified by credible structural methods.

Although the main focus of this project was to assess the effectiveness of the overlay material when it is applied to one side of the wall, it is worth noting that the walls exhibited significant out-of-plane shear strength. It is possible that this strength could have been enhanced by the overlay material.

References

Sabnis, Gajanan M., Harry G. Harris, Richard N. White, and M. Saeed Mirza, *Structural Modeling and Experimental Techniques* (Prentice-Hall, Inc., Englewood Cliffs, NJ, 1983).

Hasan, Husein A., and Joe V. Peyton, *Earthquake Evaluation of the Switch House Structures at Cordova and Weakley Electric Substations*, draft report (Tennessee Valley Authority, May 1998).

Appendix A: Figures Showing the Testing Process and Modes of Failure

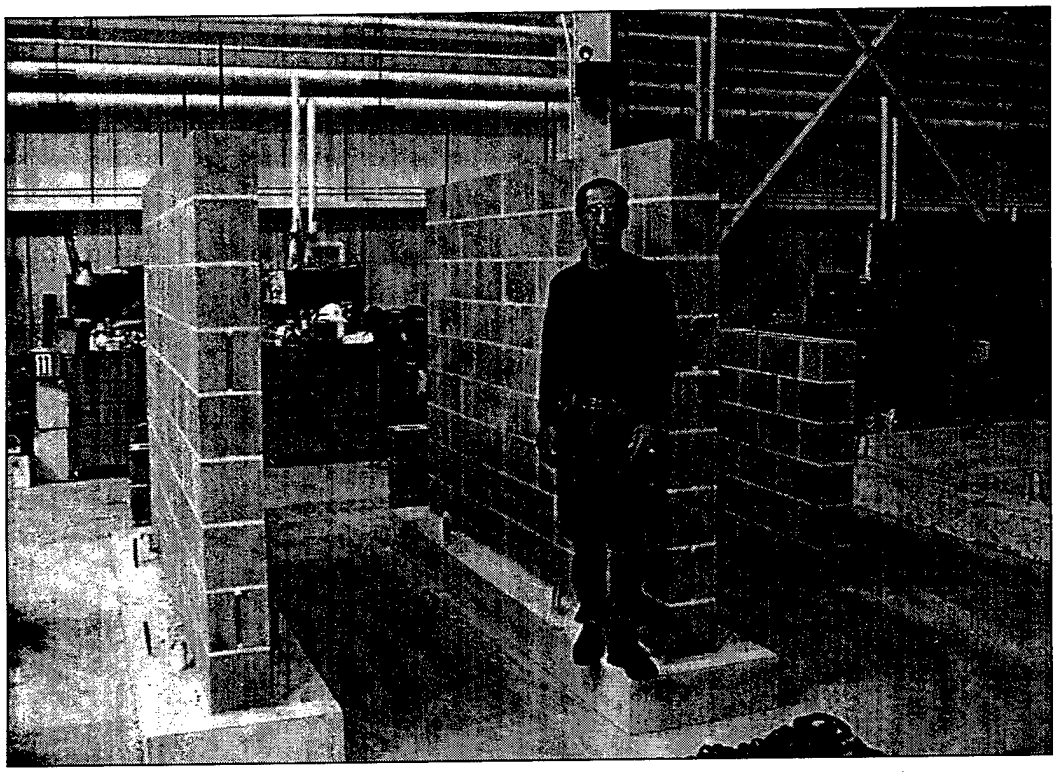

Figure A1. Two walls and one 4 ft x 4 ft racking specimen.

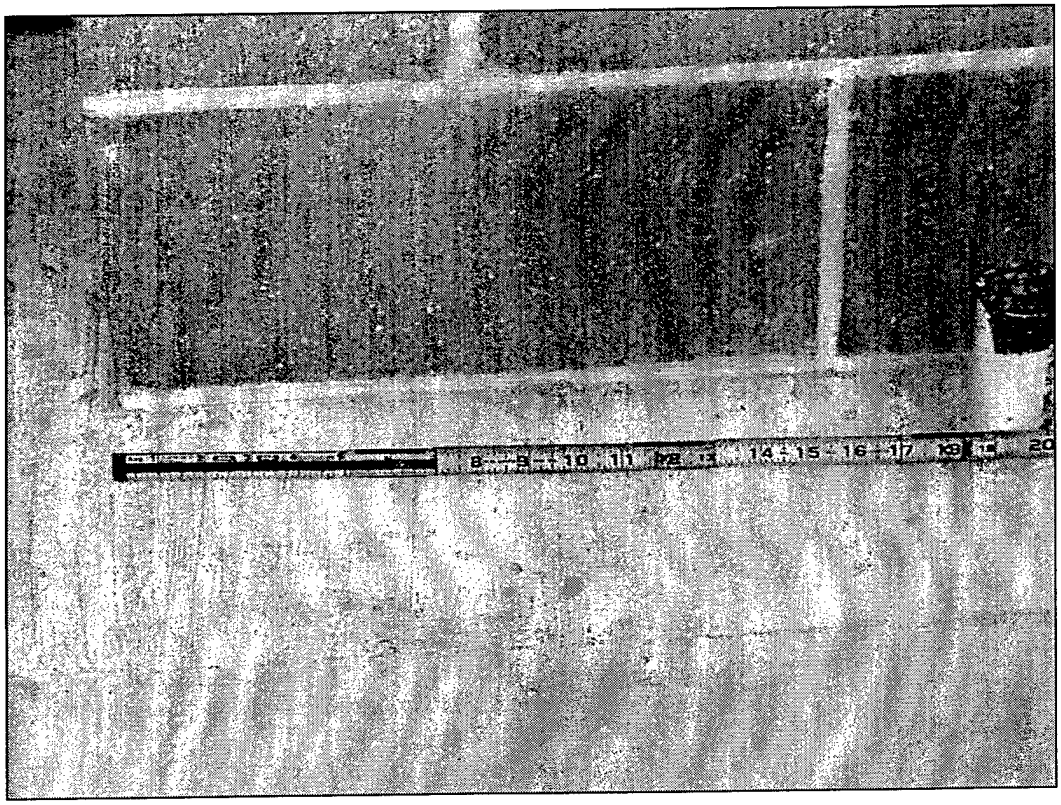

Figure A2. Edge distance between an anchor hole and edge of the wall.

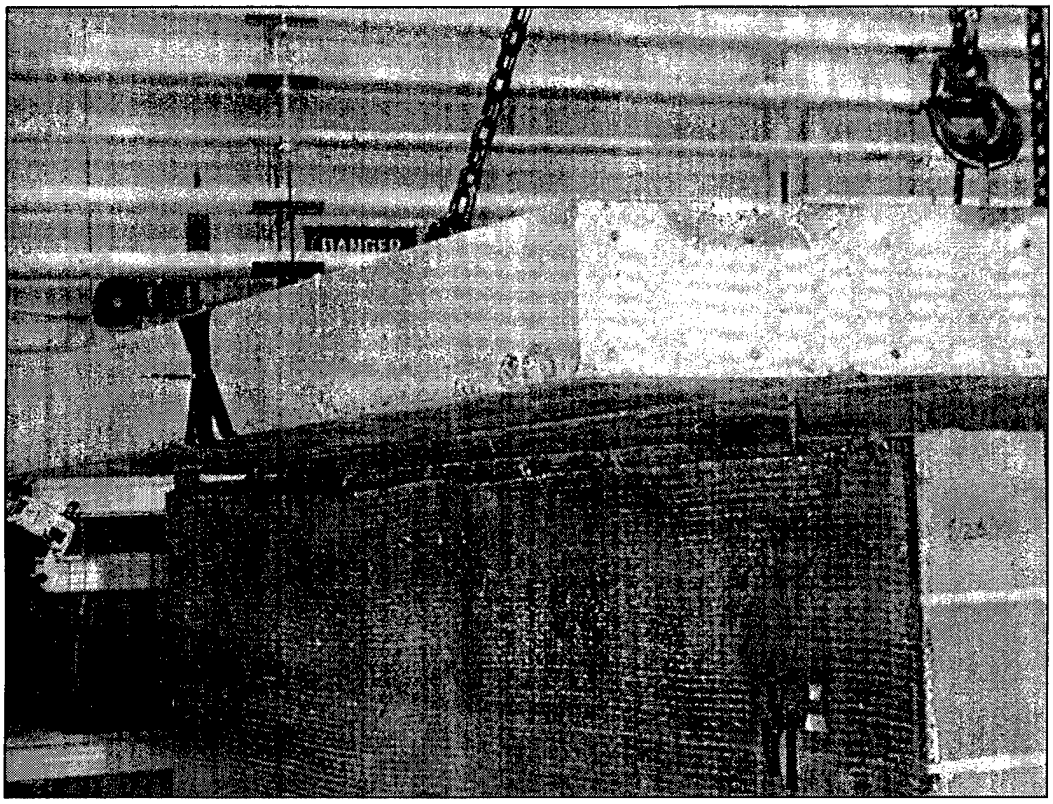

Figure A3. Three #3 bars connecting the slab to each wall.

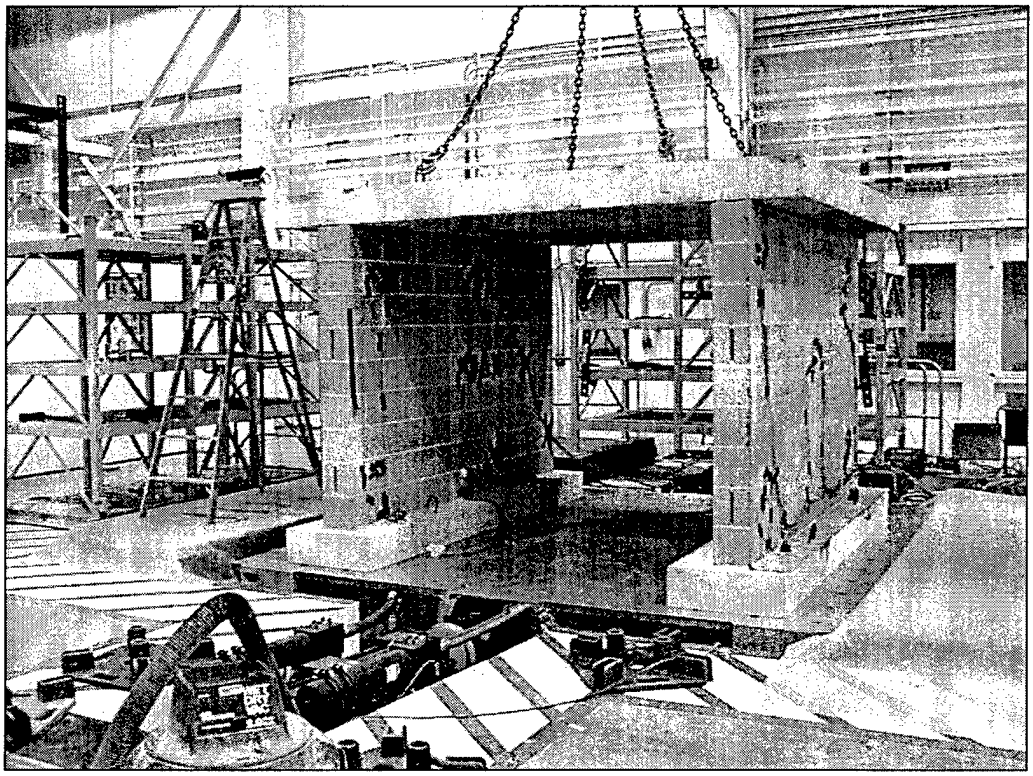

Figure A4. The testing specimen assembled on the shake table.

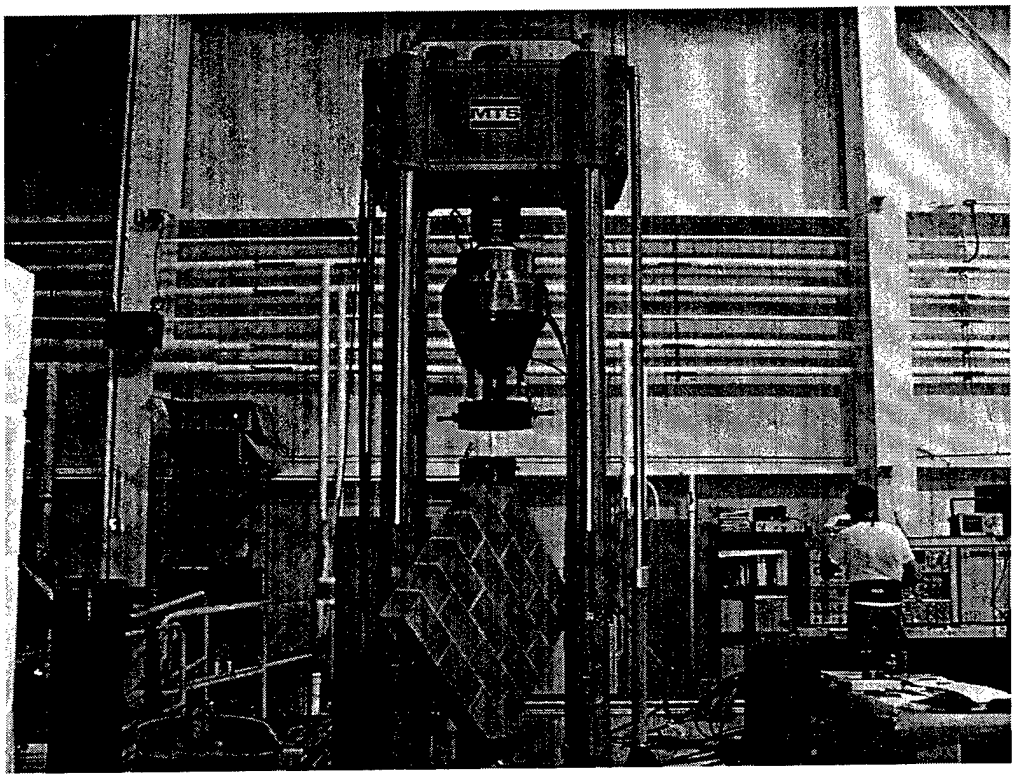

Figure A5. Racking test specimen.

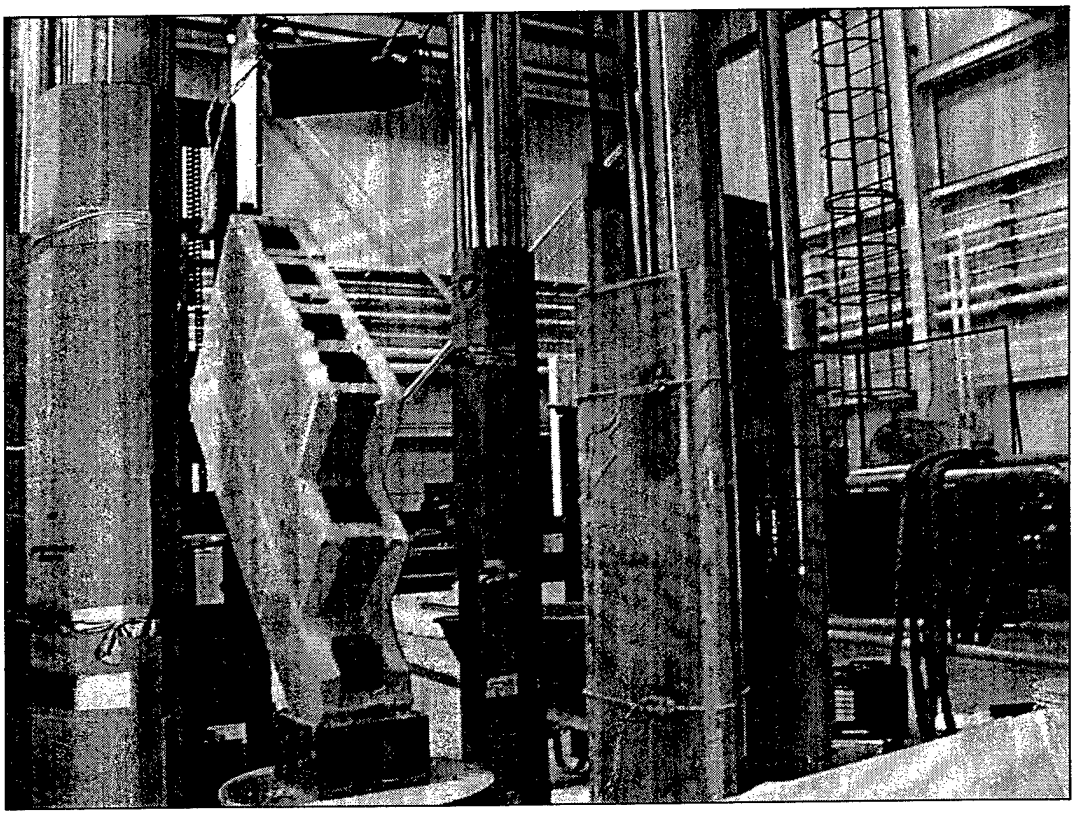

Figure A6. Mode of failure of the racking test.

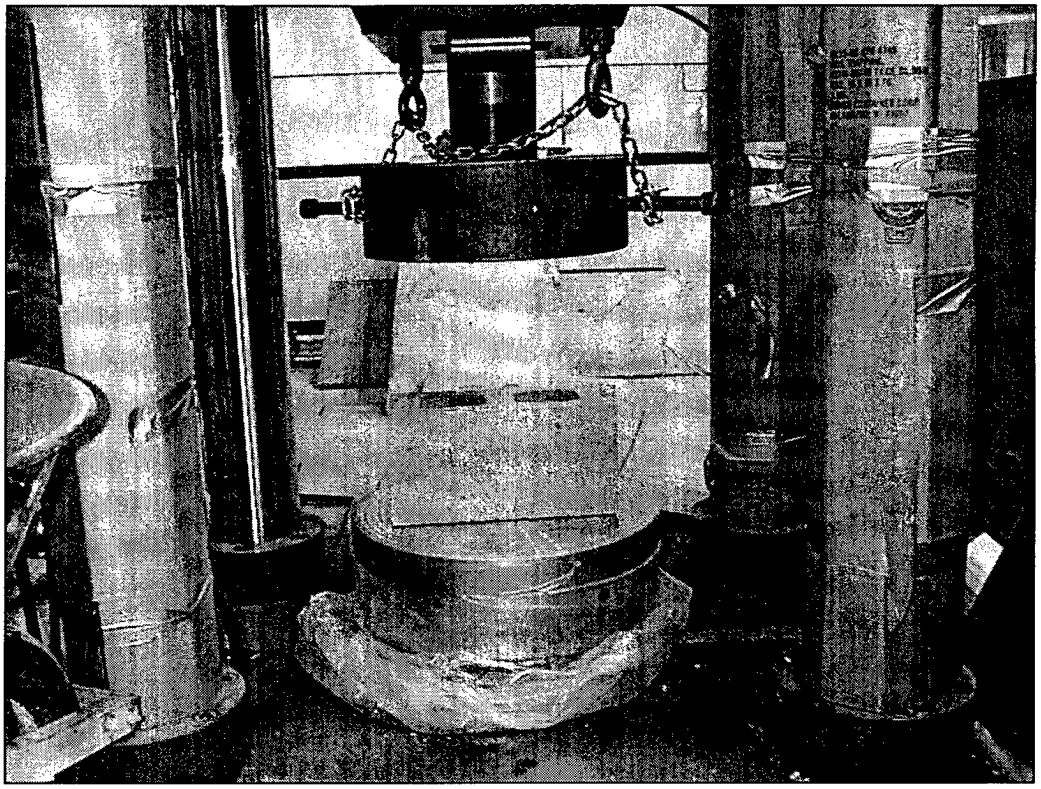

Figure A7. Compressive strength test for a concrete masonry unit.

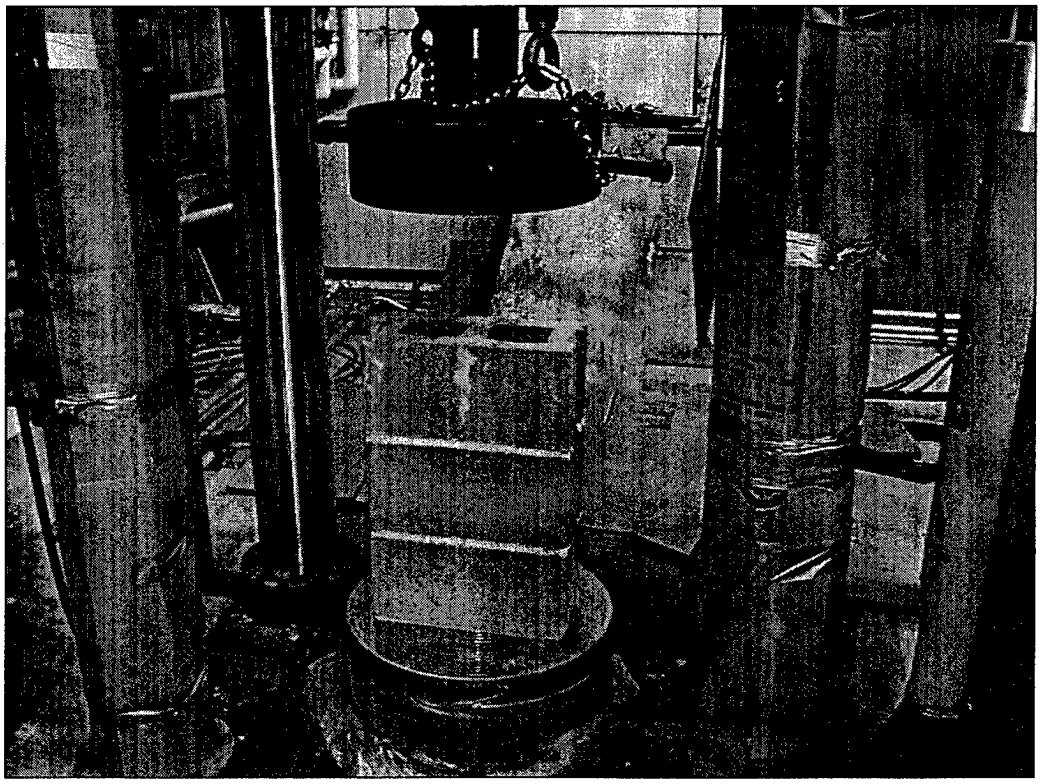

Figure A8. Prism strength test.

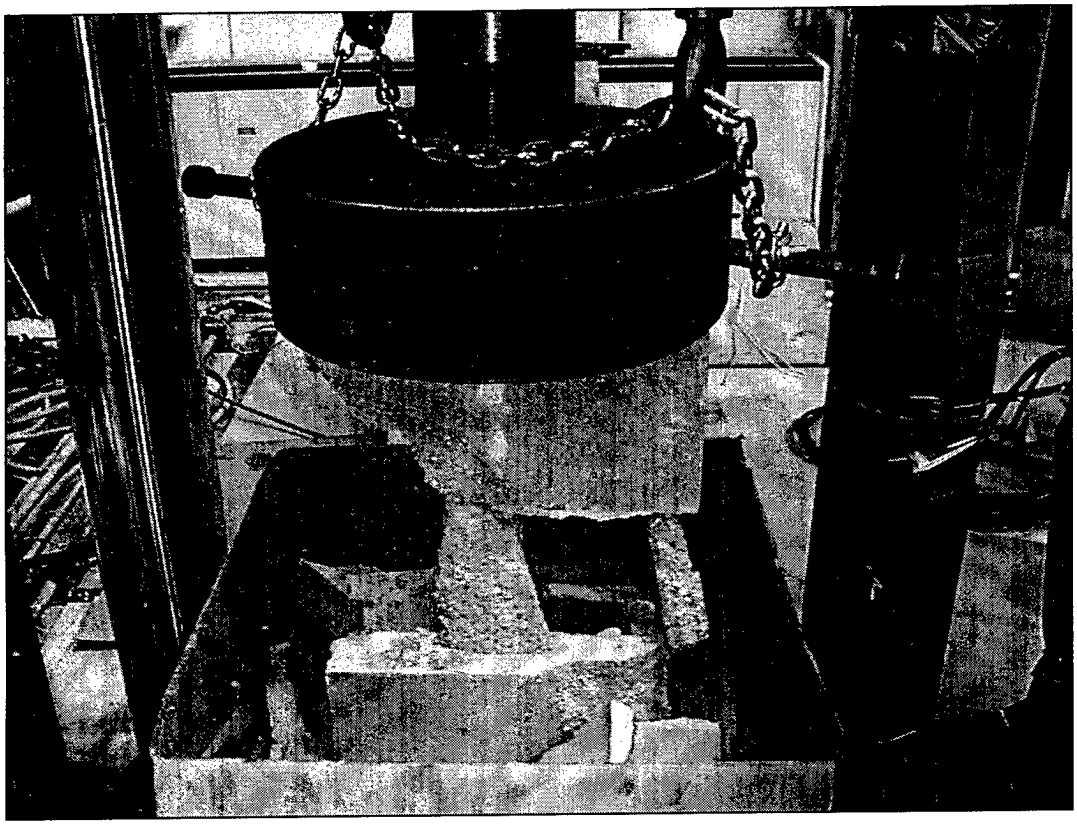

Figure A9. Failure of a prism specimen.

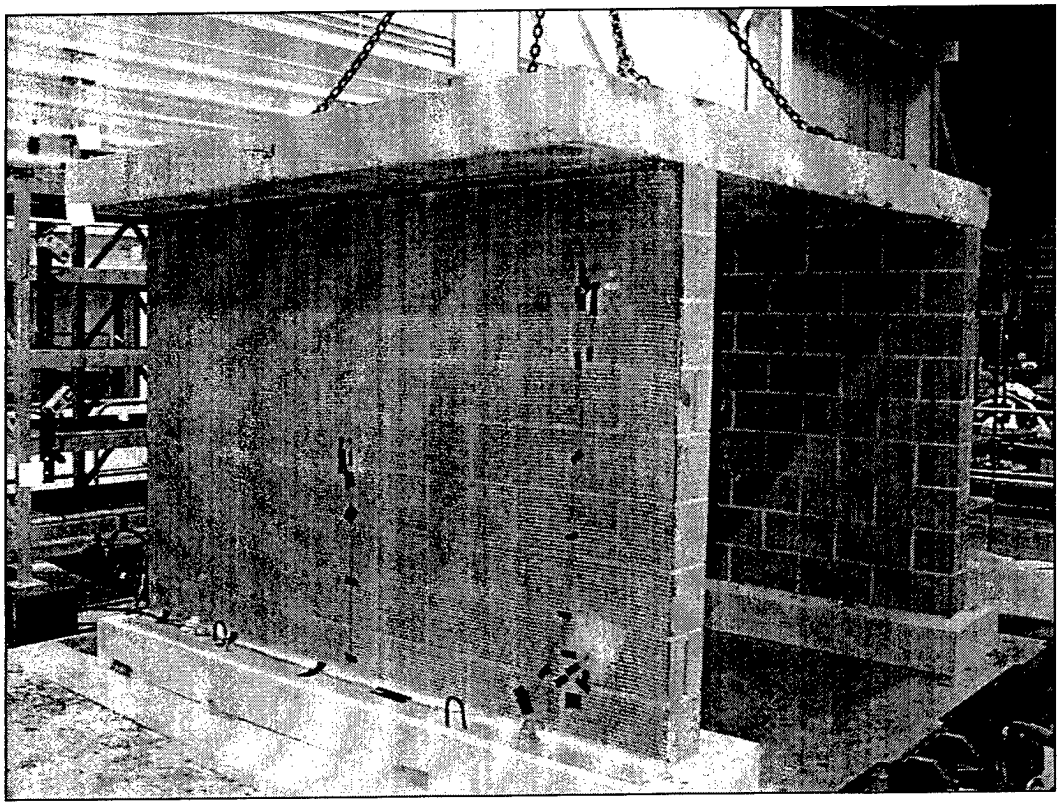

Figure A10. Specimens with both walls protected (Seismic Tests EQ-2 through EQ-7).

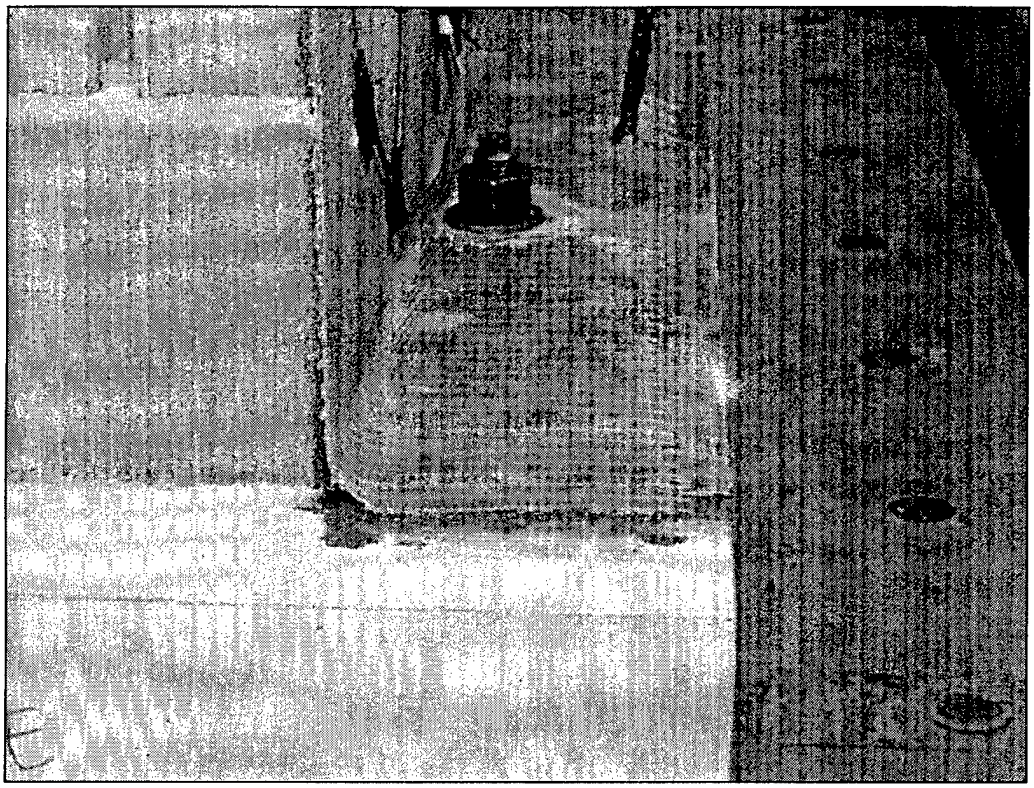

Figure A11. FIBRWRAP™ as applied on the wall and the concrete base beam.

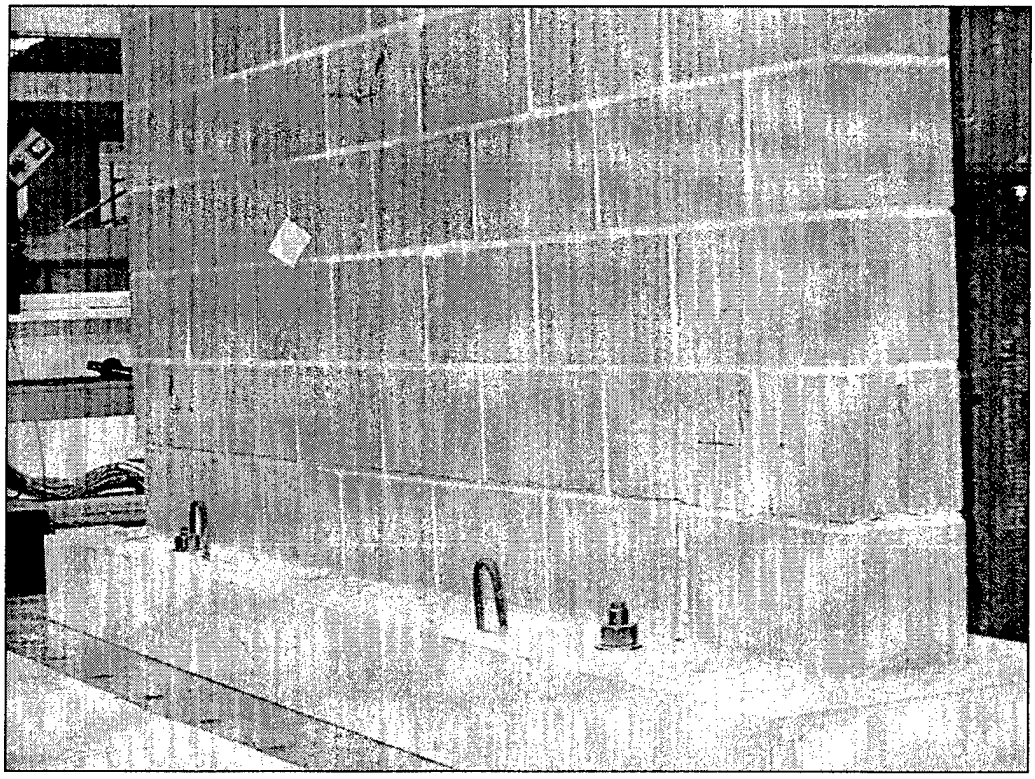

Figure A12. Formation of a crack on the outside of the unprotected wall from Seismic Test EQ-1, outside view.

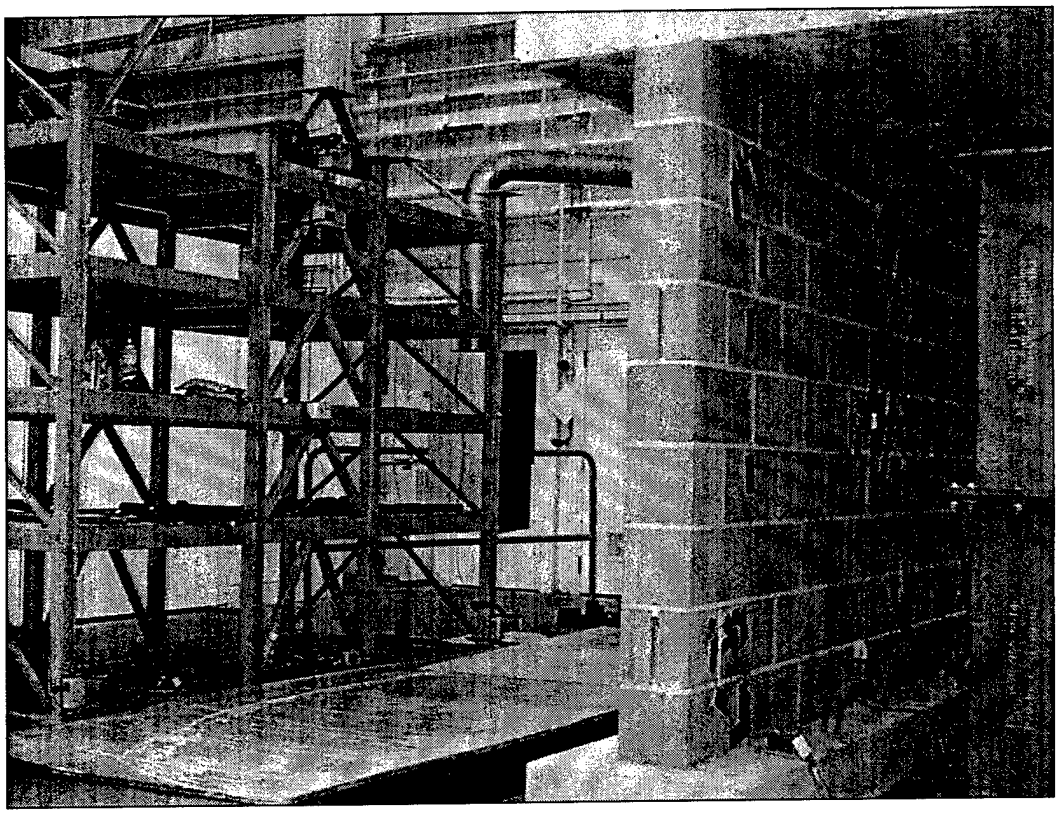

Figure A13. Formation of a crack on the inside of the unprotected wall from Seismic Test EQ-1, inside view.

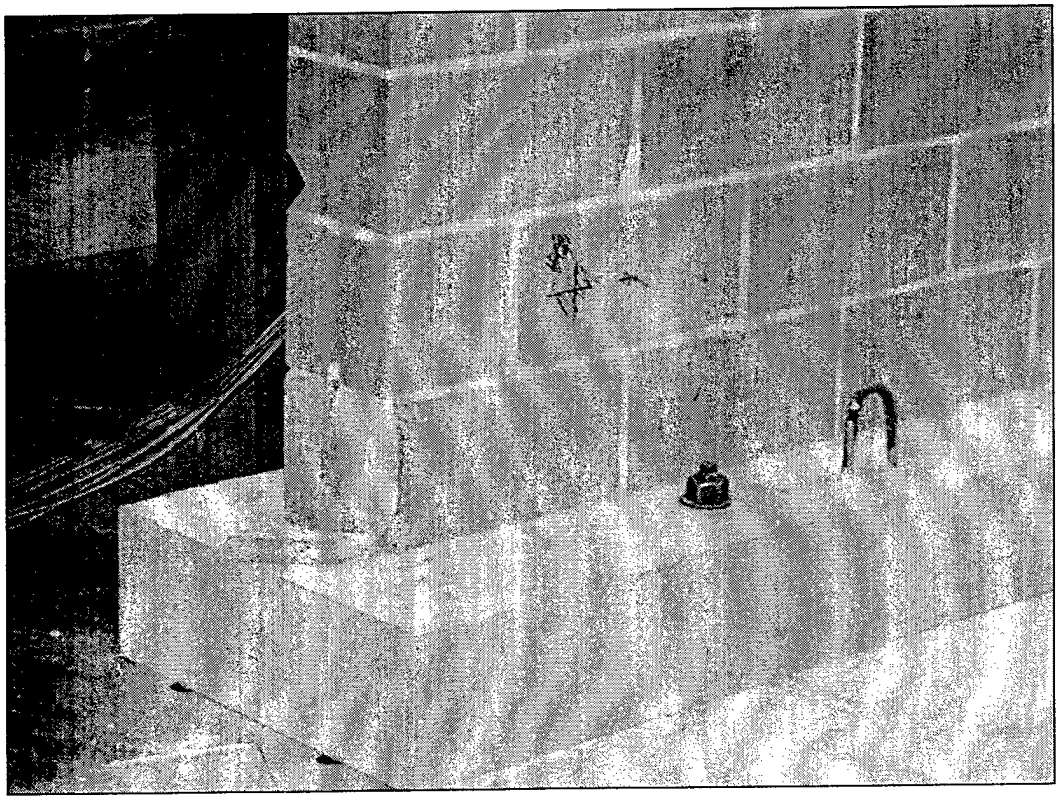

Figure A14. Edge spalling resulted from Seismic Test EQ-1 of the unprotected south wall.

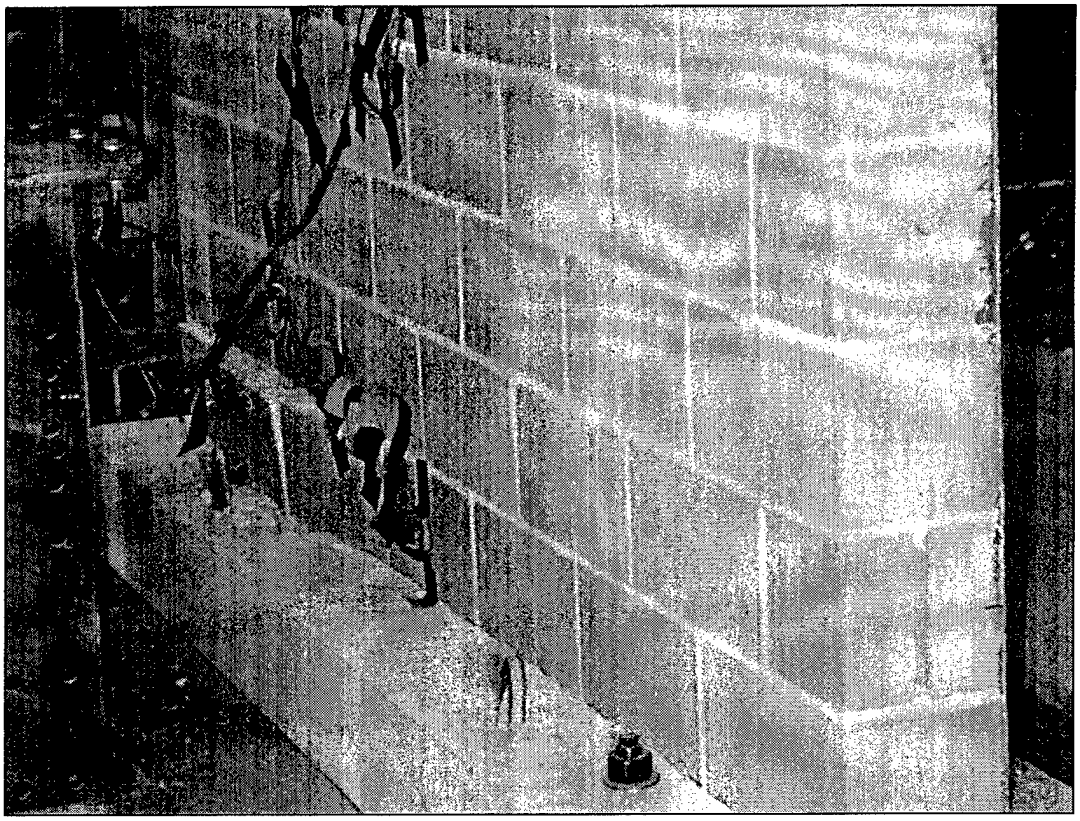

Figure A15. Out-of-plane facial slippage of bottom course CMU, inside of the north wall.

Appendix B: Static Analysis

Load Capacity of the Unreinforced Bearing Wall Model Subjected to Concentric Axial Compression

Te allowable vertical load capacity of the unreinforced wall per the UBC 2406 (c)-1 requirements.

Given Data:

Prism for CMU ---	fm := 3920·(1.07)	psi	"1.07 correction factor for slenderness ratio"
Clear height ---	h := 72	in	
CMU thickness ---	t := 7.63	in	
Width of the wall:	L := 111.75	in	

per NCMA TEK 141A for face shell bedding ---

Anet := 30.0	in^2	Per foot
Inet := 308.7	in^4	Per foot
Snet := 81.0	in^2	Per foot
r := 2.84	in	Per foot

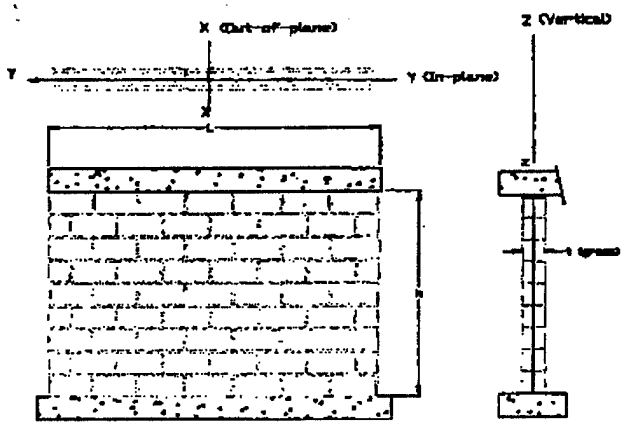

Weight of the slab: $W_s := (150) \cdot \left(\frac{8}{12} \cdot 9.29 \cdot 10.85\right)$

$W_s = 10080$ lbs

Weight of each wall: $W_w := 44.5 \cdot (9.29) \cdot (6)$

$W_w = 2480$ lbs

Total tributary weight per one foot wall: $W_t := \left(W_s + 2\frac{W_w}{2}\right) \cdot \frac{1}{2\frac{L}{12}}$

$W_t = 674$ lb/ft

Prisms have been tested and special inspection has been provided during construction.

$$F_a := 0.20 \cdot f_m \cdot \left[1 - \left(\frac{h}{42 \cdot t}\right)^3\right]$$

$F_a = 829$ psi

$\frac{h}{t} = 9.44$

$P_a := F_a \cdot A_{net}$

$P_a = 24881$ lbs/ft

The capacity/demand ratio under pure compression:

$$R := \frac{P_a}{W_t}$$

$R = 36.9$

Load Capacity of the Unreinforced Bearing Wall Model Subjected to Axial Compression and Lateral Out-of-Plane Loads

Axial load per ft. $p := Wt$

Actual axial stress: $fa := \frac{Wt}{Anet}$

$fa = 22$ psi

O/P moment for one g: $Ww := 44.5$

$$Mw := \left(\frac{\frac{Ww}{12} \cdot h^2}{8} \right)$$

$Mw = 2403$ lb-in, @ the mid height of the wall

$Mp := p \frac{h}{2}$

$Mp = 24277$ lb-in, @ the top of the wall

Actual bending stress: $fb := \frac{Mp}{Snet}$

$fb = 300$ psi

Allowable axial stress: $Fa = 829$ psi

Allowable Tensile Stresses: $Ft := 19$ psi per ACI Table 6.3.1.1 nd UBC Sec. 2406 (C) 4 for type N mortar and tension normal to bed joints.

Allowable flexural compressive stress:

$Fb := 0.33 \cdot fm$

$Fb = 1384$ psi

Tension criterion: $-fa + fb = 277$ > $1.33 \cdot Ft = 25$ NG

"0.16 P will meet the tension criteria"

Compression criterion: $\frac{fa}{Fa} + \frac{fb}{Fb} = 0.244$ < 1.33 OK

The estimated capacity/demand ratio under combined loads of out-of-plane loading equals the tributary load and the gravity load is 0.16 Wt:

Load Capacity of the Unreinforced Bearing Wall Model Subjected to Axial Compression, Bending, and Shear

lateral load per one wall: $P\_in\_plane := \frac{Ws + 2\cdot\frac{Ww}{2}}{2}$

$P\_in\_plane = 5062$ lbs/wall

$M\_p\_in\_plane := P\_in\_plane \cdot h$

$M\_p\_in\_plane = 364469$ lb-in

$tnet := 2.5$ in

$Anet := tnet \cdot L$

$Anet = 279$ in^2

$S\_in\_plane := \frac{tnet \cdot L^2}{6}$

$S\_in\_plane = 5203$ in^2

$fb := \frac{M\_p\_in\_plane}{S\_in\_plane}$

$fb = 70$ psi

Tension criterion: $-fa + fb = 48 > 1.33 \cdot Ft = 25$ NG

"0.682 p_in_plane will meet the tension criteria"

Compression criterion: $\frac{fa}{Fa} + \frac{fb}{Fb} = 0.078 < 1.33$ ok

The estimated capacity/demand ratio under combined loads of in-plane lateral load equals the tributary load and the gravity load:

$0.682 \cdot Wt$ per one foot.

Load Capacity of the Unreinforced Bearing Wall Model Subjected to Pure Shear Load

Allowable shear per a laboratory test:

$$Vall := 209 \quad psi$$

Actuat shear for one g in-plane loading:

$$v := \frac{P\_in\_plane}{L \cdot tnet}$$

$$v = 18 \quad psi \quad < \quad Vall = 209 \quad ok$$

The estimated in-plan acceleration needed to fail the model in pure shear based on static analysis:

$$\frac{Vall}{v} = 11.5 \quad g$$

Appendix C: Finite Element and Dynamic Analysis

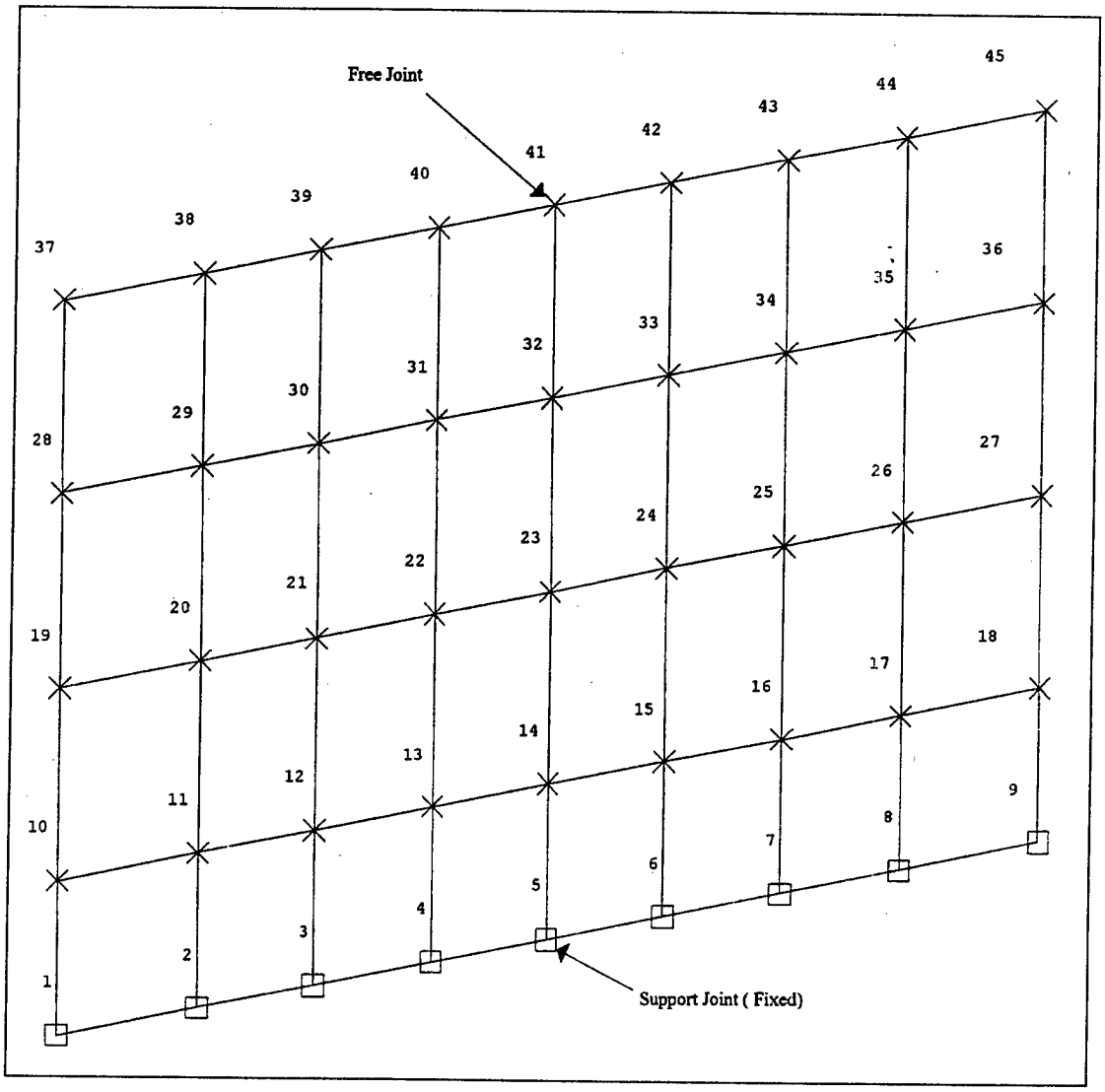

Figure C1. GT STRUDL Model 1.

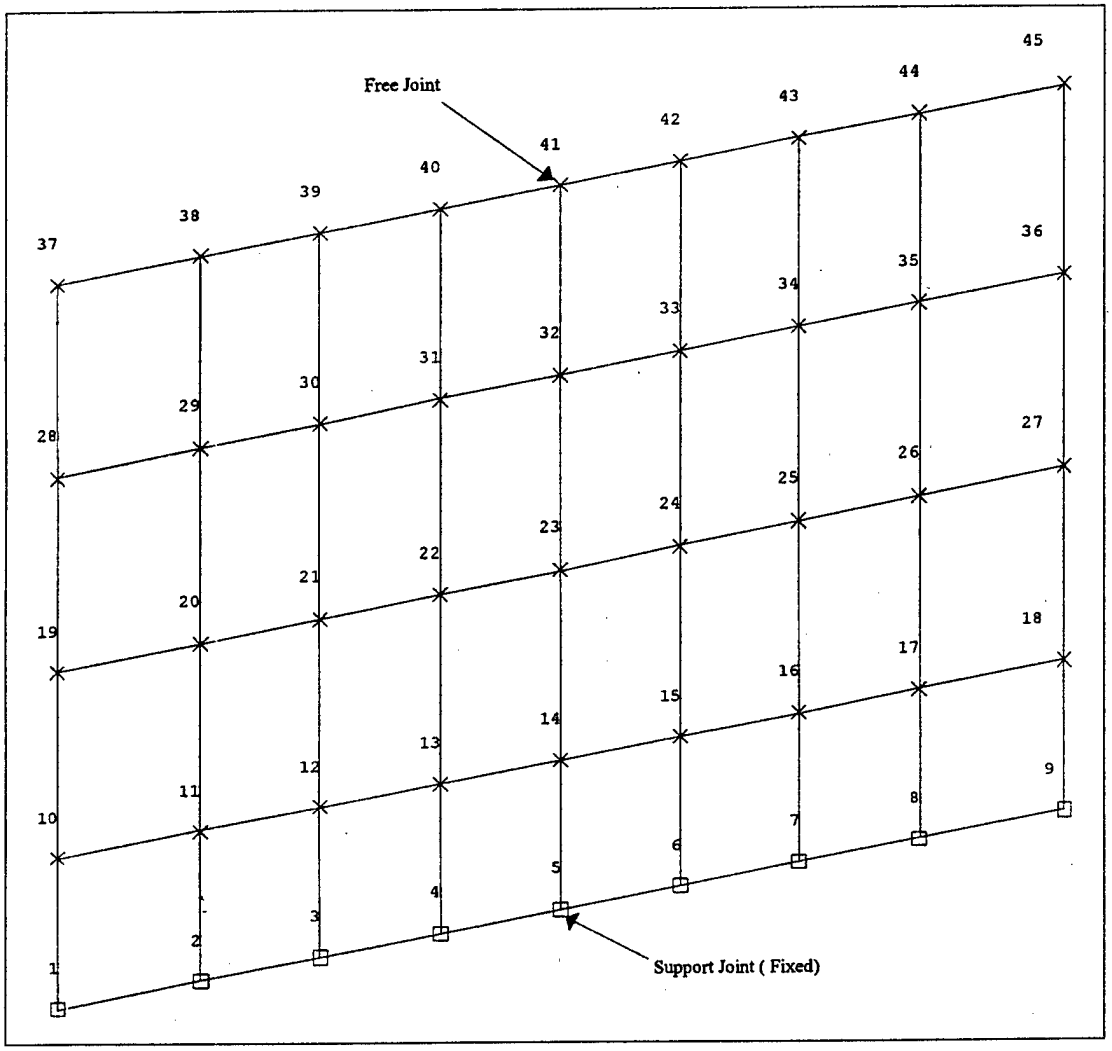

Figure C2. GT STRUDL Model 2.

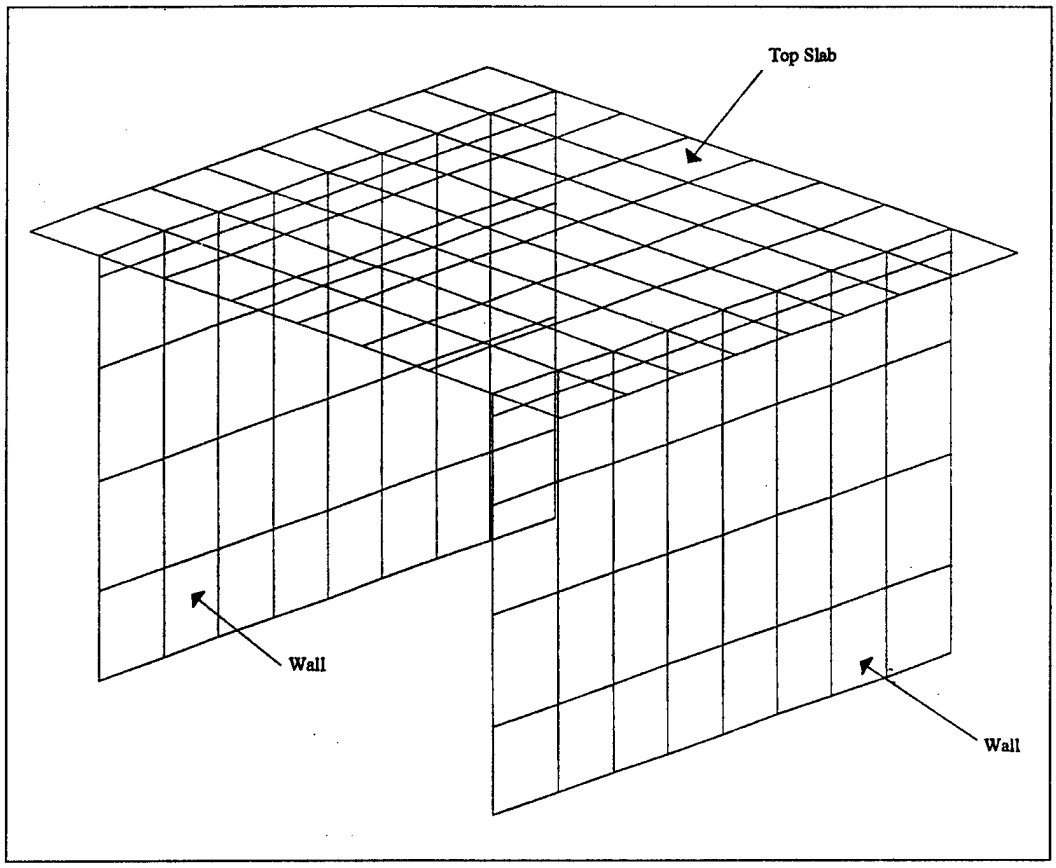

Figure C3. GT STRUDL Model 3.

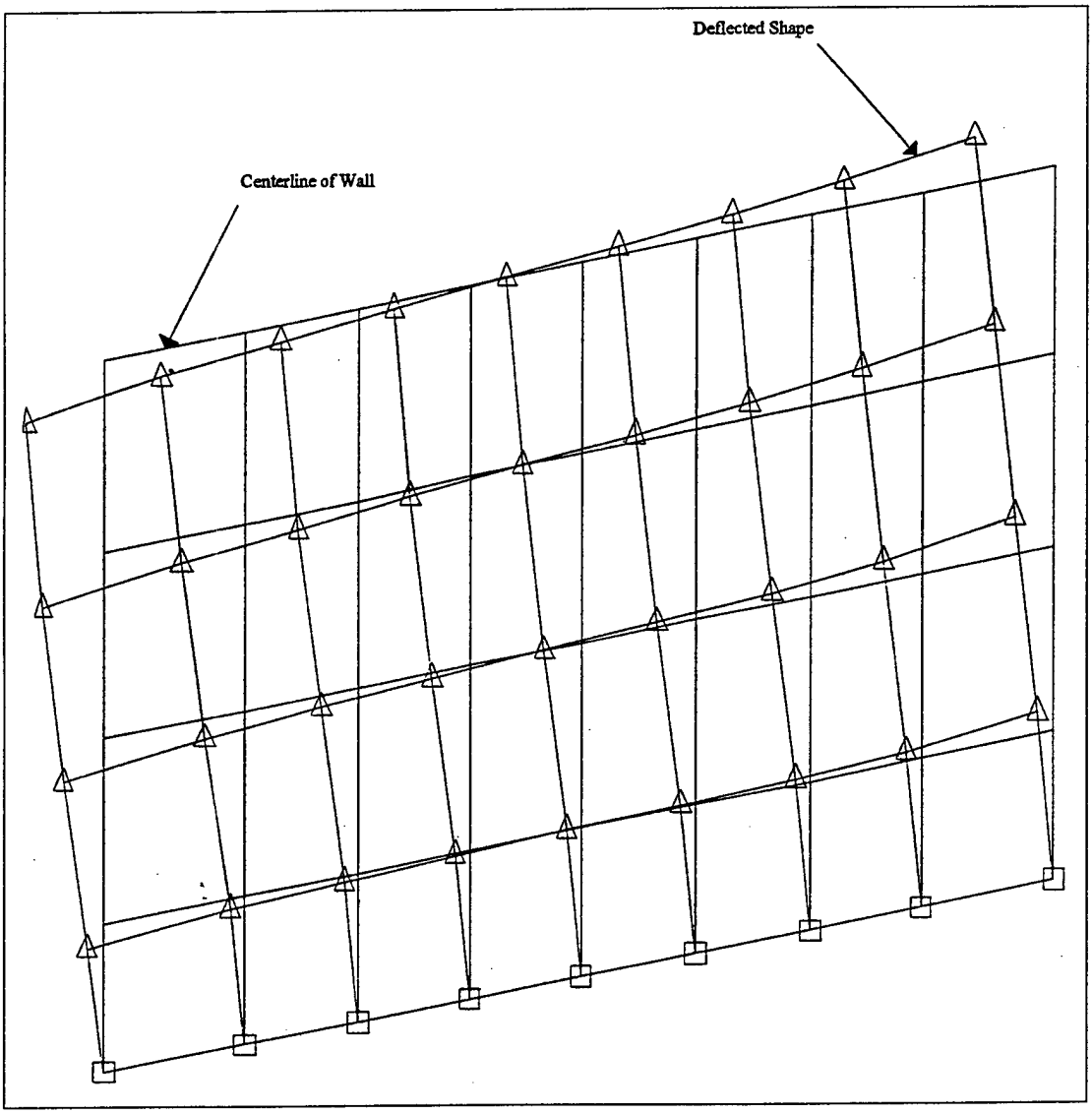

Figure C4. GT STRUDL Model 1, first mode of vibration, 183.7 Hz, in-plane (X direction).

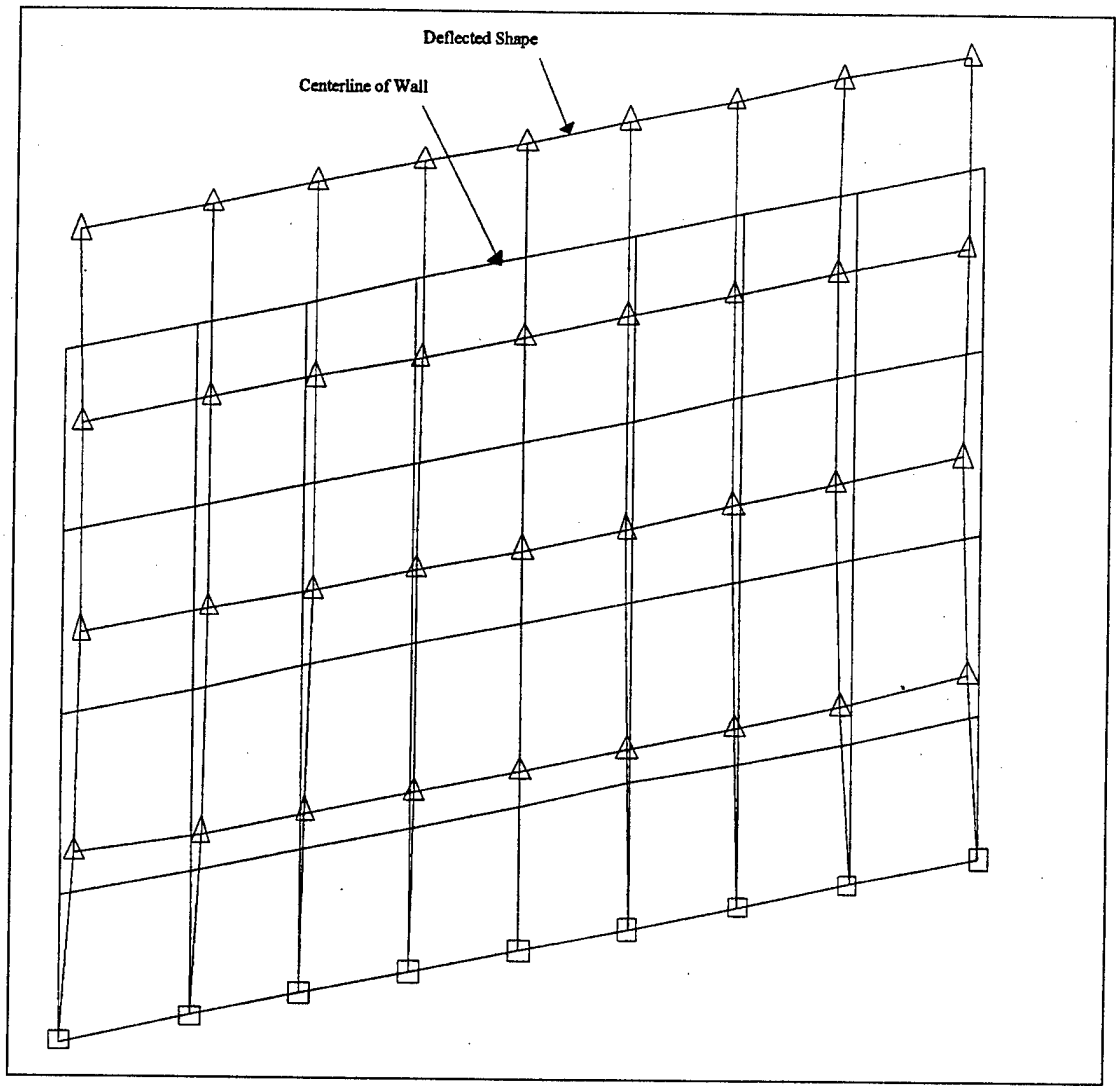

Figure C5. GT STRUDL Model 1, first mode of vibration, 369.2 Hz, vertical (Y direction).

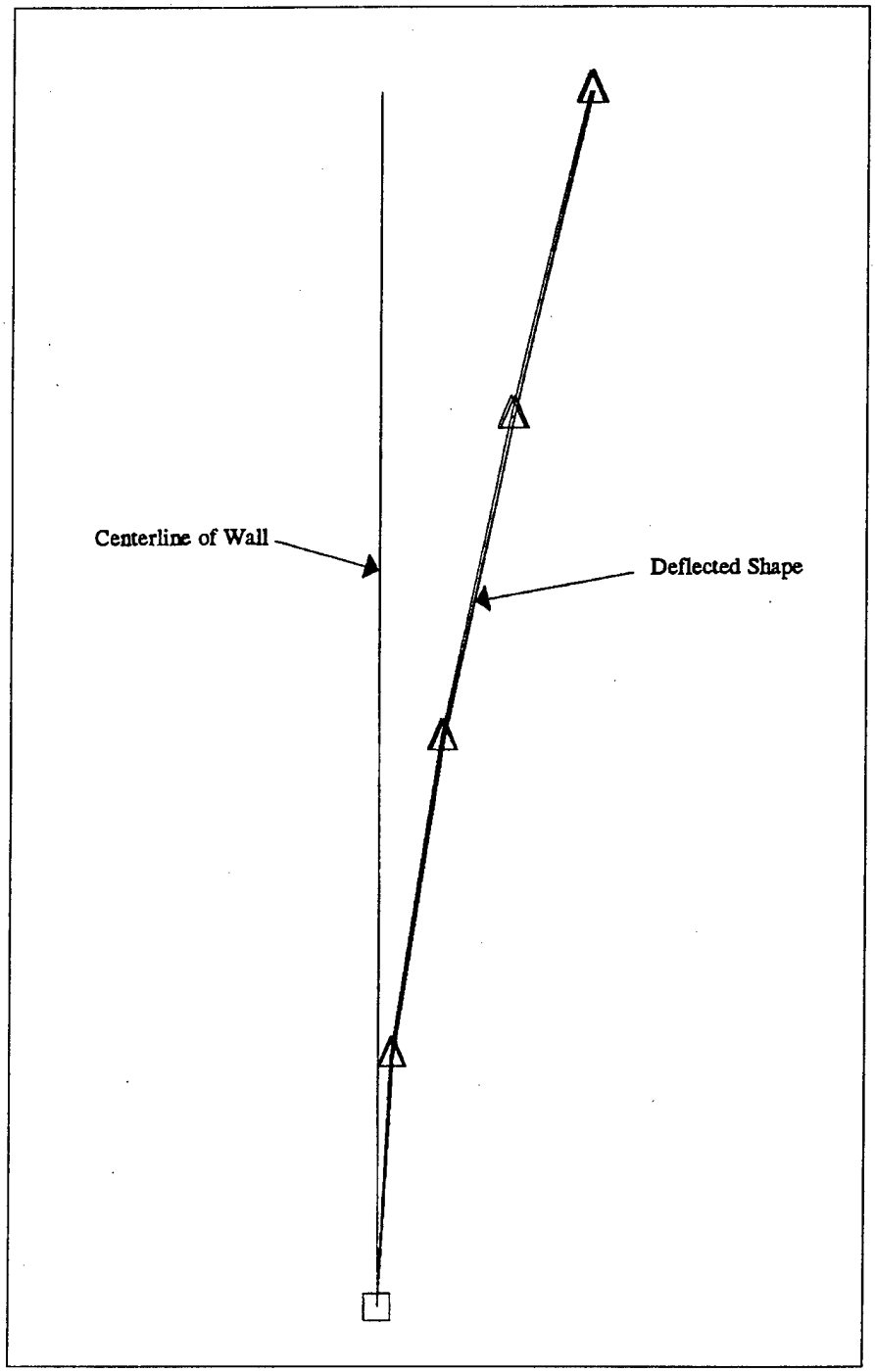

Figure C6. GT STRUDL Model 1, first mode of vibration, 20.9 Hz, out-of-plane (Z direction).

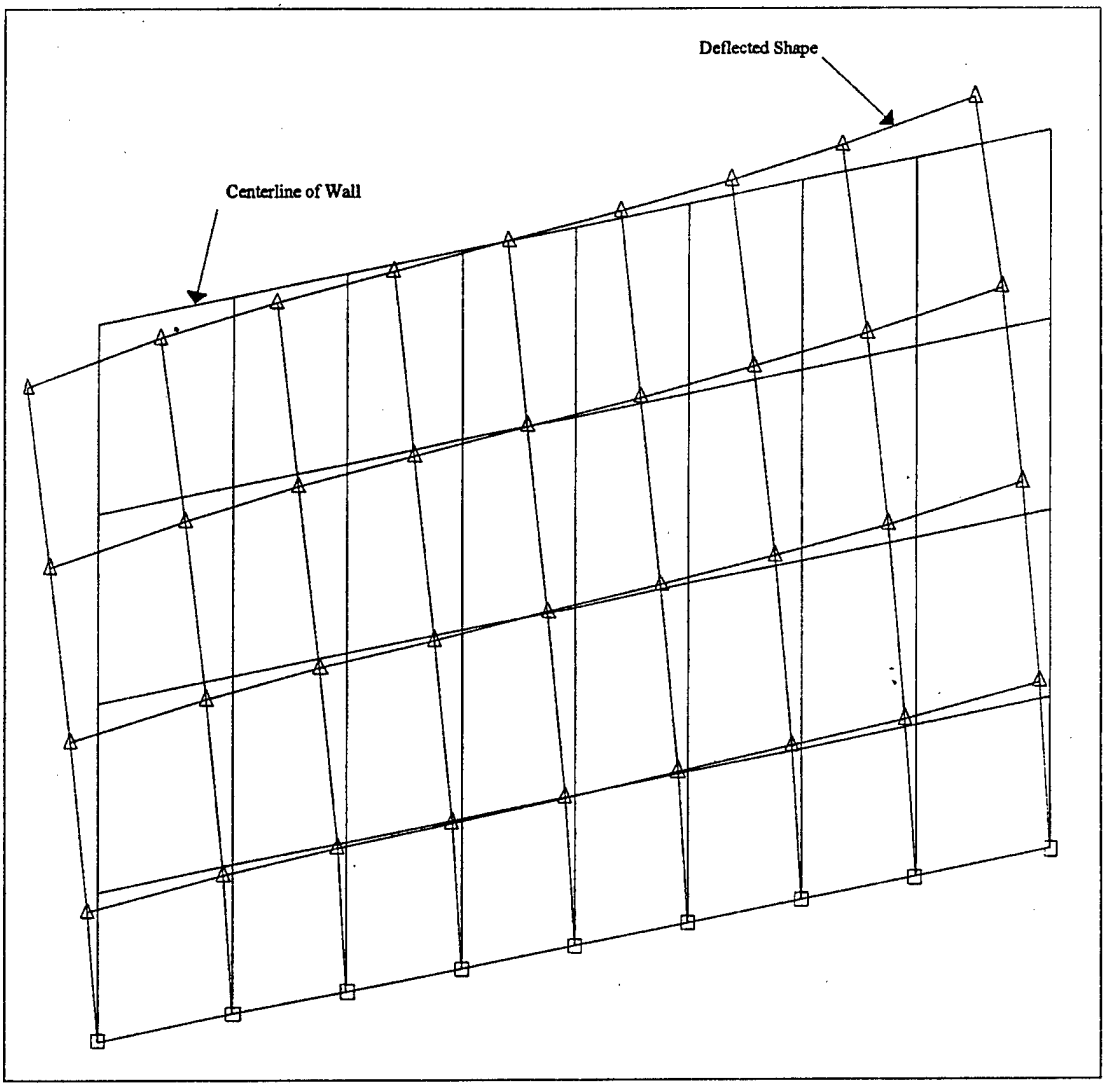

Figure C7. GT STRUDL Model 2, first mode of vibration, 71.2 Hz, in-plane (X direction).

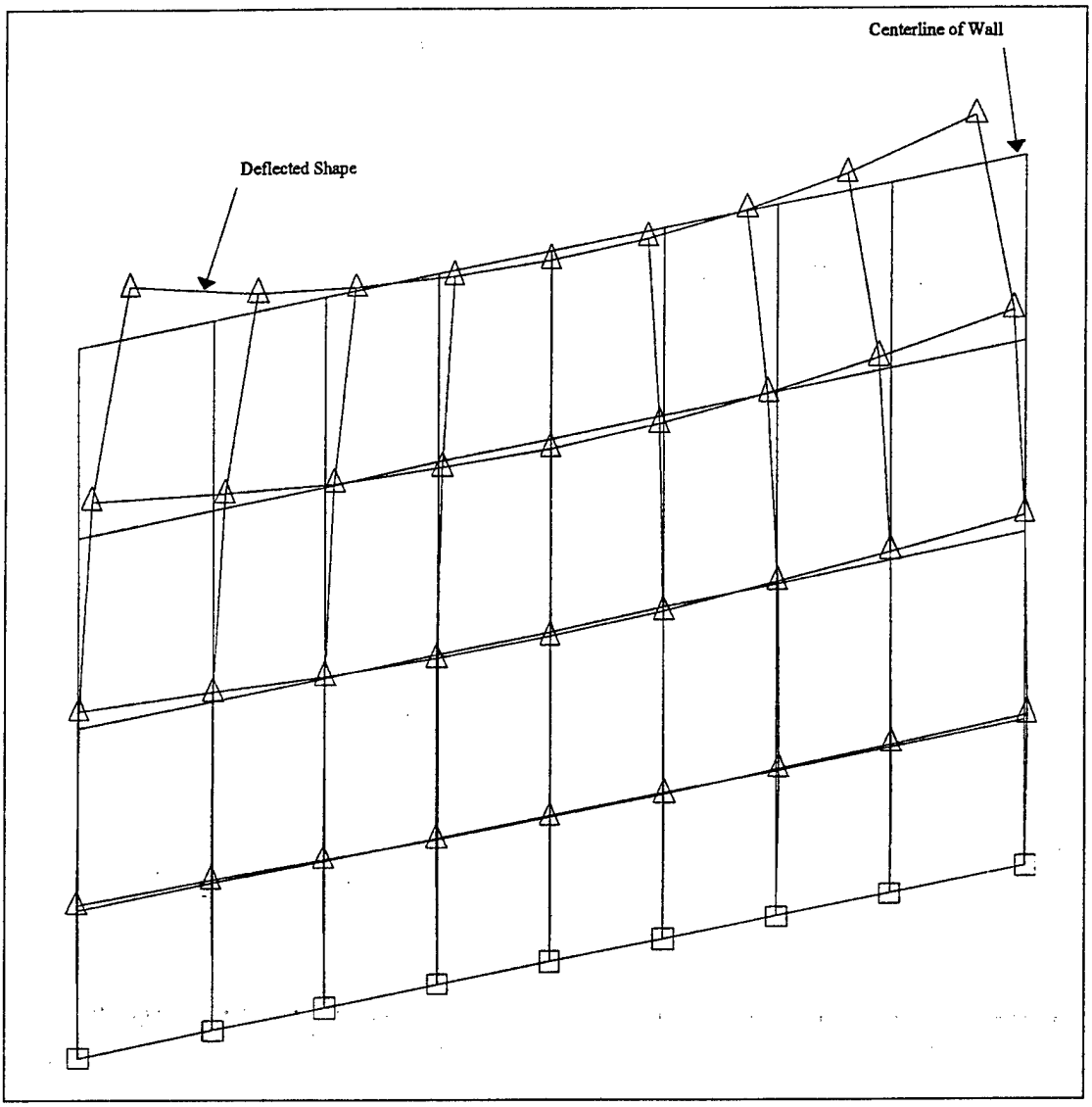

Figure C8. GT STRUDL Model 2, first mode of vibration, 138.1 Hz, vertical (Y direction).

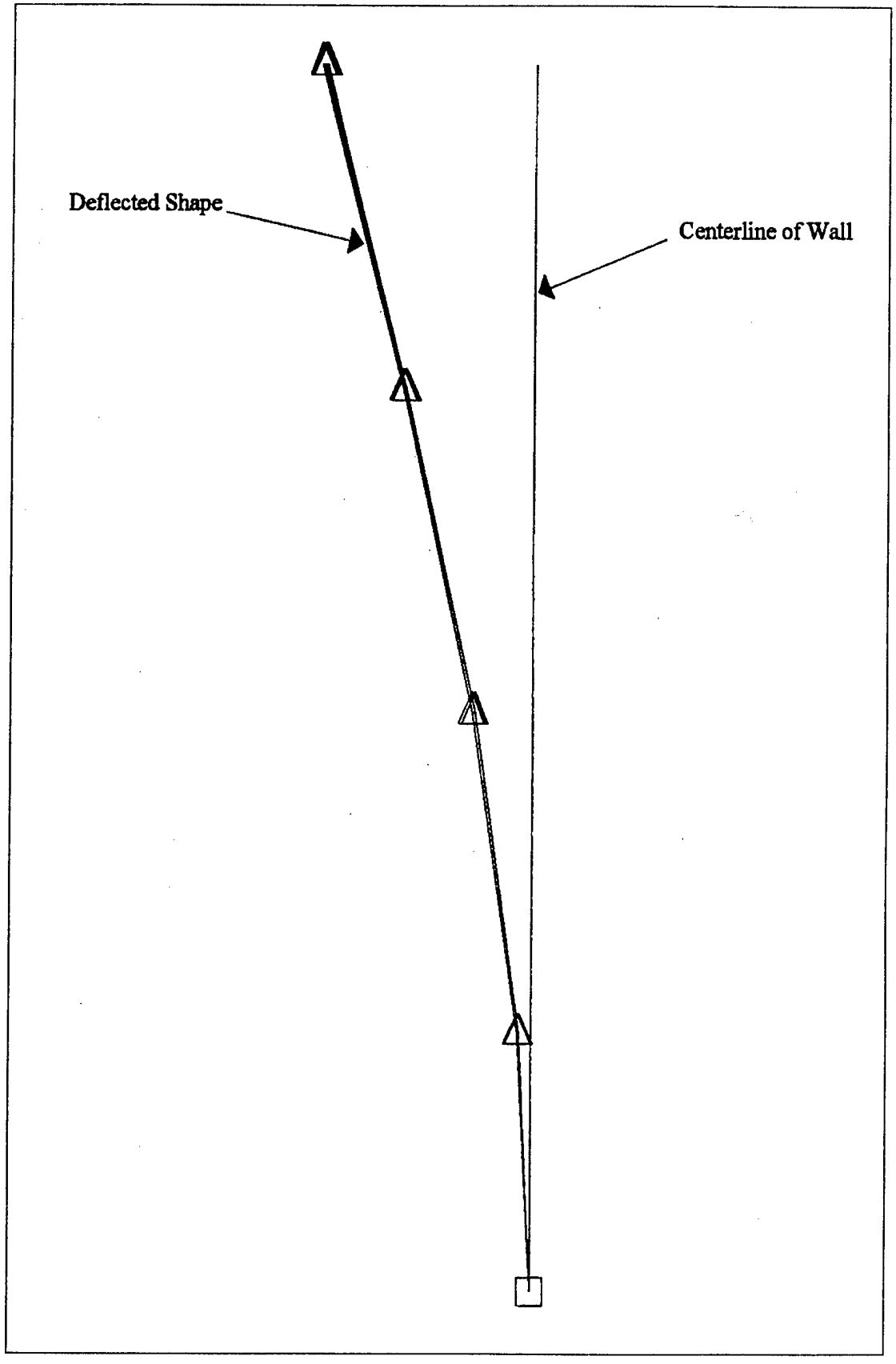

Figure C9. GT STRUDL Model 2, first mode of vibration, 7.2 Hz, out-of-plane (Z direction).

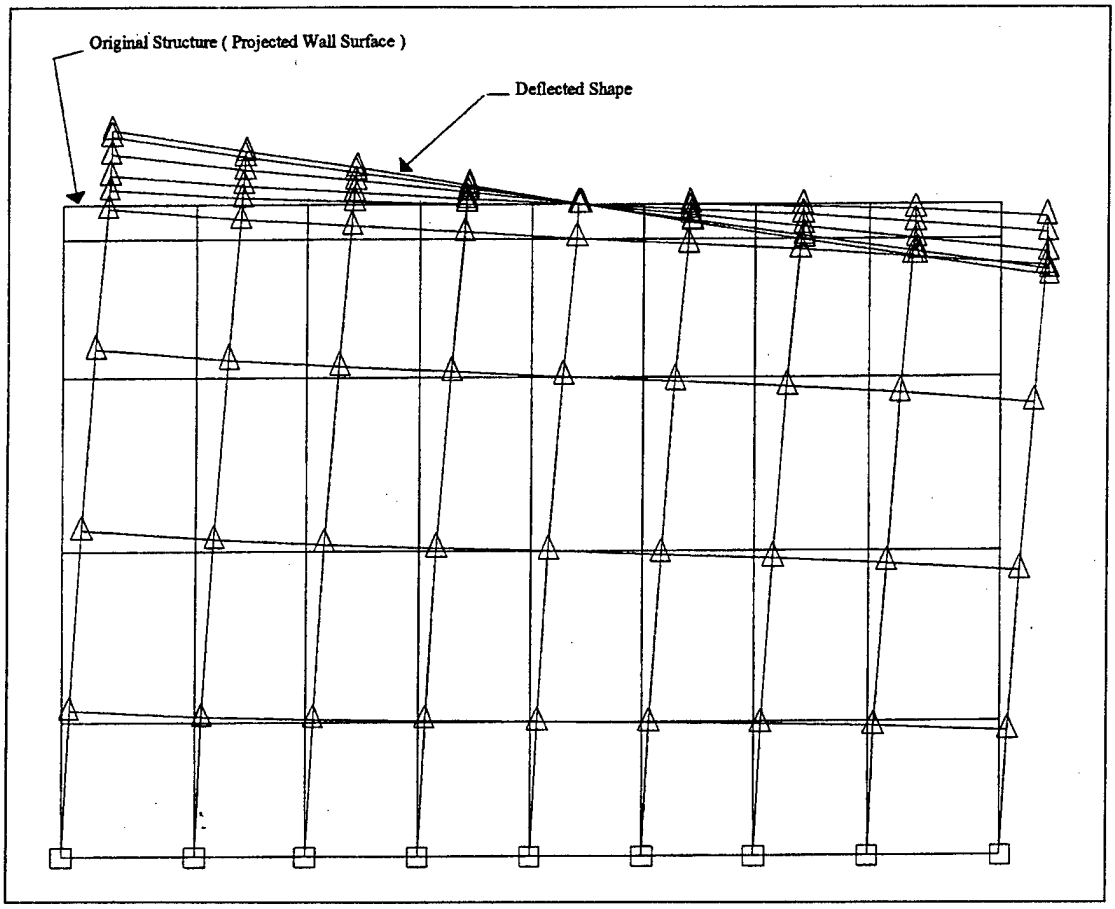

Figure C10. GT STRUDL Model 3, first mode of vibration, 70.5 Hz, in-plane (X direction).

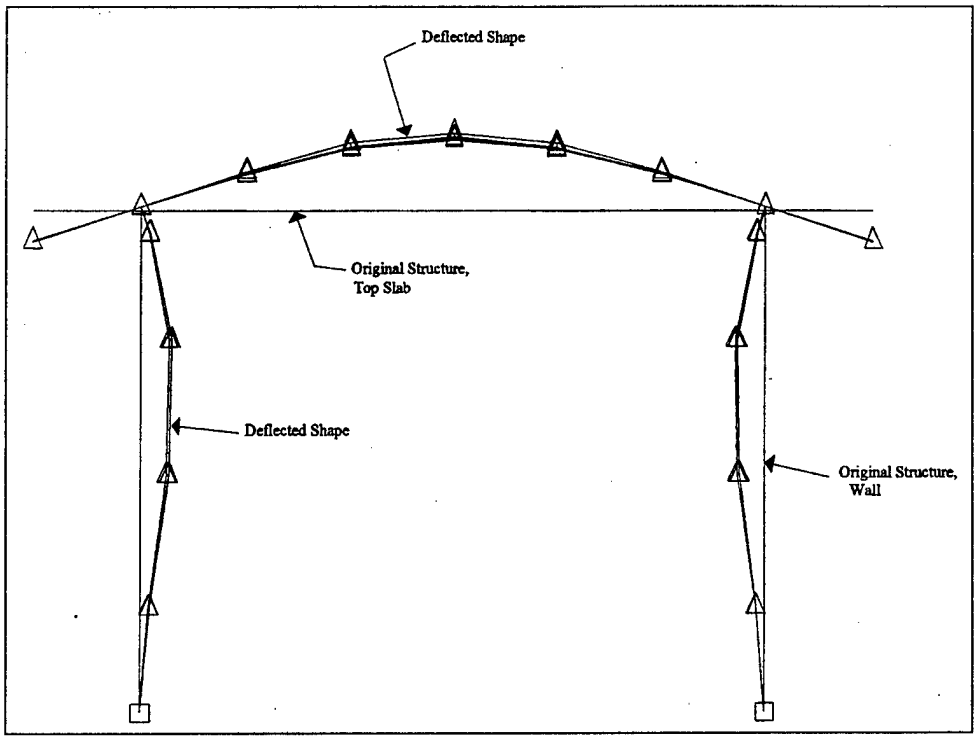

Figure C11. GT STRUDL Model 3, first mode of vibration, 55.8 Hz, vertical (Y direction).

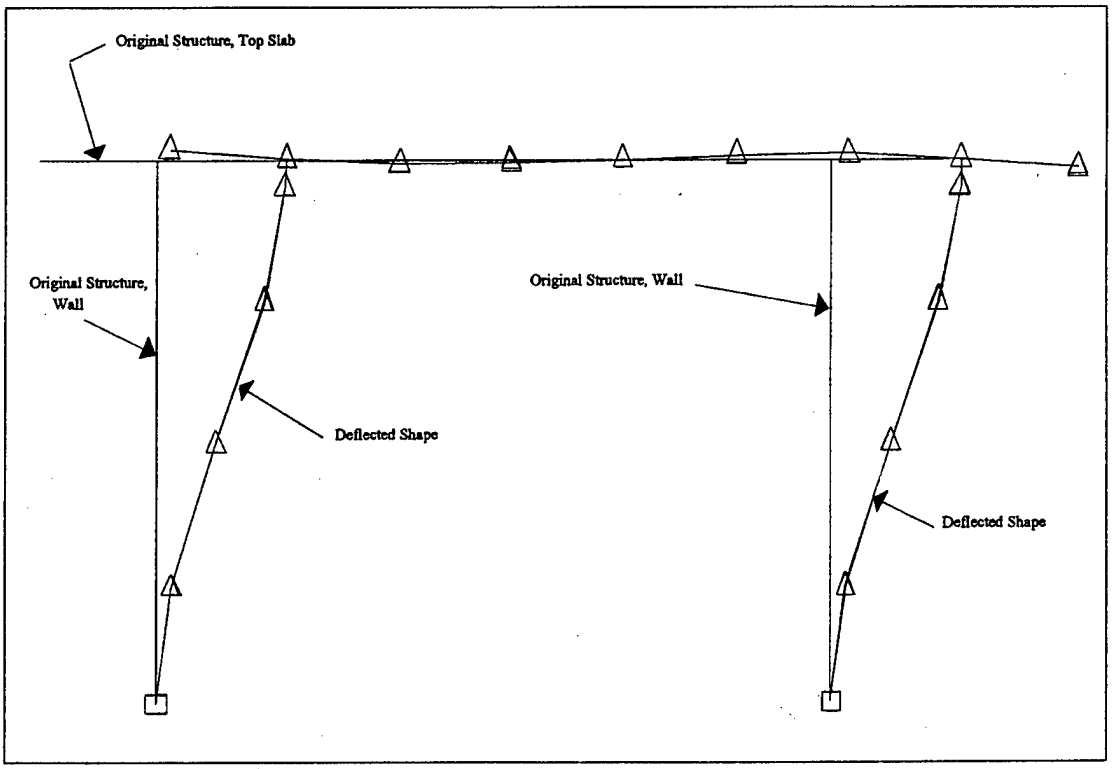

Figure C12. GT STRUDL Model 3, first mode of vibration, 14.0 Hz, out-of-plane (Z direction).

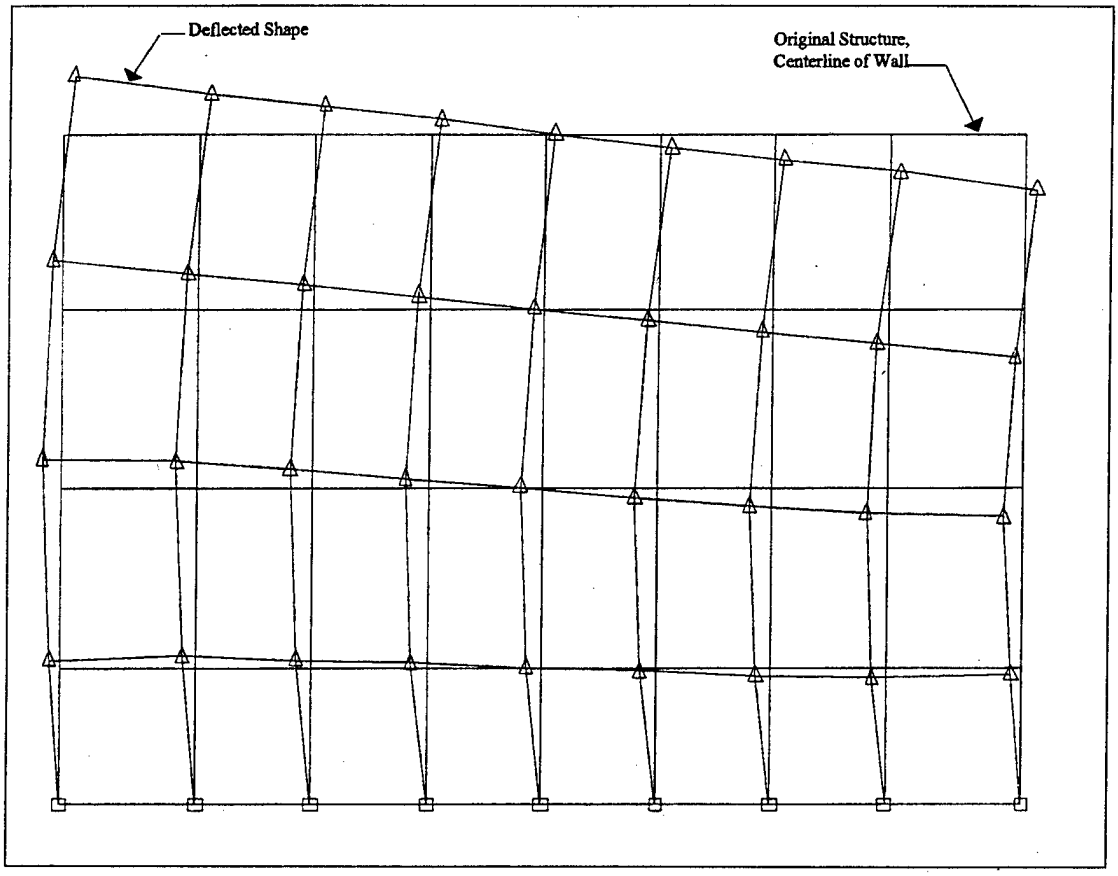

Figure C13. GT STRUDL Model1, second mode of vibration, 407.9 Hz, in-plane (X direction).

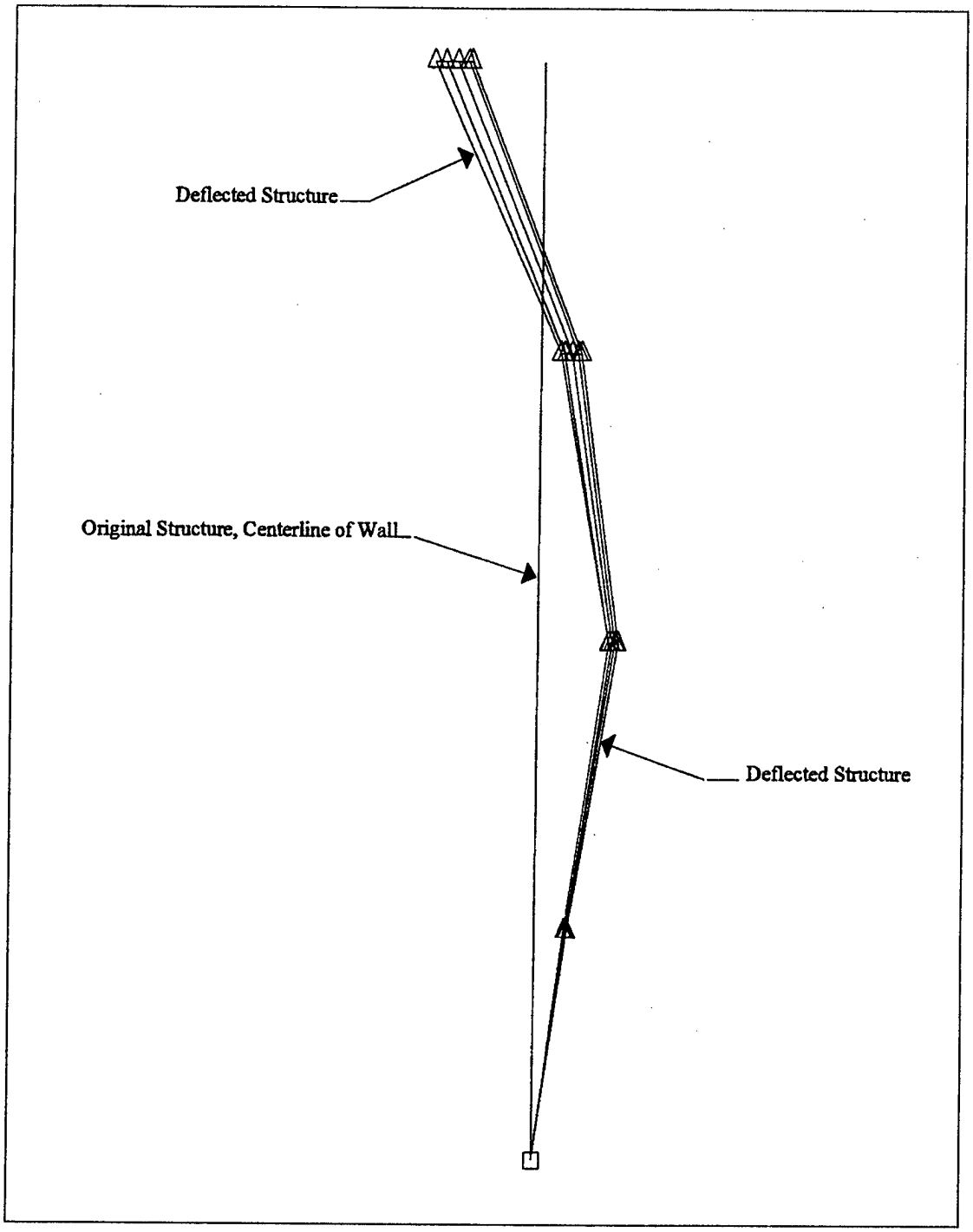

Figure C14. GT STRUDL Model 1, third mode of vibration, 122.8 Hz, out-of-plane (Z direction).

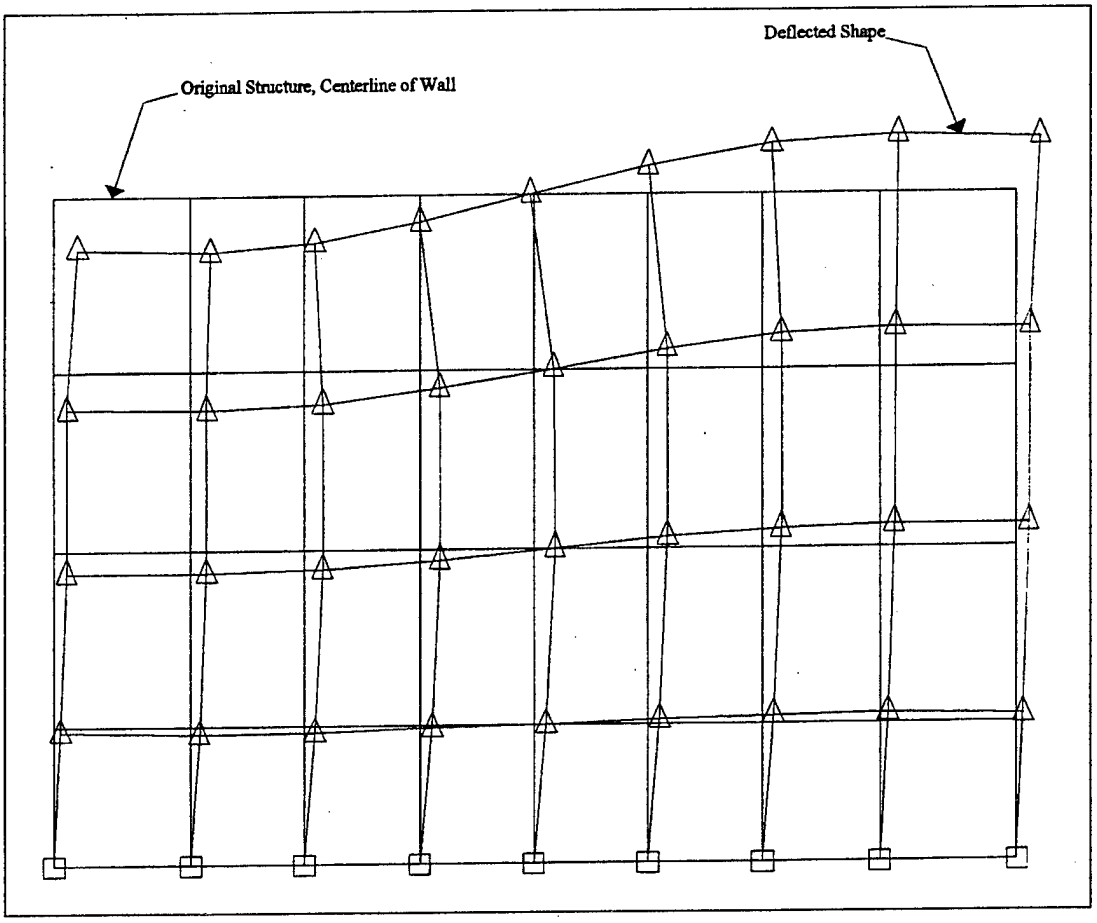

Figure C15. GT STRUDL Model 2, second mode of vibration, 190.2 Hz, in-plane (X direction).

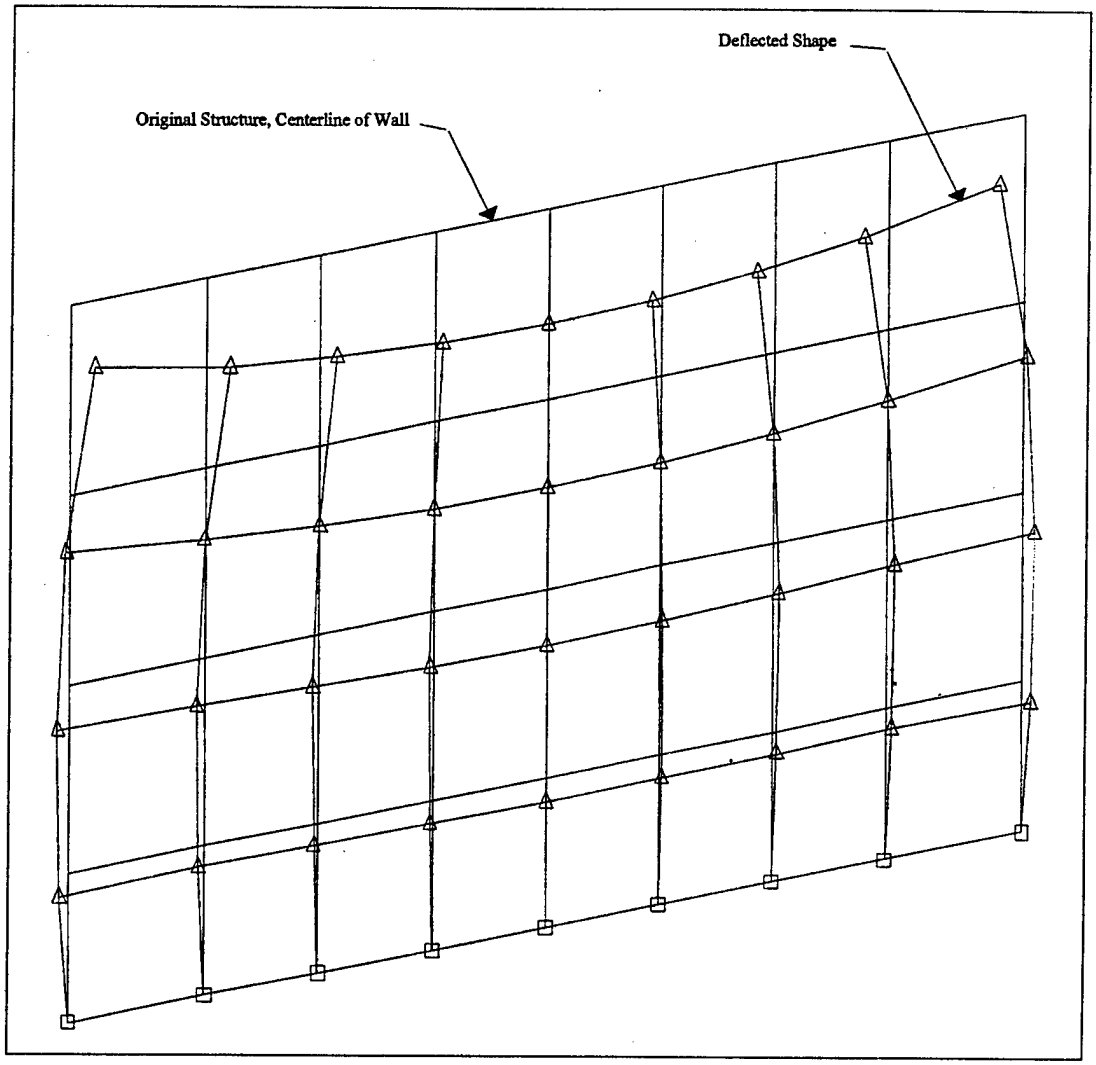

Figure C16. GT STRUDL Model 2, second mode of vibration, 158.0 Hz, vertical (Y direction).

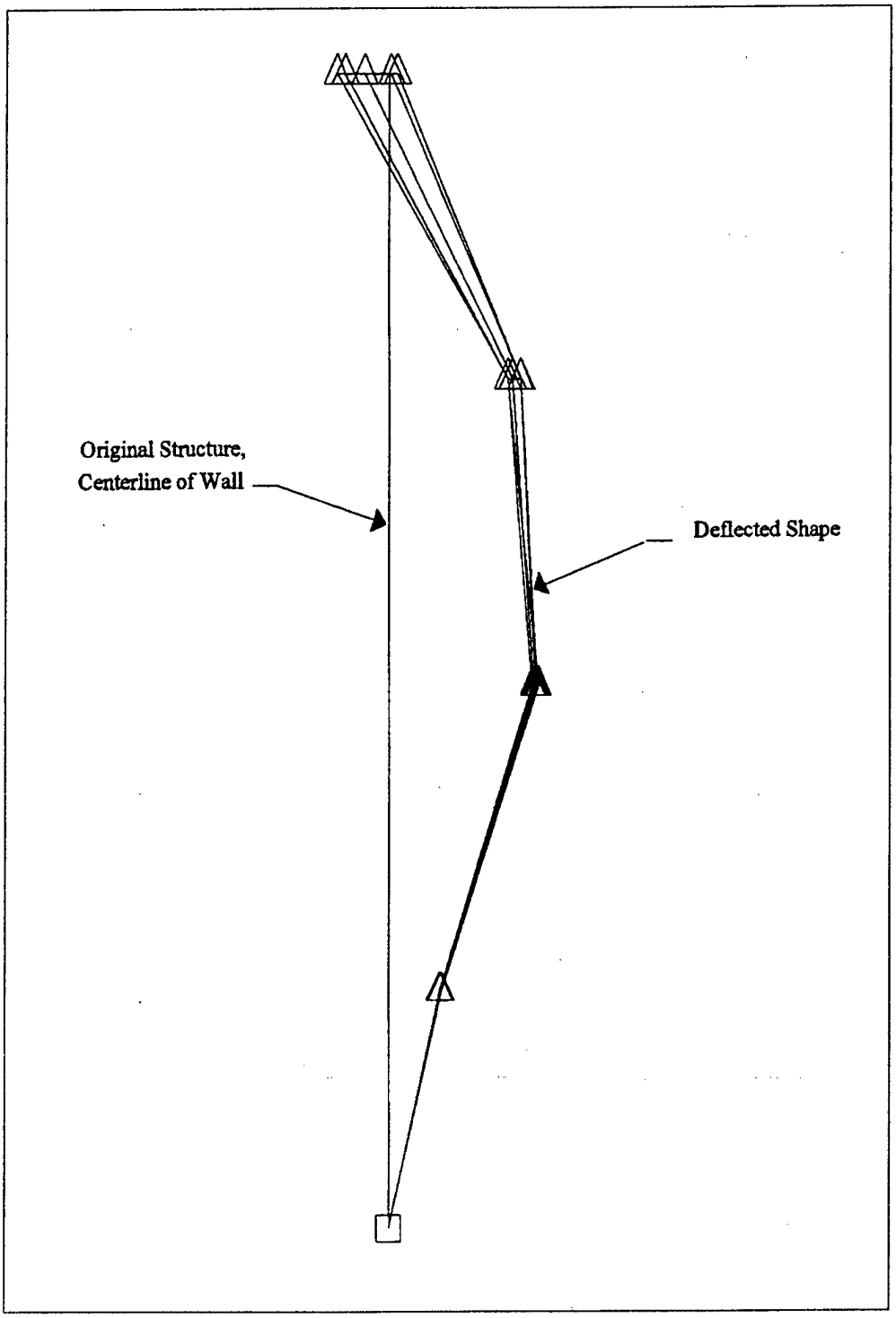

Figure C17. GT STRUDL Model 2, fourth mode of vibration, 97.1 Hz, out-of-plane (Z direction).

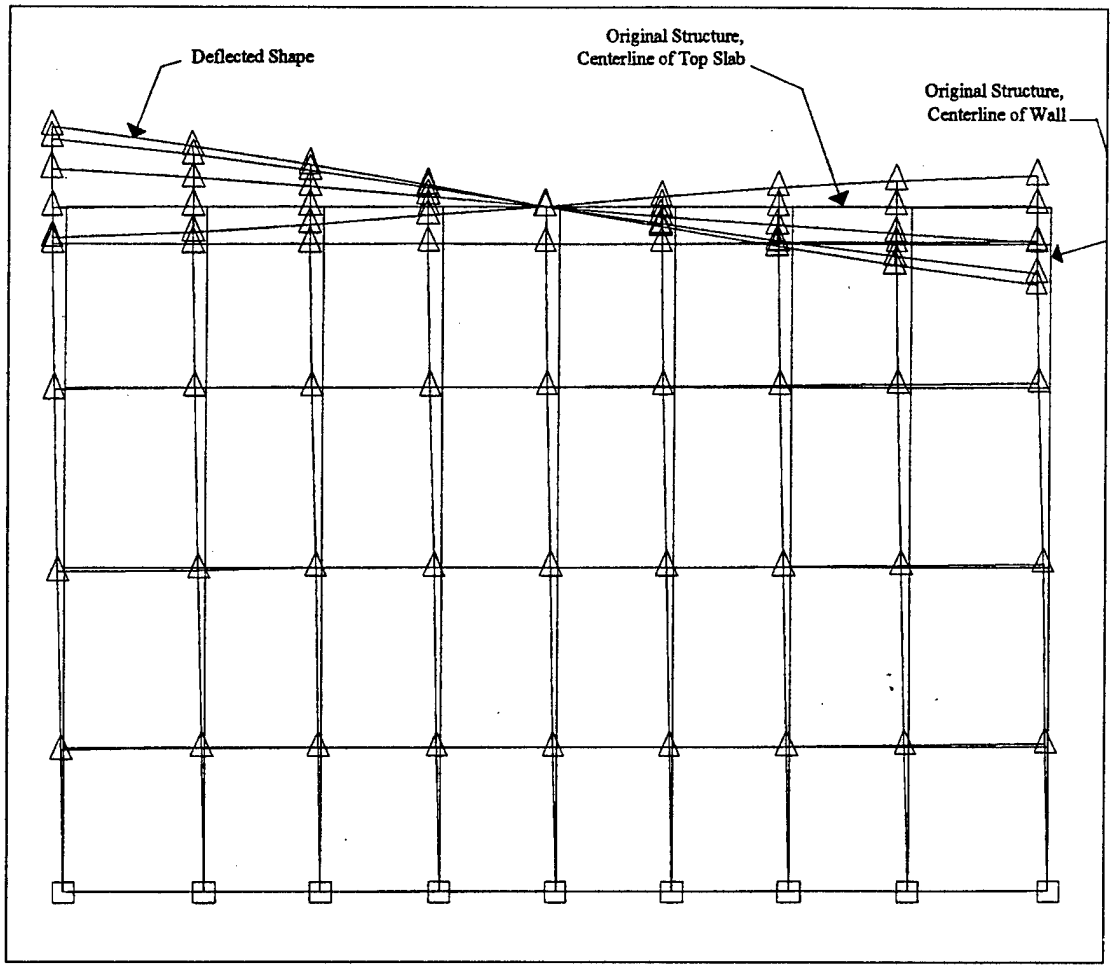

Figure C18. GT STRUDL Model 3, second mode of vibration, 89.0 Hz, in-plane (X direction).

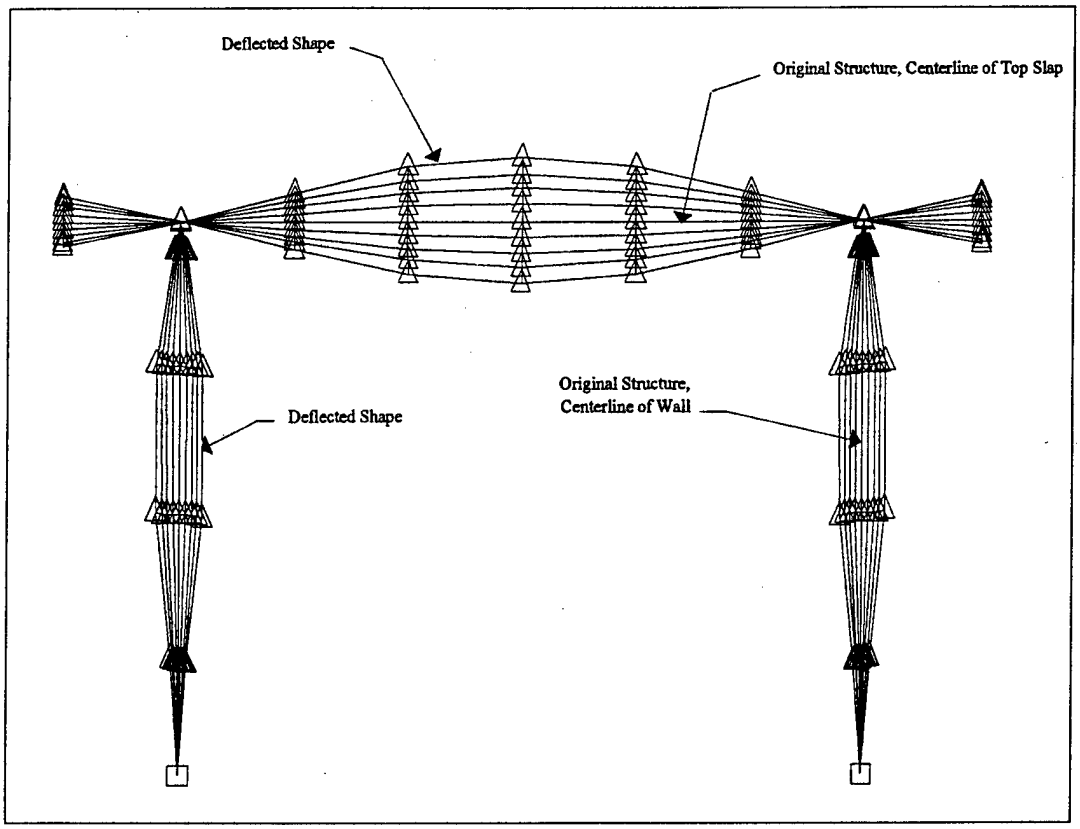

Figure C19. GT STRUDL Model 3, second mode of vibration, 89.0 Hz, in-plane (X direction).

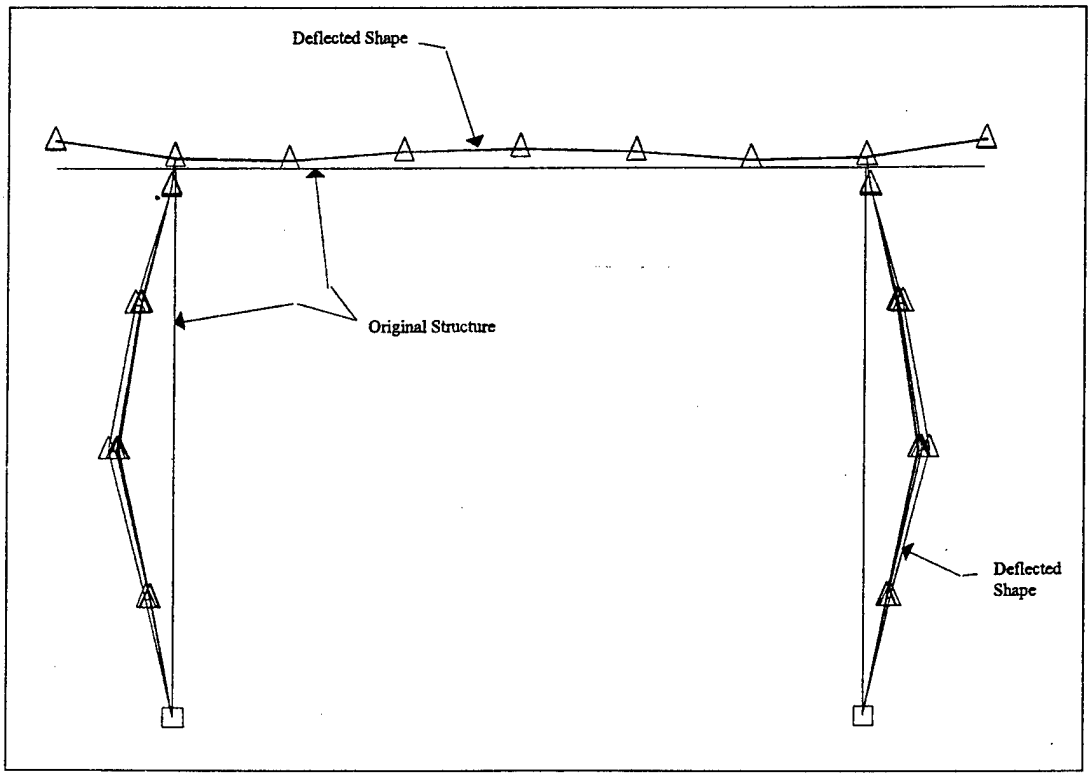

Figure C20. GT STRUDL Model 3, second mode of vibration, 138.8 Hz, vertical (Y direction).

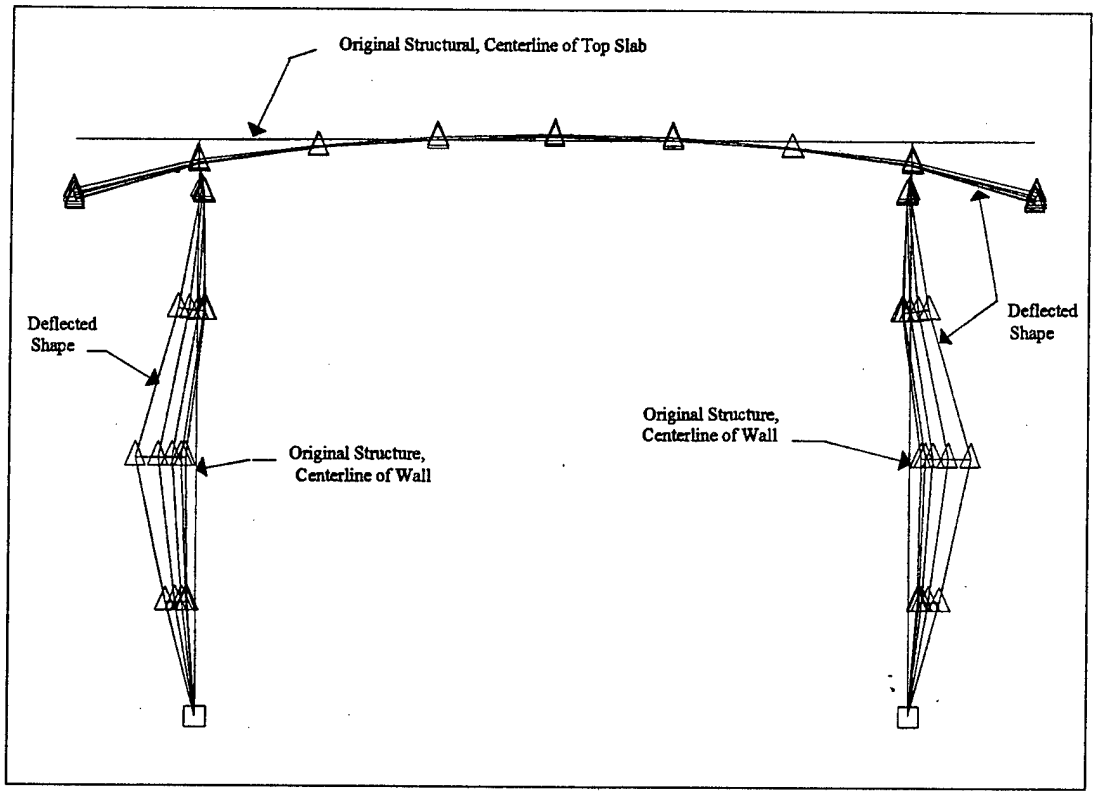

Figure C21. GT STRUDL Model 3, third mode of vibration, 191.6 Hz, vertical (Y direction).

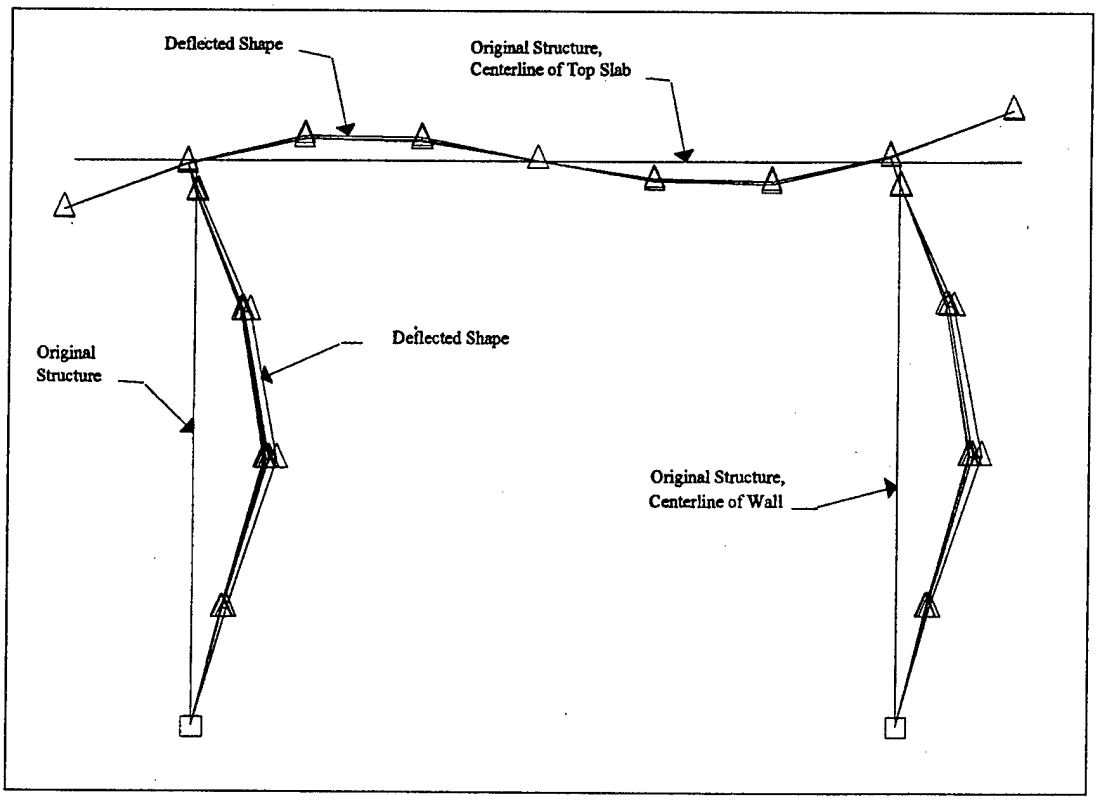

Figure C22. GT STRUDL Model 3, second mode of vibration, 126.3 Hz, out-of-plane (Z direction).

Appendix D: Test Data

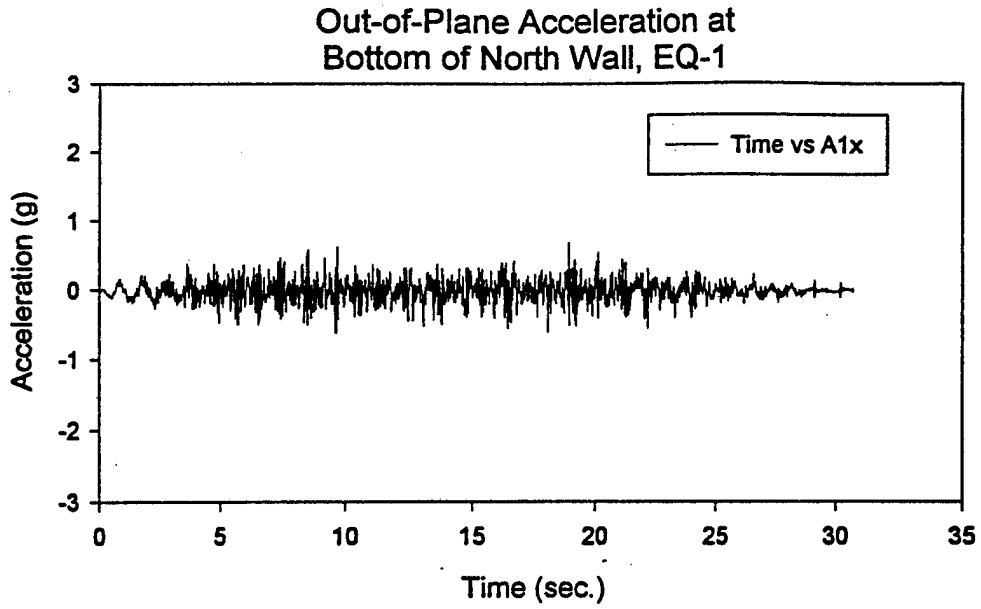
Out-of-Plane Acceleration at
Bottom of North Wall, EQ-1
Time vs A1x
Acceleration (g)
3
2
1
0
-1
-2
-3
0
5
10
15
20
25
30
35
Time (sec.)

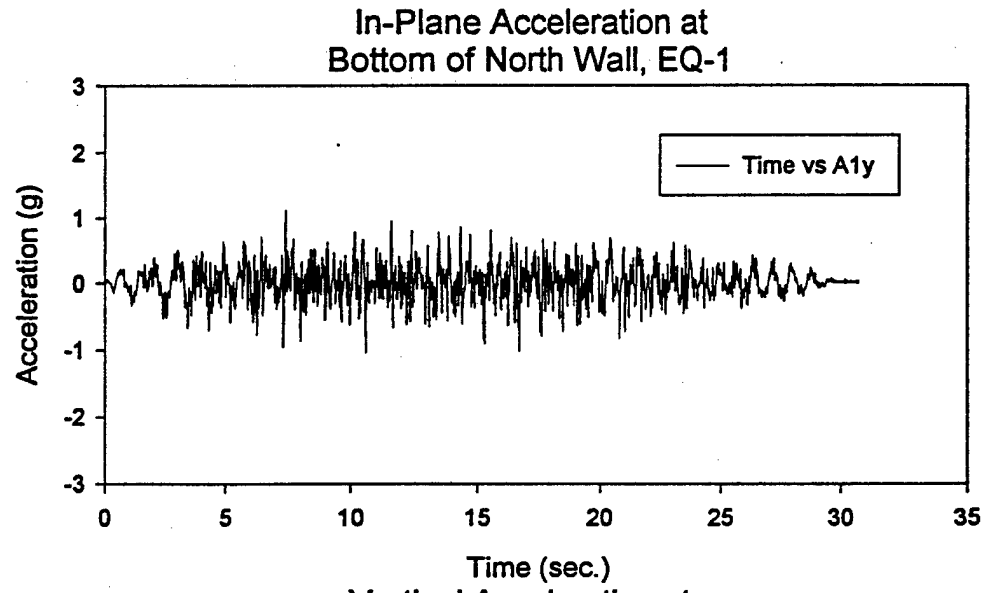
In-Plane Acceleration at
Bottom of North Wall, EQ-1
Time vs A1y
Acceleration (g)
3
2
1
0
-1
-2
-3
0
5
10
15
20
25
30
35
Time (sec.)

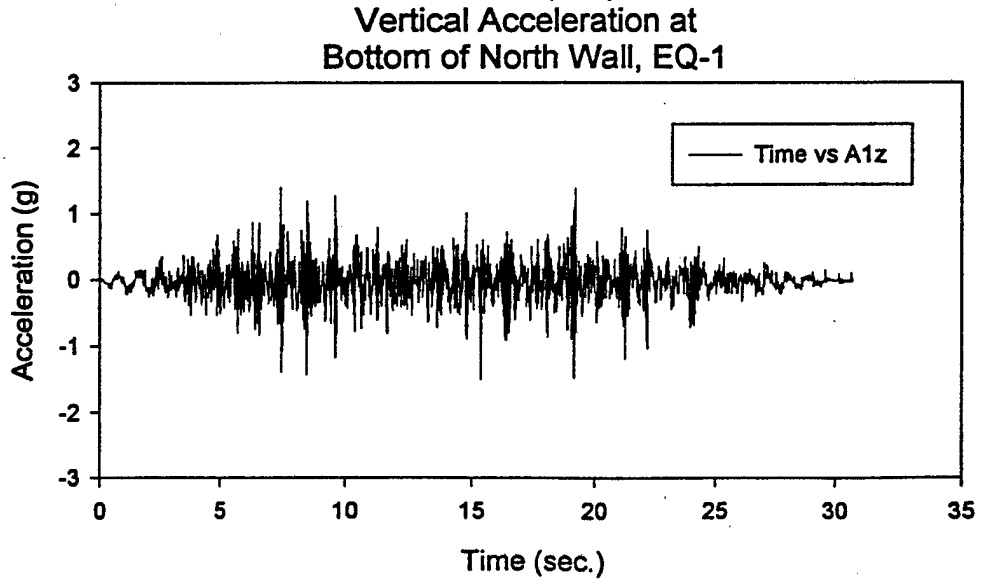
Vertical Acceleration at
Bottom of North Wall, EQ-1
Time vs A1z
Acceleration (g)
3
2
1
0
-1
-2
-3
0
5
10
15
20
25
30
35
Time (sec.)

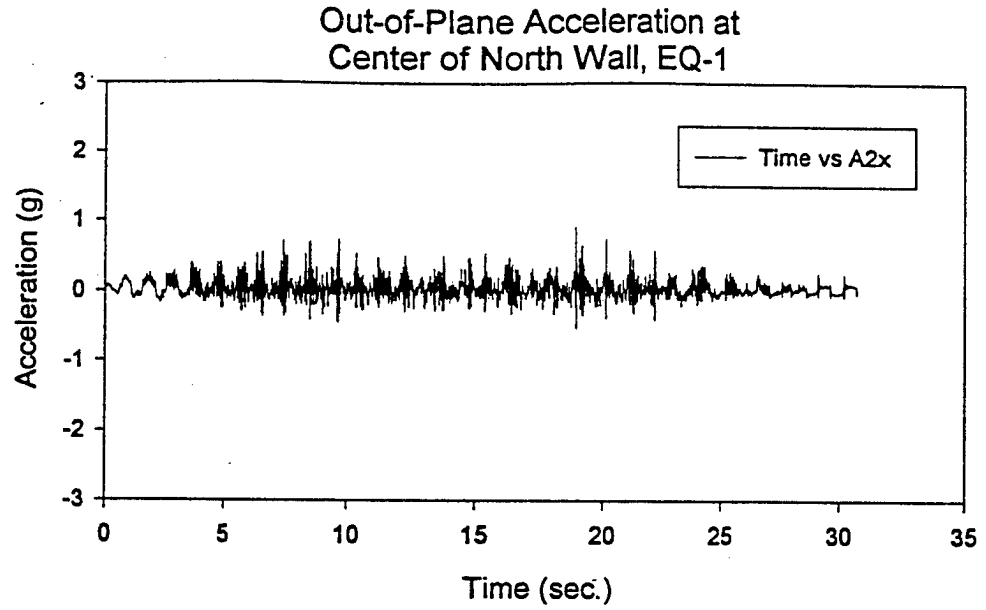
Out-of-Plane Acceleration at
Center of North Wall, EQ-1
Time vs A2x
Acceleration (g)
3
2
1
0
-1
-2
-3
0
5
10
15
20
25
30
35
Time (sec.)

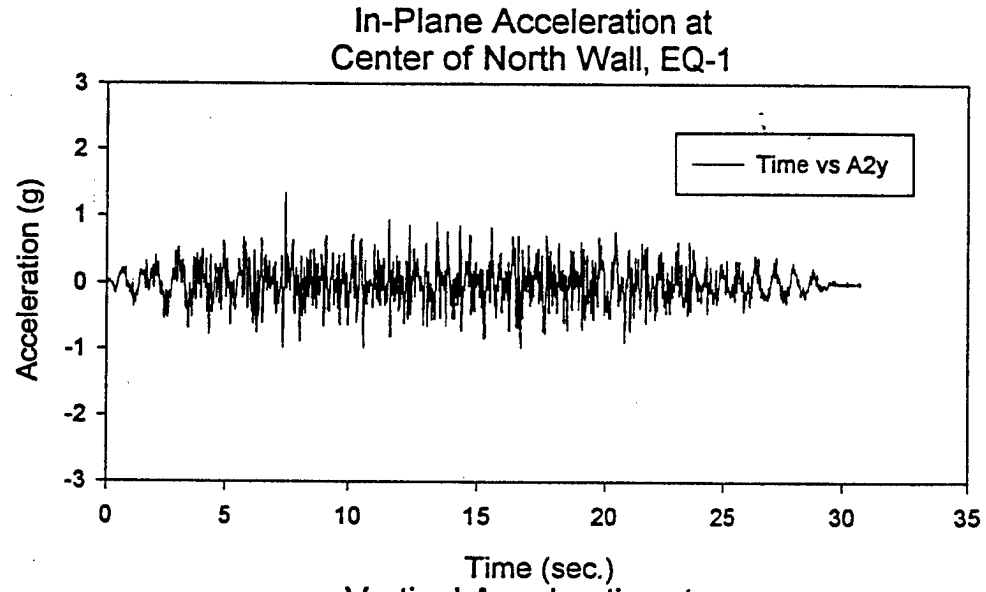
In-Plane Acceleration at
Center of North Wall, EQ-1
Time vs A2y
Acceleration (g)
3
2
1
0
-1
-2
-3
0
5
10
15
20
25
30
35
Time (sec.)

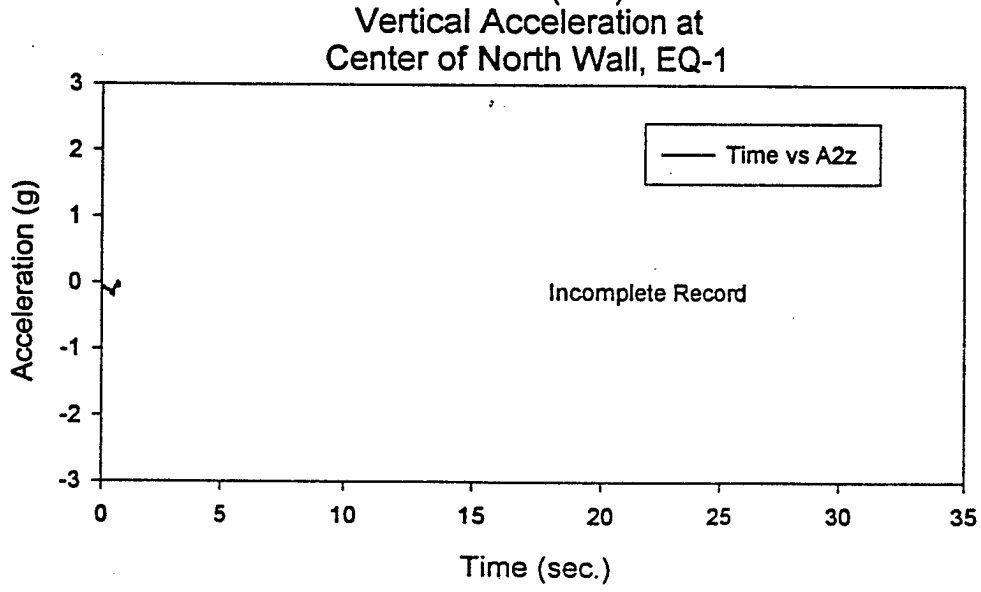
Vertical Acceleration at
Center of North Wall, EQ-1
Time vs A2z
Incomplete Record
Acceleration (g)
3
2
1
0
-1
-2
-3
0
5
10
15
20
25
30
35
Time (sec.)

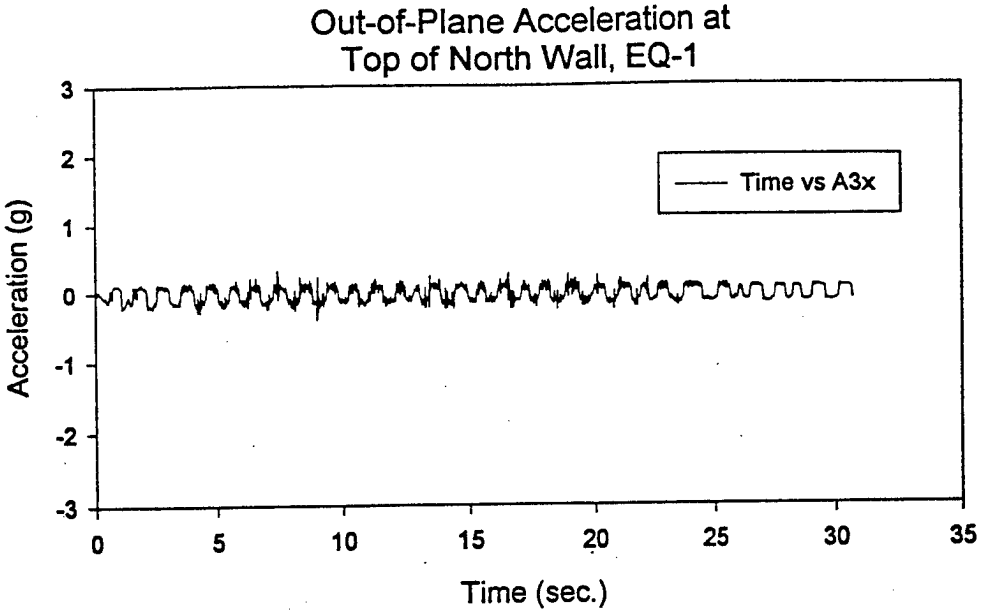
Out-of-Plane Acceleration at
Top of North Wall, EQ-1
Time vs A3x
Acceleration (g)
Time (sec.)

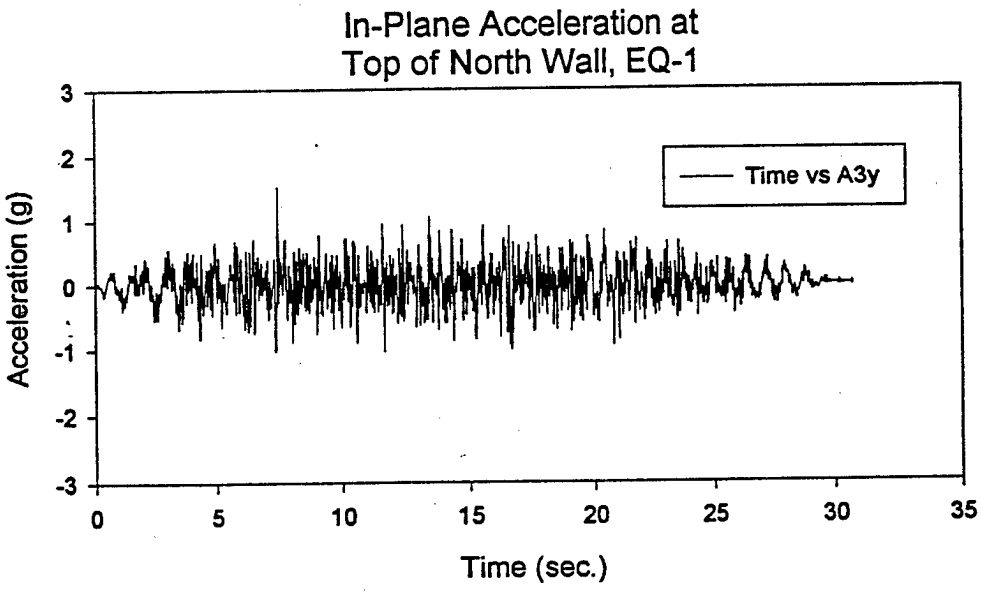
In-Plane Acceleration at
Top of North Wall, EQ-1
Time vs A3y
Acceleration (g)
Time (sec.)

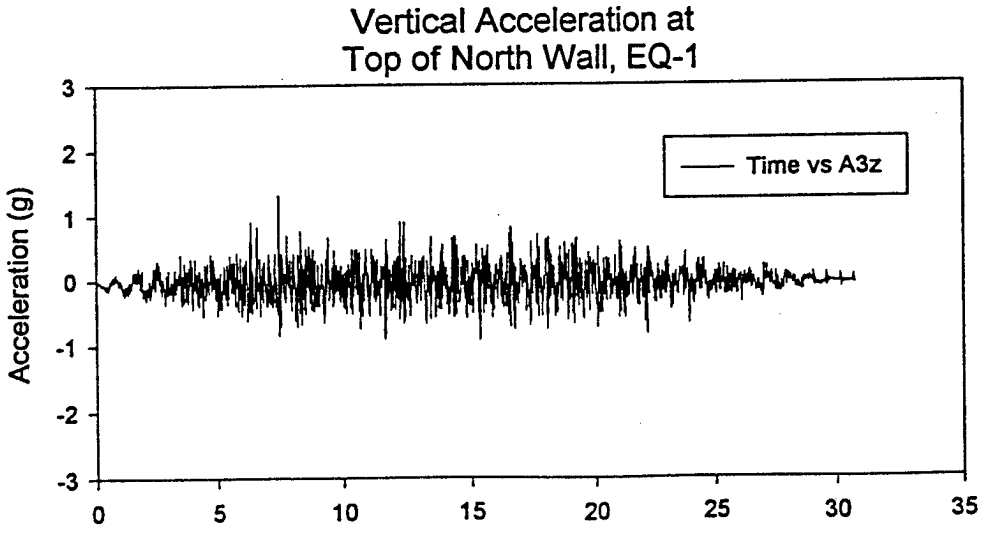
Vertical Acceleration at
Top of North Wall, EQ-1
Time vs A3z
Acceleration (g)

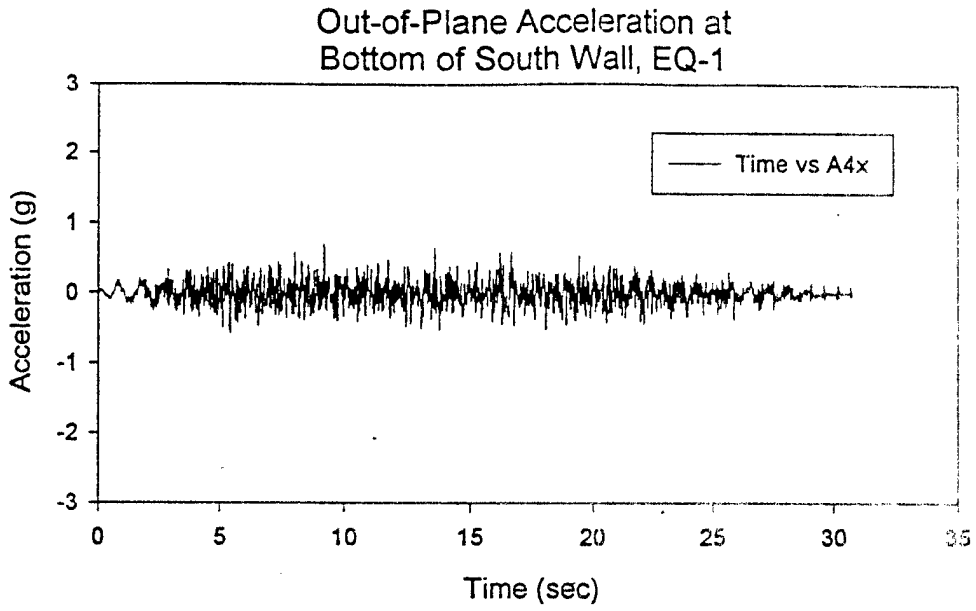
Out-of-Plane Acceleration at
Bottom of South Wall, EQ-1
Time vs A4x
Acceleration (g)
Time (sec)

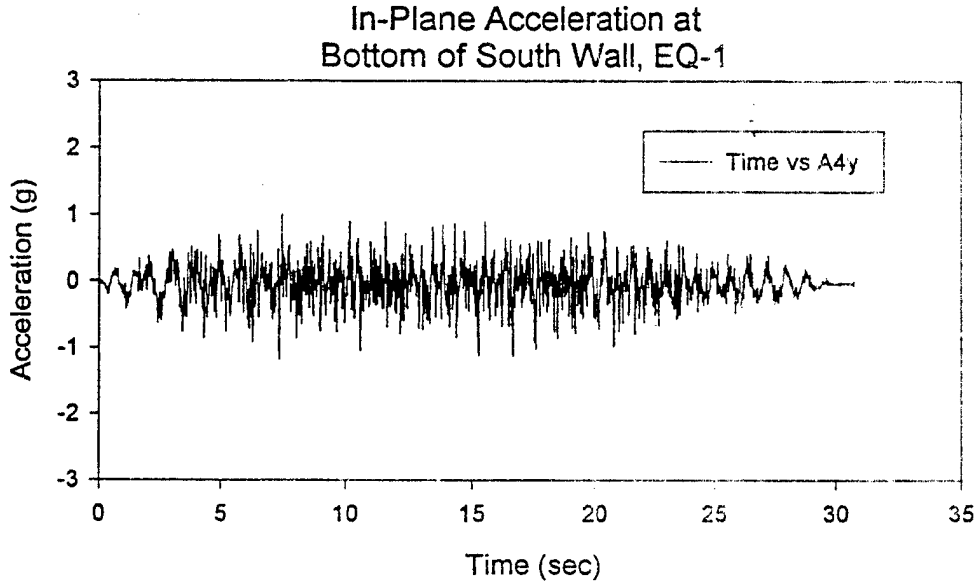
In-Plane Acceleration at
Bottom of South Wall, EQ-1
Time vs A4y
Acceleration (g)
Time (sec)

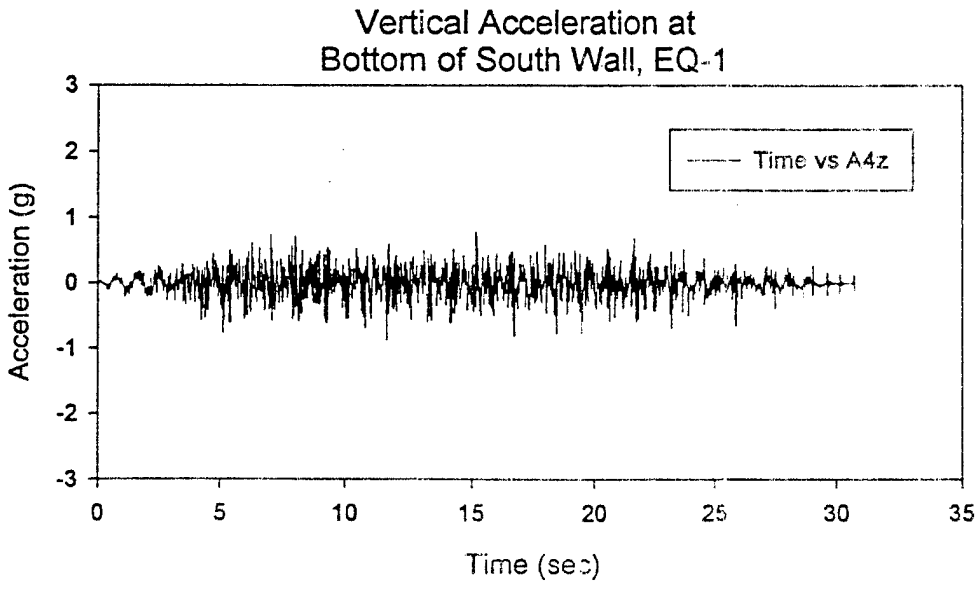
Vertical Acceleration at
Bottom of South Wall, EQ-1
Time vs A4z
Acceleration (g)
Time (sec)

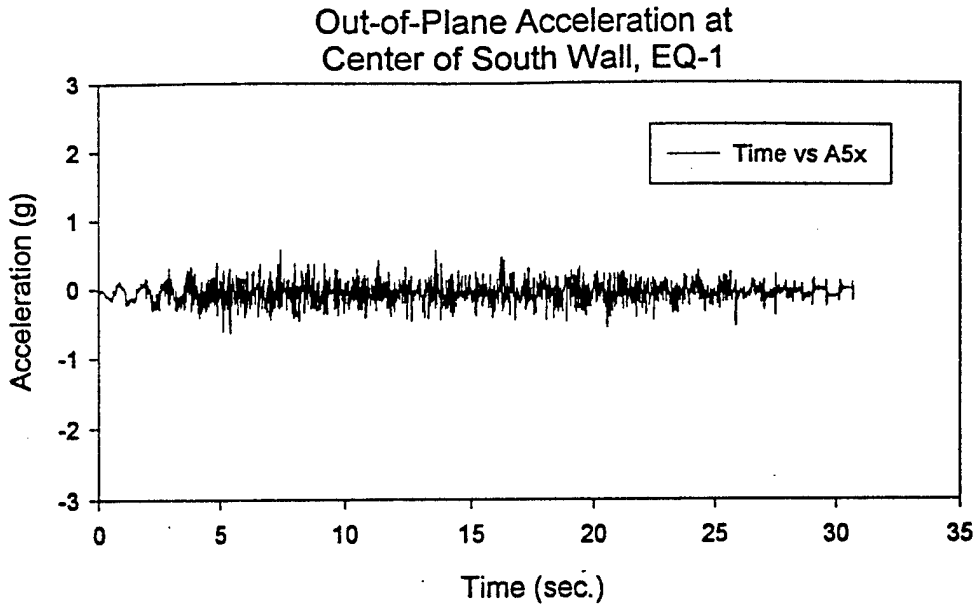
Out-of-Plane Acceleration at
Center of South Wall, EQ-1
Time vs A5x
Acceleration (g)
Time (sec.)

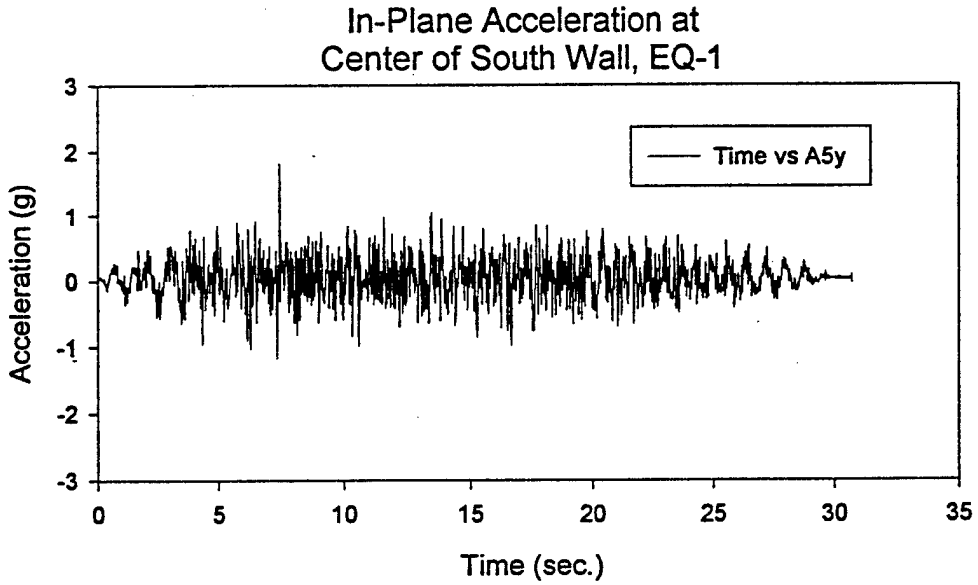
In-Plane Acceleration at
Center of South Wall, EQ-1
Time vs A5y
Acceleration (g)
Time (sec.)

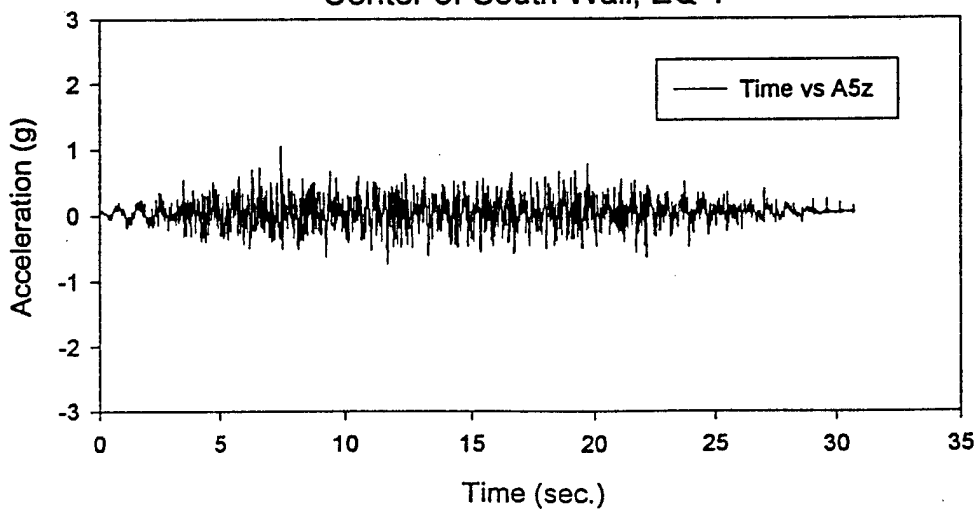
Vertical Acceleration at
Center of South Wall, EQ-1
Time vs A5z
Acceleration (g)
Time (sec.)

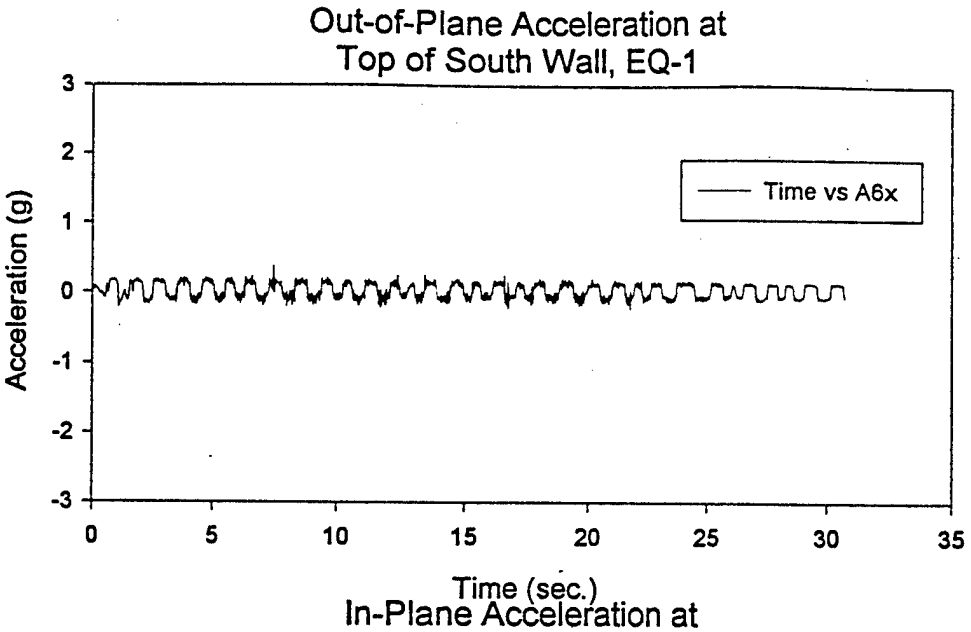
Out-of-Plane Acceleration at
Top of South Wall, EQ-1
Time vs A6x
Acceleration (g)
Time (sec.)

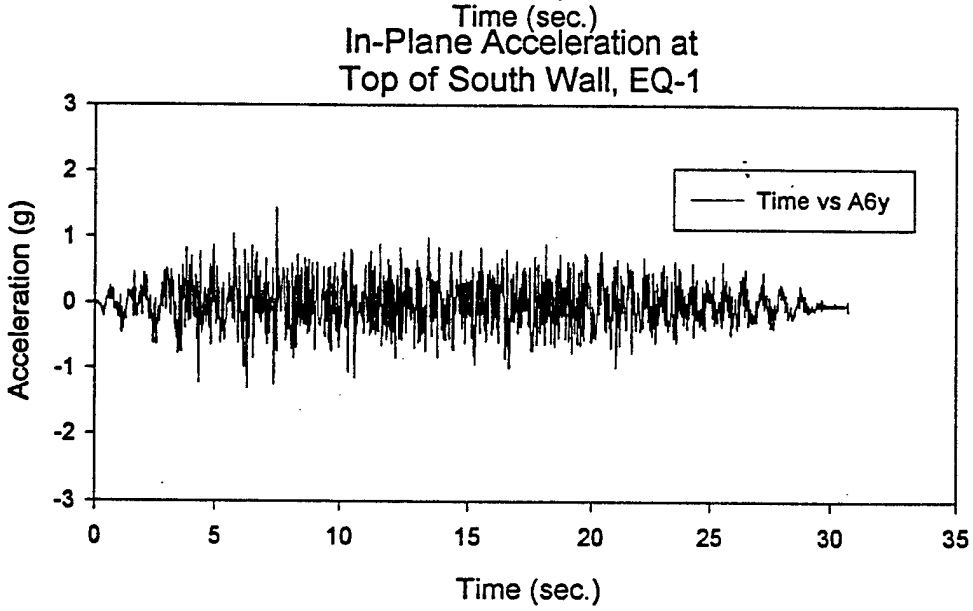
In-Plane Acceleration at
Top of South Wall, EQ-1
Time vs A6y
Acceleration (g)
Time (sec.)

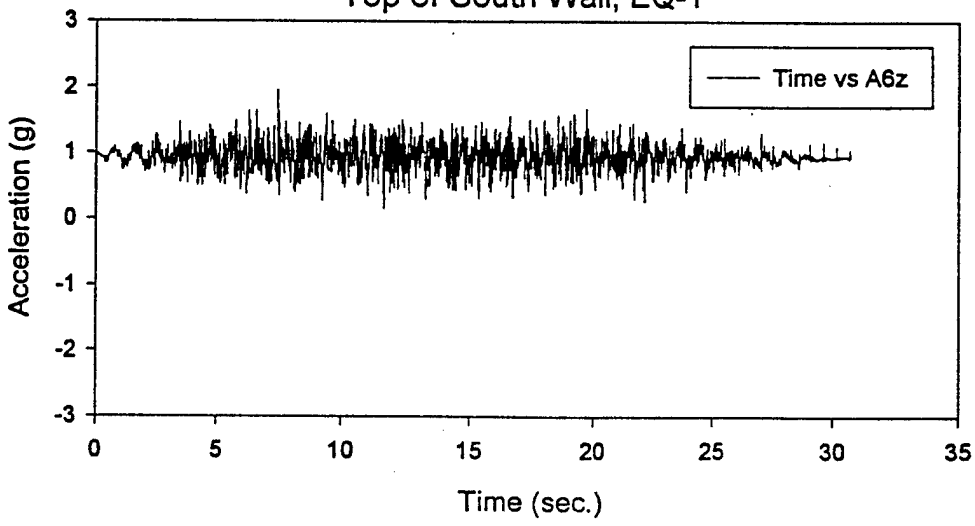
Vertical Acceleration at
Top of South Wall, EQ-1
Time vs A6z
Acceleration (g)
Time (sec.)

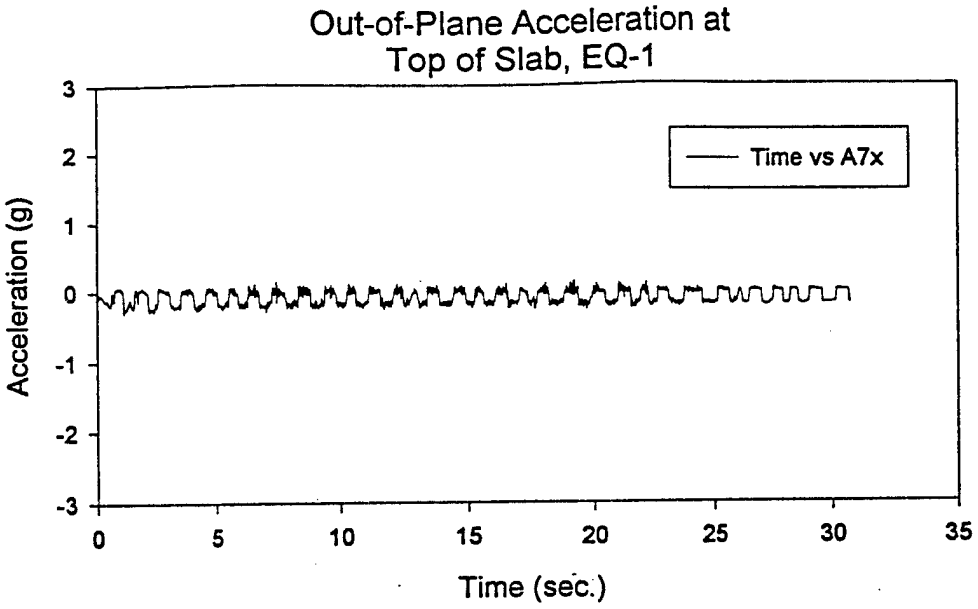
Out-of-Plane Acceleration at
Top of Slab, EQ-1
Time vs A7x
Acceleration (g)
3
2
1
0
-1
-2
-3
0
5
10
15
20
25
30
35
Time (sec.)

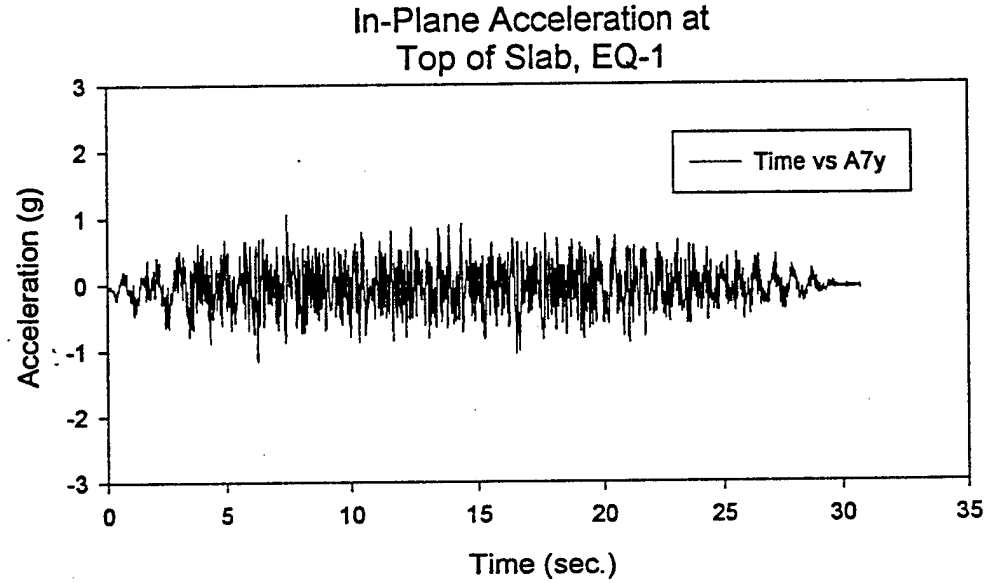
In-Plane Acceleration at
Top of Slab, EQ-1
Time vs A7y
Acceleration (g)
3
2
1
0
-1
-2
-3
0
5
10
15
20
25
30
35
Time (sec.)

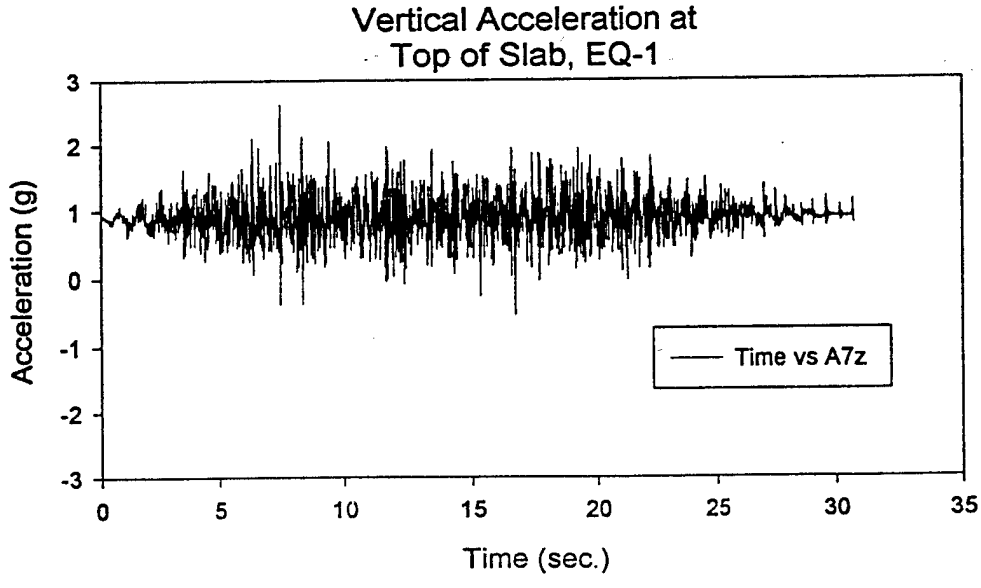
Vertical Acceleration at
Top of Slab, EQ-1
Time vs A7z
Acceleration (g)
3
2
1
0
-1
-2
-3
0
5
10
15
20
25
30
35
Time (sec.)

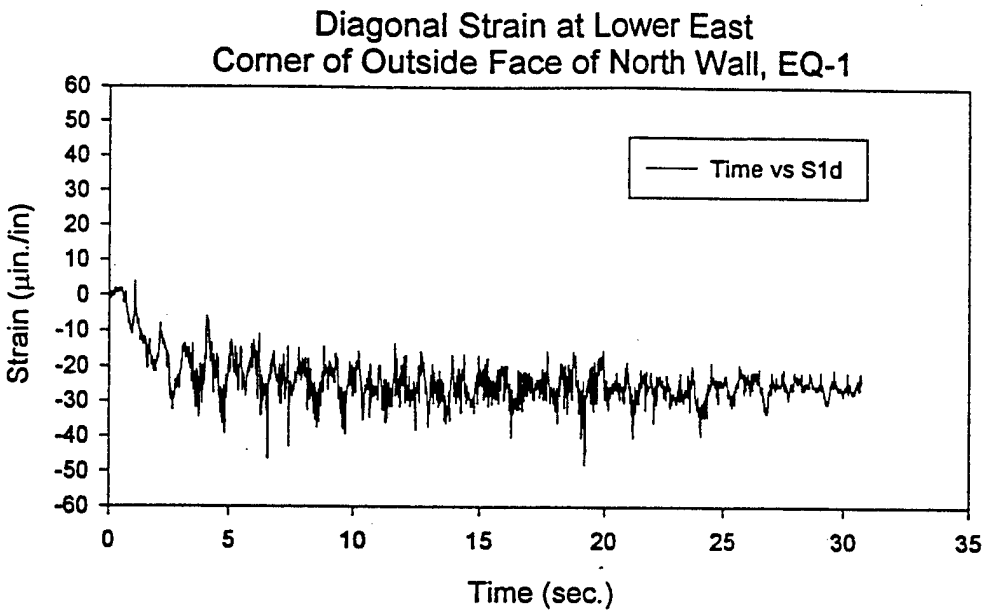
Diagonal Strain at Lower East
Corner of Outside Face of North Wall, EQ-1
Strain (µin./in)
60
50
40
30
20
10
0
-10
-20
-30
-40
-50
-60
0
5
10
15
20
25
30
35
Time (sec.)
Time vs S1d

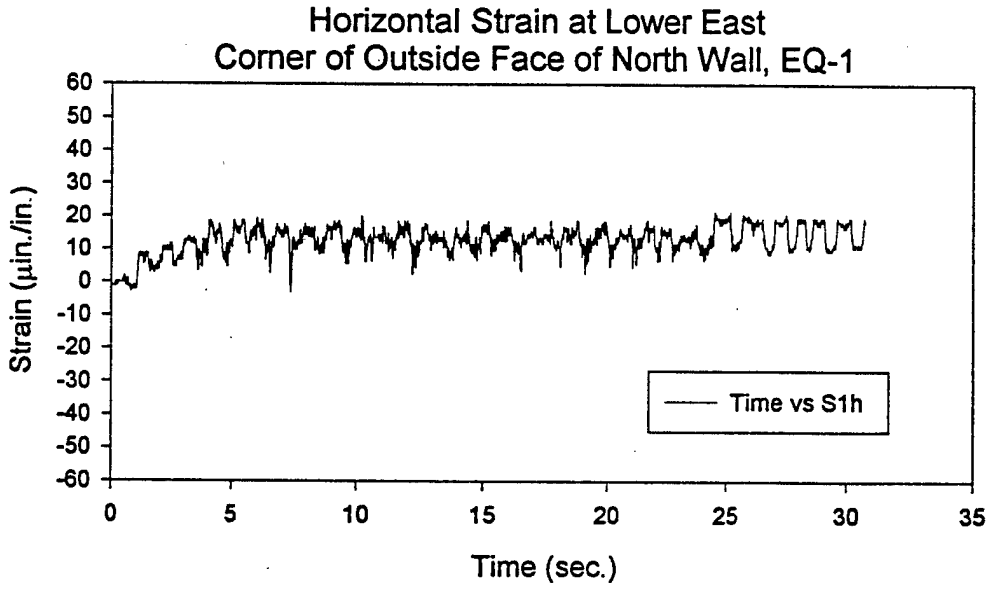
Horizontal Strain at Lower East
Corner of Outside Face of North Wall, EQ-1
Strain (µin./in.)
60
50
40
30
20
10
0
-10
-20
-30
-40
-50
-60
0
5
10
15
20
25
30
35
Time (sec.)
Time vs S1h

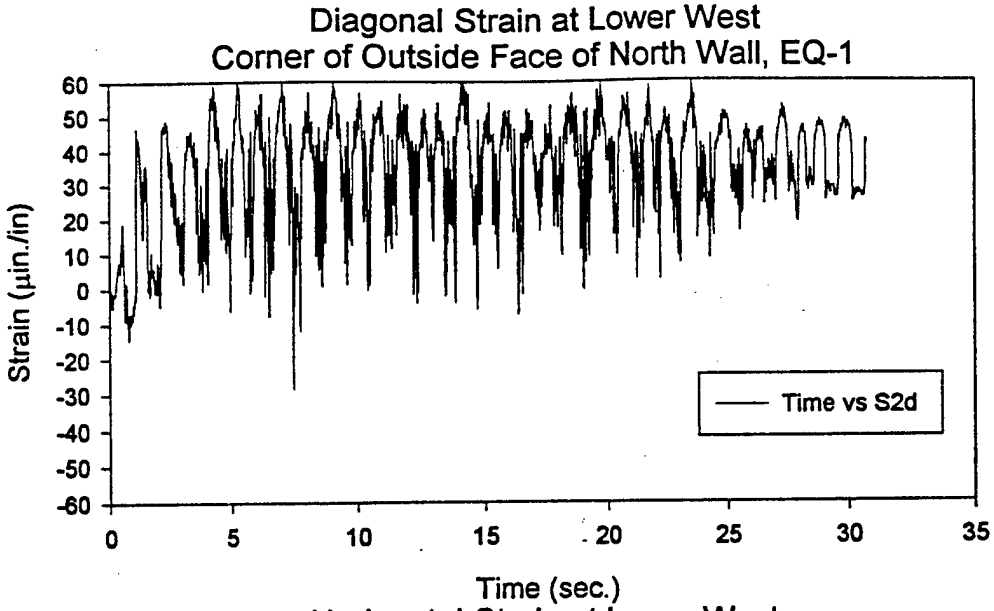
Diagonal Strain at Lower West
Corner of Outside Face of North Wall, EQ-1
Strain (µin./in)
60
50
40
30
20
10
0
-10
-20
-30
-40
-50
-60
0
5
10
15
20
25
30
35
Time (sec.)
Time vs S2d

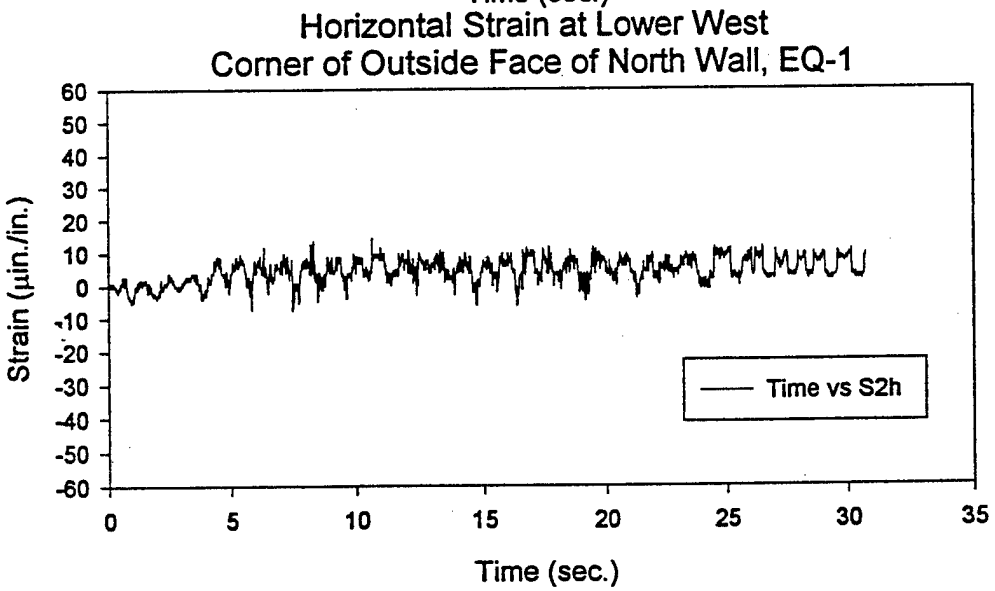
Horizontal Strain at Lower West
Corner of Outside Face of North Wall, EQ-1
Strain (µin./in.)
60
50
40
30
20
10
0
-10
-20
-30
-40
-50
-60
0
5
10
15
20
25
30
35
Time (sec.)
Time vs S2h

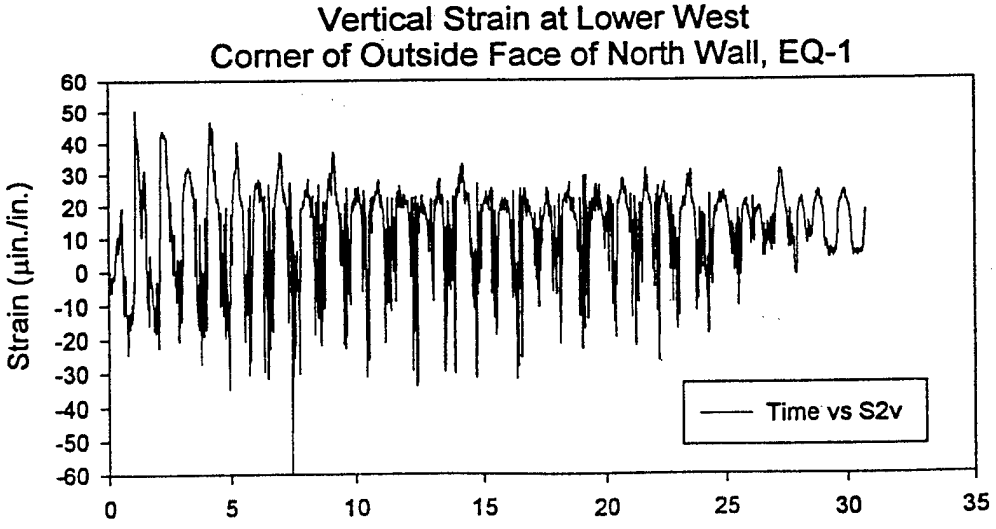
Vertical Strain at Lower West
Corner of Outside Face of North Wall, EQ-1
Strain (µin./in.)
60
50
40
30
20
10
0
-10
-20
-30
-40
-50
-60
0
5
10
15
20
25
30
35
Time vs S2v

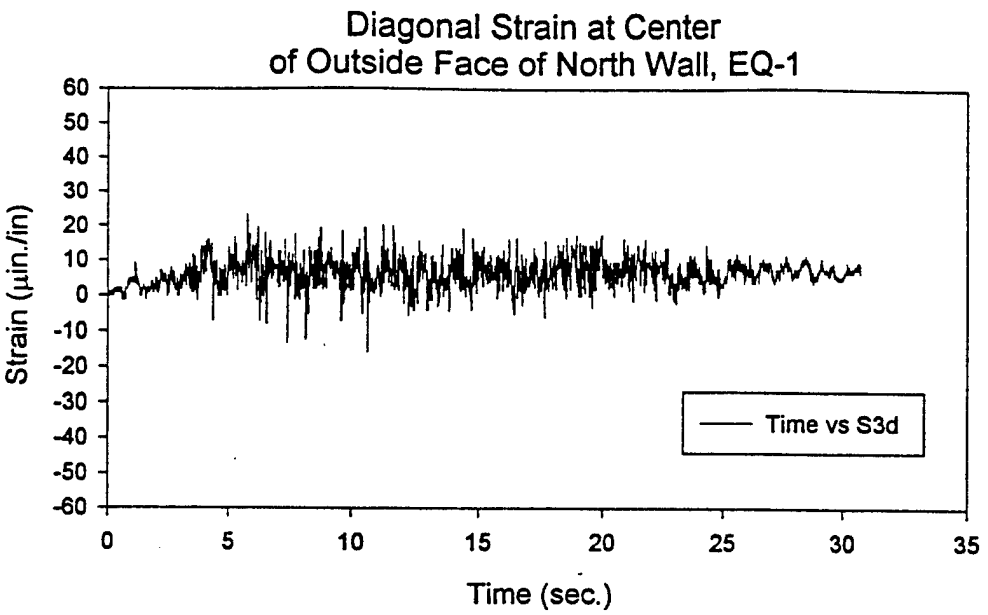
Diagonal Strain at Center
of Outside Face of North Wall, EQ-1
Strain (μin./in)
60
50
40
30
20
10
0
-10
-20
-30
-40
-50
-60
0
5
10
15
20
25
30
35
Time (sec.)
Time vs S3d

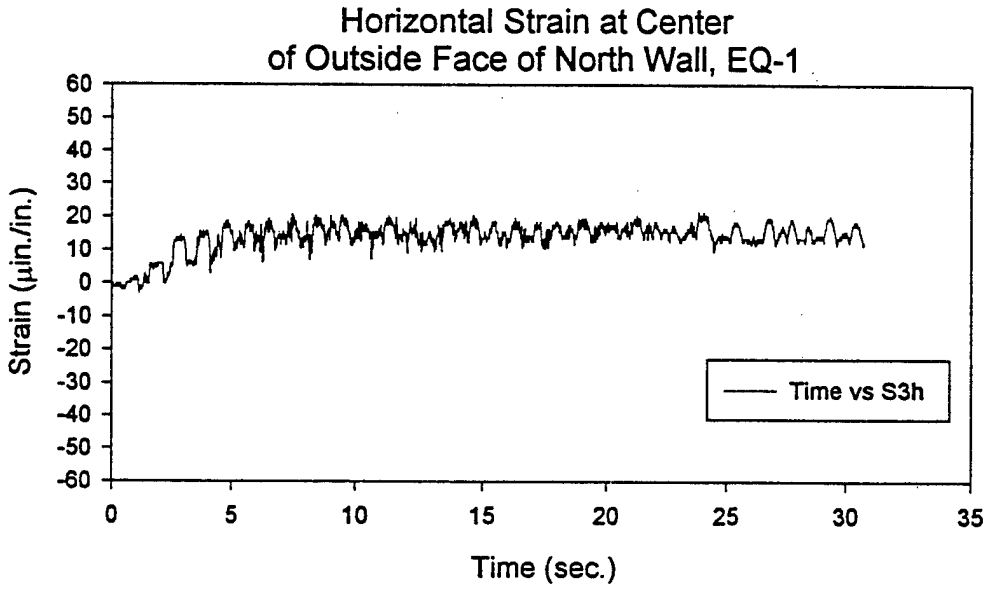
Horizontal Strain at Center
of Outside Face of North Wall, EQ-1
Strain (μin./in.)
60
50
40
30
20
10
0
-10
-20
-30
-40
-50
-60
0
5
10
15
20
25
30
35
Time (sec.)
Time vs S3h

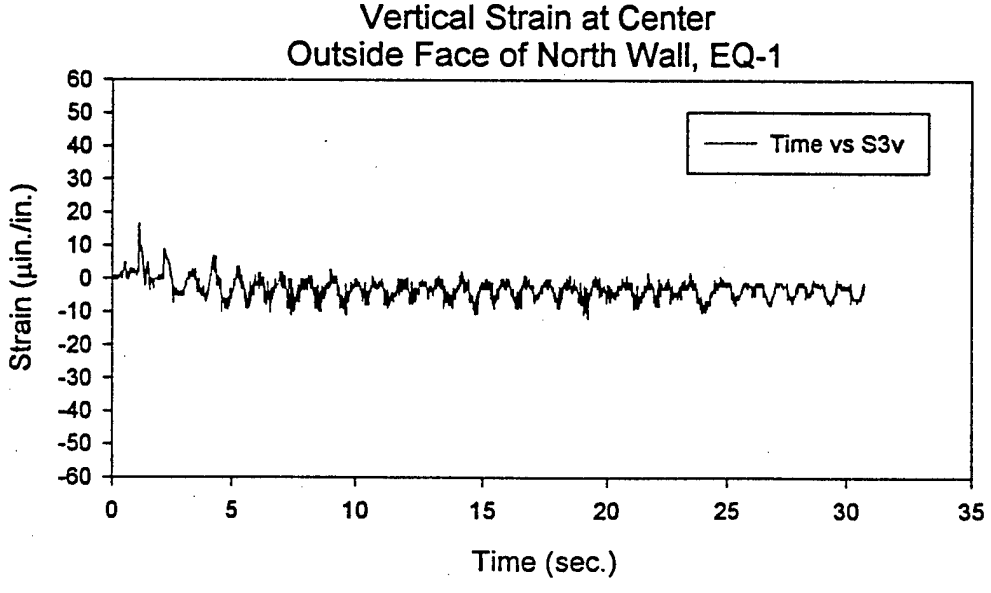
Vertical Strain at Center
Outside Face of North Wall, EQ-1
Strain (μin./in.)
60
50
40
30
20
10
0
-10
-20
-30
-40
-50
-60
0
5
10
15
20
25
30
35
Time (sec.)
Time vs S3v

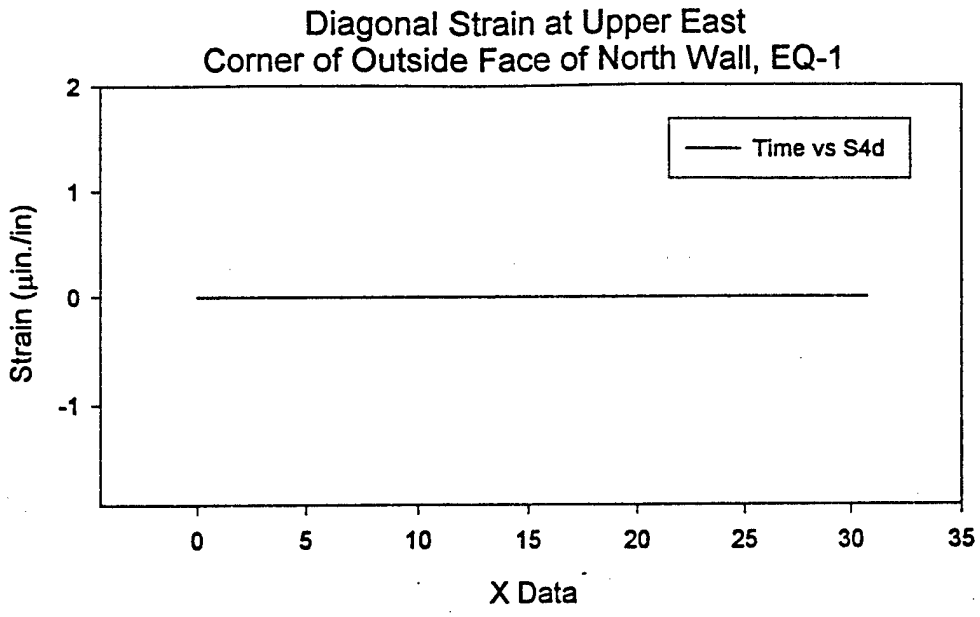
Diagonal Strain at Upper East
Corner of Outside Face of North Wall, EQ-1
Time vs S4d
Strain (µin./in)
X Data

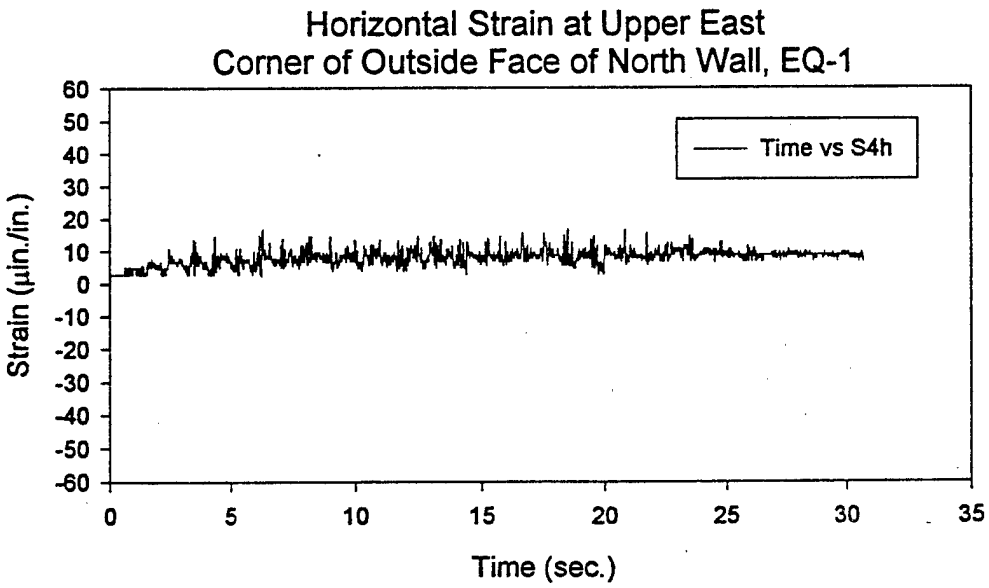
Horizontal Strain at Upper East
Corner of Outside Face of North Wall, EQ-1
Time vs S4h
Strain (µin./in.)
Time (sec.)

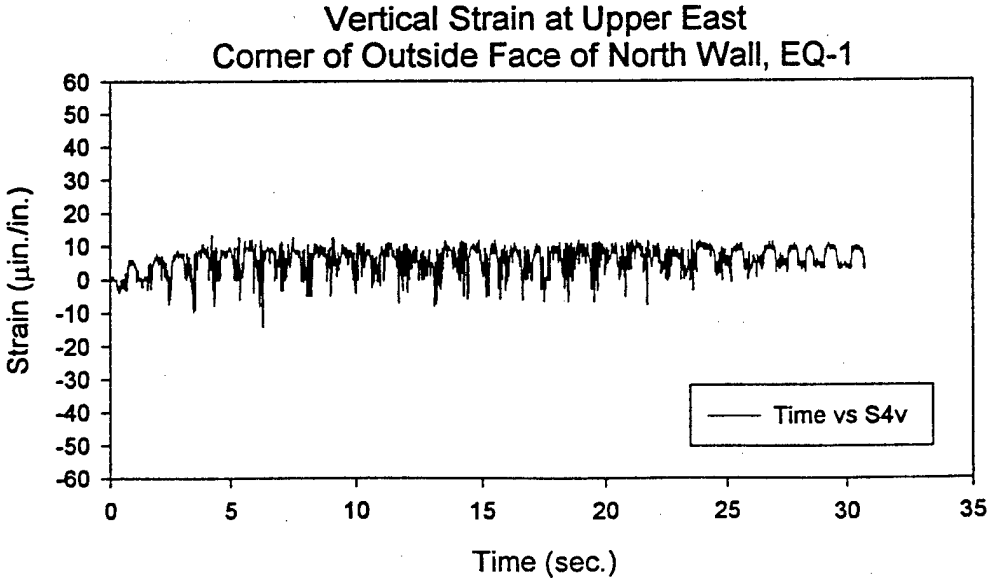
Vertical Strain at Upper East
Corner of Outside Face of North Wall, EQ-1
Time vs S4v
Strain (µin./in.)
Time (sec.)

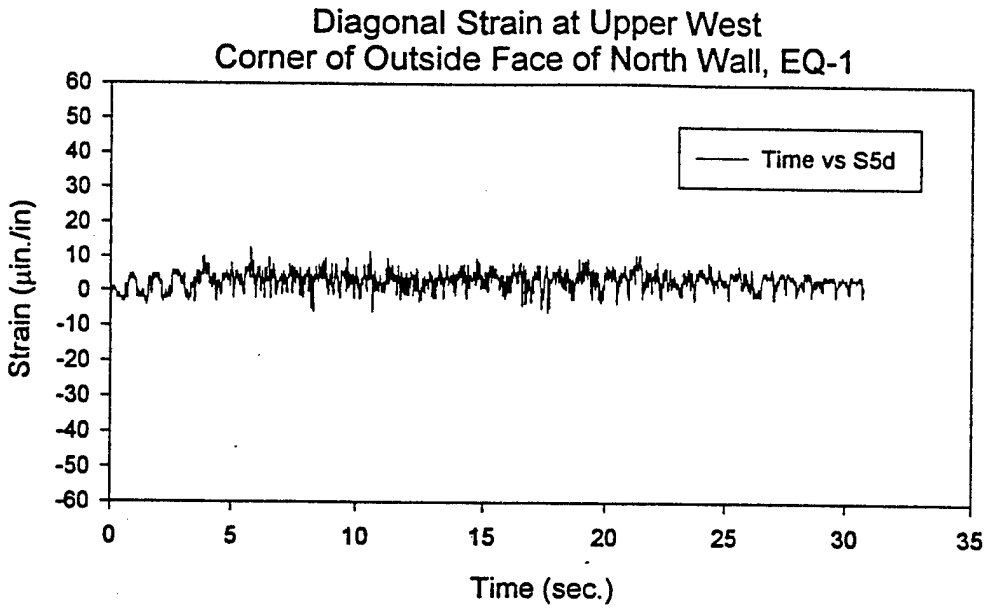
Diagonal Strain at Upper West
Corner of Outside Face of North Wall, EQ-1
Time vs S5d
Strain (µin./in)
Time (sec.)

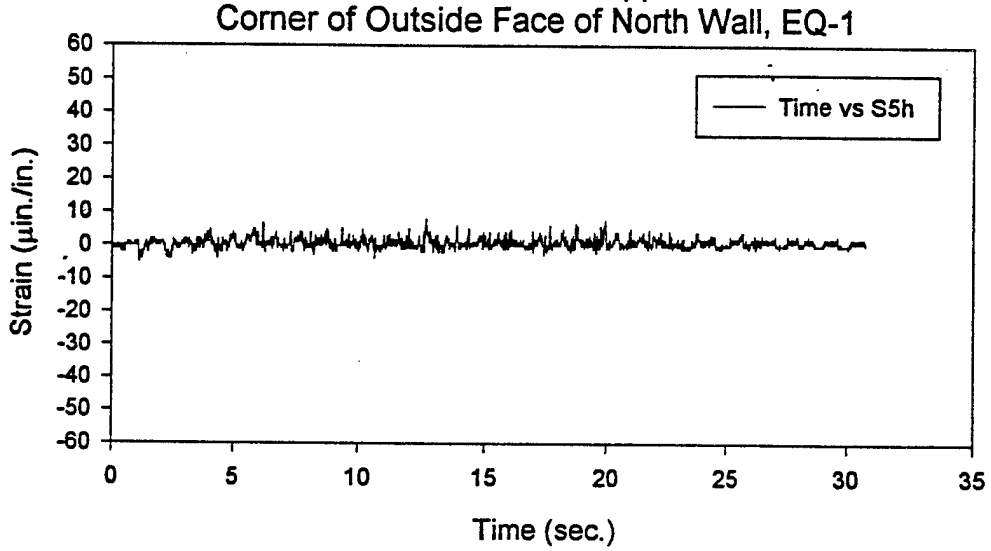
Horizontal Strain at Upper West
Corner of Outside Face of North Wall, EQ-1
Time vs S5h
Strain (µin./in.)
Time (sec.)

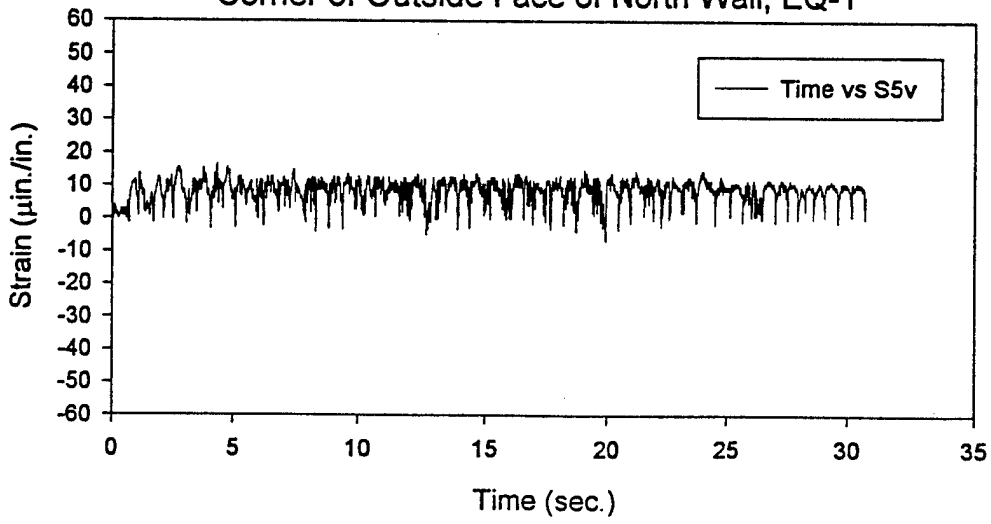
Vertical Strain at Upper West
Corner of Outside Face of North Wall, EQ-1
Time vs S5v
Strain (µin./in.)
Time (sec.)

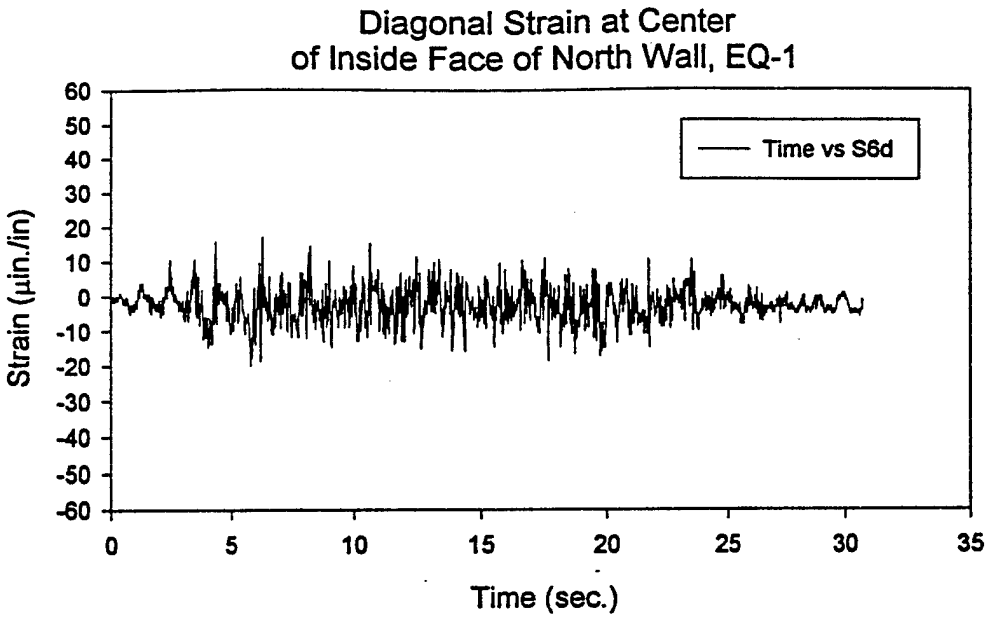
Diagonal Strain at Center
of Inside Face of North Wall, EQ-1
Time vs S6d
Strain (µin./in)
60
50
40
30
20
10
0
-10
-20
-30
-40
-50
-60
0
5
10
15
20
25
30
35
Time (sec.)

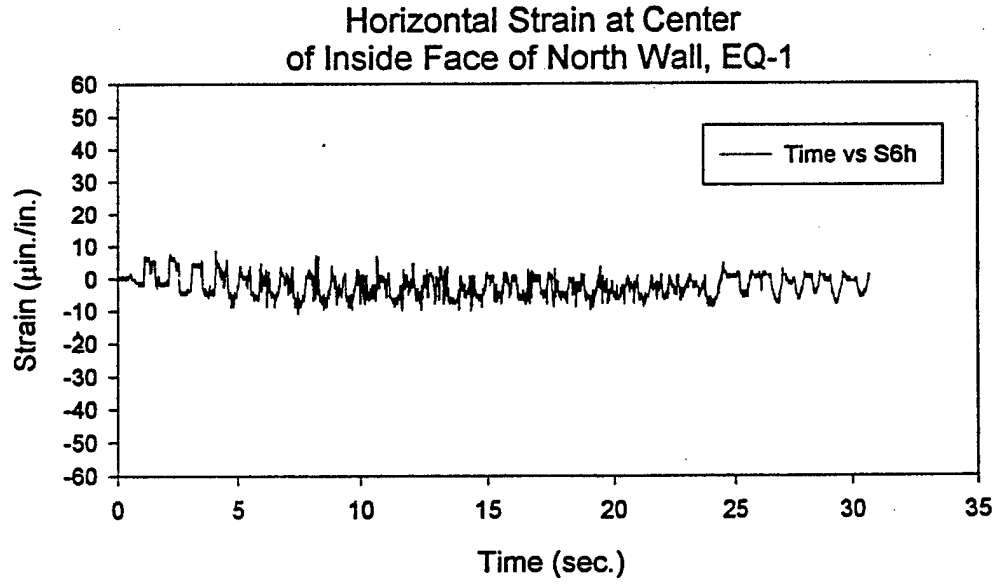
Horizontal Strain at Center
of Inside Face of North Wall, EQ-1
Time vs S6h
Strain (µin./in.)
60
50
40
30
20
10
0
-10
-20
-30
-40
-50
-60
0
5
10
15
20
25
30
35
Time (sec.)

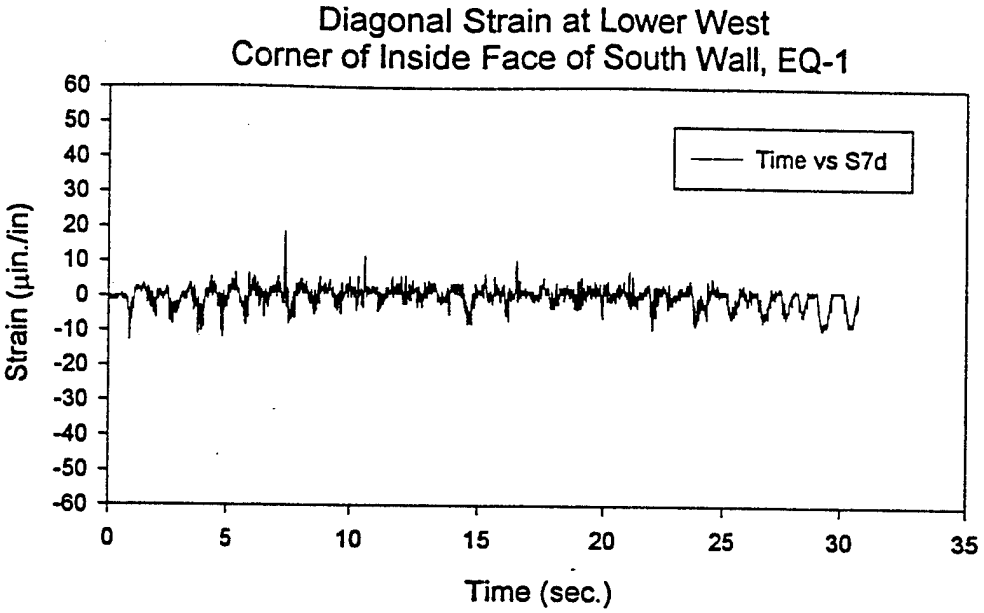
Diagonal Strain at Lower West
Corner of Inside Face of South Wall, EQ-1
Strain (µin./in)
Time vs S7d
Time (sec.)

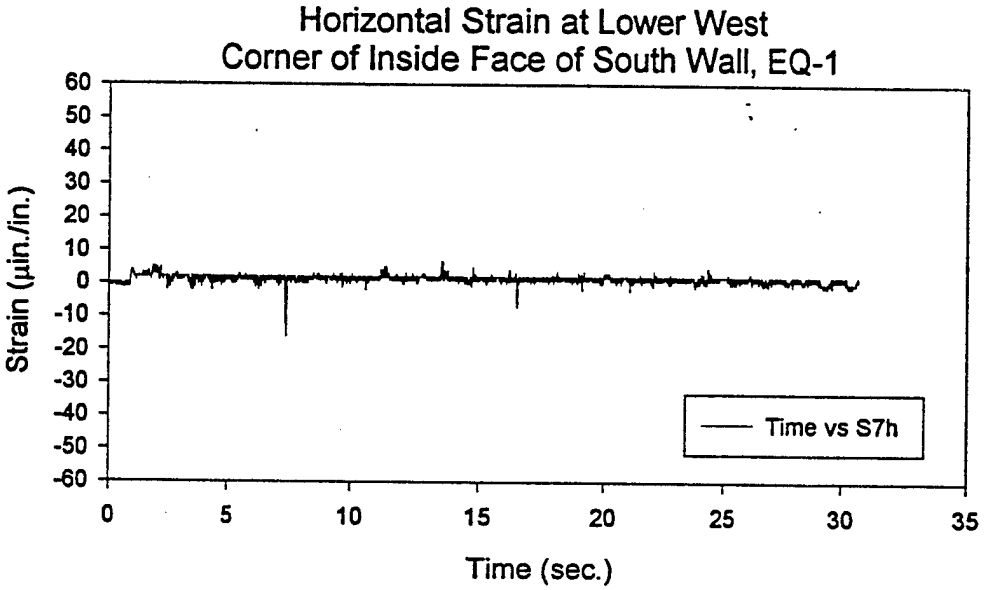
Horizontal Strain at Lower West
Corner of Inside Face of South Wall, EQ-1
Strain (µin./in.)
Time vs S7h
Time (sec.)

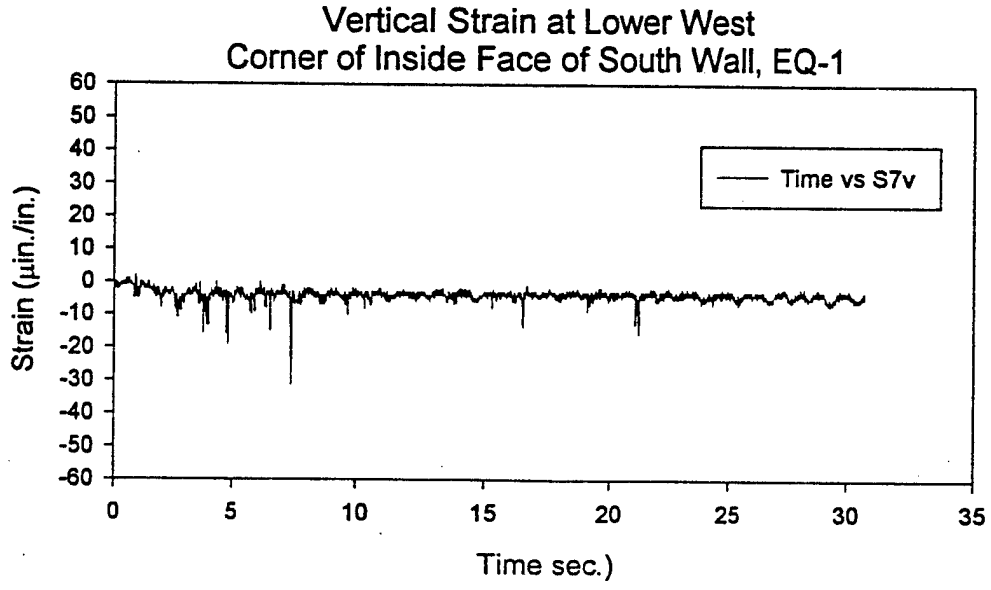
Vertical Strain at Lower West
Corner of Inside Face of South Wall, EQ-1
Strain (µin./in.)
Time vs S7v
Time sec.)

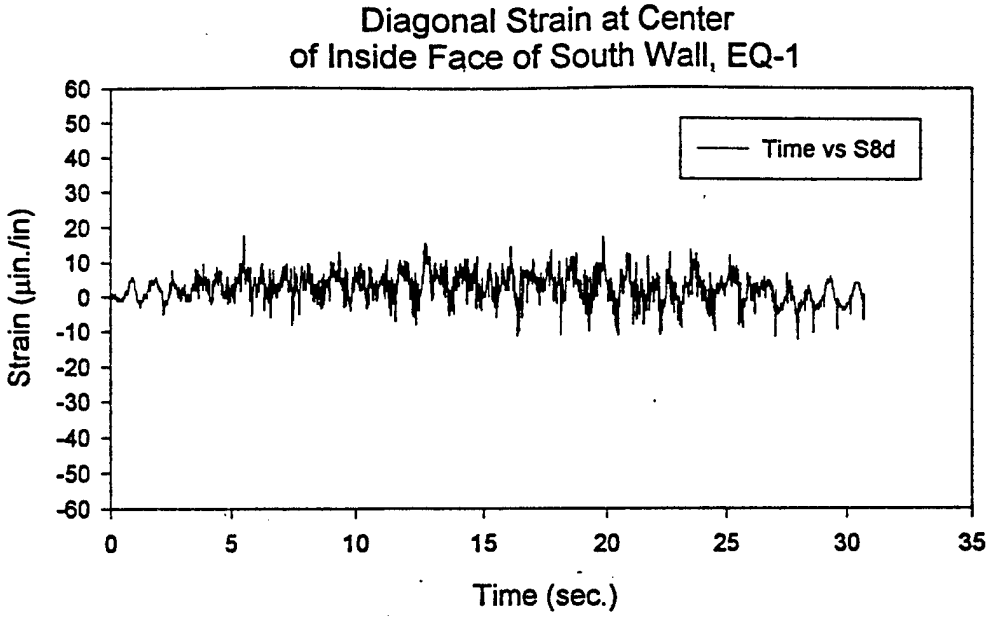
Diagonal Strain at Center
of Inside Face of South Wall, EQ-1
Time vs S8d
Strain (µin./in)
Time (sec.)

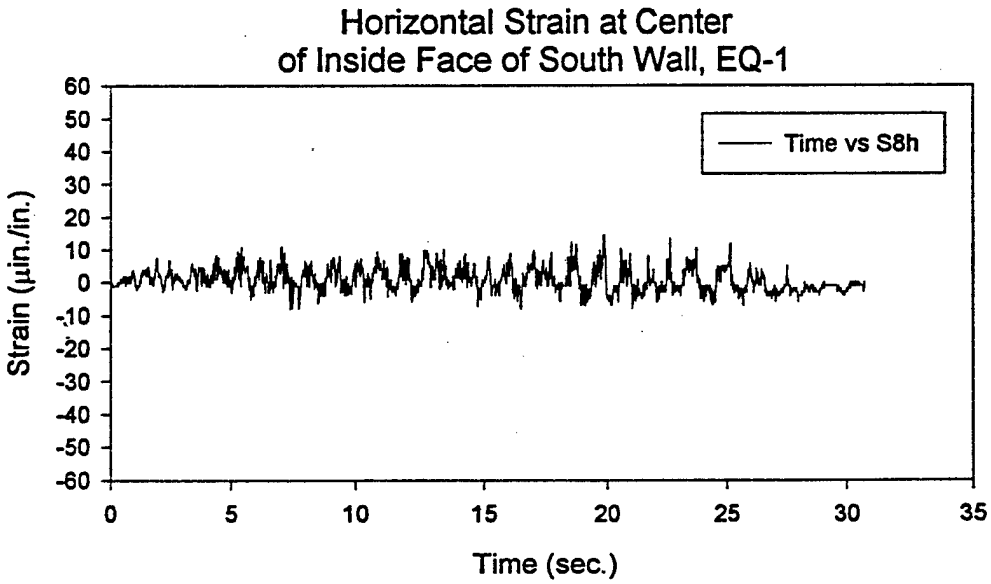
Horizontal Strain at Center
of Inside Face of South Wall, EQ-1
Time vs S8h
Strain (µin./in.)
Time (sec.)

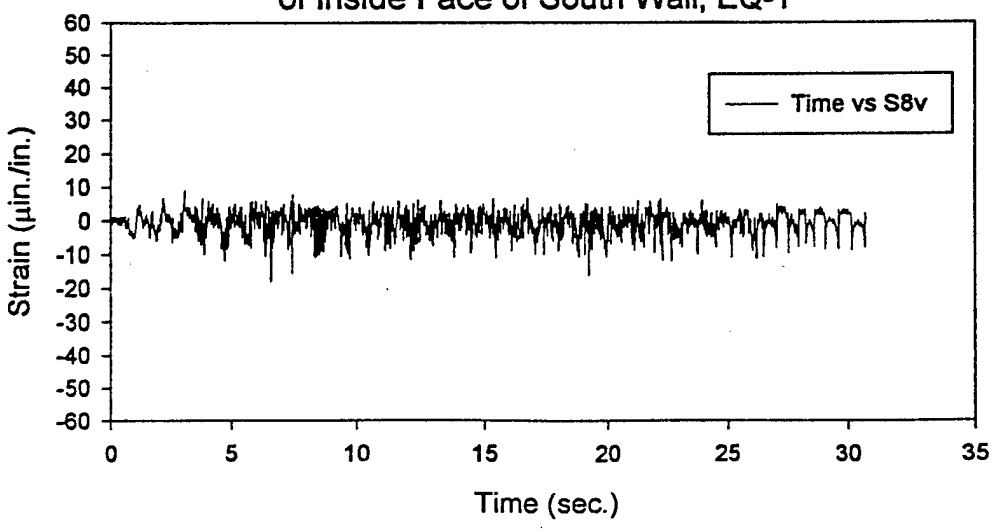
Vertical Strain at Center
of Inside Face of South Wall, EQ-1
Time vs S8v
Strain (µin./in.)
Time (sec.)

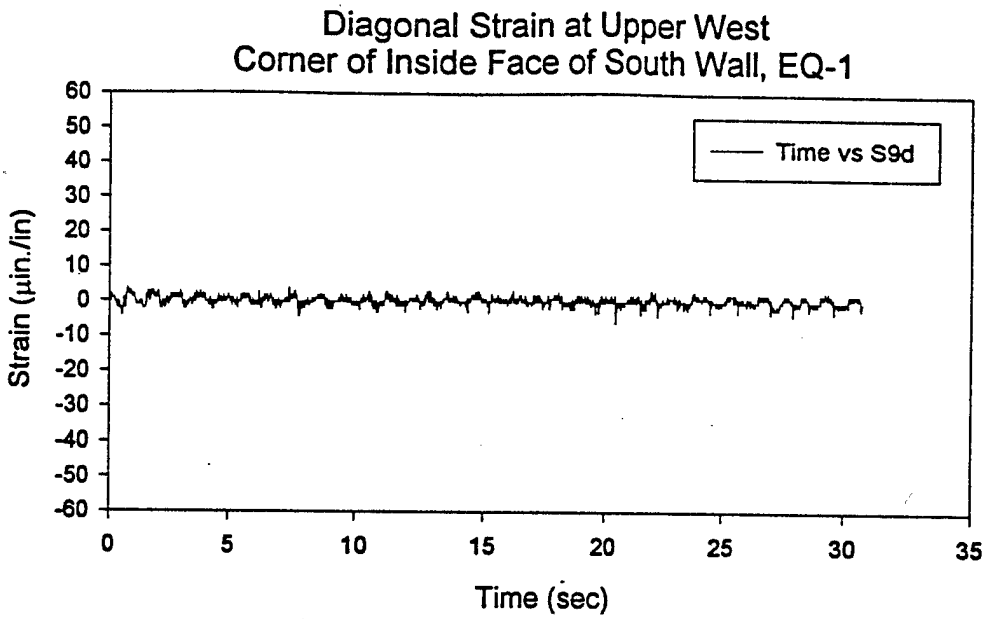
Diagonal Strain at Upper West
Corner of Inside Face of South Wall, EQ-1
Time vs S9d
Strain (µin./in)
60
50
40
30
20
10
0
-10
-20
-30
-40
-50
-60
0
5
10
15
20
25
30
35
Time (sec)

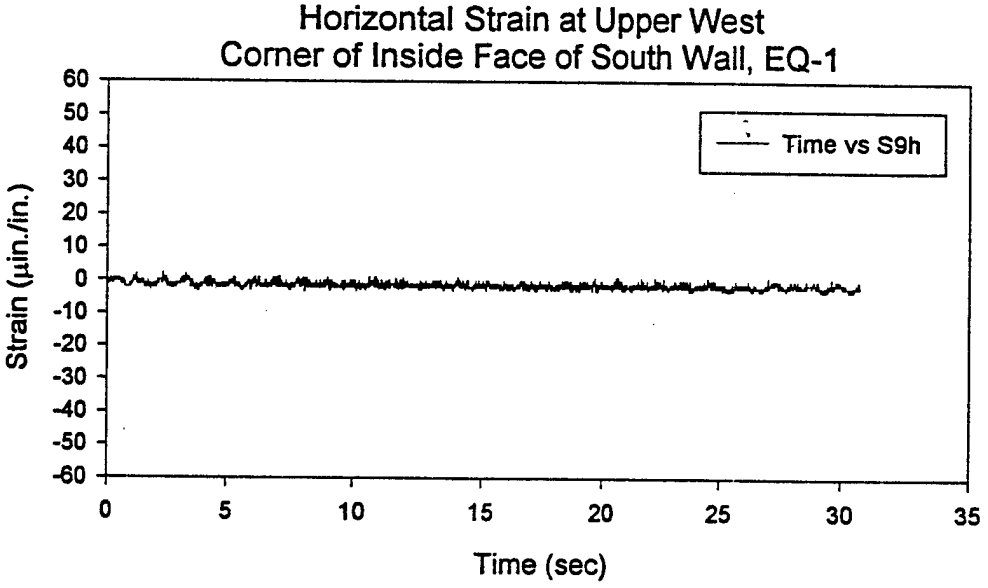
Horizontal Strain at Upper West
Corner of Inside Face of South Wall, EQ-1
Time vs S9h
Strain (µin./in.)
60
50
40
30
20
10
0
-10
-20
-30
-40
-50
-60
0
5
10
15
20
25
30
35
Time (sec)

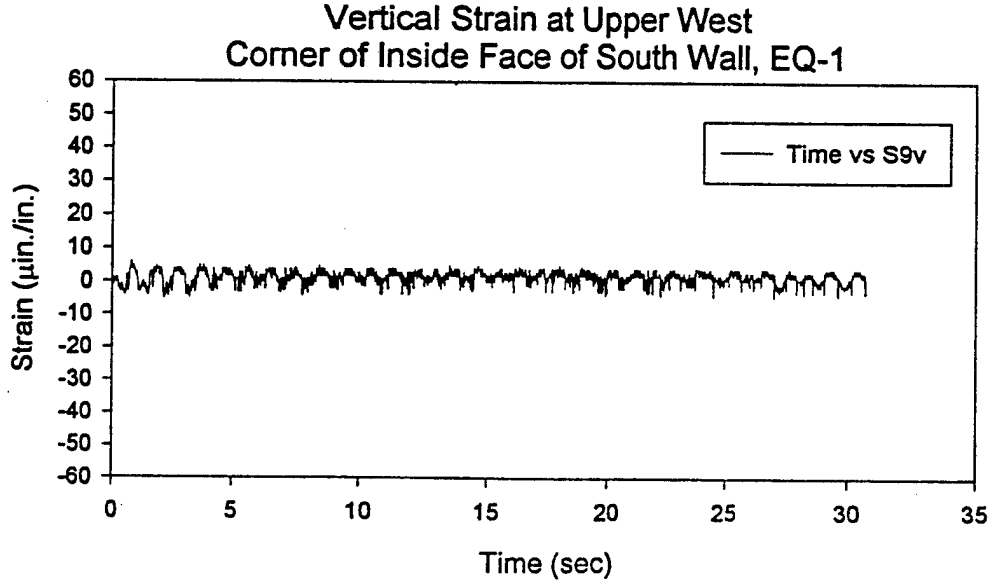
Vertical Strain at Upper West
Corner of Inside Face of South Wall, EQ-1
Time vs S9v
Strain (µin./in.)
60
50
40
30
20
10
0
-10
-20
-30
-40
-50
-60
0
5
10
15
20
25
30
35
Time (sec)

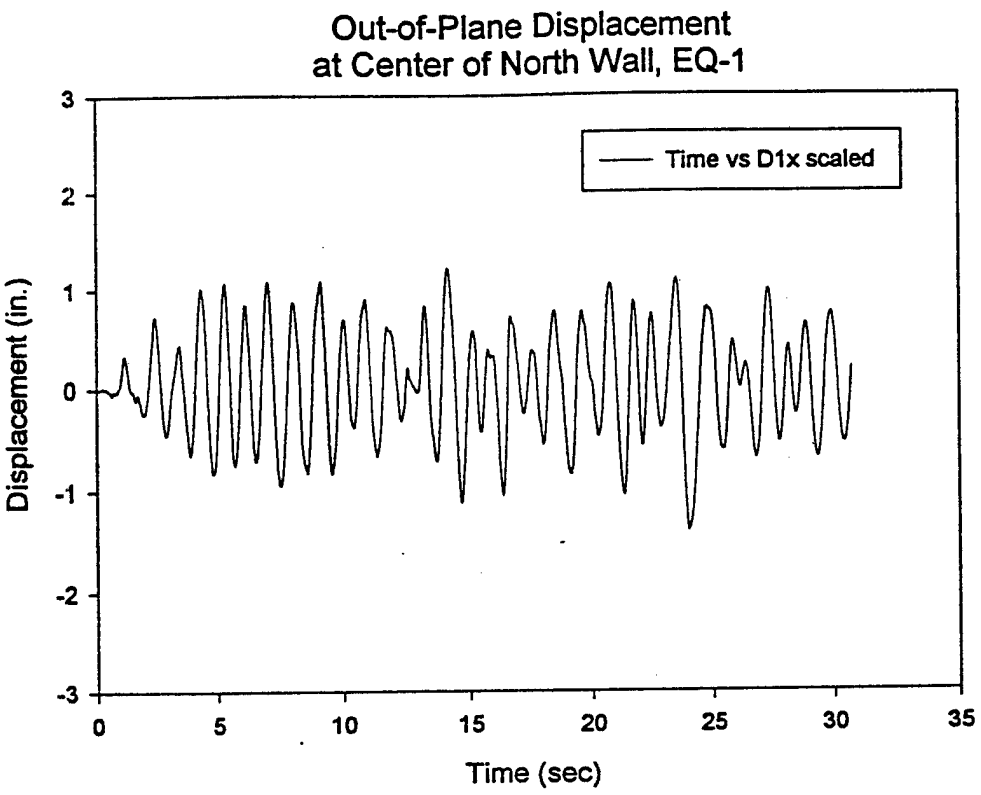
Out-of-Plane Displacement
at Center of North Wall, EQ-1
Time vs D1x scaled
Displacement (in.)
3
2
1
0
-1
-2
-3
0
5
10
15
20
25
30
35
Time (sec)

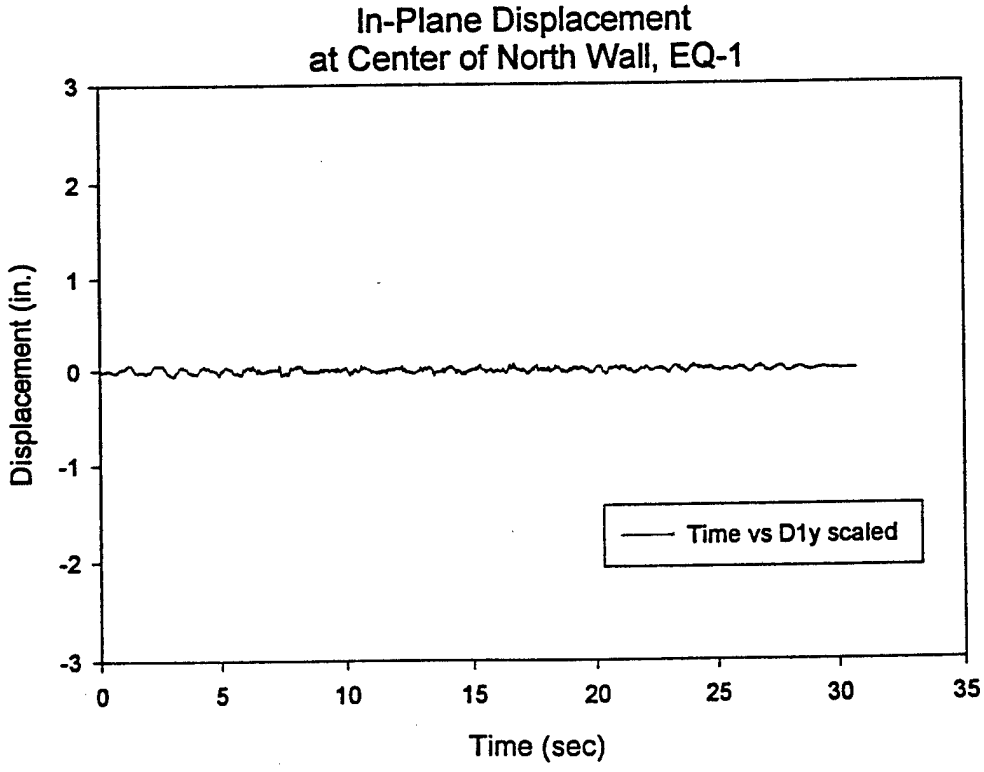
In-Plane Displacement
at Center of North Wall, EQ-1
Time vs D1y scaled
Displacement (in.)
3
2
1
0
-1
-2
-3
0
5
10
15
20
25
30
35
Time (sec)

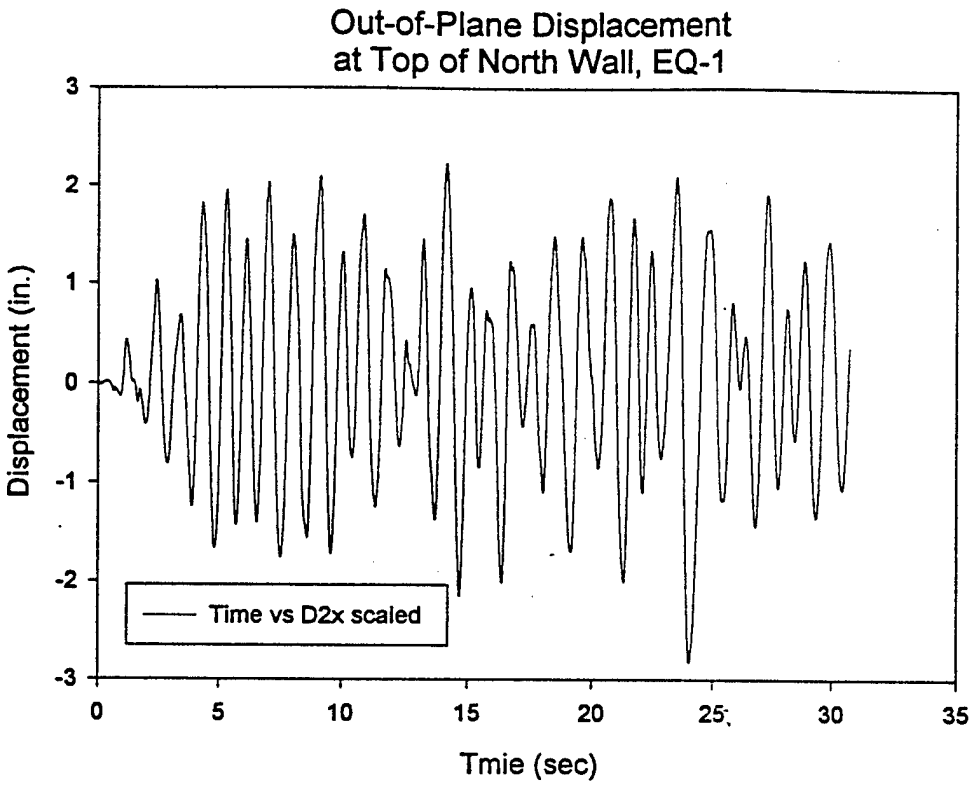
Out-of-Plane Displacement
at Top of North Wall, EQ-1
Displacement (in.)
3
2
1
0
-1
-2
-3
0
5
10
15
20
25
30
35
Tmie (sec)
Time vs D2x scaled

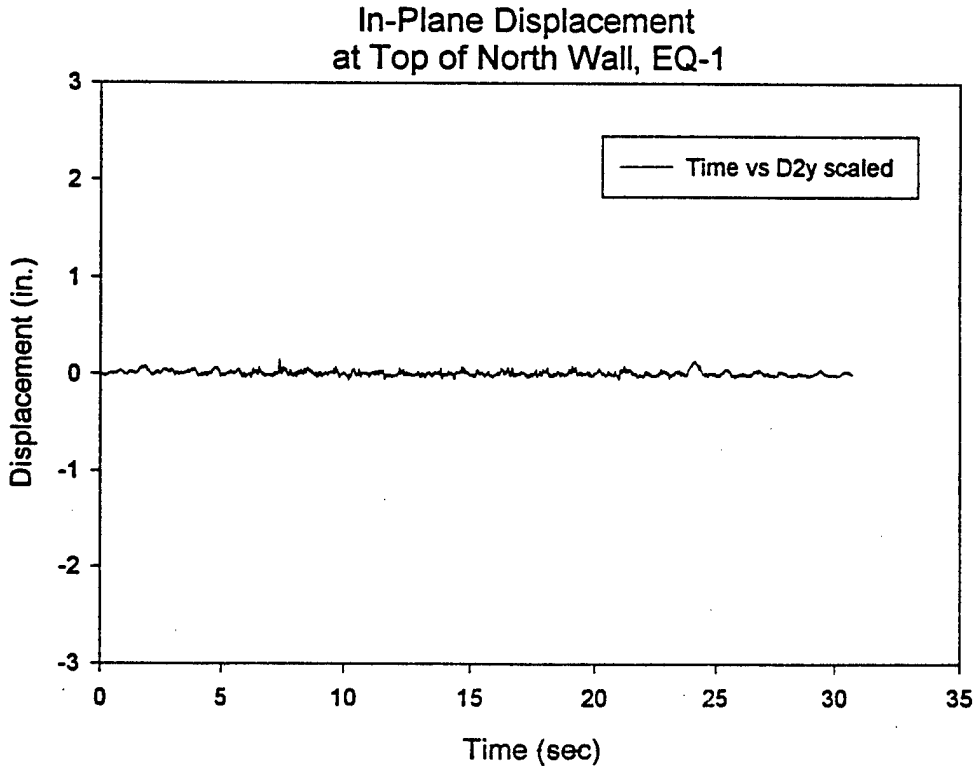
In-Plane Displacement
at Top of North Wall, EQ-1
Displacement (in.)
3
2
1
0
-1
-2
-3
0
5
10
15
20
25
30
35
Time (sec)
Time vs D2y scaled

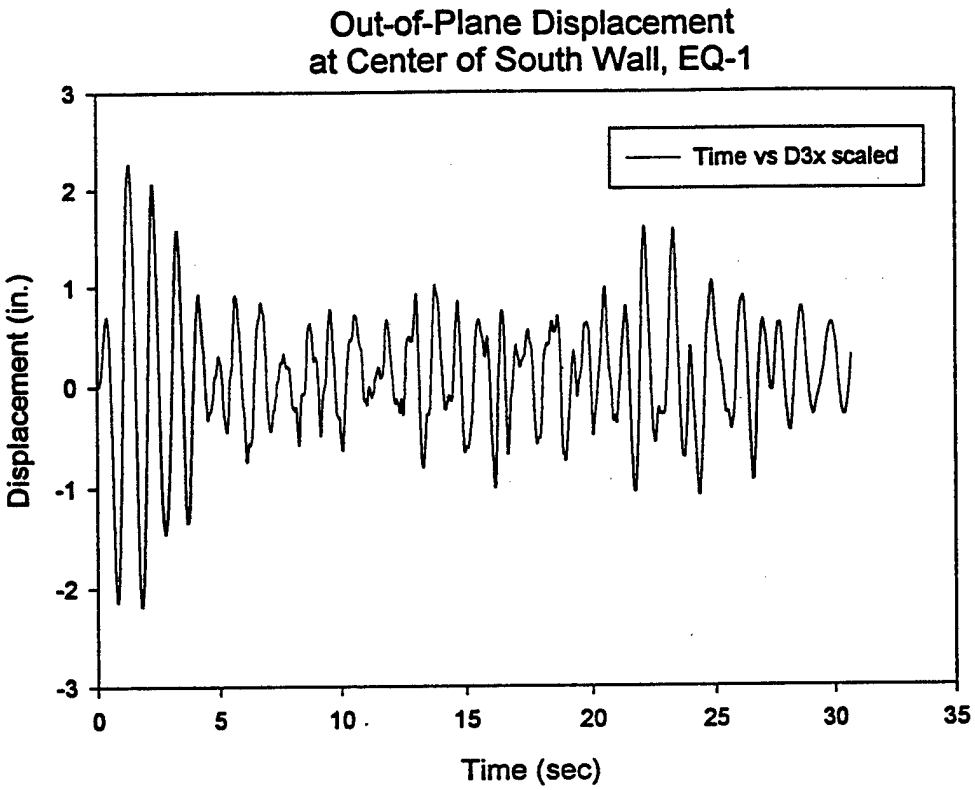
Out-of-Plane Displacement
at Center of South Wall, EQ-1
Time vs D3x scaled
Displacement (in.)
3
2
1
0
-1
-2
-3
0
5
10
15
20
25
30
35
Time (sec)

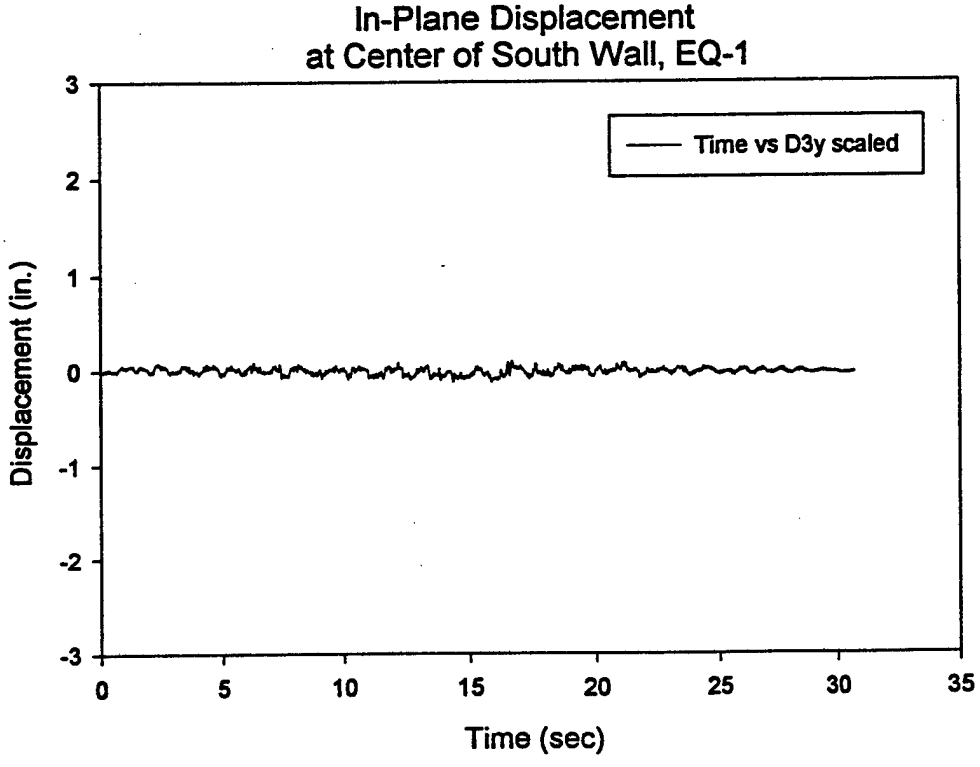
In-Plane Displacement
at Center of South Wall, EQ-1
Time vs D3y scaled
Displacement (in.)
3
2
1
0
-1
-2
-3
0
5
10
15
20
25
30
35
Time (sec)

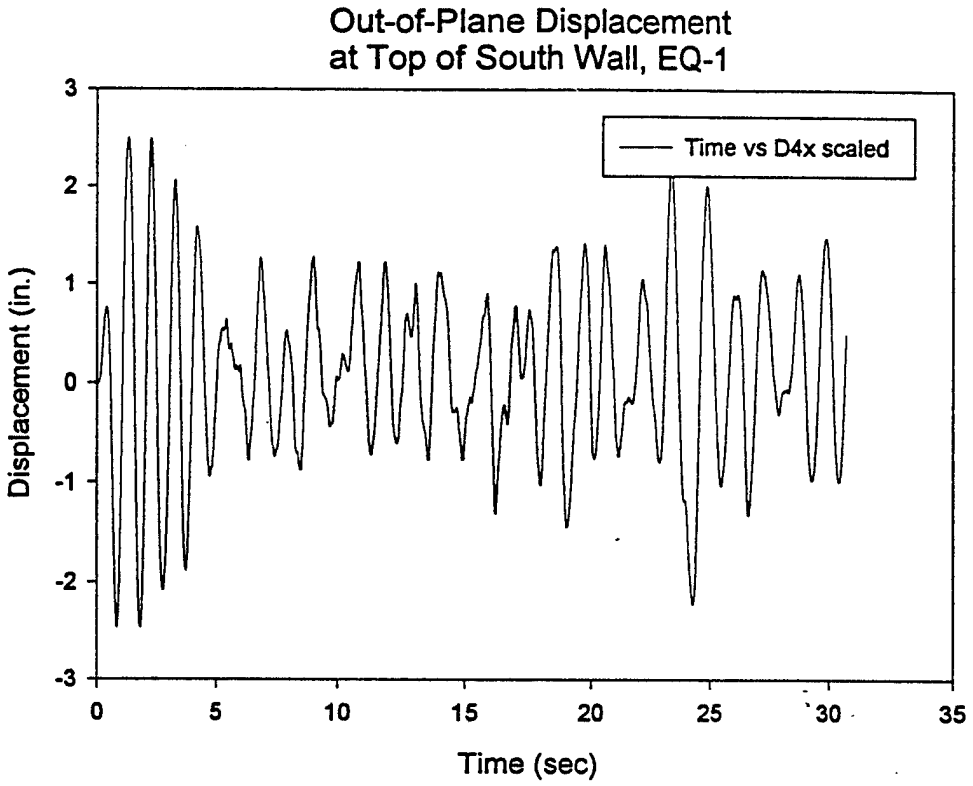
Out-of-Plane Displacement
at Top of South Wall, EQ-1
Time vs D4x scaled
Displacement (in.)
3
2
1
0
-1
-2
-3
0
5
10
15
20
25
30
35
Time (sec)

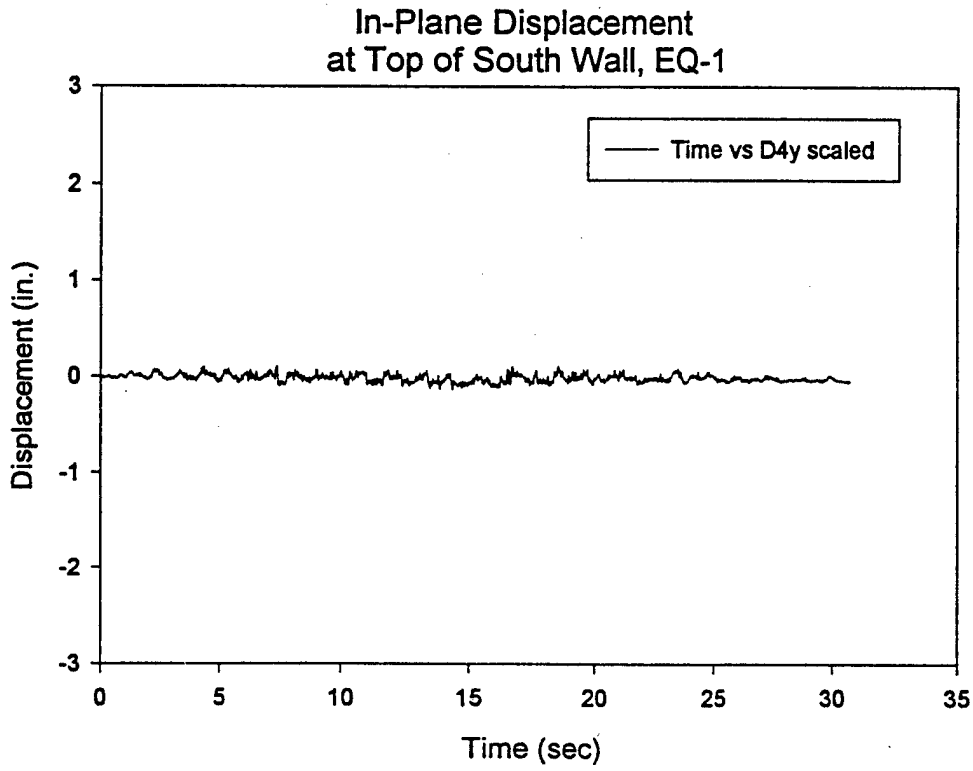
In-Plane Displacement
at Top of South Wall, EQ-1
Time vs D4y scaled
Displacement (in.)
3
2
1
0
-1
-2
-3
0
5
10
15
20
25
30
35
Time (sec)

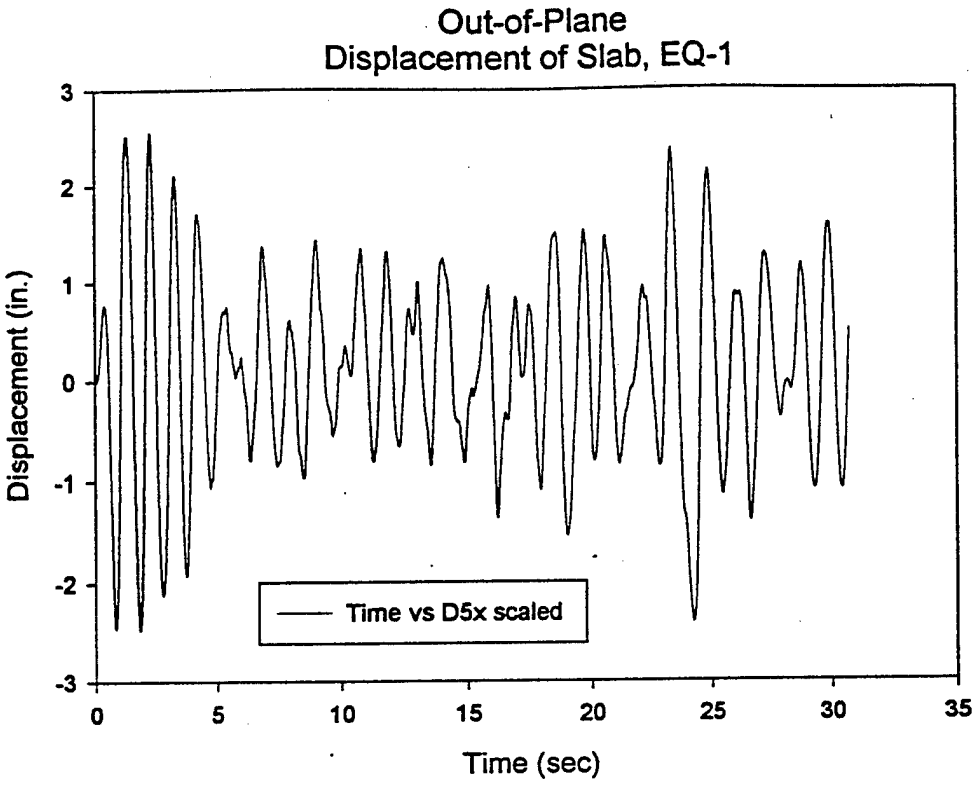
Out-of-Plane
Displacement of Slab, EQ-1
Displacement (in.)
3
2
1
0
-1
-2
-3
0
5
10
15
20
25
30
35
Time (sec)
Time vs D5x scaled

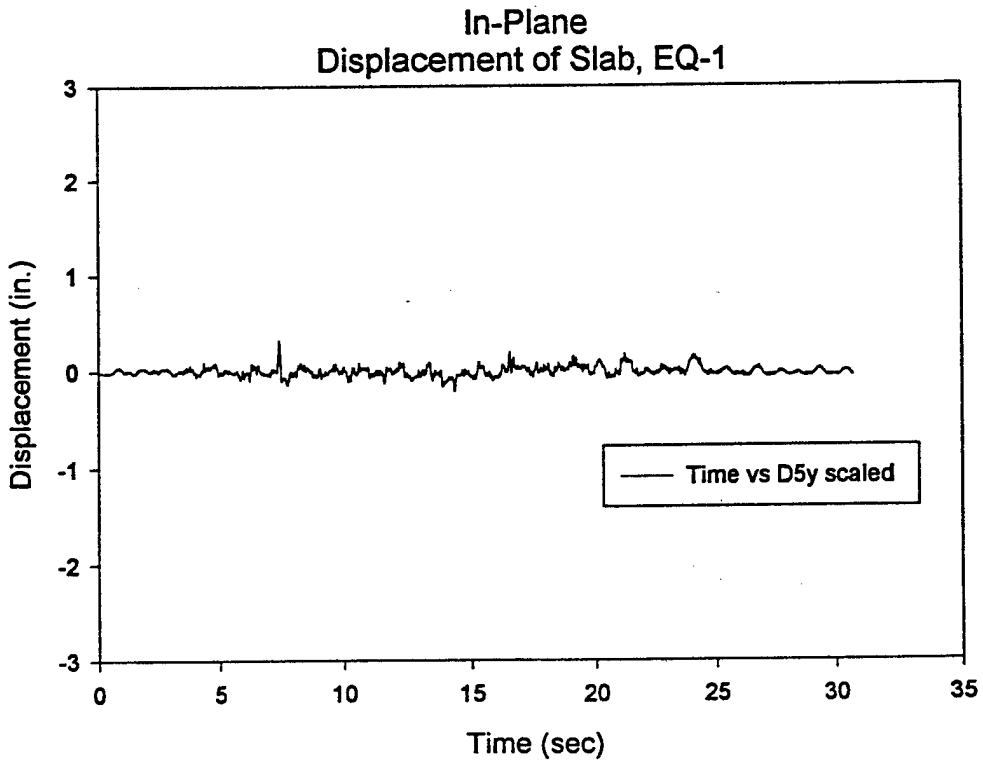
In-Plane
Displacement of Slab, EQ-1
Displacement (in.)
3
2
1
0
-1
-2
-3
0
5
10
15
20
25
30
35
Time (sec)
Time vs D5y scaled

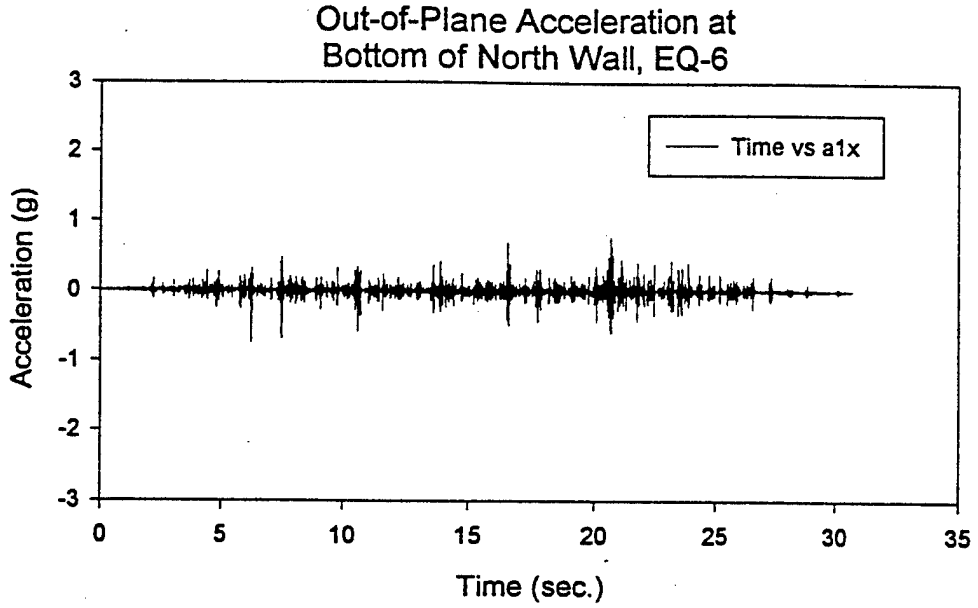
Out-of-Plane Acceleration at
Bottom of North Wall, EQ-6
Time vs a1x
Acceleration (g)
Time (sec.)

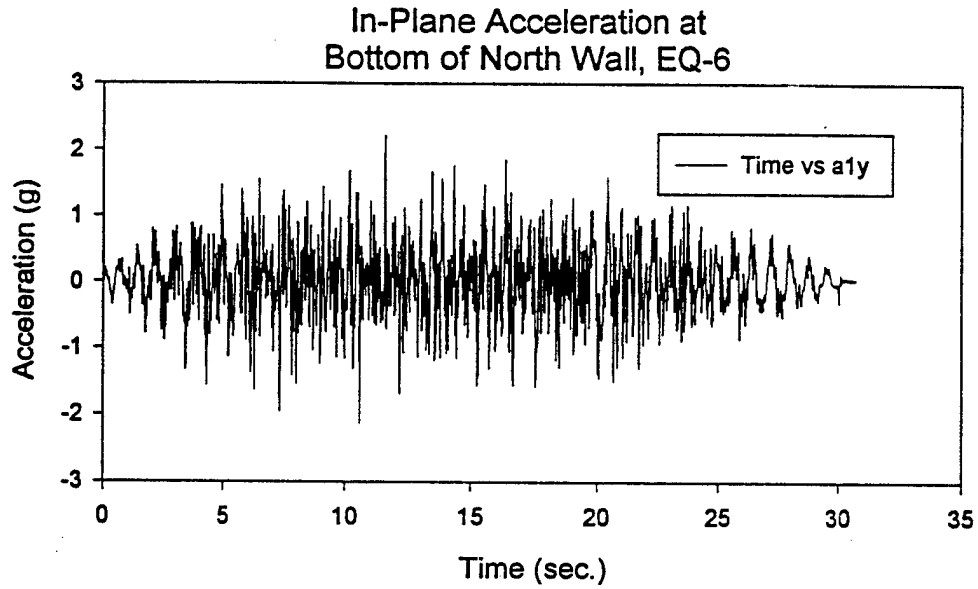
In-Plane Acceleration at
Bottom of North Wall, EQ-6
Time vs a1y
Acceleration (g)
Time (sec.)

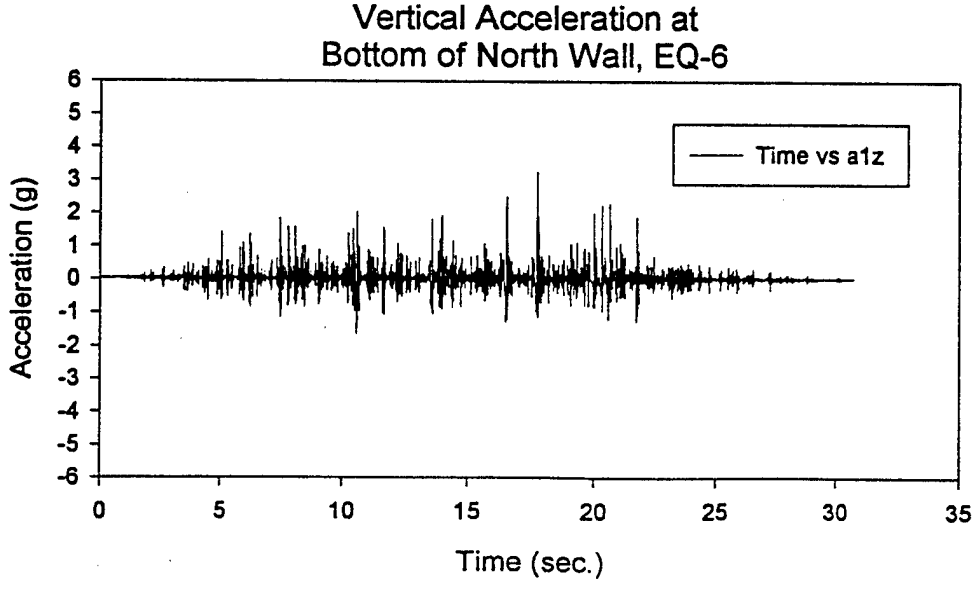
Vertical Acceleration at
Bottom of North Wall, EQ-6
Time vs a1z
Acceleration (g)
Time (sec.)

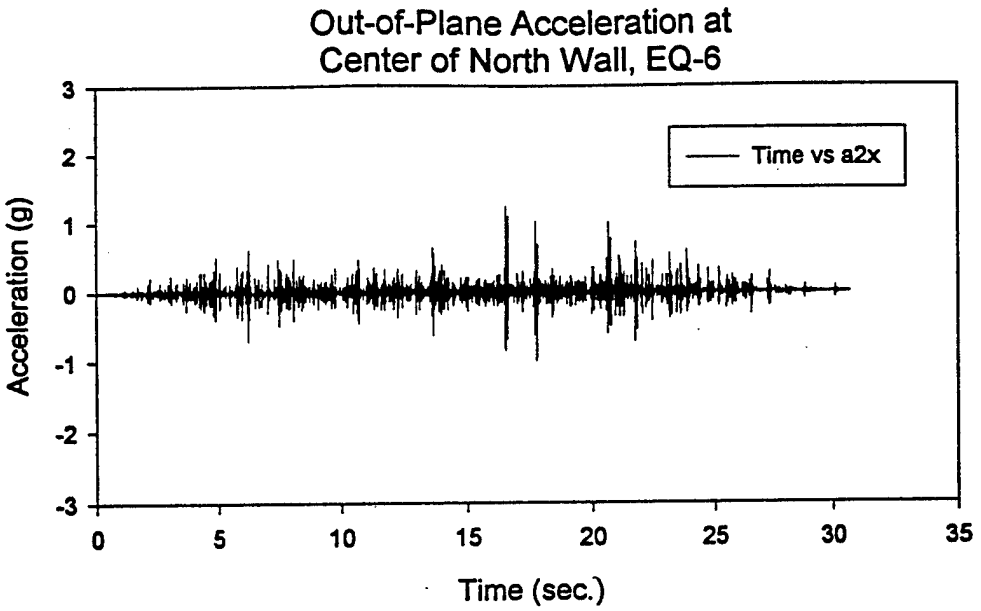
Out-of-Plane Acceleration at
Center of North Wall, EQ-6
Time vs a2x
Acceleration (g)
Time (sec.)

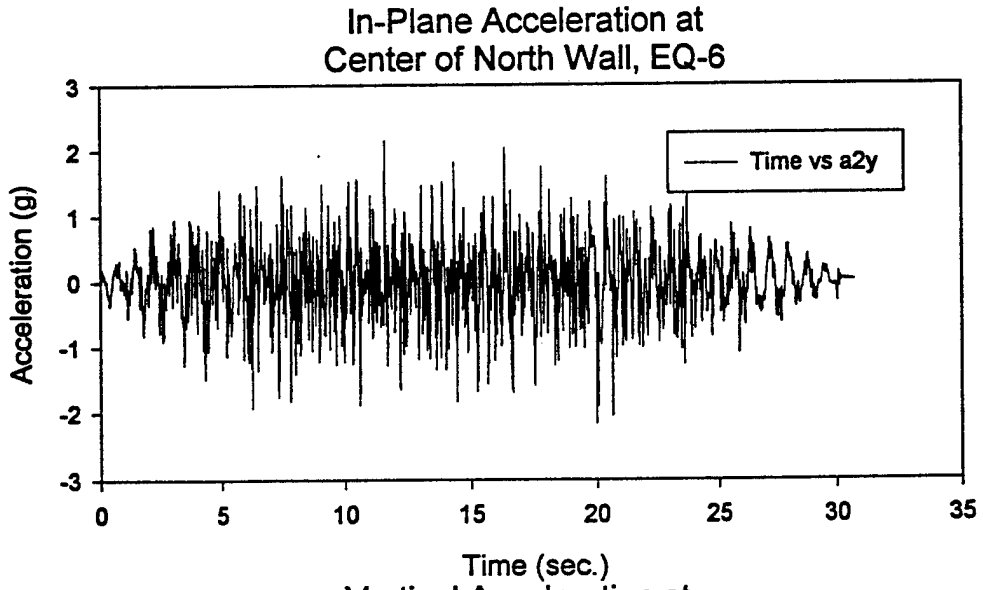
In-Plane Acceleration at
Center of North Wall, EQ-6
Time vs a2y
Acceleration (g)
Time (sec.)

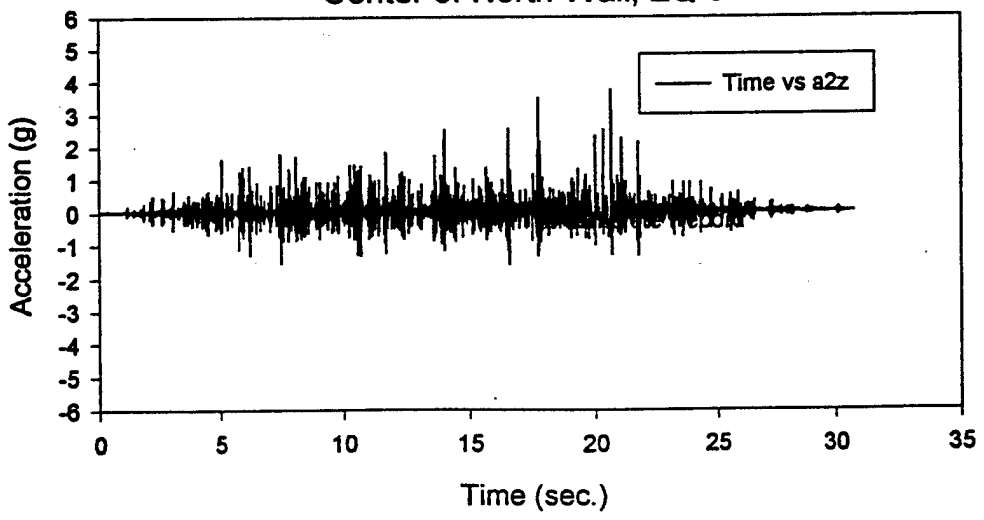
Vertical Acceleration at
Center of North Wall, EQ-6
Time vs a2z
Acceleration (g)
Time (sec.)

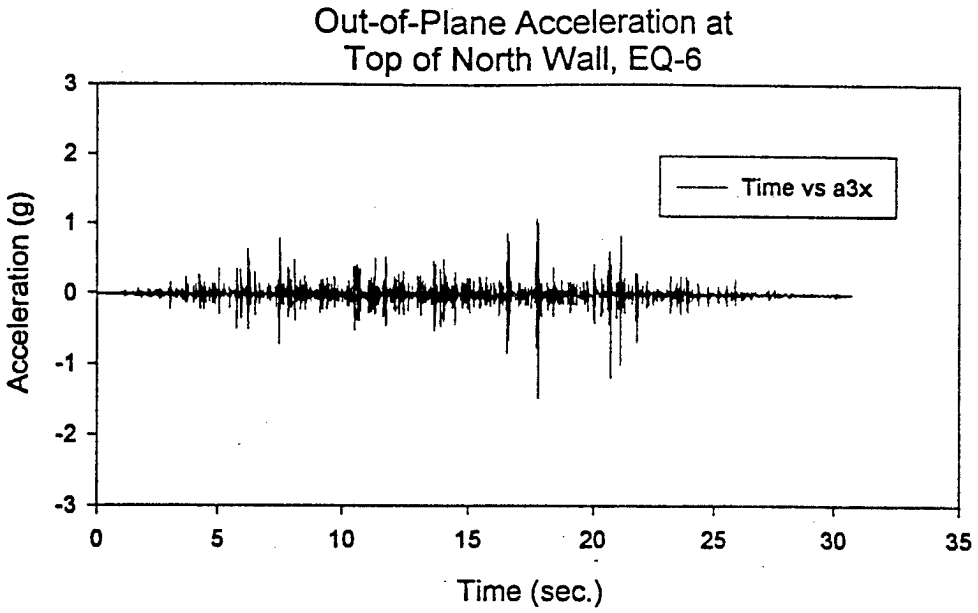
Out-of-Plane Acceleration at
Top of North Wall, EQ-6
Time vs a3x
Acceleration (g)
Time (sec.)

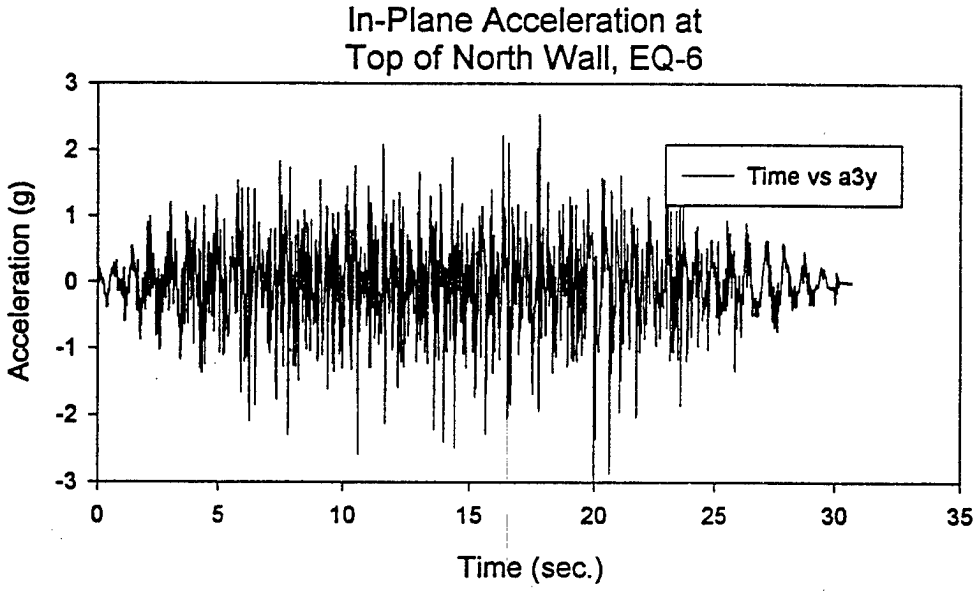
In-Plane Acceleration at
Top of North Wall, EQ-6
Time vs a3y
Acceleration (g)
Time (sec.)

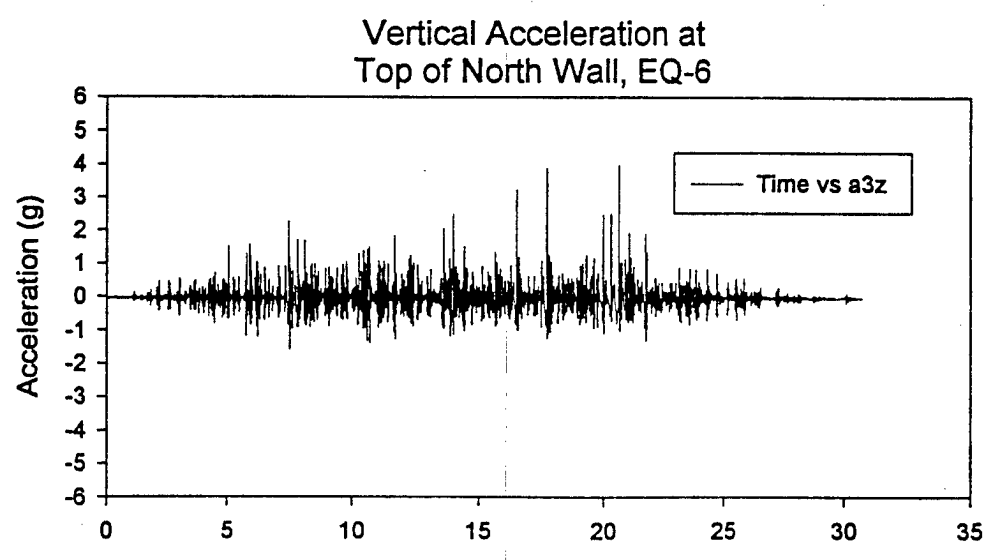
Vertical Acceleration at
Top of North Wall, EQ-6
Time vs a3z
Acceleration (g)

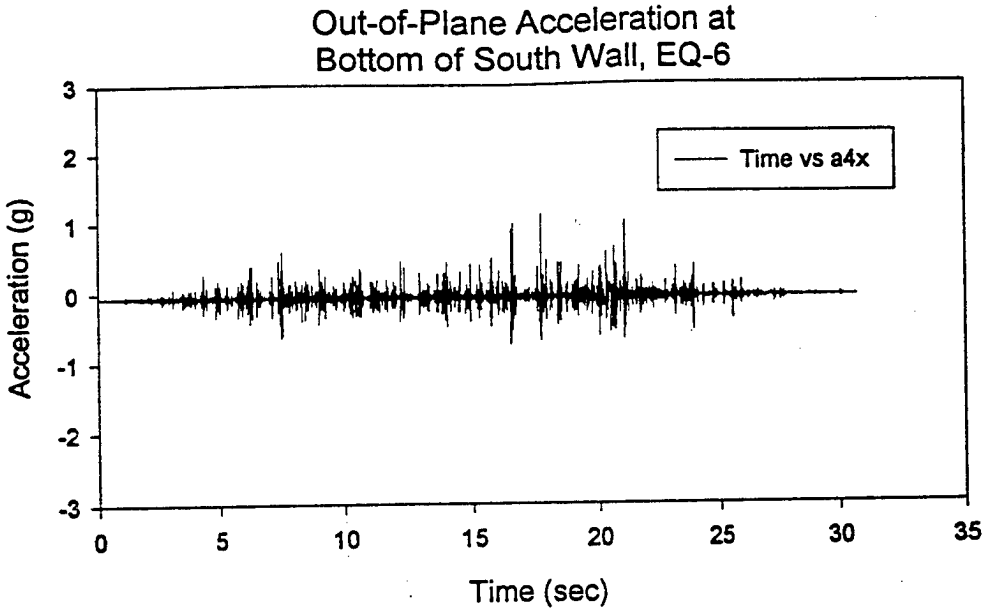
Out-of-Plane Acceleration at
Bottom of South Wall, EQ-6
Time vs a4x
Acceleration (g)
Time (sec)

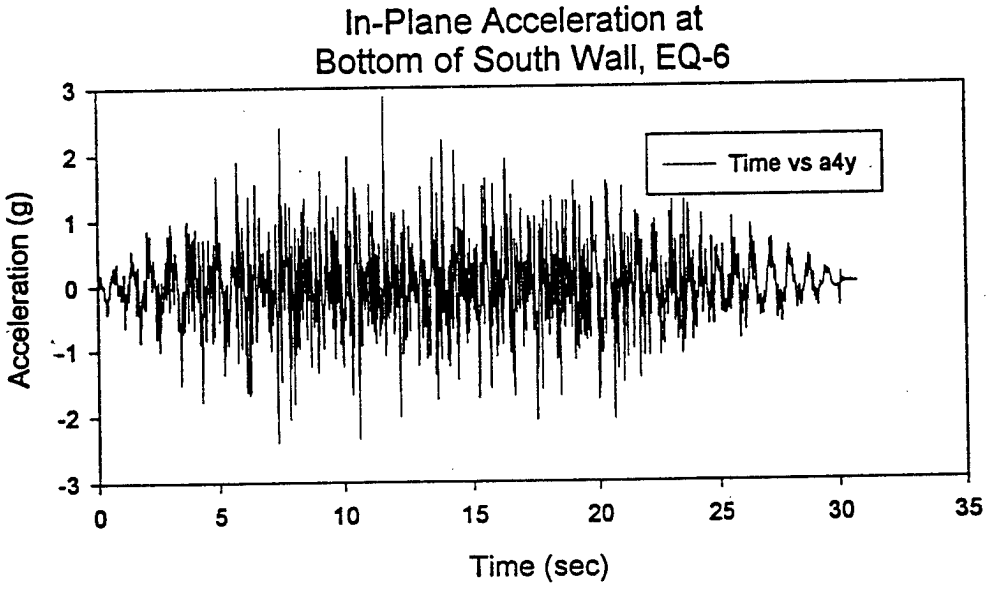
In-Plane Acceleration at
Bottom of South Wall, EQ-6
Time vs a4y
Acceleration (g)
Time (sec)

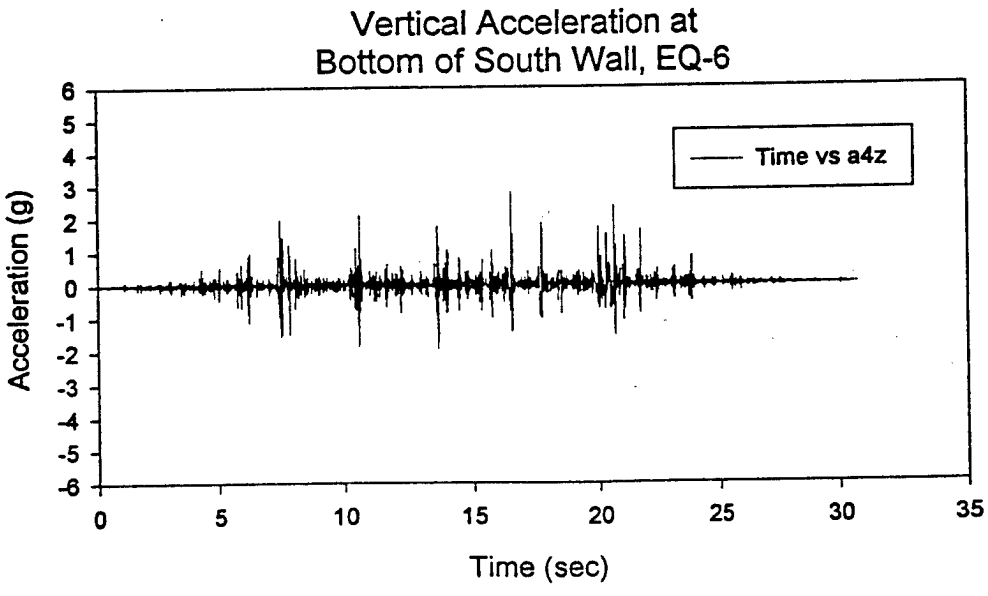
Vertical Acceleration at
Bottom of South Wall, EQ-6
Time vs a4z
Acceleration (g)
Time (sec)

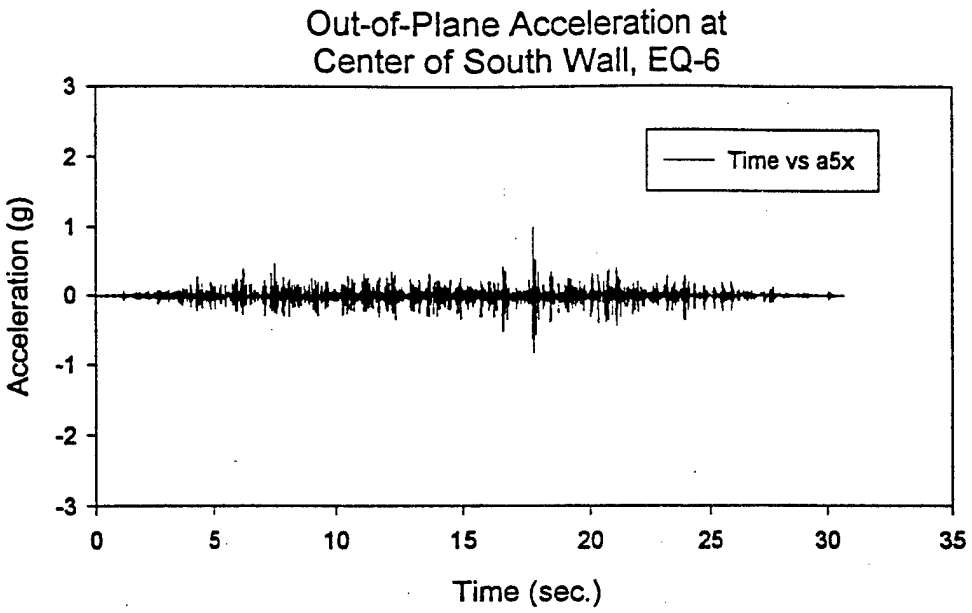
Out-of-Plane Acceleration at
Center of South Wall, EQ-6
Time vs a5x
Acceleration (g)
Time (sec.)

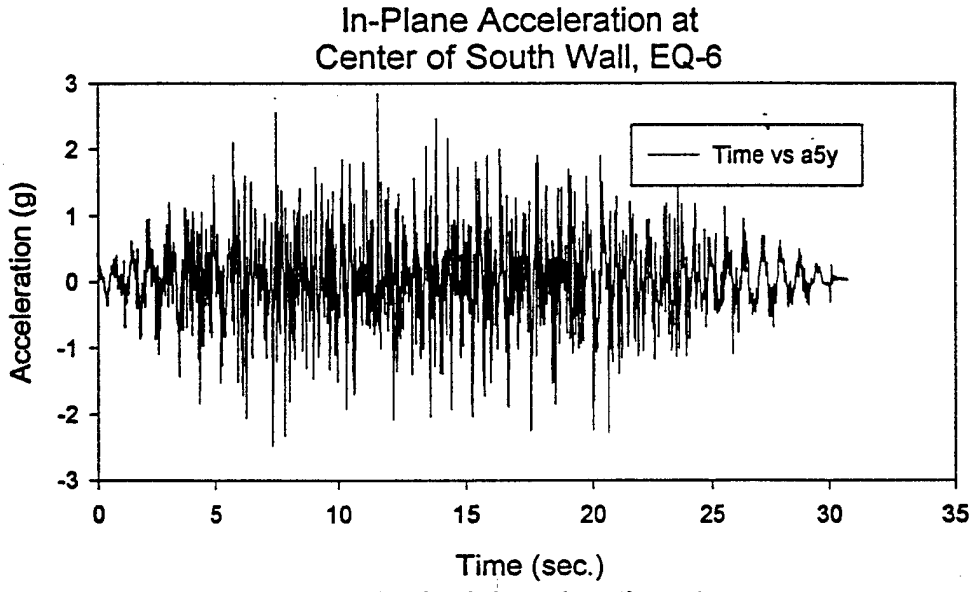
In-Plane Acceleration at
Center of South Wall, EQ-6
Time vs a5y
Acceleration (g)
Time (sec.)

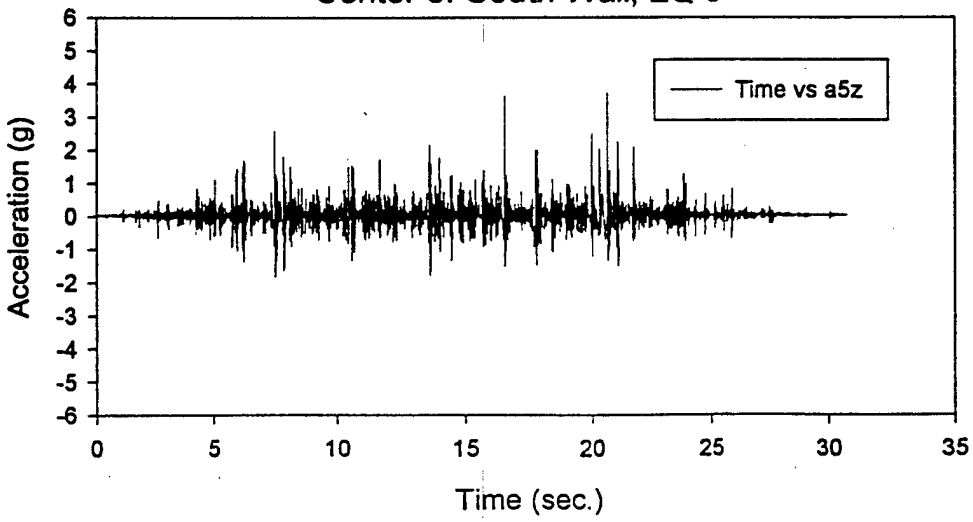
Vertical Acceleration at
Center of South Wall, EQ-6
Time vs a5z
Acceleration (g)
Time (sec.)

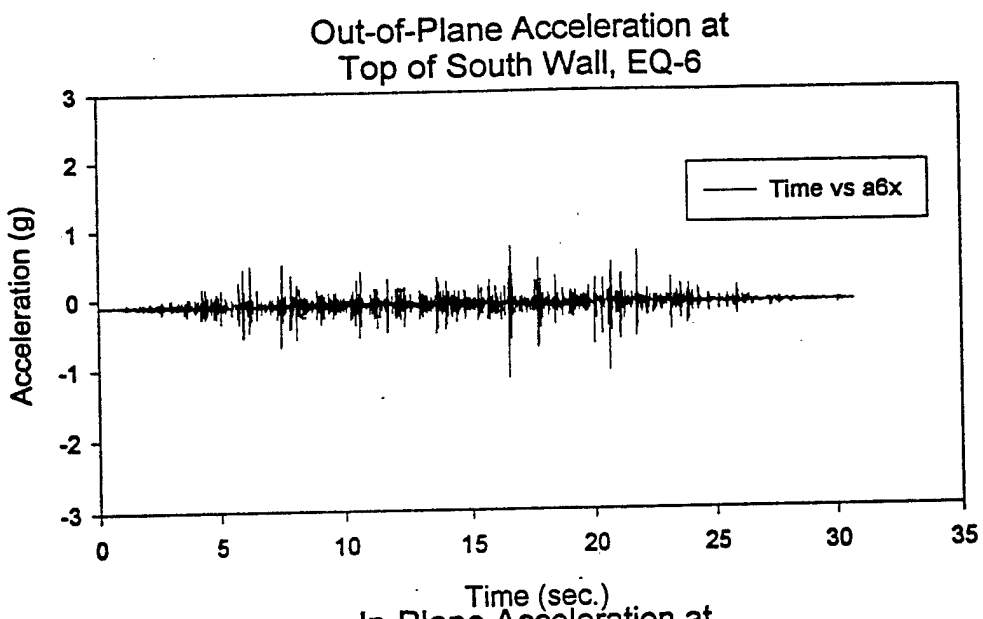
Out-of-Plane Acceleration at
Top of South Wall, EQ-6
Time vs a6x
Acceleration (g)
3
2
1
0
-1
-2
-3
0
5
10
15
20
25
30
35
Time (sec.)

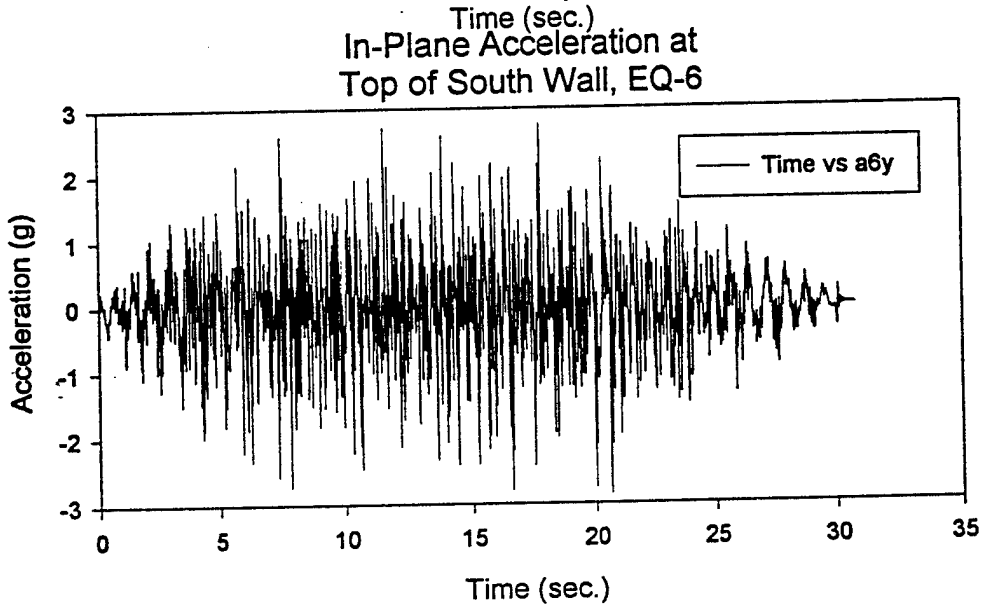
In-Plane Acceleration at
Top of South Wall, EQ-6
Time vs a6y
Acceleration (g)
3
2
1
0
-1
-2
-3
0
5
10
15
20
25
30
35
Time (sec.)

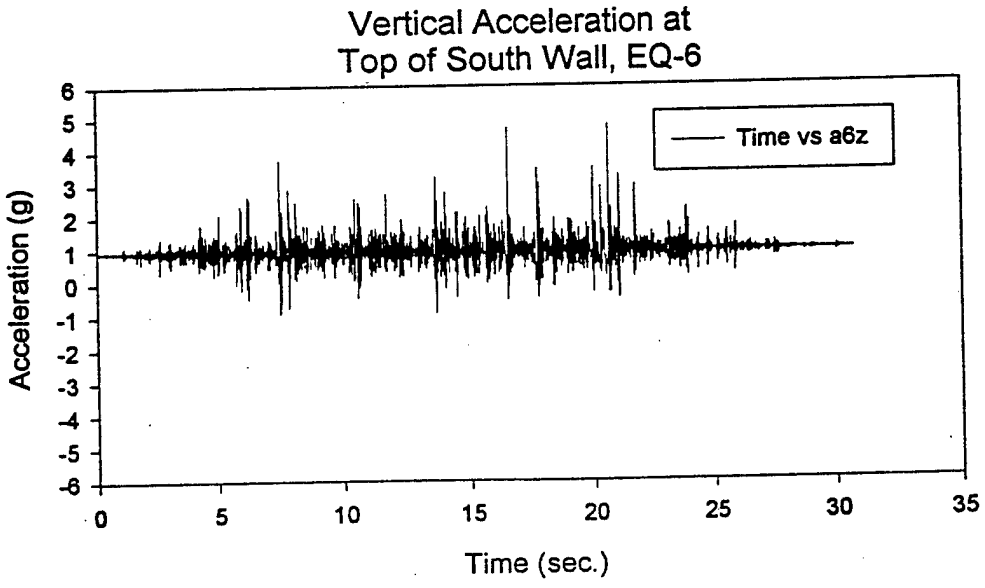
Vertical Acceleration at
Top of South Wall, EQ-6
Time vs a6z
Acceleration (g)
6
5
4
3
2
1
0
-1
-2
-3
-4
-5
-6
0
5
10
15
20
25
30
35
Time (sec.)

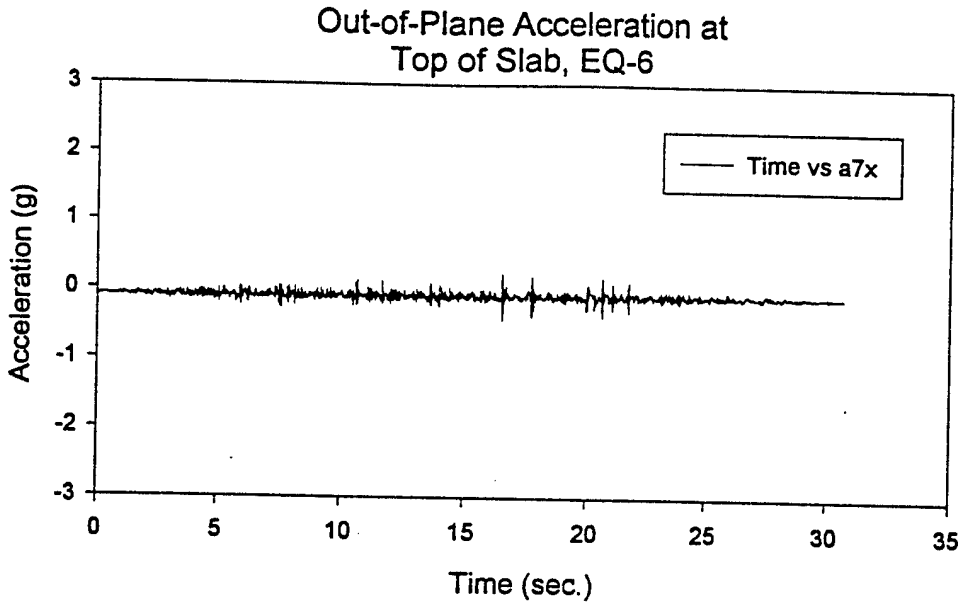
Out-of-Plane Acceleration at
Top of Slab, EQ-6
Time vs a7x
Acceleration (g)
3
2
1
0
-1
-2
-3
0
5
10
15
20
25
30
35
Time (sec.)

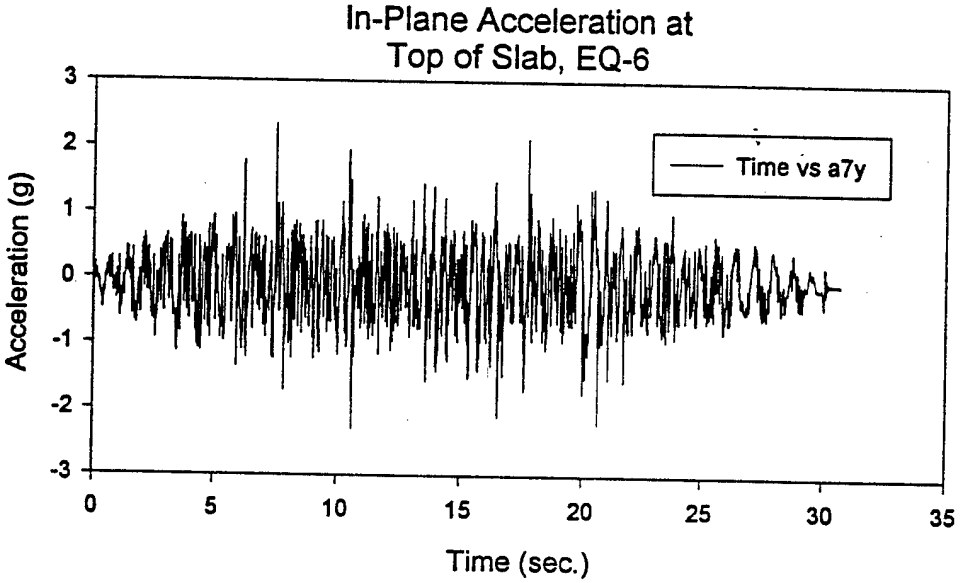
In-Plane Acceleration at
Top of Slab, EQ-6
Time vs a7y
Acceleration (g)
3
2
1
0
-1
-2
-3
0
5
10
15
20
25
30
35
Time (sec.)

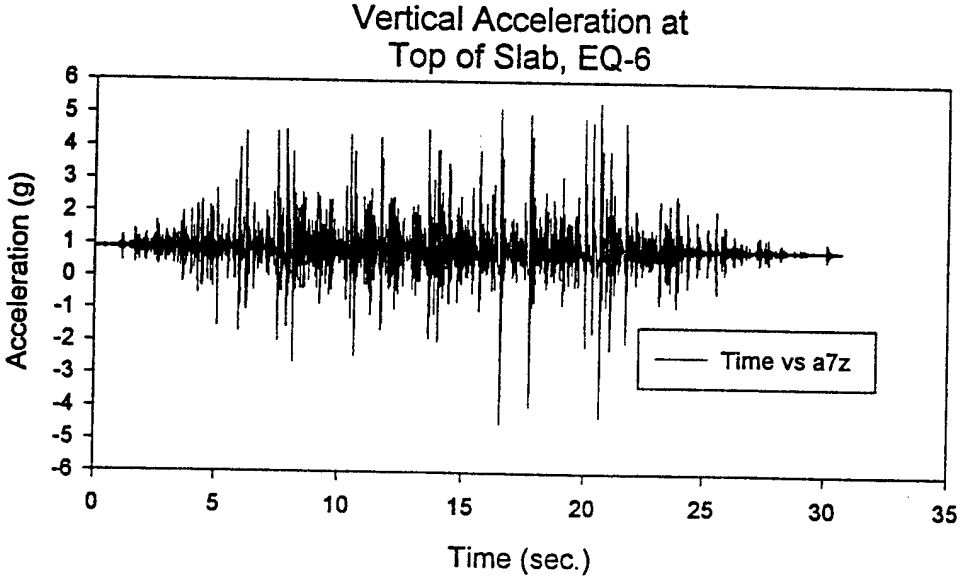
Vertical Acceleration at
Top of Slab, EQ-6
Time vs a7z
Acceleration (g)
6
5
4
3
2
1
0
-1
-2
-3
-4
-5
-6
0
5
10
15
20
25
30
35
Time (sec.)

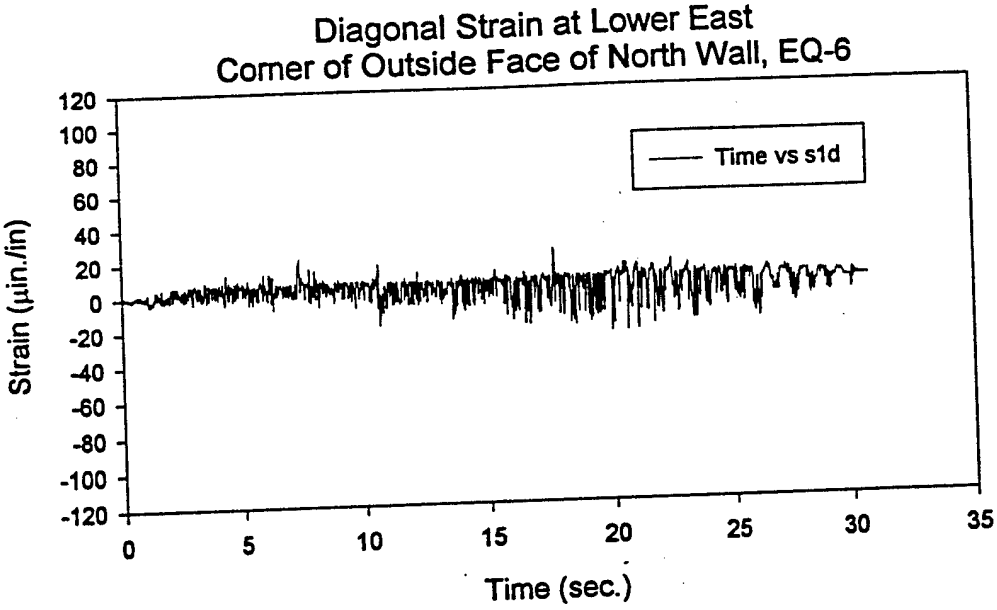
Diagonal Strain at Lower East
Corner of Outside Face of North Wall, EQ-6
Strain (µin./in)
120
100
80
60
40
20
0
-20
-40
-60
-80
-100
-120
0
5
10
15
20
25
30
35
Time (sec.)
Time vs s1d

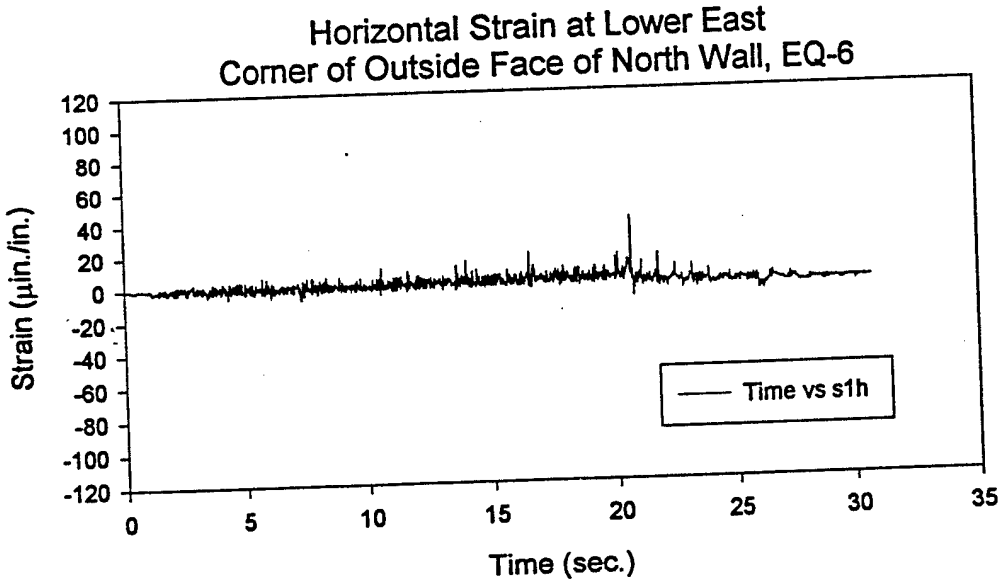
Horizontal Strain at Lower East
Corner of Outside Face of North Wall, EQ-6
Strain (µin./in.)
120
100
80
60
40
20
0
-20
-40
-60
-80
-100
-120
0
5
10
15
20
25
30
35
Time (sec.)
Time vs s1h

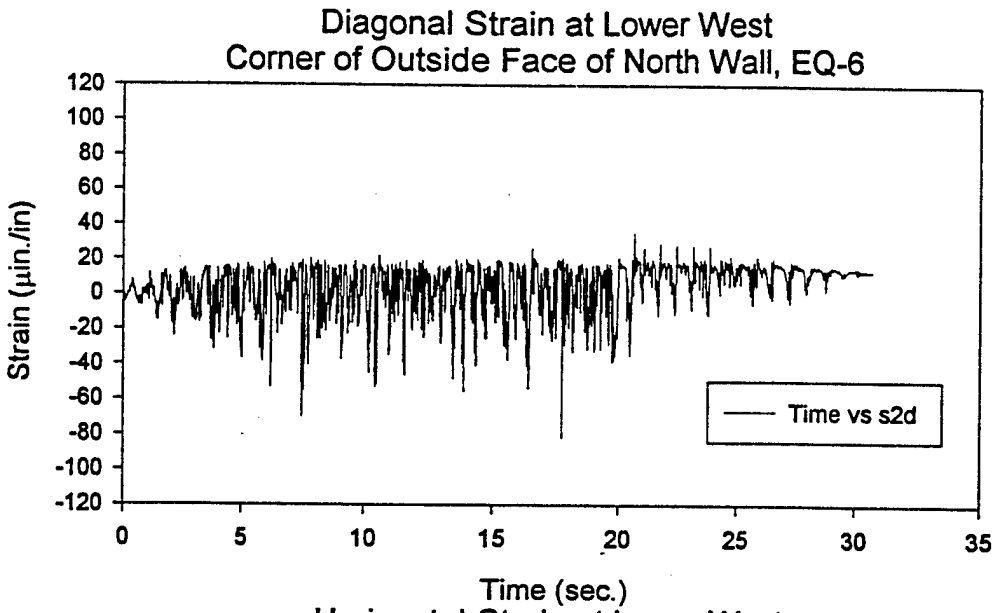
Diagonal Strain at Lower West
Corner of Outside Face of North Wall, EQ-6
Strain (μin./in)
120
100
80
60
40
20
0
-20
-40
-60
-80
-100
-120
0
5
10
15
20
25
30
35
Time (sec.)
Time vs s2d

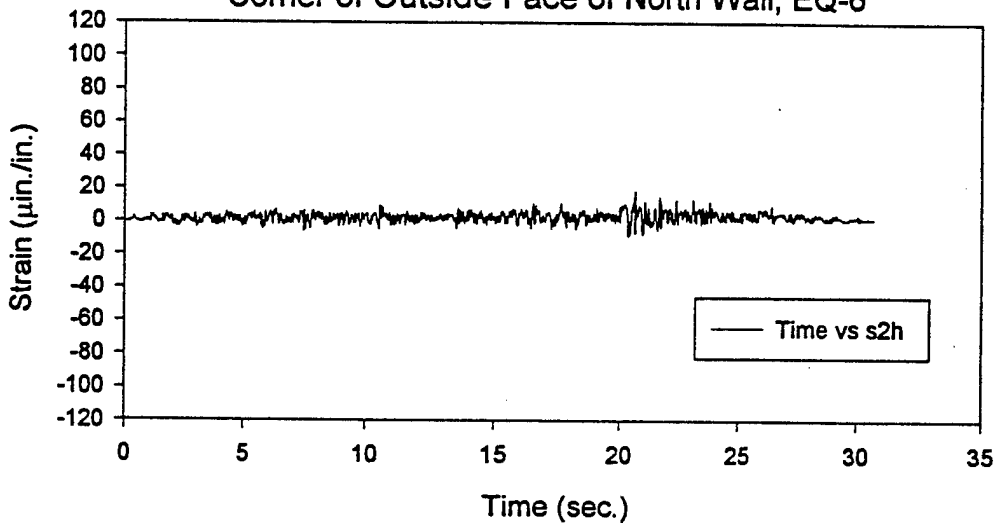
Horizontal Strain at Lower West
Corner of Outside Face of North Wall, EQ-6
Strain (μin./in.)
120
100
80
60
40
20
0
-20
-40
-60
-80
-100
-120
0
5
10
15
20
25
30
35
Time (sec.)
Time vs s2h

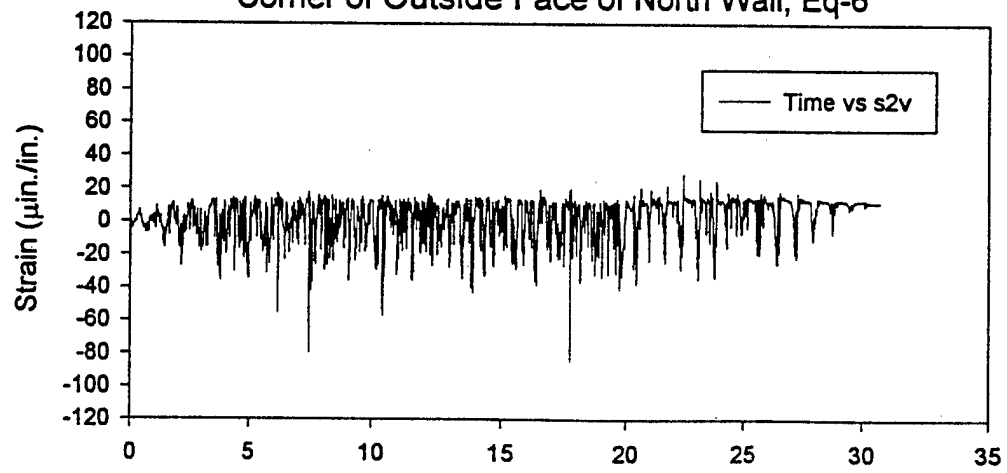
Vertical Strain at Lower West
Corner of Outside Face of North Wall, Eq-6
Strain (μin./in.)
120
100
80
60
40
20
0
-20
-40
-60
-80
-100
-120
0
5
10
15
20
25
30
35
Time vs s2v

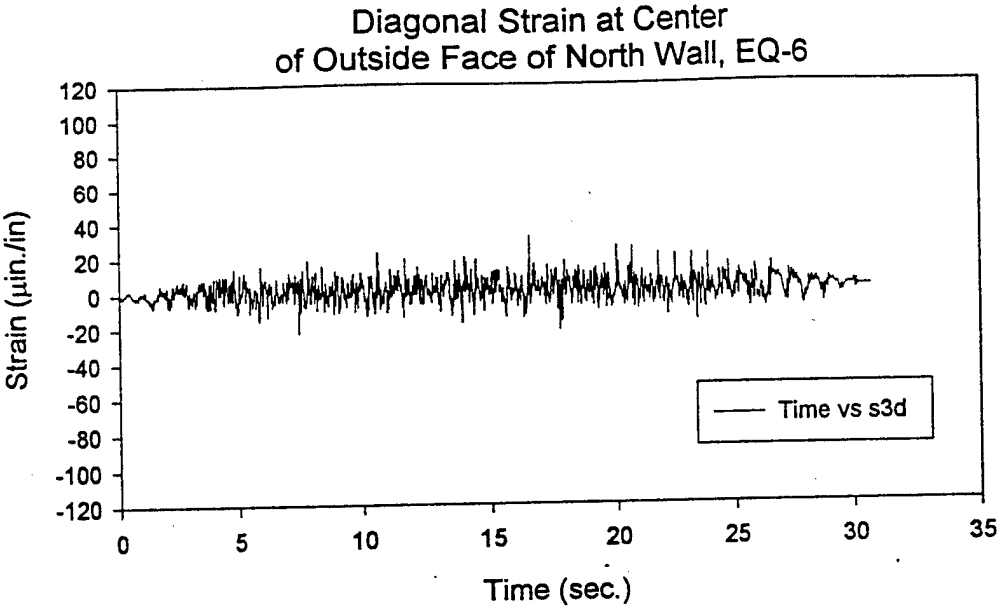
Diagonal Strain at Center
of Outside Face of North Wall, EQ-6
Strain (μin./in)
120
100
80
60
40
20
0
-20
-40
-60
-80
-100
-120
0
5
10
15
20
25
30
35
Time (sec.)
Time vs s3d

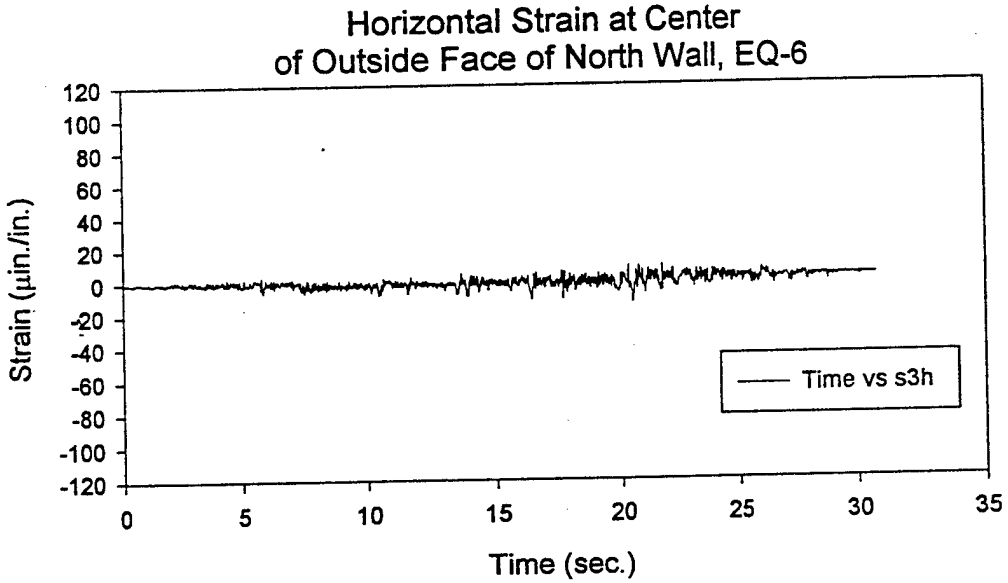
Horizontal Strain at Center
of Outside Face of North Wall, EQ-6
Strain (μin./in.)
120
100
80
60
40
20
0
-20
-40
-60
-80
-100
-120
0
5
10
15
20
25
30
35
Time (sec.)
Time vs s3h

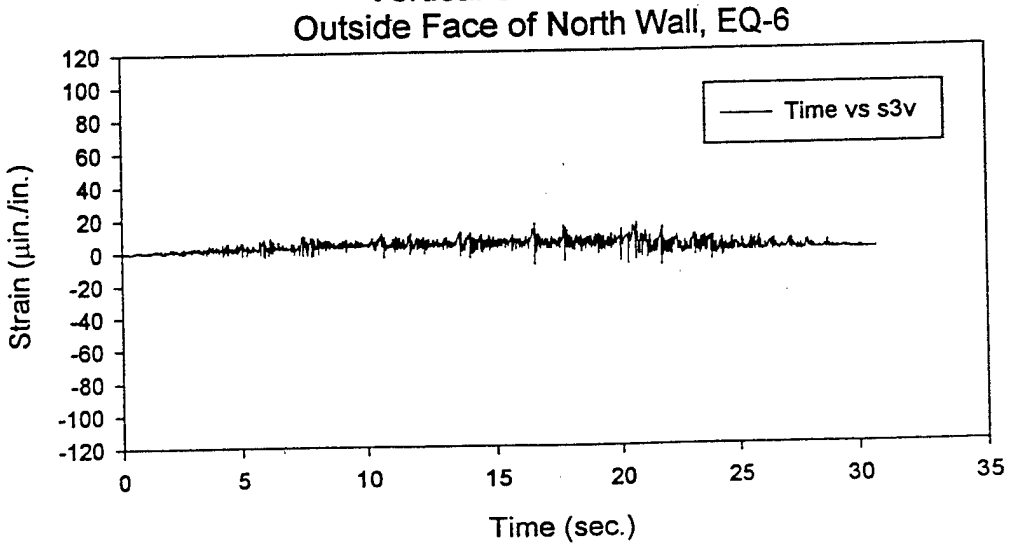
Vertical Strain at Center
Outside Face of North Wall, EQ-6
Strain (μin./in.)
120
100
80
60
40
20
0
-20
-40
-60
-80
-100
-120
0
5
10
15
20
25
30
35
Time (sec.)
Time vs s3v

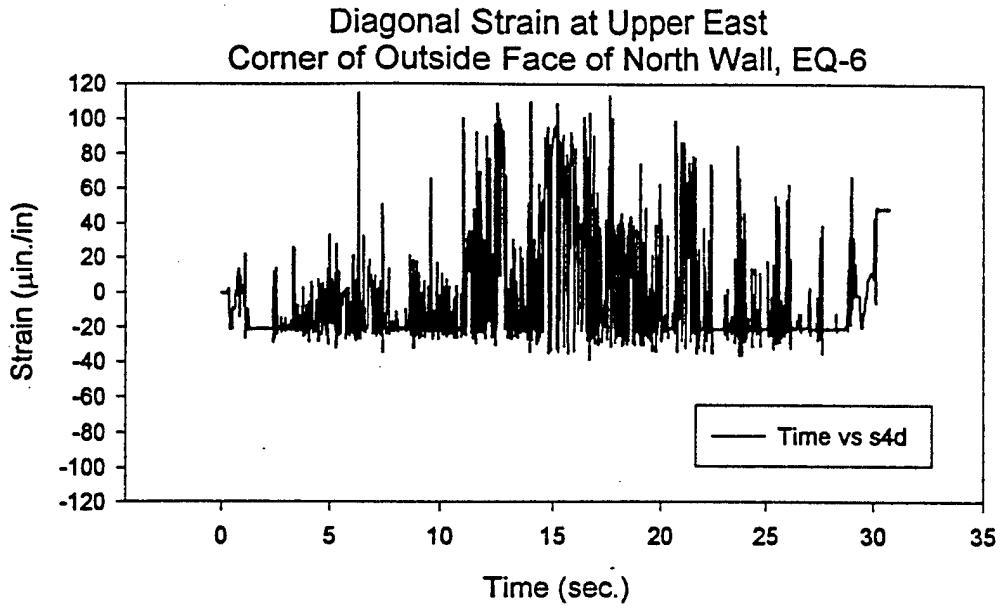
Diagonal Strain at Upper East
Corner of Outside Face of North Wall, EQ-6
Strain (µin./in)
Time (sec.)
Time vs s4d

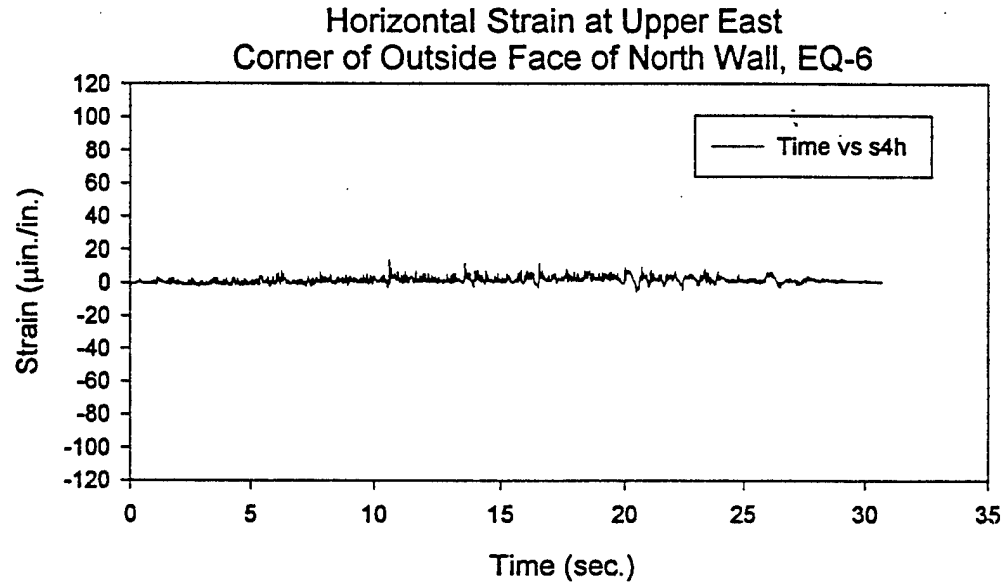
Horizontal Strain at Upper East
Corner of Outside Face of North Wall, EQ-6
Strain (µin./in.)
Time (sec.)
Time vs s4h

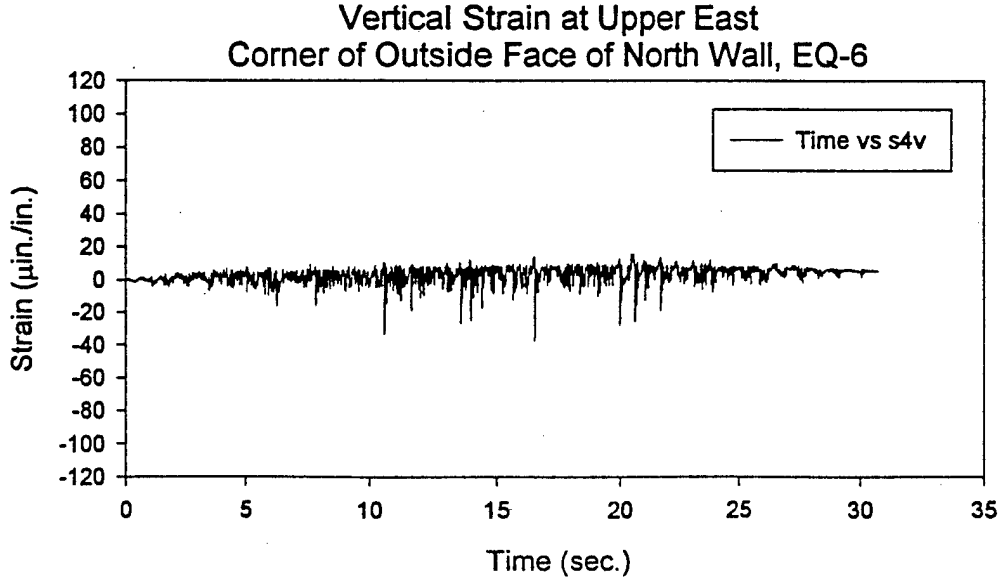
Vertical Strain at Upper East
Corner of Outside Face of North Wall, EQ-6
Strain (µin./in.)
Time (sec.)
Time vs s4v

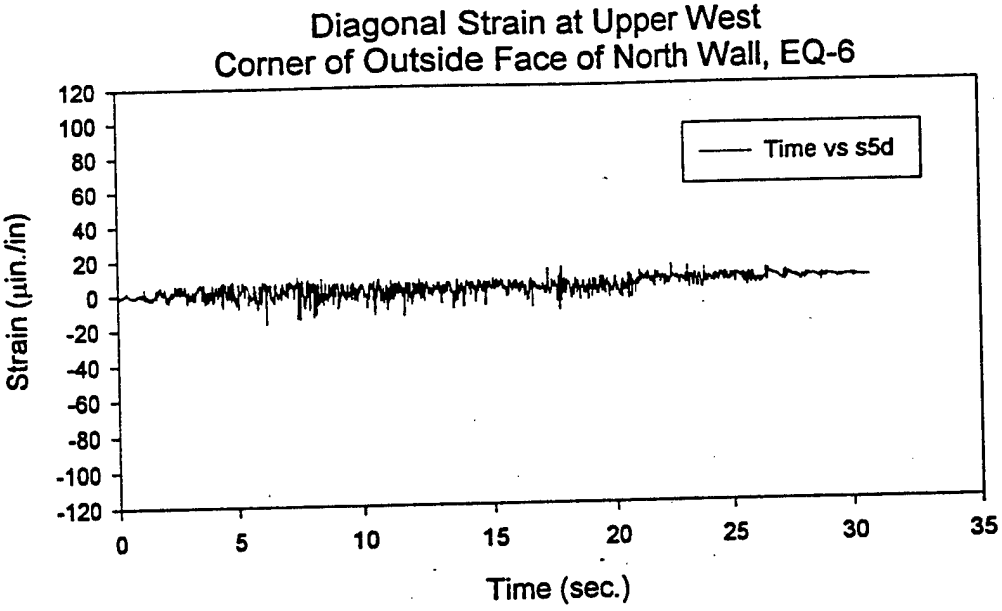
Diagonal Strain at Upper West
Corner of Outside Face of North Wall, EQ-6
Time vs s5d
Strain (µin./in)
120
100
80
60
40
20
0
-20
-40
-60
-80
-100
-120
0
5
10
15
20
25
30
35
Time (sec.)

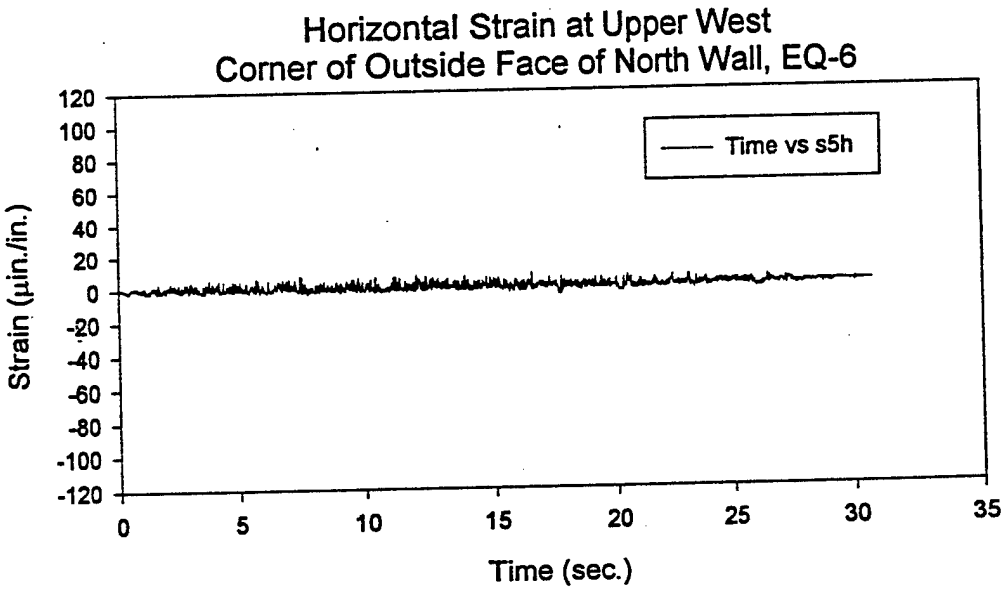
Horizontal Strain at Upper West
Corner of Outside Face of North Wall, EQ-6
Time vs s5h
Strain (µin./in.)
120
100
80
60
40
20
0
-20
-40
-60
-80
-100
-120
0
5
10
15
20
25
30
35
Time (sec.)

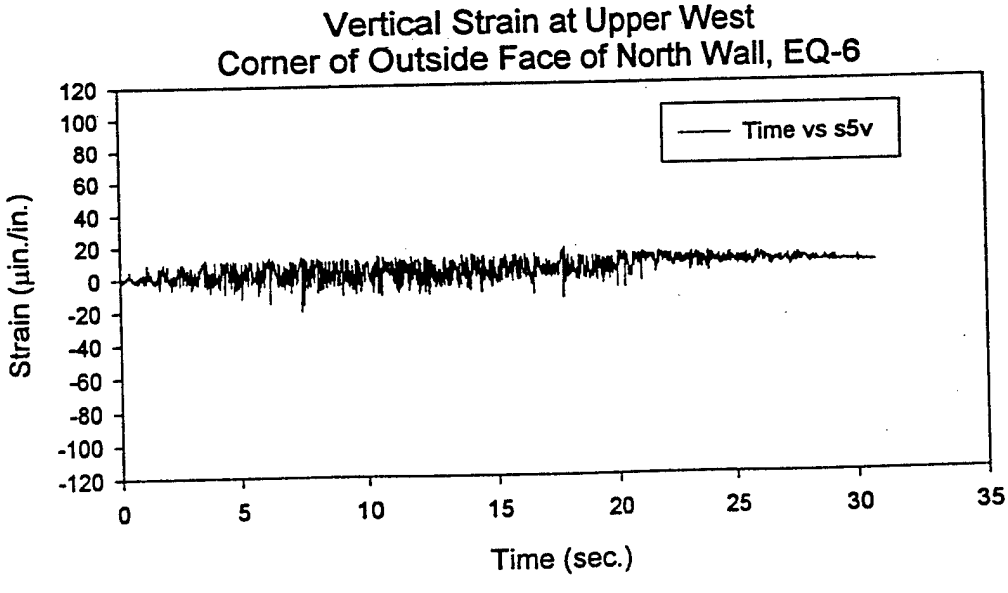
Vertical Strain at Upper West
Corner of Outside Face of North Wall, EQ-6
Time vs s5v
Strain (µin./in.)
120
100
80
60
40
20
0
-20
-40
-60
-80
-100
-120
0
5
10
15
20
25
30
35
Time (sec.)

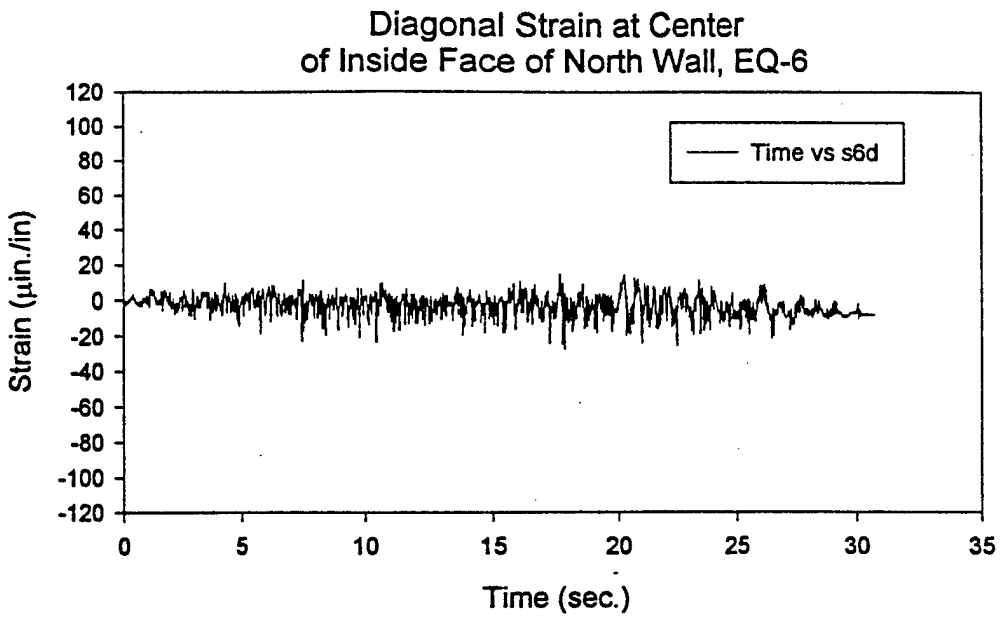
Diagonal Strain at Center
of Inside Face of North Wall, EQ-6
Time vs s6d
Strain (µin./in)
120
100
80
60
40
20
0
-20
-40
-60
-80
-100
-120
0
5
10
15
20
25
30
35
Time (sec.)

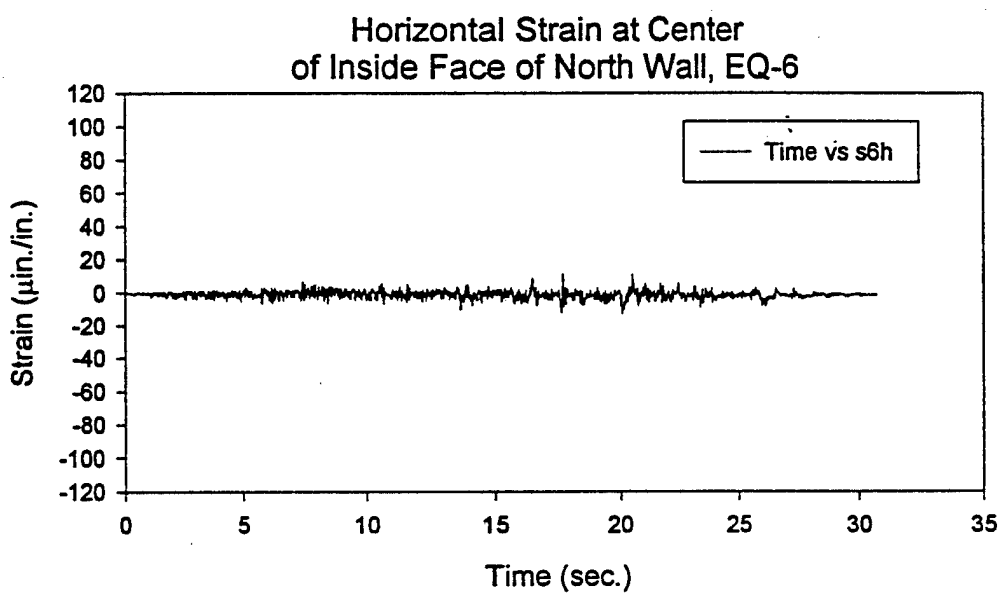
Horizontal Strain at Center
of Inside Face of North Wall, EQ-6
Time vs s6h
Strain (µin./in.)
120
100
80
60
40
20
0
-20
-40
-60
-80
-100
-120
0
5
10
15
20
25
30
35
Time (sec.)

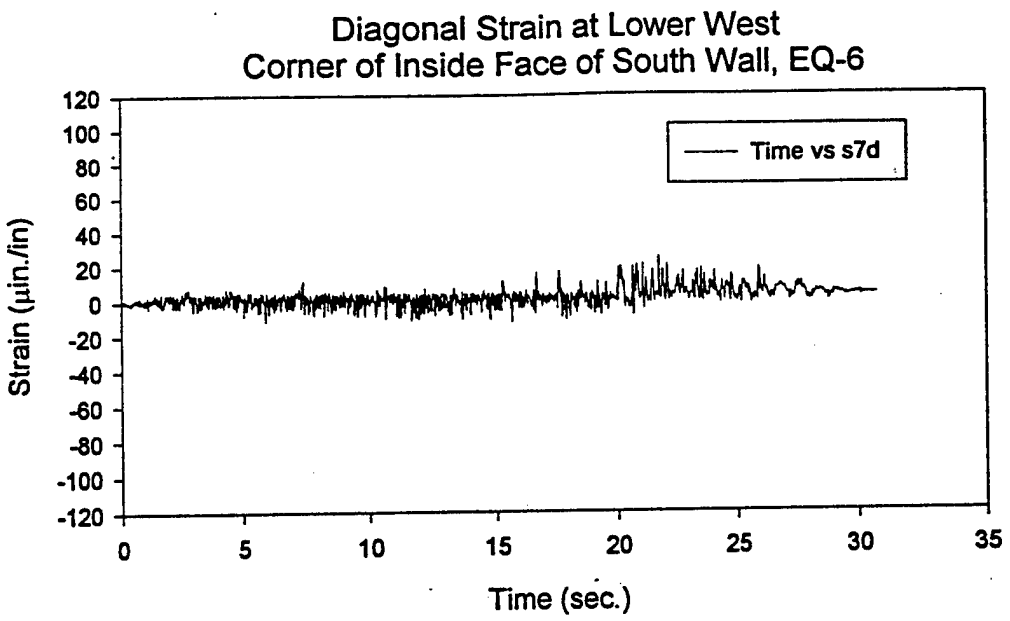
Diagonal Strain at Lower West
Corner of Inside Face of South Wall, EQ-6
Time vs s7d
Strain (µin./in)
120
100
80
60
40
20
0
-20
-40
-60
-80
-100
-120
0
5
10
15
20
25
30
35
Time (sec.)

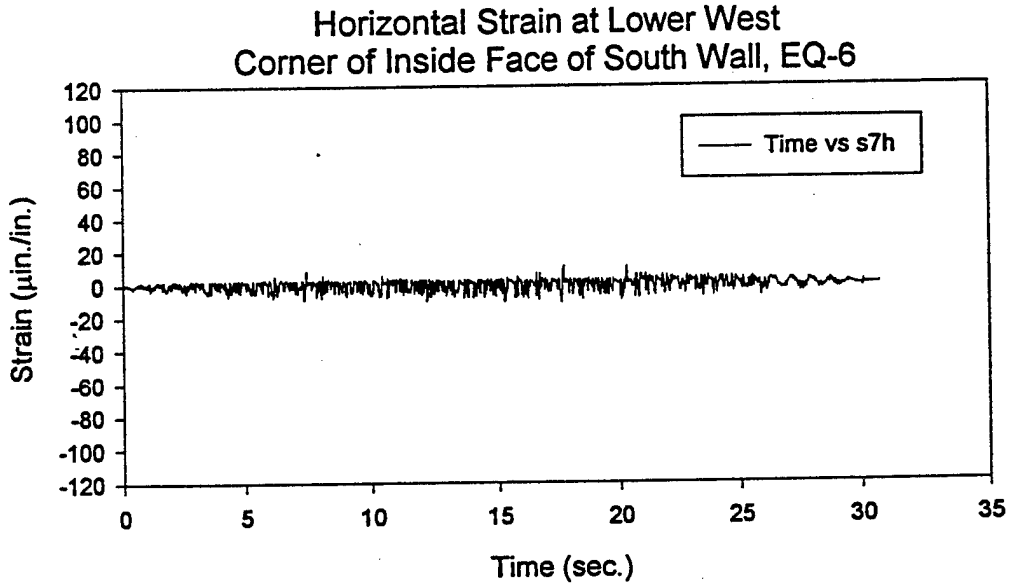
Horizontal Strain at Lower West
Corner of Inside Face of South Wall, EQ-6
Time vs s7h
Strain (µin./in.)
120
100
80
60
40
20
0
-20
-40
-60
-80
-100
-120
0
5
10
15
20
25
30
35
Time (sec.)

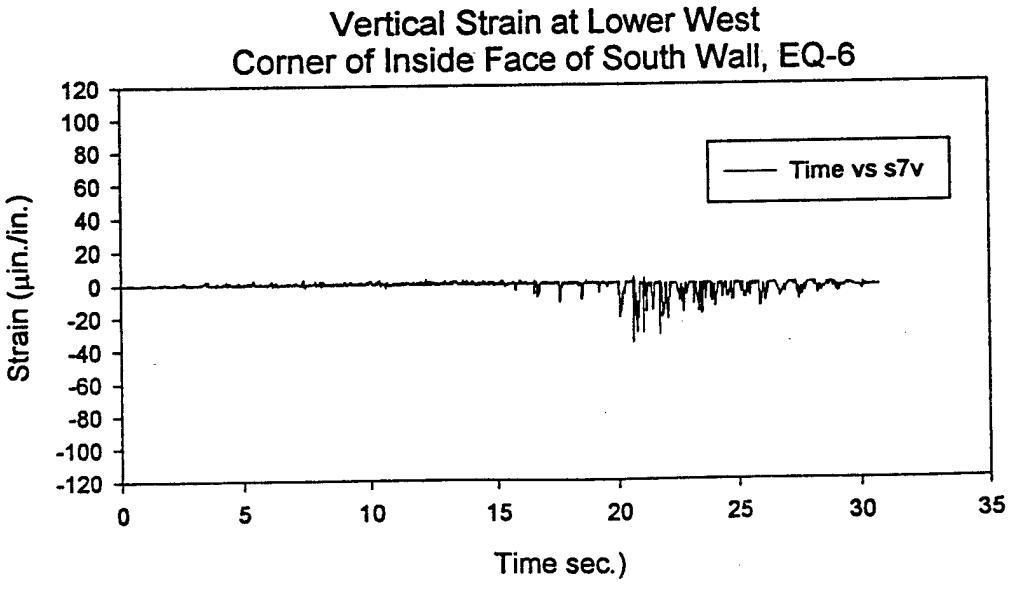
Vertical Strain at Lower West
Corner of Inside Face of South Wall, EQ-6
Time vs s7v
Strain (µin./in.)
120
100
80
60
40
20
0
-20
-40
-60
-80
-100
-120
0
5
10
15
20
25
30
35
Time sec.)

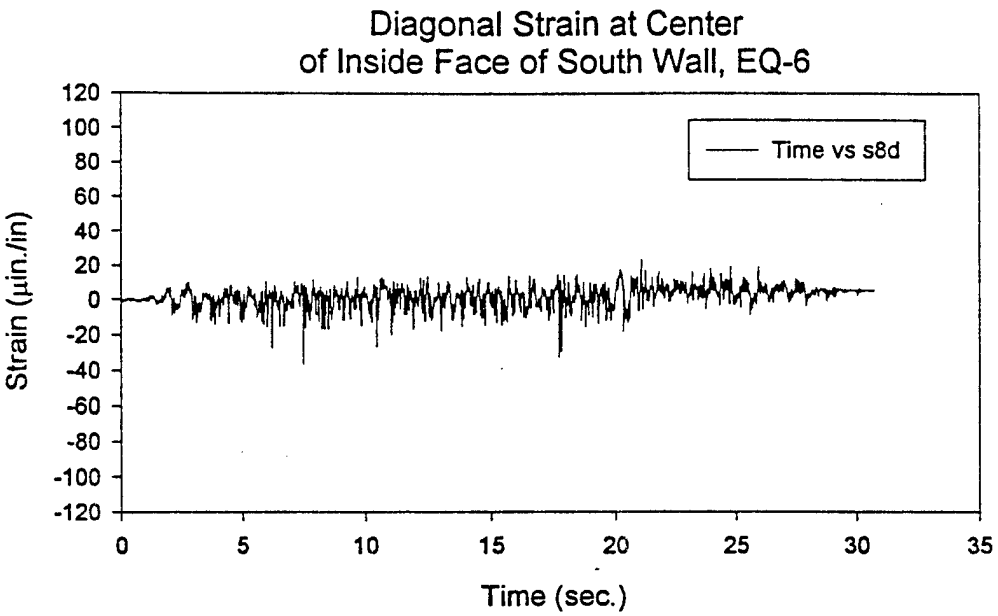
Diagonal Strain at Center
of Inside Face of South Wall, EQ-6
Time vs s8d
Strain (µin./in)
Time (sec.)

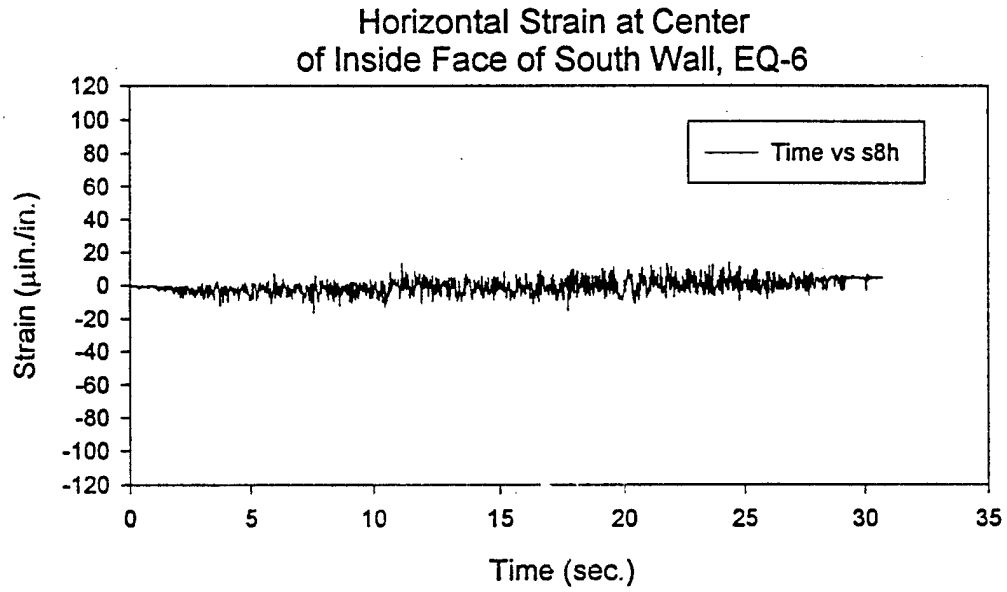
Horizontal Strain at Center
of Inside Face of South Wall, EQ-6
Time vs s8h
Strain (µin./in.)
Time (sec.)

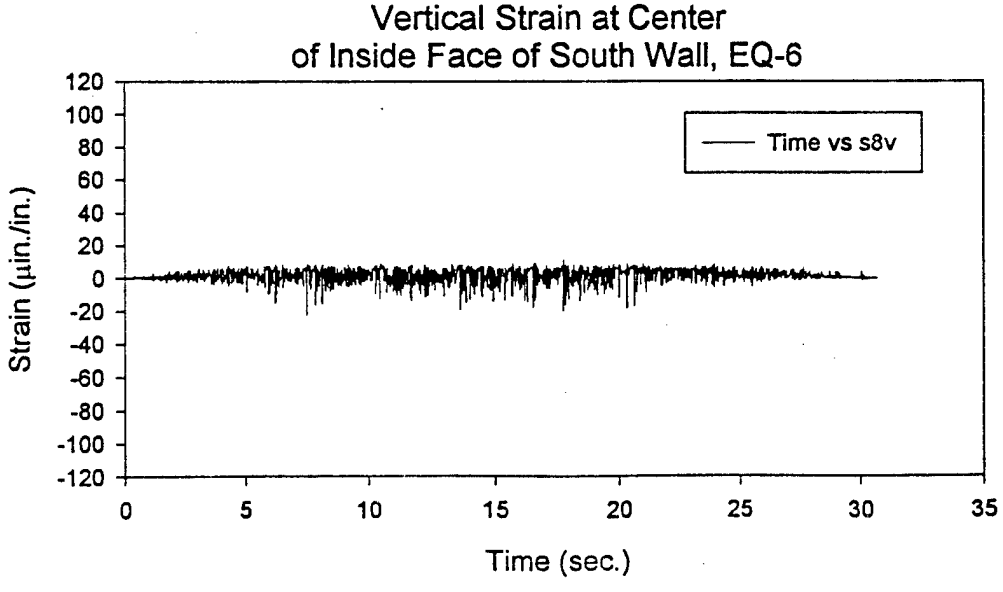
Vertical Strain at Center
of Inside Face of South Wall, EQ-6
Time vs s8v
Strain (µin./in.)
Time (sec.)

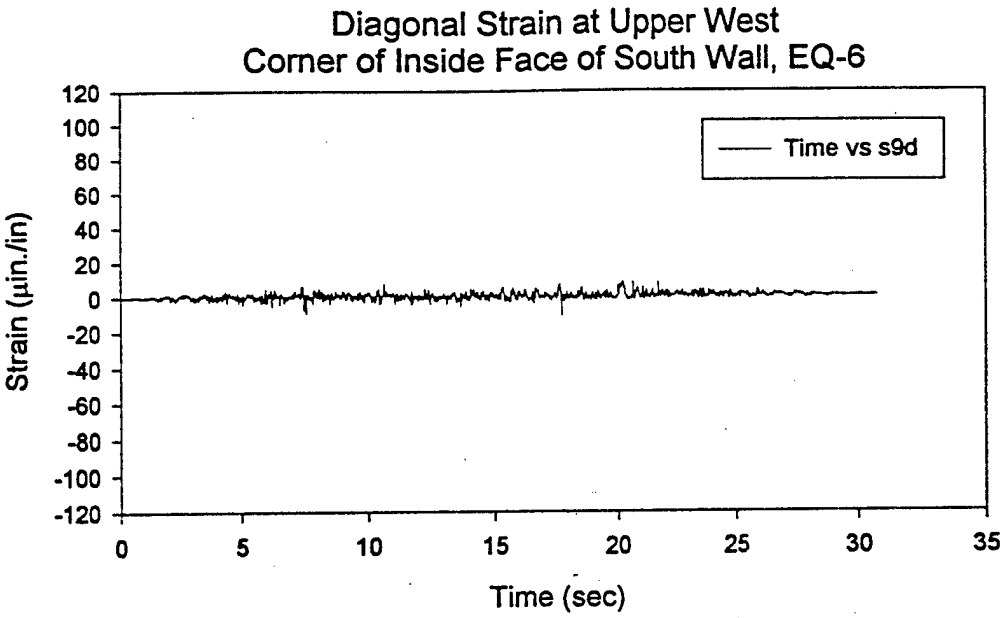
Diagonal Strain at Upper West
Corner of Inside Face of South Wall, EQ-6
Time vs s9d
Strain (µin./in)
Time (sec)

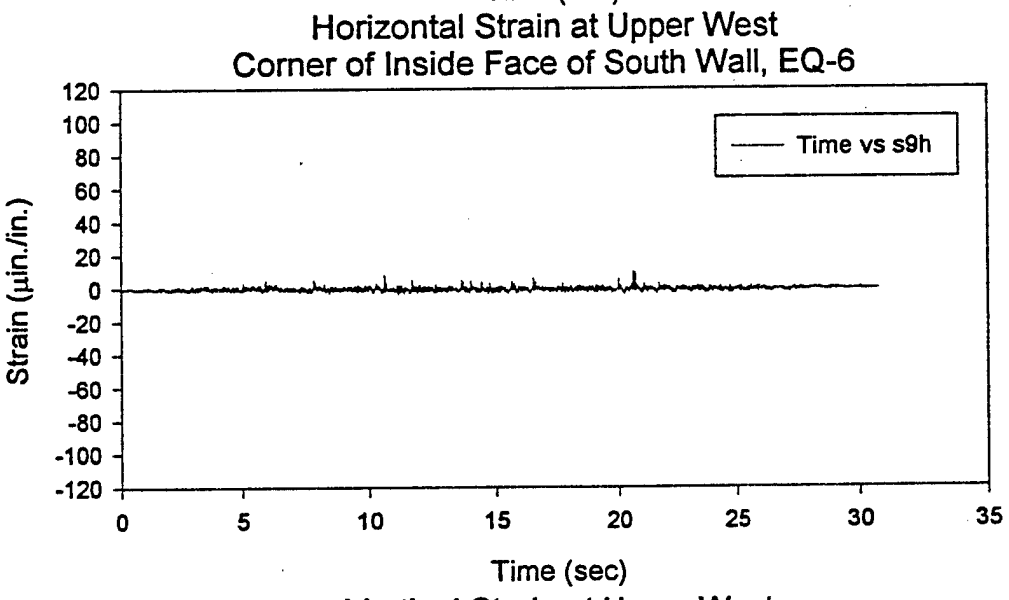
Horizontal Strain at Upper West
Corner of Inside Face of South Wall, EQ-6
Time vs s9h
Strain (µin./in.)
Time (sec)

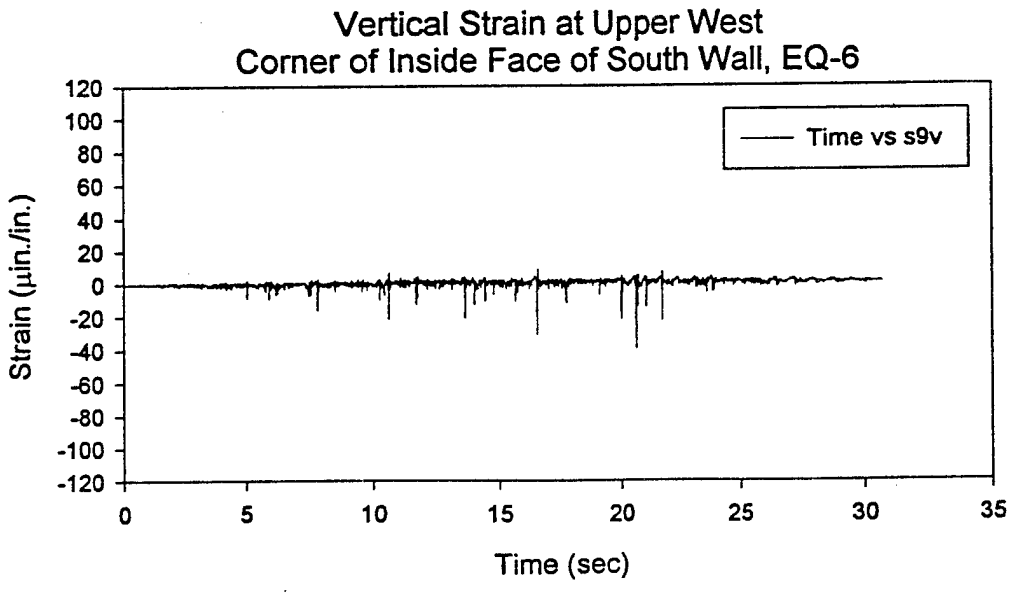
Vertical Strain at Upper West
Corner of Inside Face of South Wall, EQ-6
Time vs s9v
Strain (µin./in.)
Time (sec)

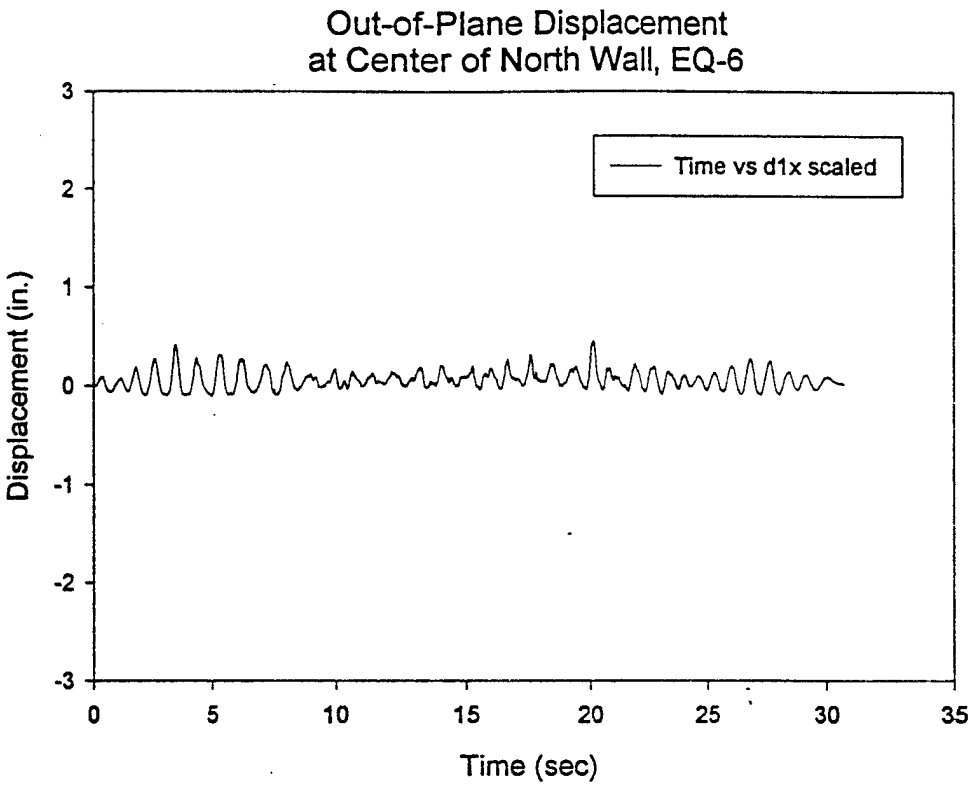
Out-of-Plane Displacement
at Center of North Wall, EQ-6
Time vs d1x scaled
Displacement (in.)
3
2
1
0
-1
-2
-3
0
5
10
15
20
25
30
35
Time (sec)

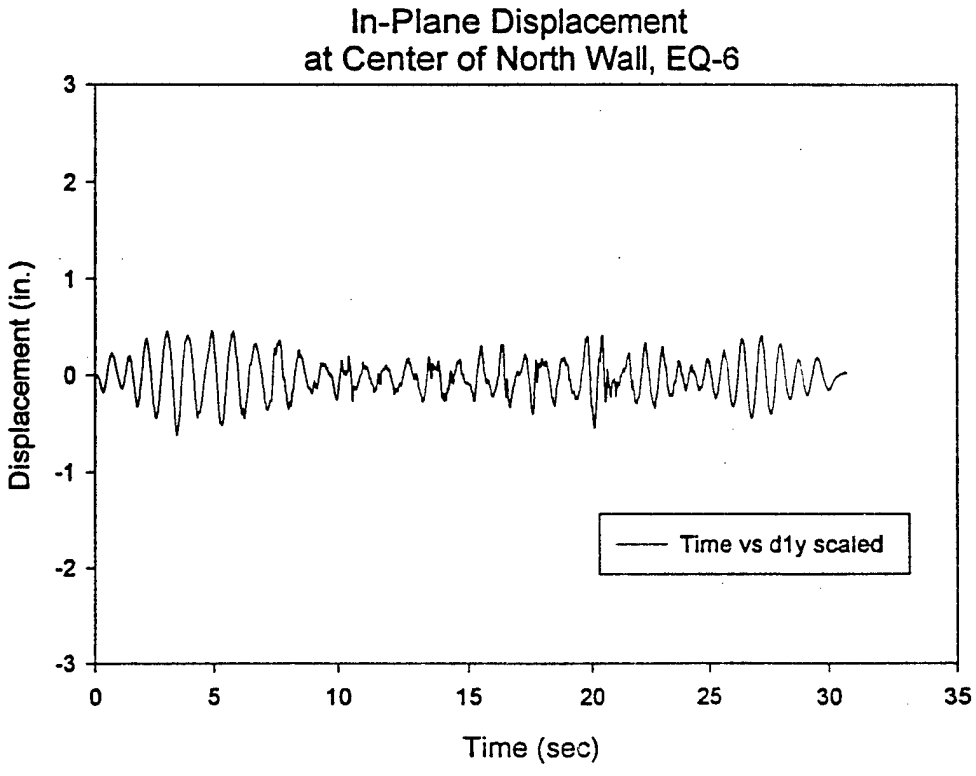
In-Plane Displacement
at Center of North Wall, EQ-6
Time vs d1y scaled
Displacement (in.)
3
2
1
0
-1
-2
-3
0
5
10
15
20
25
30
35
Time (sec)

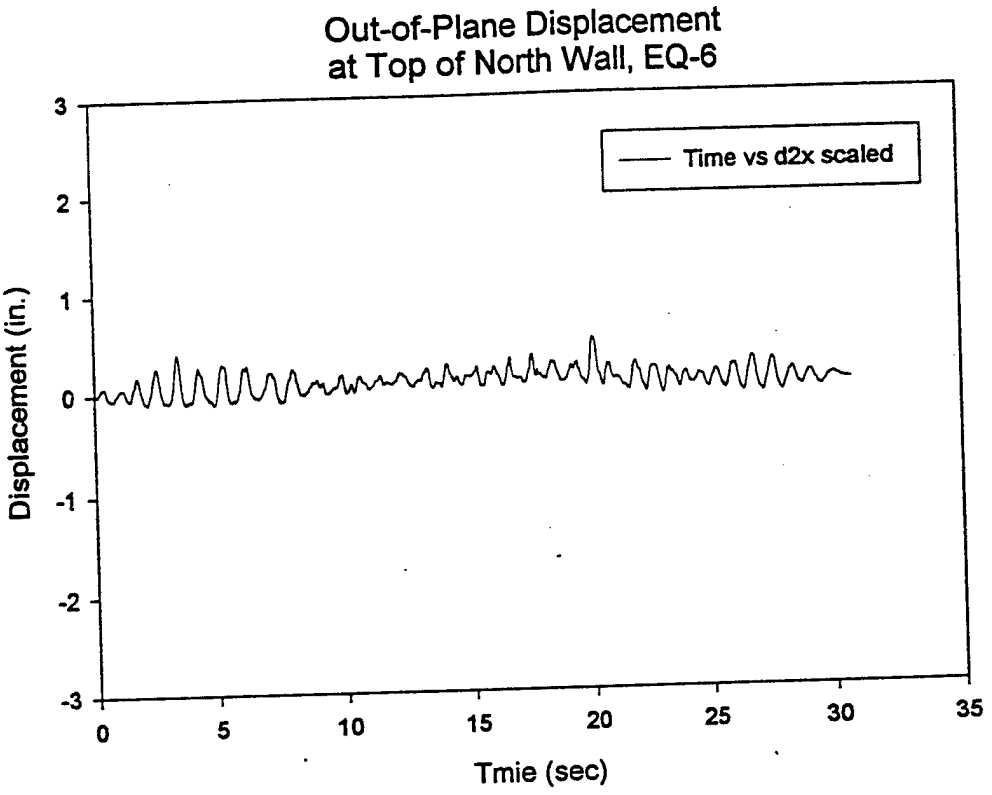
Out-of-Plane Displacement
at Top of North Wall, EQ-6
Time vs d2x scaled
Displacement (in.)
3
2
1
0
-1
-2
-3
0
5
10
15
20
25
30
35
Tmie (sec)

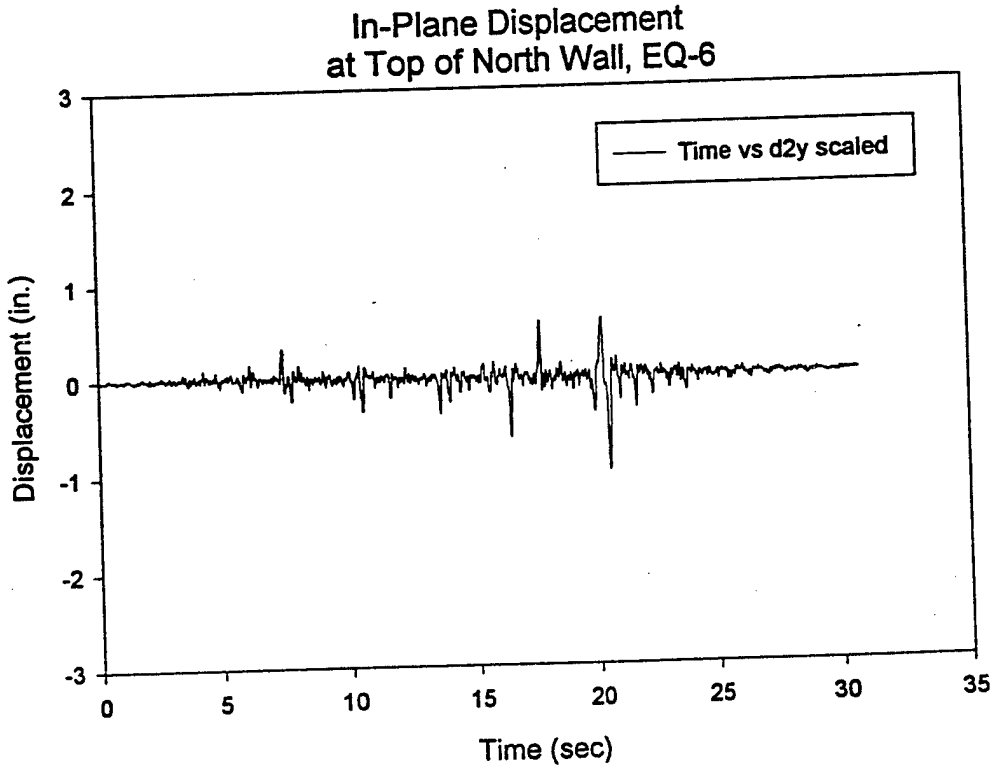
In-Plane Displacement
at Top of North Wall, EQ-6
Time vs d2y scaled
Displacement (in.)
3
2
1
0
-1
-2
-3
0
5
10
15
20
25
30
35
Time (sec)

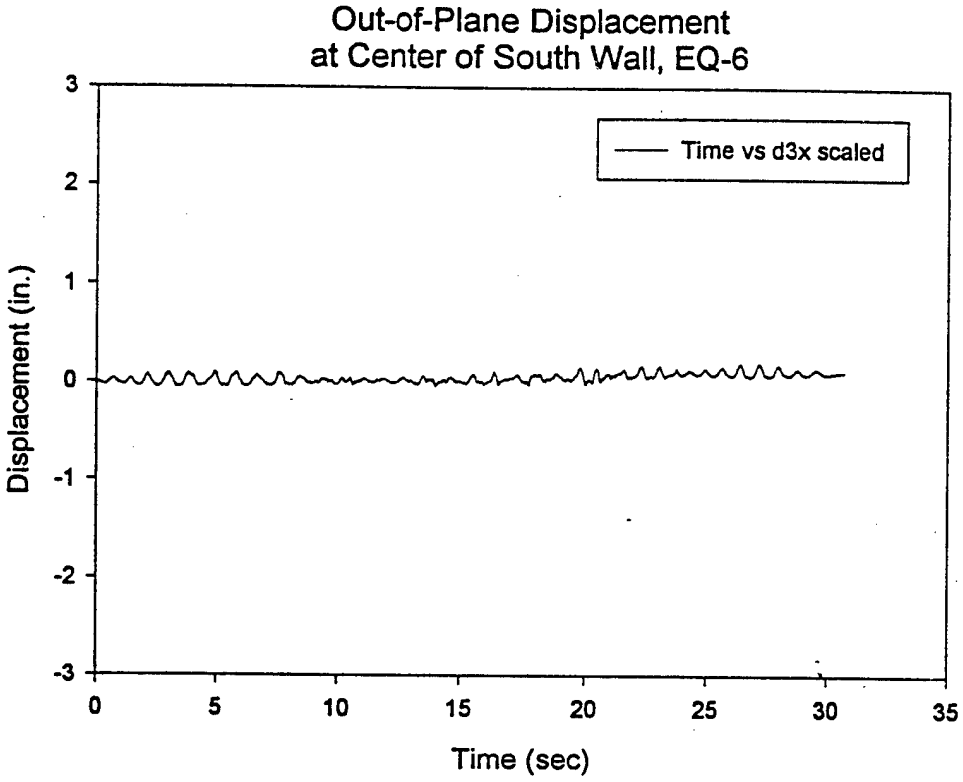
Out-of-Plane Displacement
at Center of South Wall, EQ-6
Time vs d3x scaled
Displacement (in.)
3
2
1
0
-1
-2
-3
0
5
10
15
20
25
30
35
Time (sec)

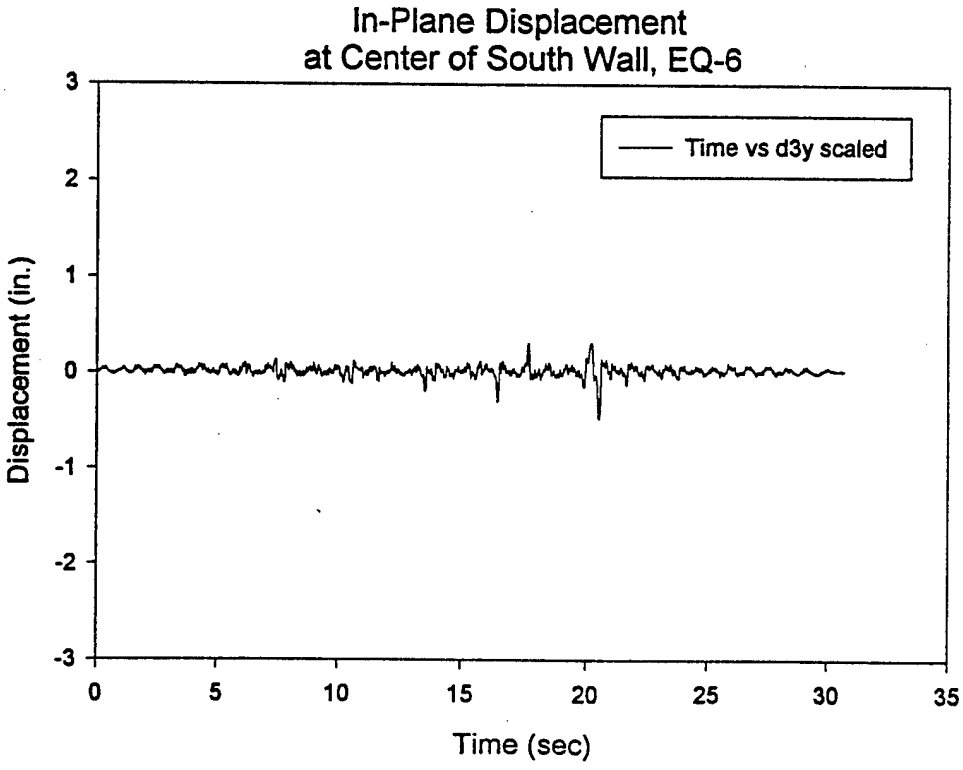
In-Plane Displacement
at Center of South Wall, EQ-6
Time vs d3y scaled
Displacement (in.)
3
2
1
0
-1
-2
-3
0
5
10
15
20
25
30
35
Time (sec)

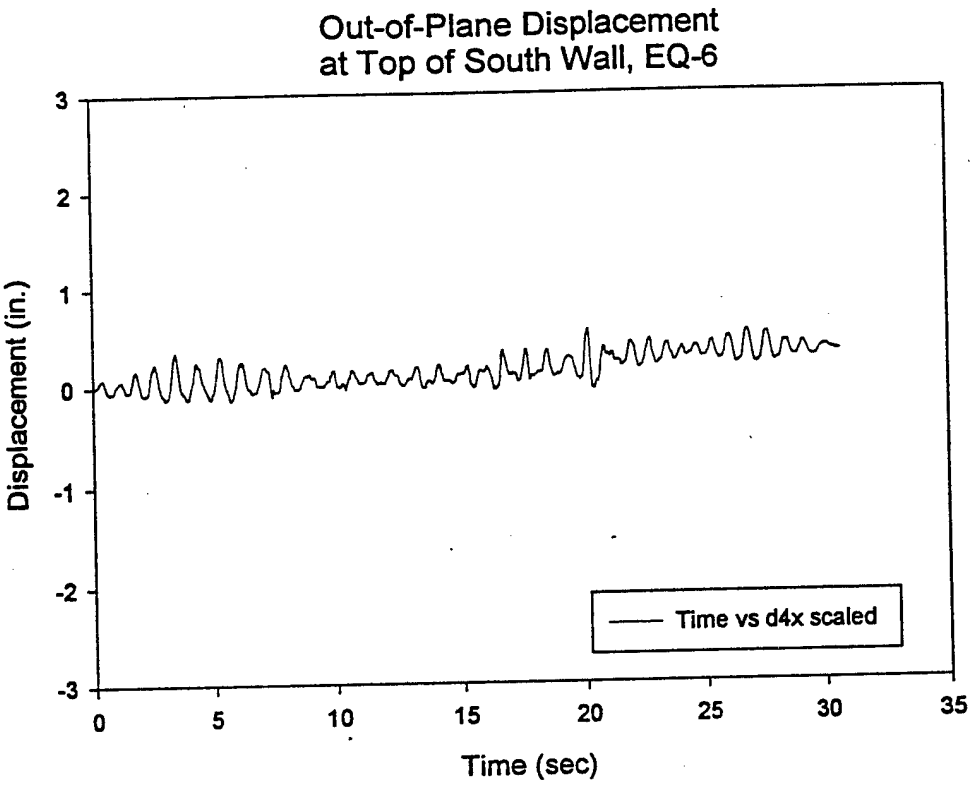
Out-of-Plane Displacement
at Top of South Wall, EQ-6
Displacement (in.)
3
2
1
0
-1
-2
-3
0
5
10
15
20
25
30
35
Time (sec)
Time vs d4x scaled

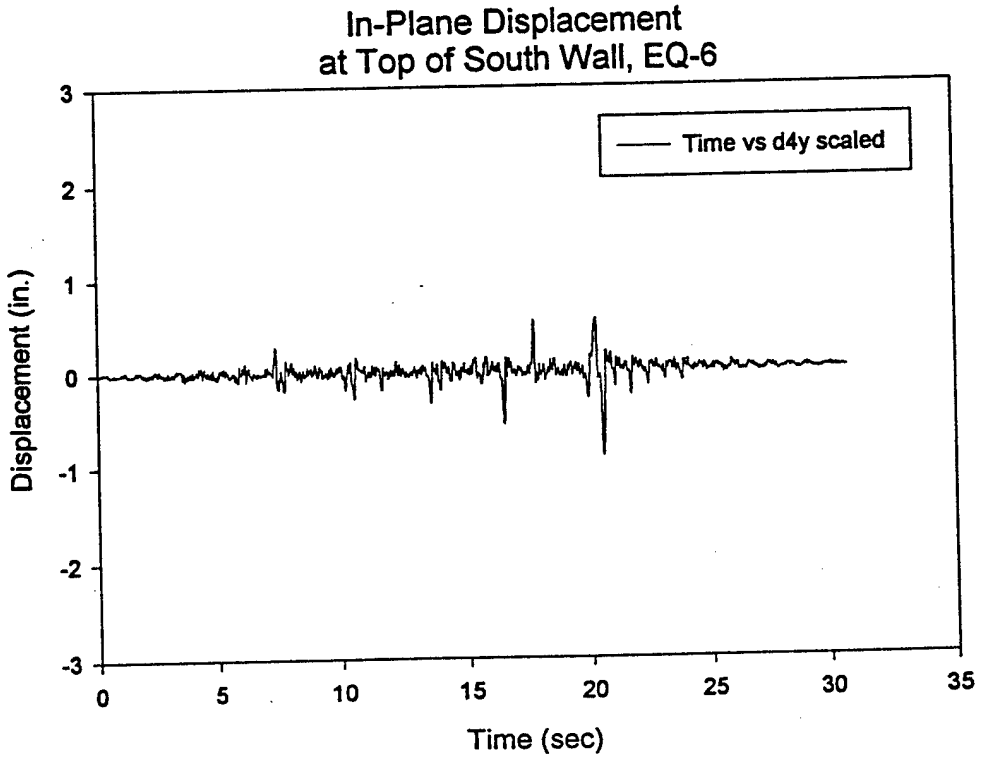
In-Plane Displacement
at Top of South Wall, EQ-6
Displacement (in.)
3
2
1
0
-1
-2
-3
0
5
10
15
20
25
30
35
Time (sec)
Time vs d4y scaled

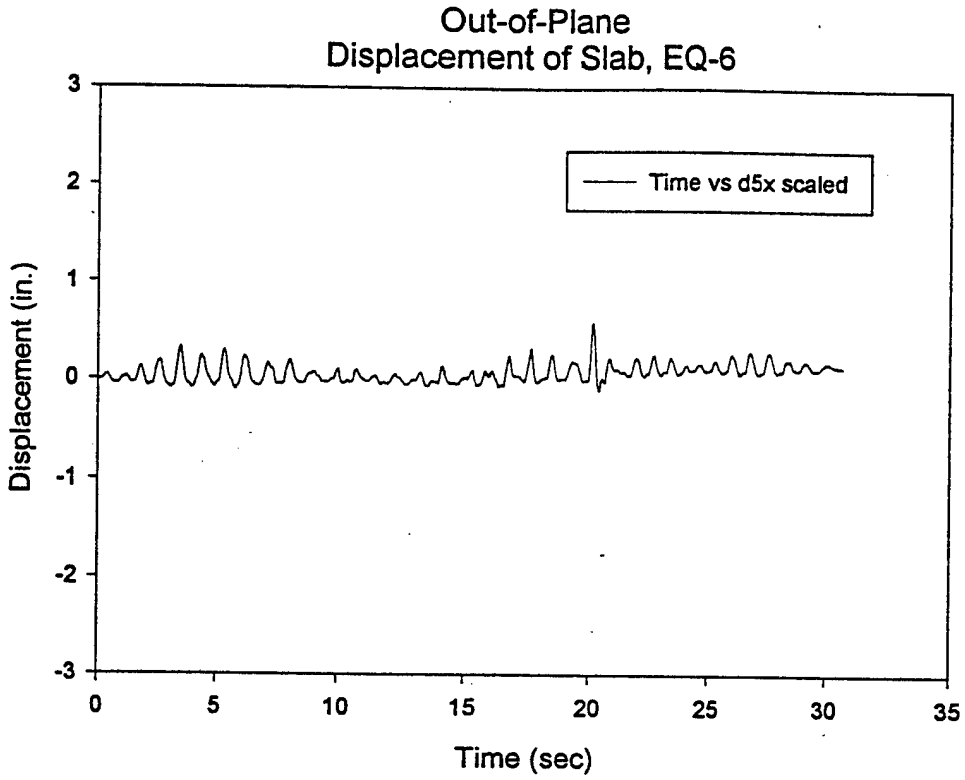
Out-of-Plane
Displacement of Slab, EQ-6
Time vs d5x scaled
Displacement (in.)
3
2
1
0
-1
-2
-3
0
5
10
15
20
25
30
35
Time (sec)

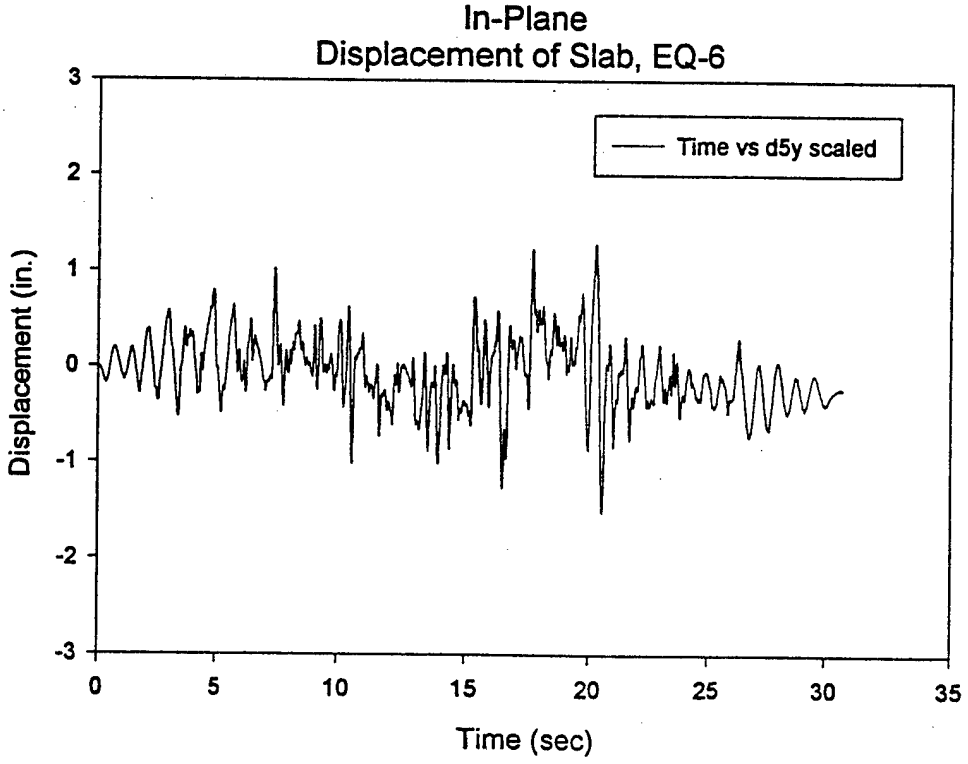
In-Plane
Displacement of Slab, EQ-6
Time vs d5y scaled
Displacement (in.)
3
2
1
0
-1
-2
-3
0
5
10
15
20
25
30
35
Time (sec)

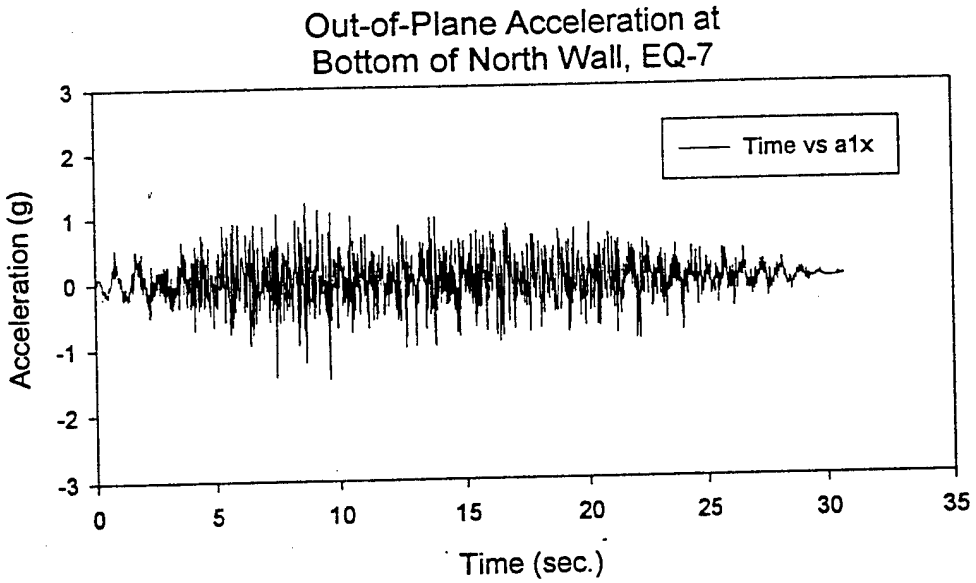
Out-of-Plane Acceleration at
Bottom of North Wall, EQ-7
Time vs a1x
Acceleration (g)
3
2
1
0
-1
-2
-3
0
5
10
15
20
25
30
35
Time (sec.)

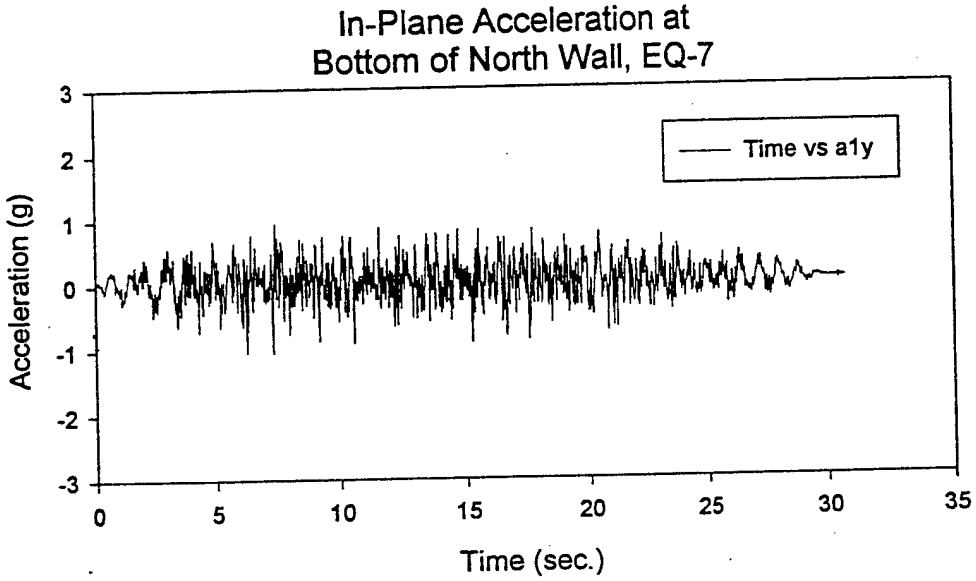
In-Plane Acceleration at
Bottom of North Wall, EQ-7
Time vs a1y
Acceleration (g)
3
2
1
0
-1
-2
-3
0
5
10
15
20
25
30
35
Time (sec.)

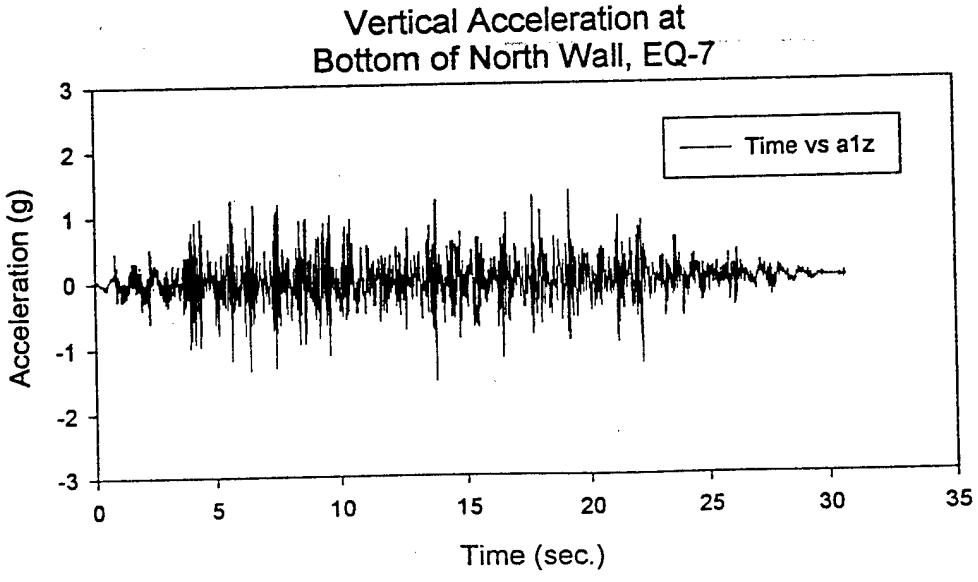
Vertical Acceleration at
Bottom of North Wall, EQ-7
Time vs a1z
Acceleration (g)
3
2
1
0
-1
-2
-3
0
5
10
15
20
25
30
35
Time (sec.)

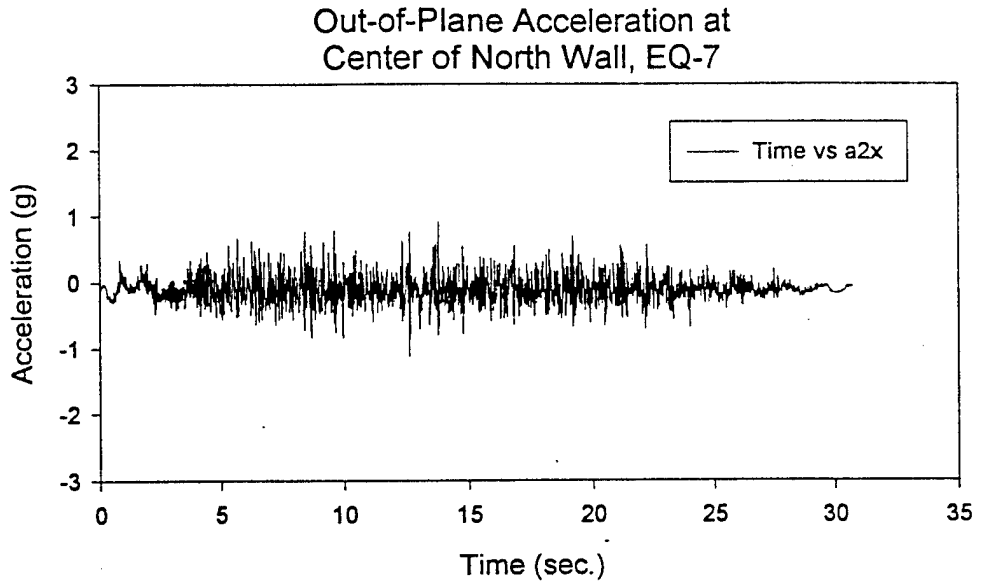
Out-of-Plane Acceleration at
Center of North Wall, EQ-7
Time vs a2x
Acceleration (g)
Time (sec.)

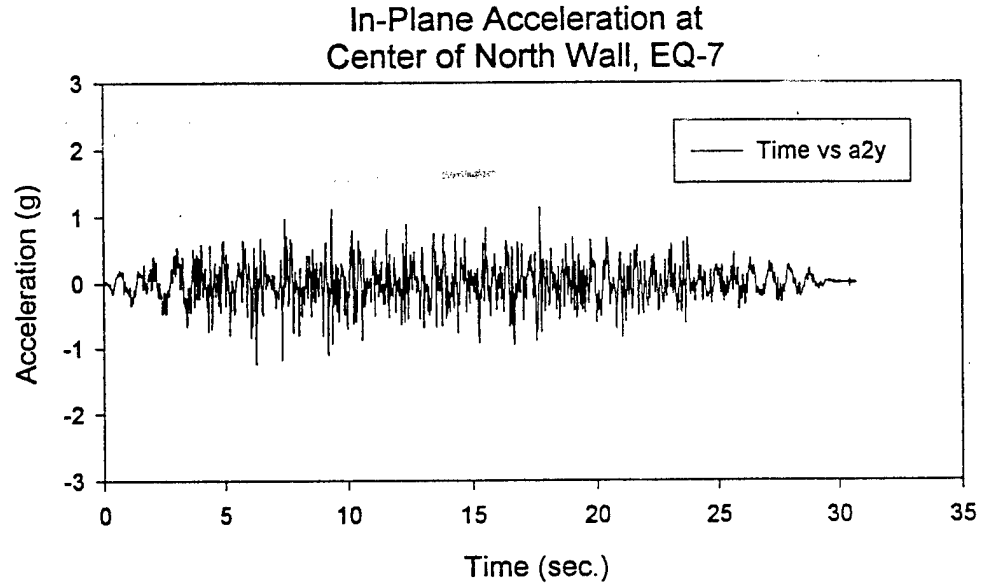
In-Plane Acceleration at
Center of North Wall, EQ-7
Time vs a2y
Acceleration (g)
Time (sec.)

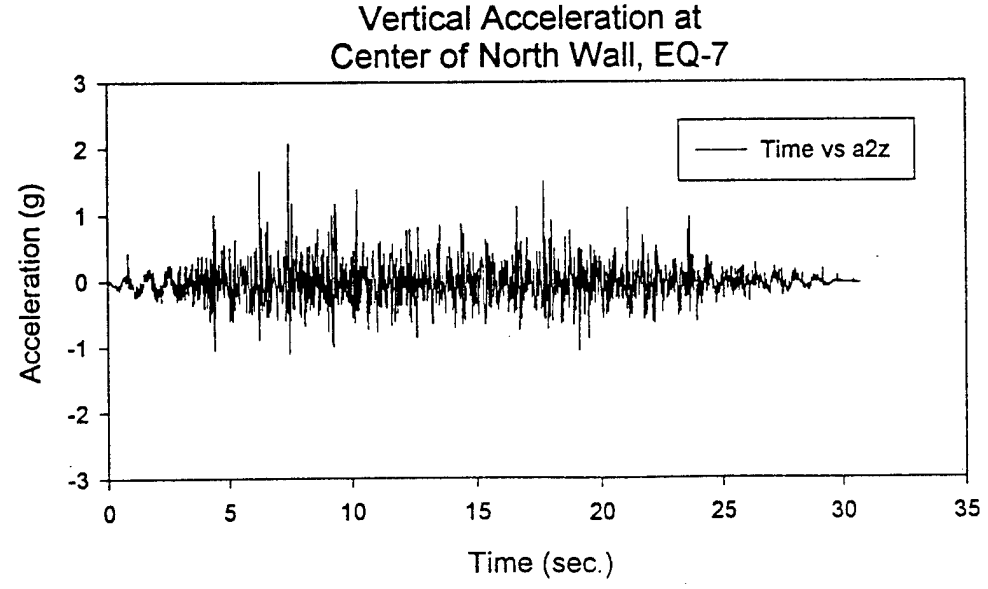
Vertical Acceleration at
Center of North Wall, EQ-7
Time vs a2z
Acceleration (g)
Time (sec.)

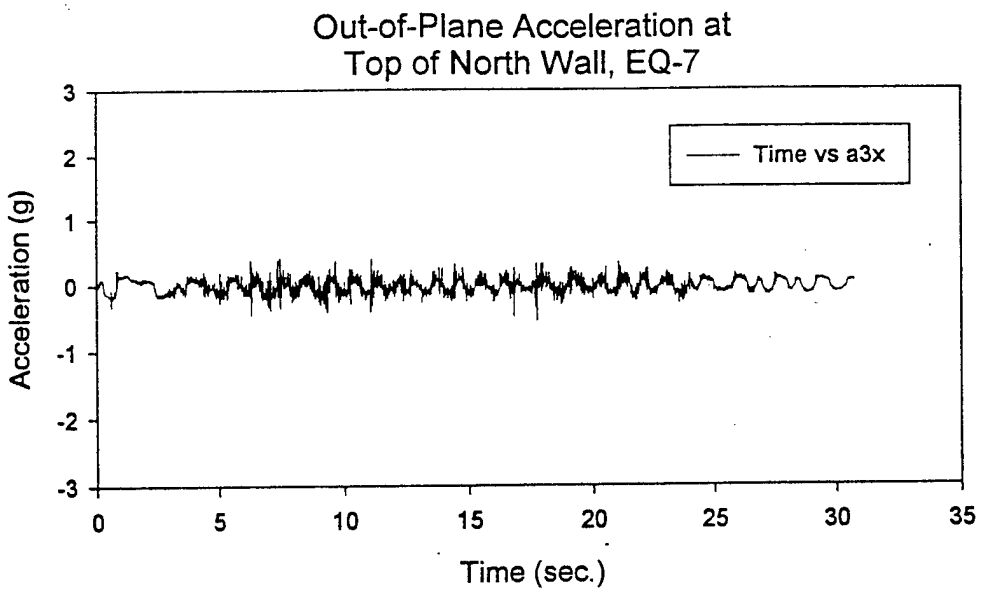
Out-of-Plane Acceleration at
Top of North Wall, EQ-7
Time vs a3x
Acceleration (g)
3
2
1
0
-1
-2
-3
0
5
10
15
20
25
30
35
Time (sec.)

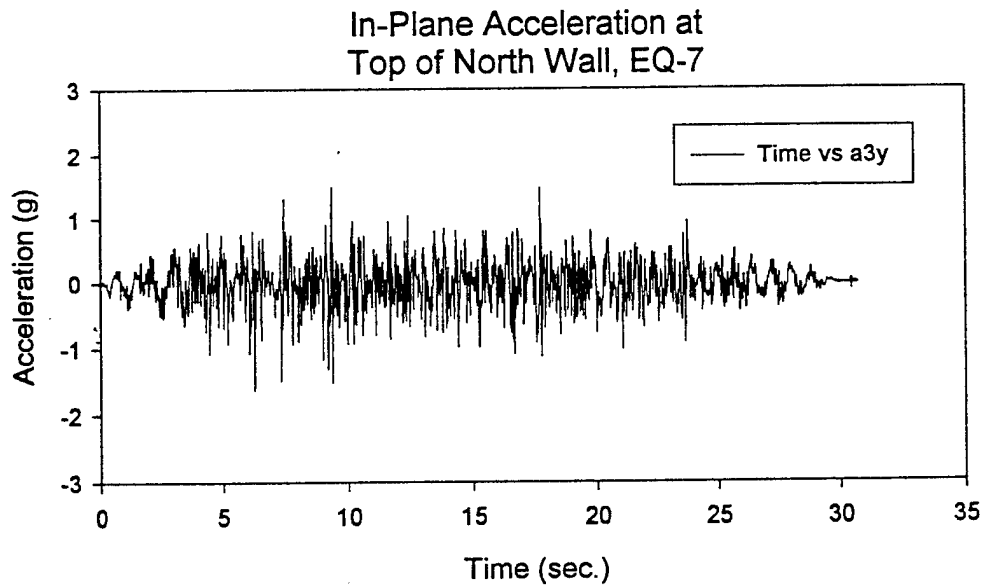
In-Plane Acceleration at
Top of North Wall, EQ-7
Time vs a3y
Acceleration (g)
3
2
1
0
-1
-2
-3
0
5
10
15
20
25
30
35
Time (sec.)

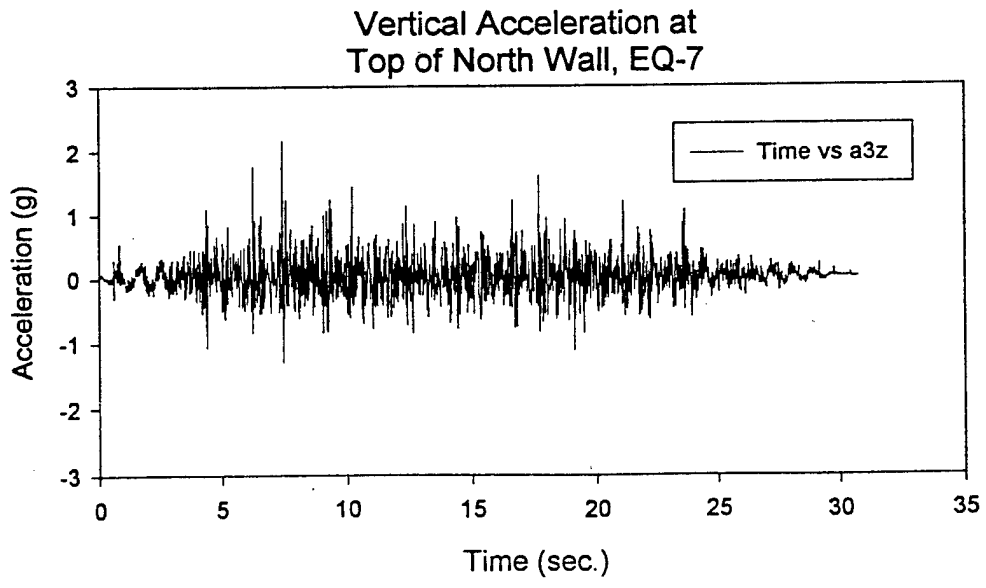
Vertical Acceleration at
Top of North Wall, EQ-7
Time vs a3z
Acceleration (g)
3
2
1
0
-1
-2
-3
0
5
10
15
20
25
30
35
Time (sec.)

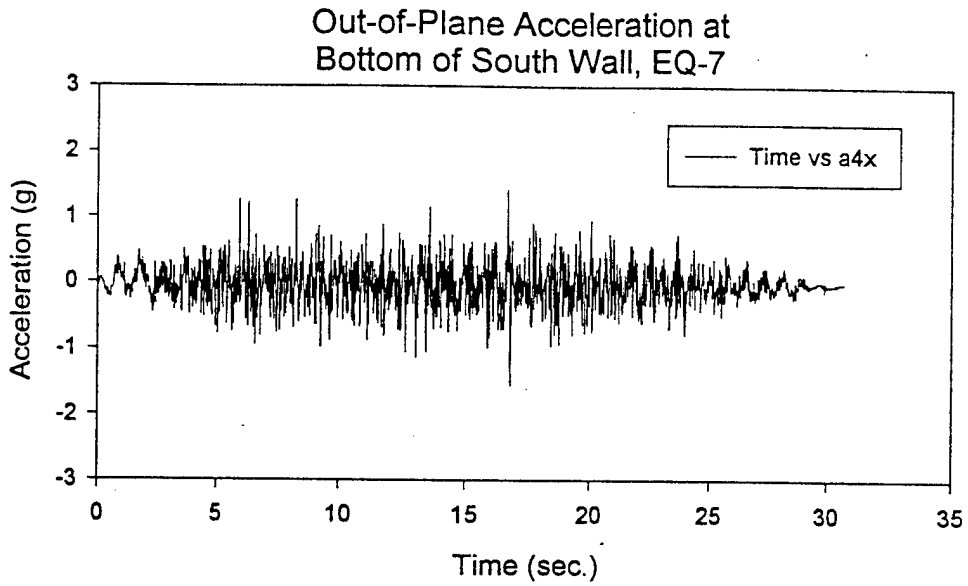
Out-of-Plane Acceleration at
Bottom of South Wall, EQ-7
Time vs a4x
Acceleration (g)
Time (sec.)

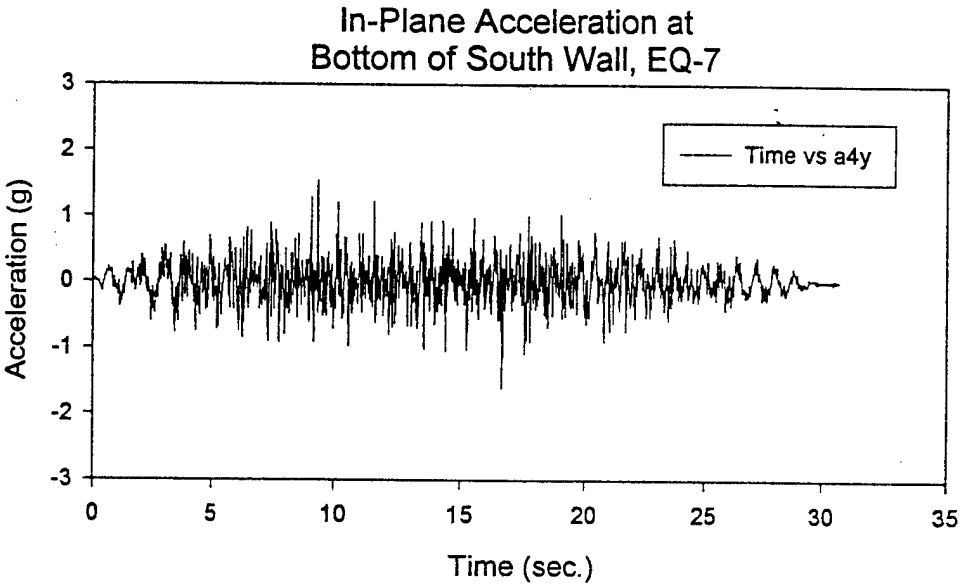
In-Plane Acceleration at
Bottom of South Wall, EQ-7
Time vs a4y
Acceleration (g)
Time (sec.)

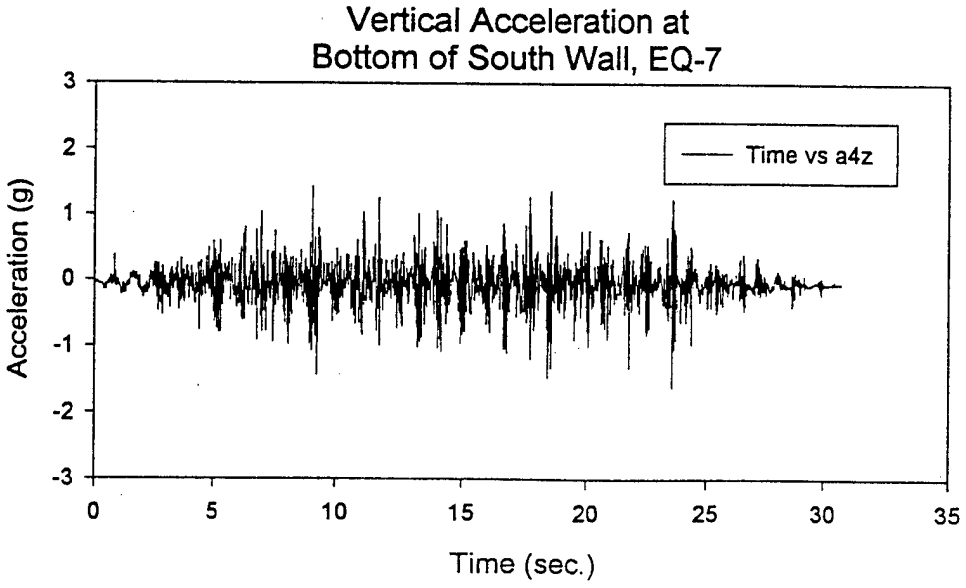
Vertical Acceleration at
Bottom of South Wall, EQ-7
Time vs a4z
Acceleration (g)
Time (sec.)

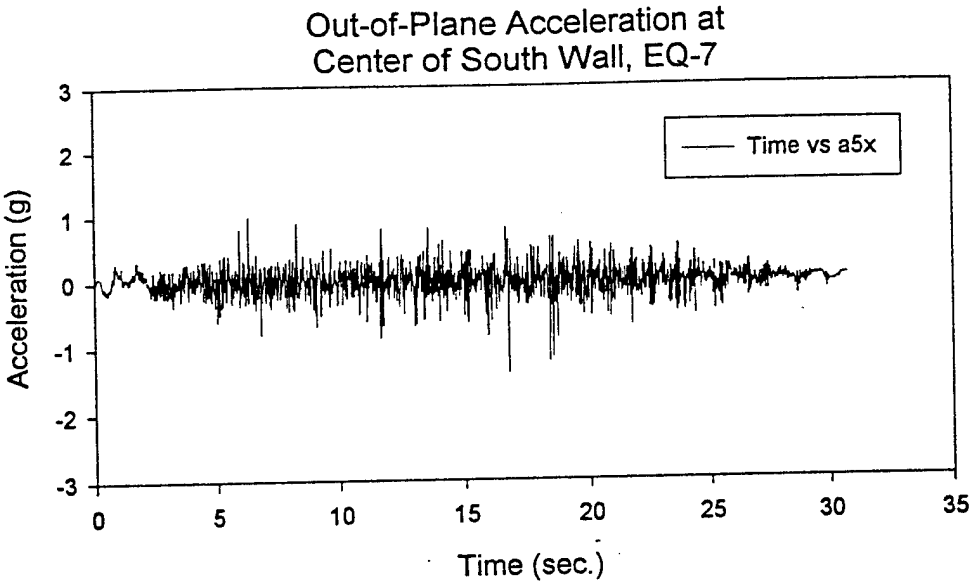
Out-of-Plane Acceleration at
Center of South Wall, EQ-7
Time vs a5x
Acceleration (g)
3
2
1
0
-1
-2
-3
0
5
10
15
20
25
30
35
Time (sec.)

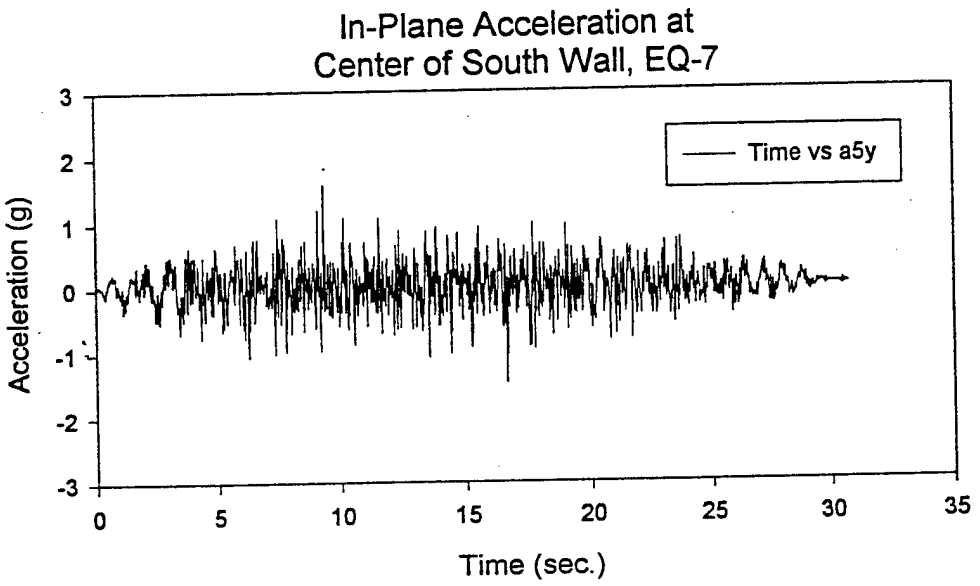
In-Plane Acceleration at
Center of South Wall, EQ-7
Time vs a5y
Acceleration (g)
3
2
1
0
-1
-2
-3
0
5
10
15
20
25
30
35
Time (sec.)

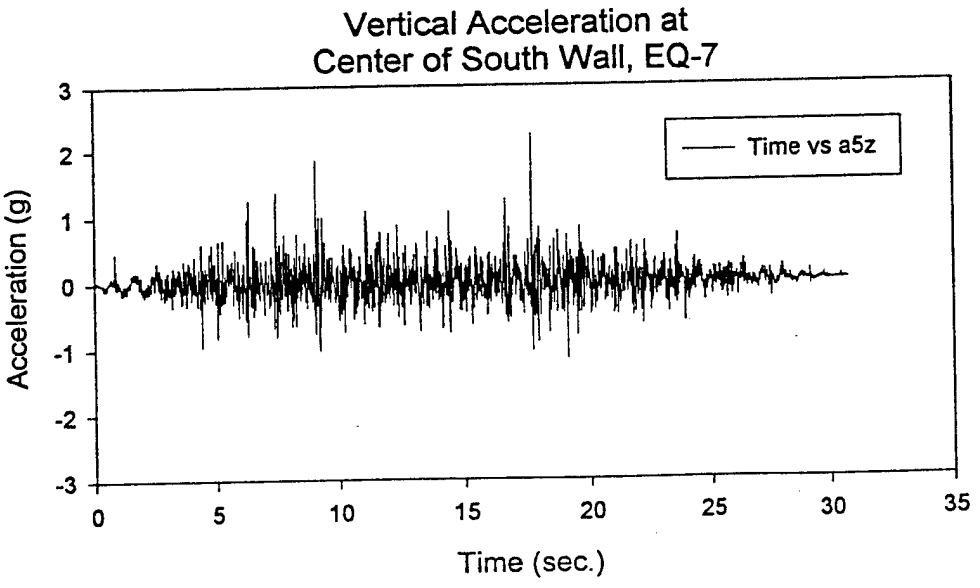
Vertical Acceleration at
Center of South Wall, EQ-7
Time vs a5z
Acceleration (g)
3
2
1
0
-1
-2
-3
0
5
10
15
20
25
30
35
Time (sec.)

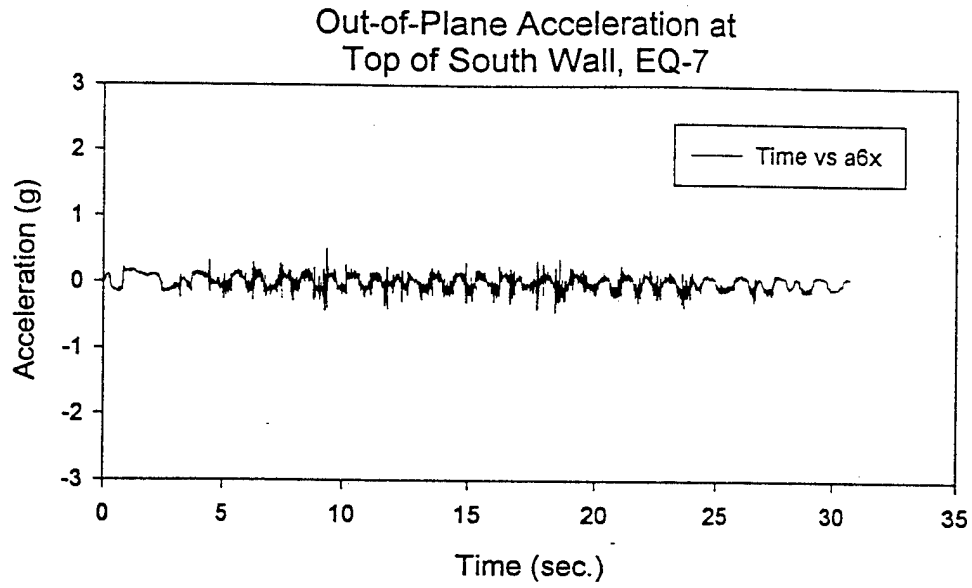
Out-of-Plane Acceleration at
Top of South Wall, EQ-7
Time vs a6x
Acceleration (g)
Time (sec.)

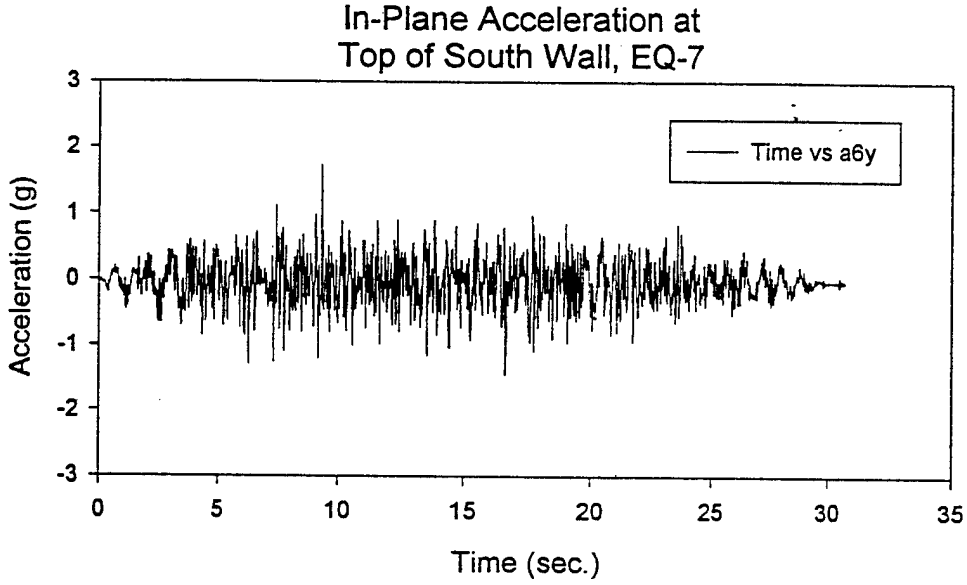
In-Plane Acceleration at
Top of South Wall, EQ-7
Time vs a6y
Acceleration (g)
Time (sec.)

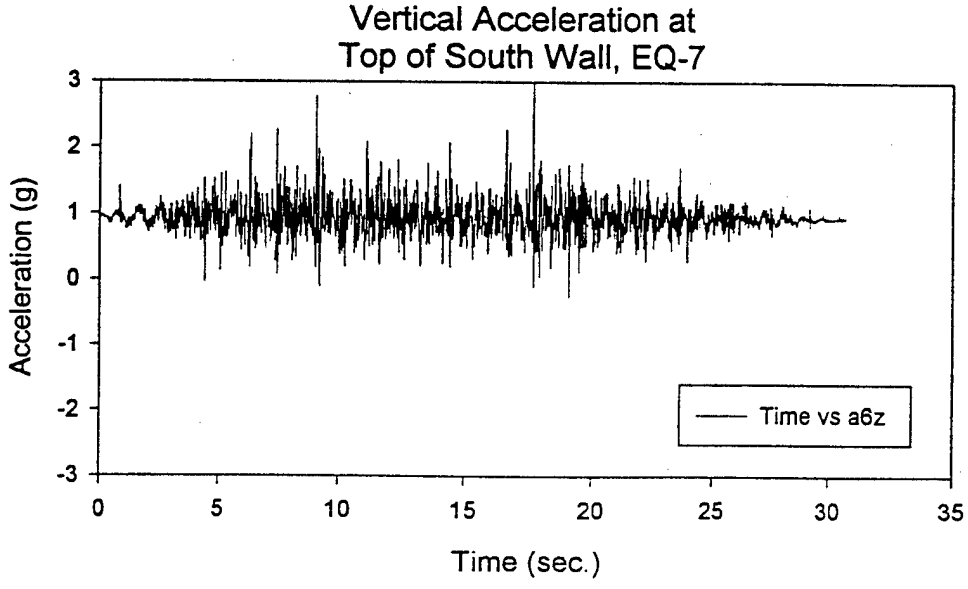
Vertical Acceleration at
Top of South Wall, EQ-7
Time vs a6z
Acceleration (g)
Time (sec.)

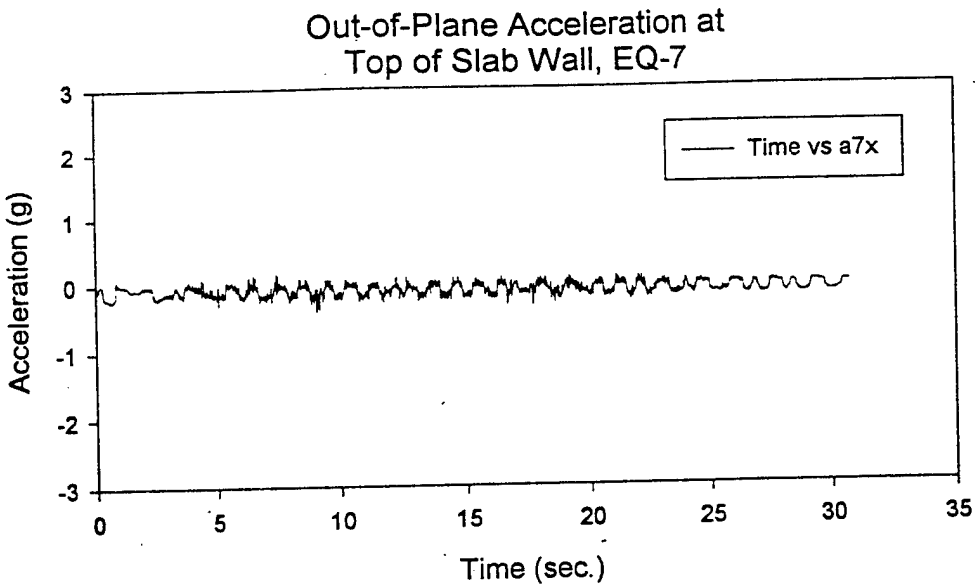
Out-of-Plane Acceleration at
Top of Slab Wall, EQ-7
Time vs a7x
Acceleration (g)
Time (sec.)

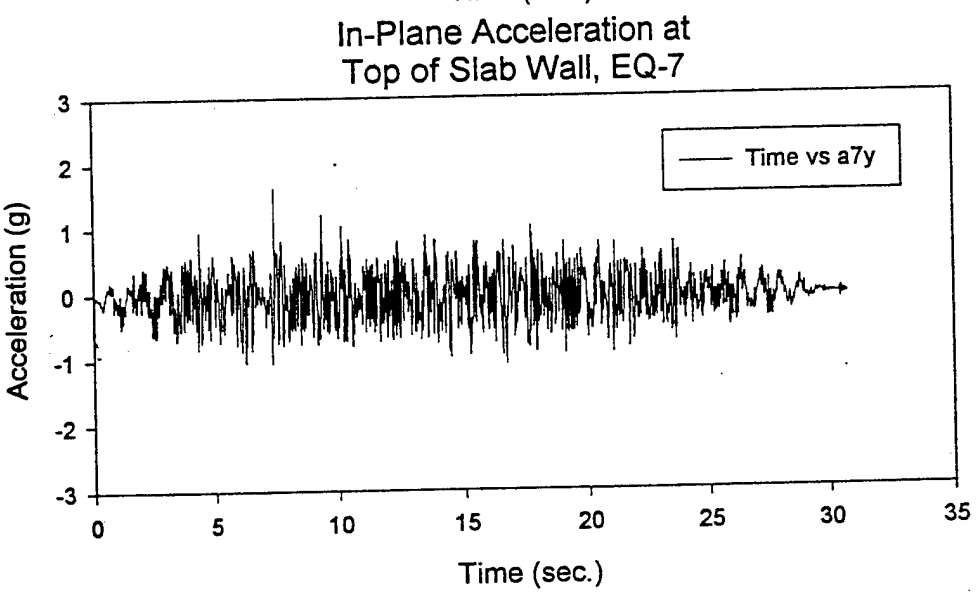
In-Plane Acceleration at
Top of Slab Wall, EQ-7
Time vs a7y
Acceleration (g)
Time (sec.)

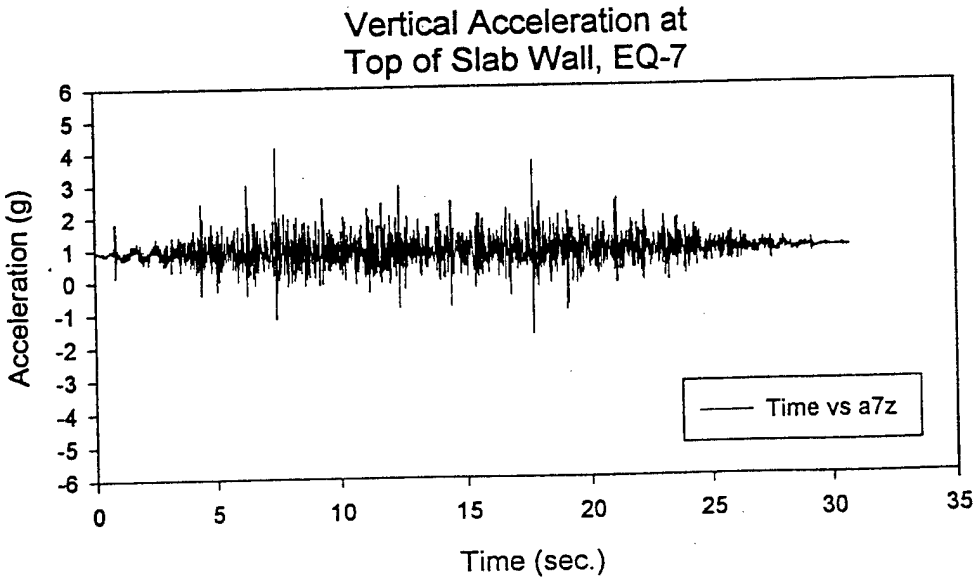
Vertical Acceleration at
Top of Slab Wall, EQ-7
Time vs a7z
Acceleration (g)
Time (sec.)

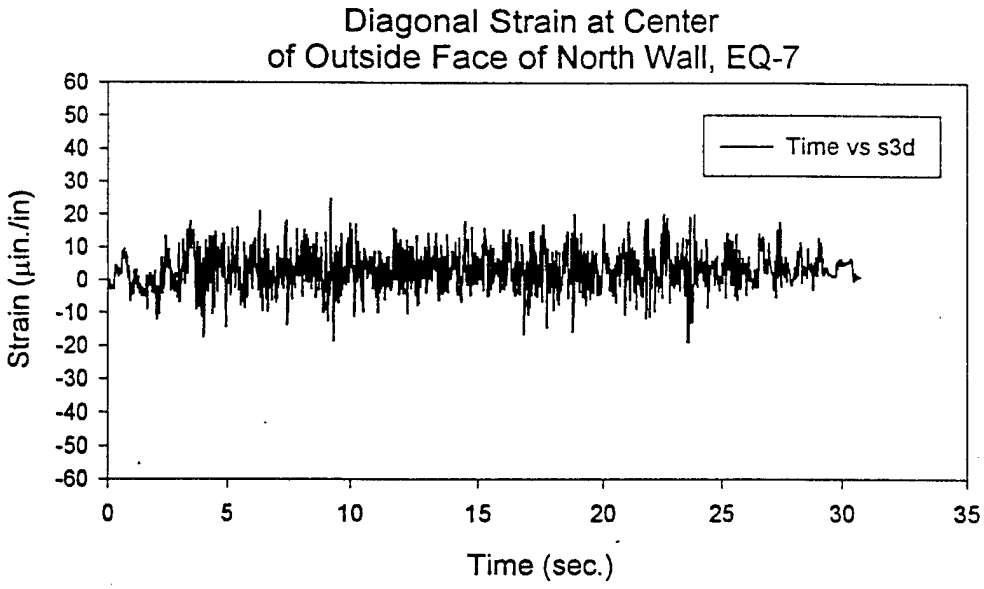
Diagonal Strain at Center
of Outside Face of North Wall, EQ-7
Time vs s3d
Strain (µin./in)
Time (sec.)

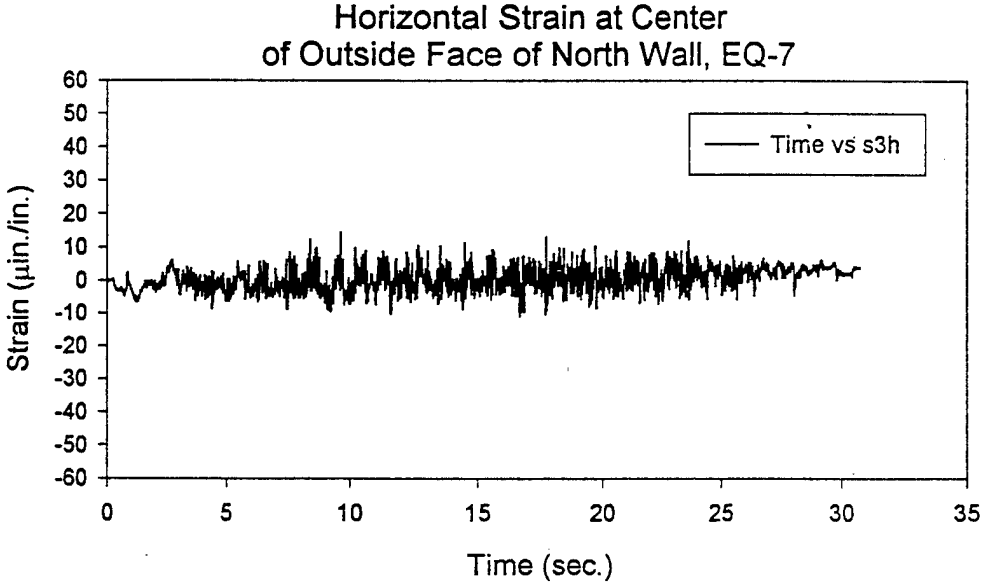
Horizontal Strain at Center
of Outside Face of North Wall, EQ-7
Time vs s3h
Strain (µin./in.)
Time (sec.)

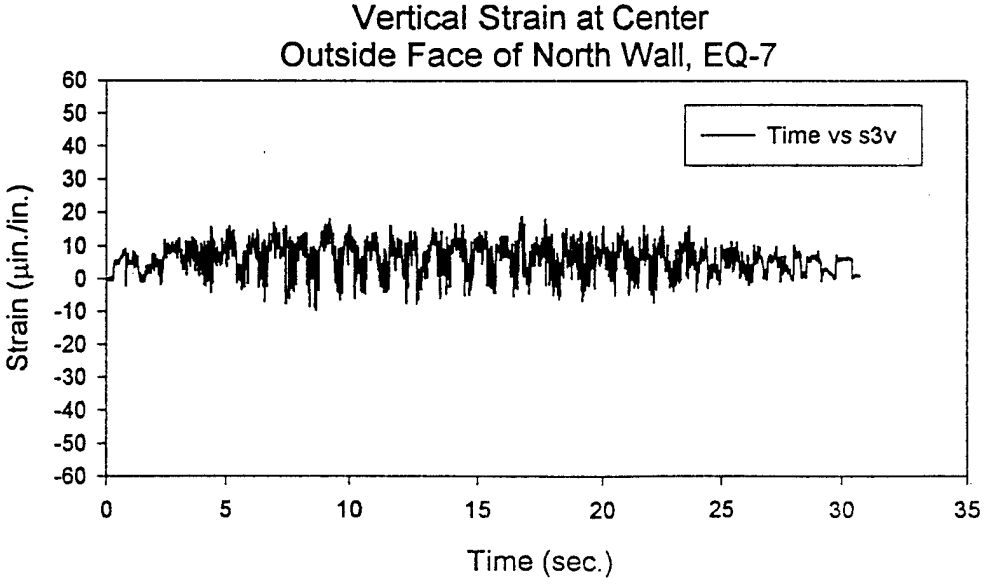
Vertical Strain at Center
Outside Face of North Wall, EQ-7
Time vs s3v
Strain (µin./in.)
Time (sec.)

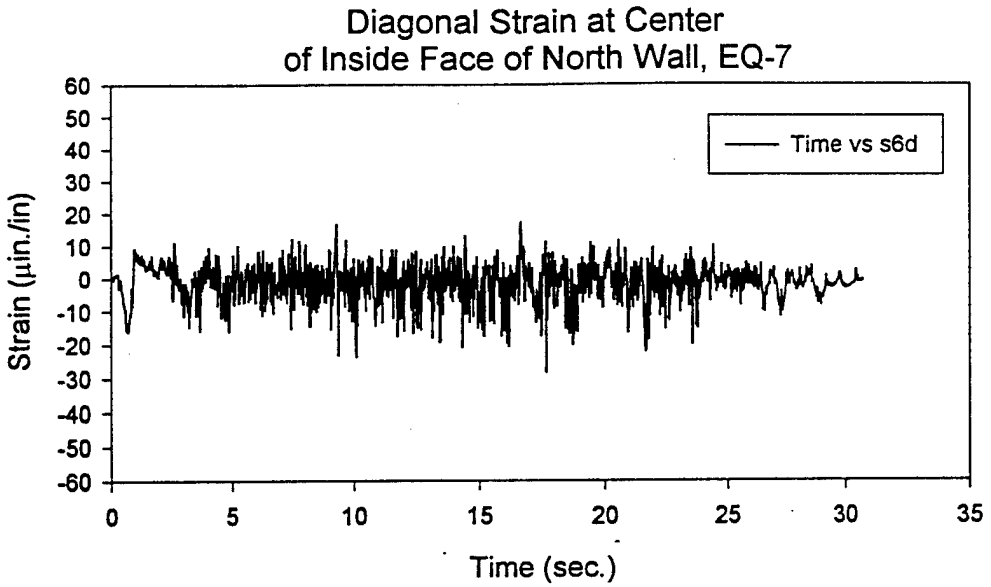
Diagonal Strain at Center
of Inside Face of North Wall, EQ-7
Time vs s6d
Strain (μin./in)
Time (sec.)

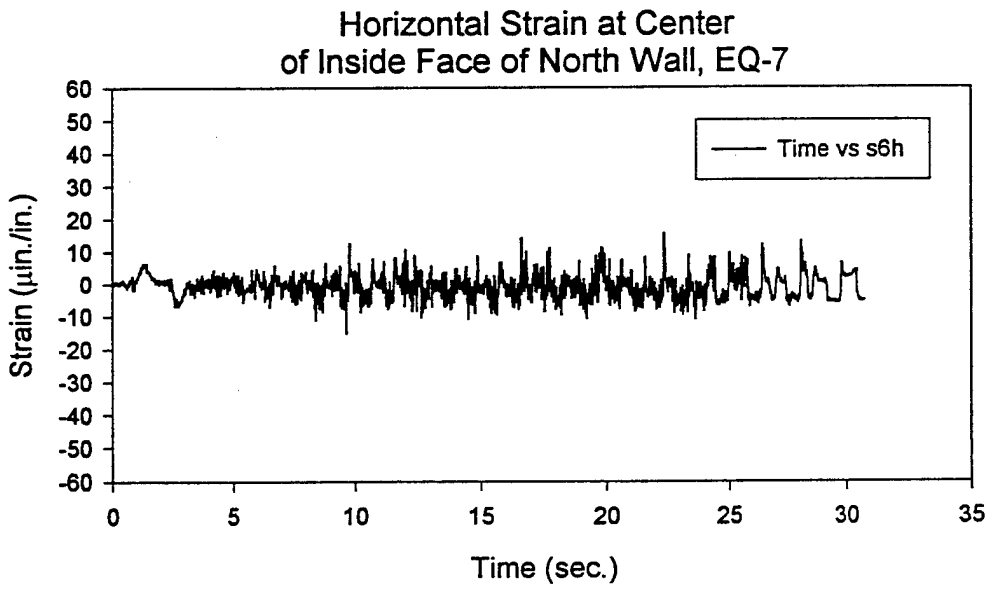
Horizontal Strain at Center
of Inside Face of North Wall, EQ-7
Time vs s6h
Strain (μin./in.)
Time (sec.)

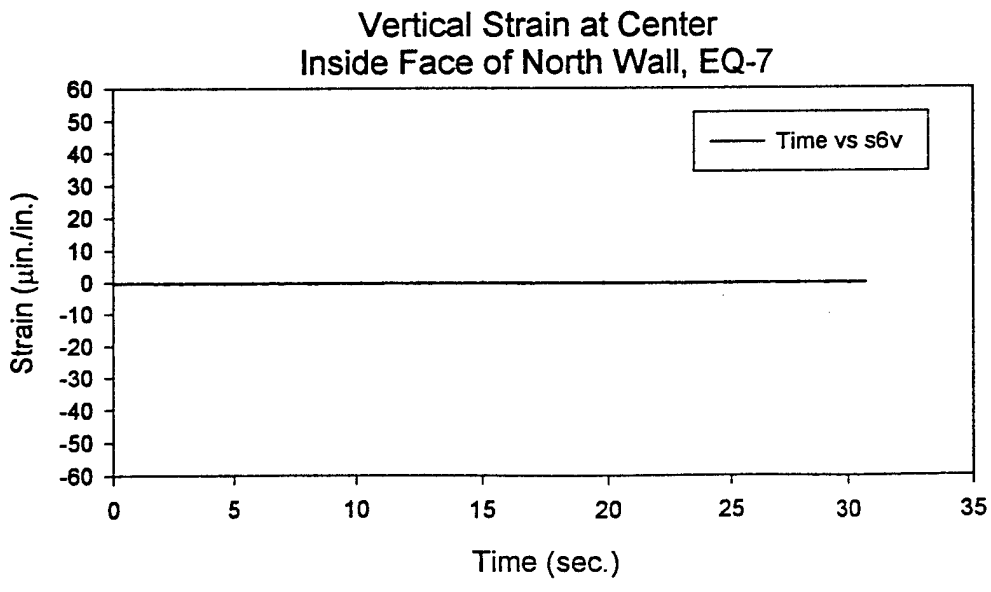
Vertical Strain at Center
Inside Face of North Wall, EQ-7
Time vs s6v
Strain (μin./in.)
Time (sec.)

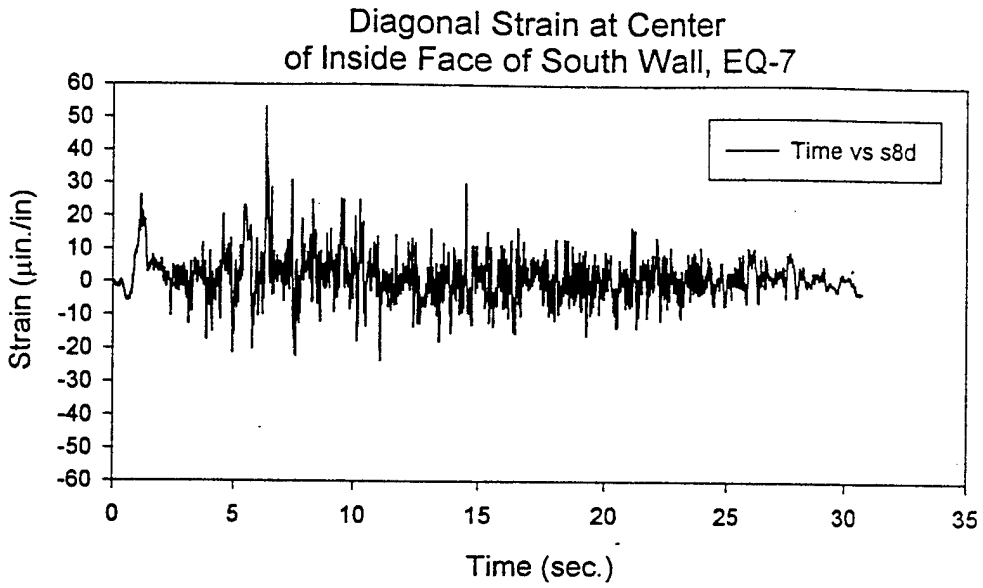
Diagonal Strain at Center
of Inside Face of South Wall, EQ-7
Time vs s8d
Strain (µin./in)
Time (sec.)

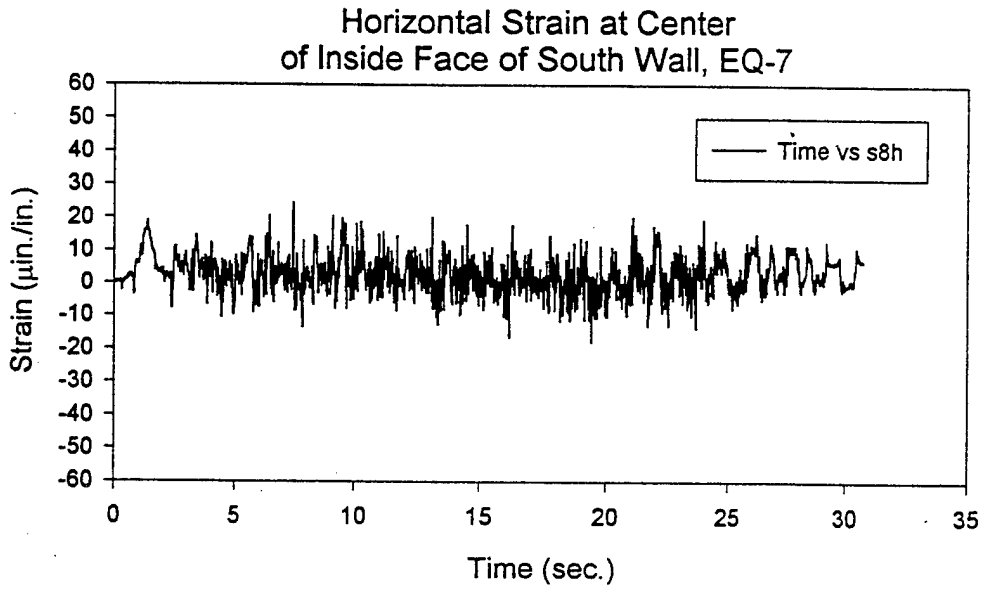
Horizontal Strain at Center
of Inside Face of South Wall, EQ-7
Time vs s8h
Strain (µin./in.)
Time (sec.)

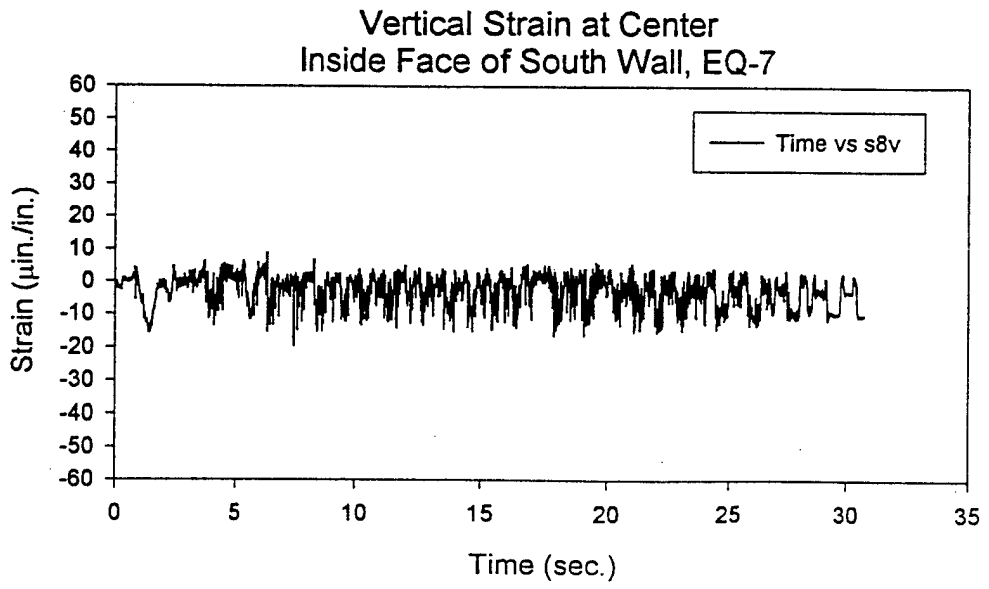
Vertical Strain at Center
Inside Face of South Wall, EQ-7
Time vs s8v
Strain (µin./in.)
Time (sec.)

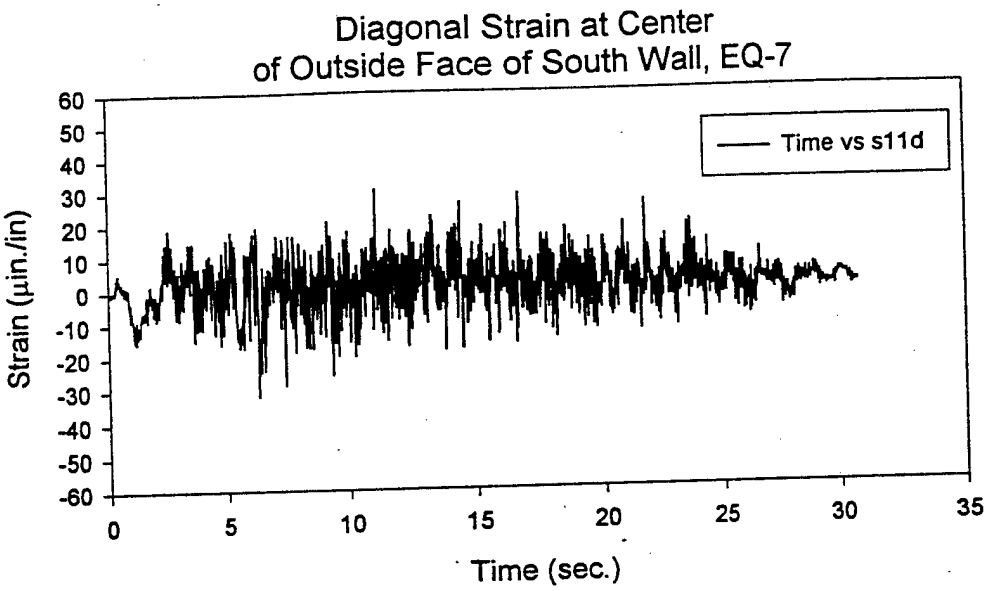
Diagonal Strain at Center
of Outside Face of South Wall, EQ-7
Time vs s11d
Strain (µin./in)
Time (sec.)

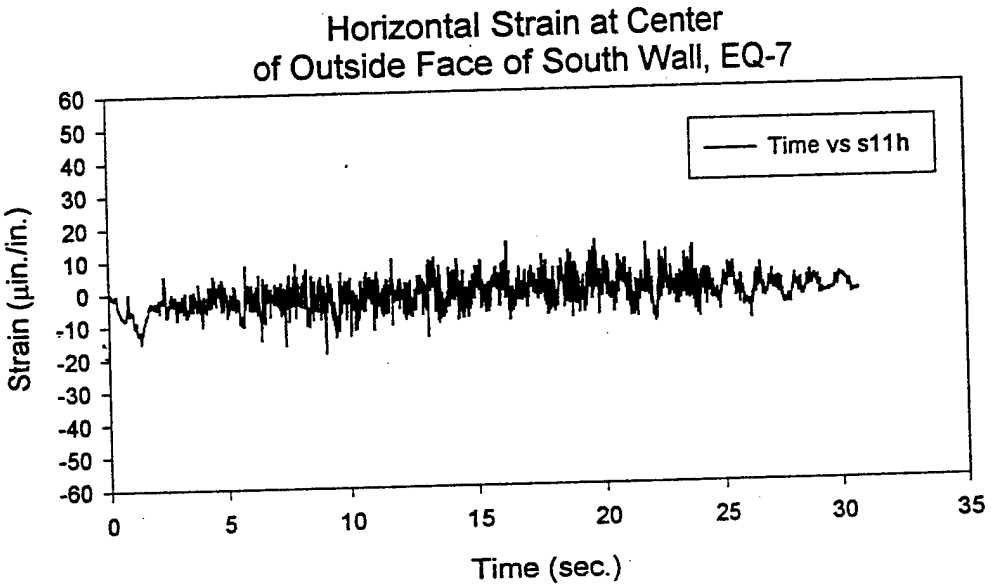
Horizontal Strain at Center
of Outside Face of South Wall, EQ-7
Time vs s11h
Strain (µin./in.)
Time (sec.)

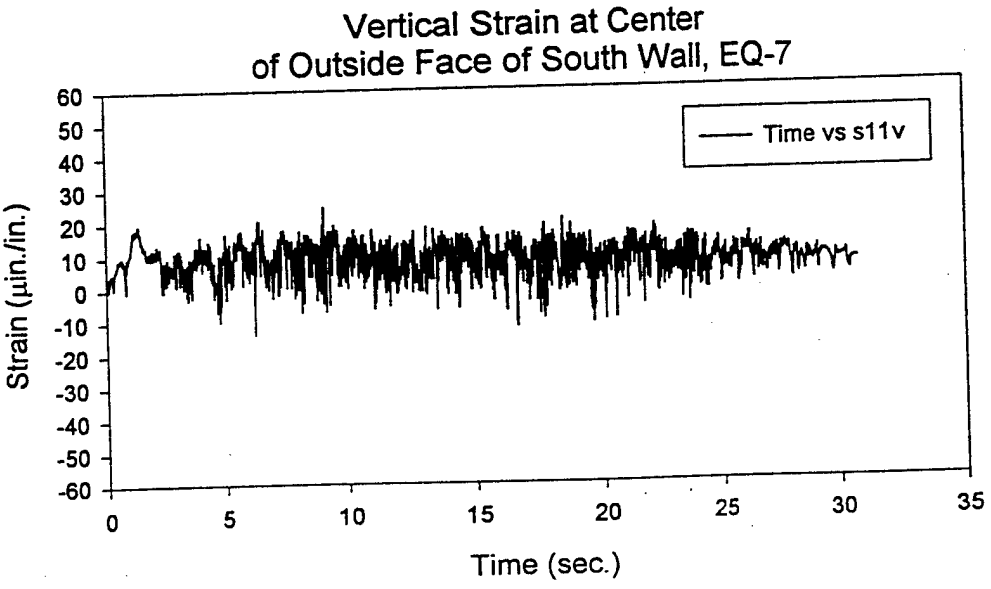
Vertical Strain at Center
of Outside Face of South Wall, EQ-7
Time vs s11v
Strain (µin./in.)
Time (sec.)

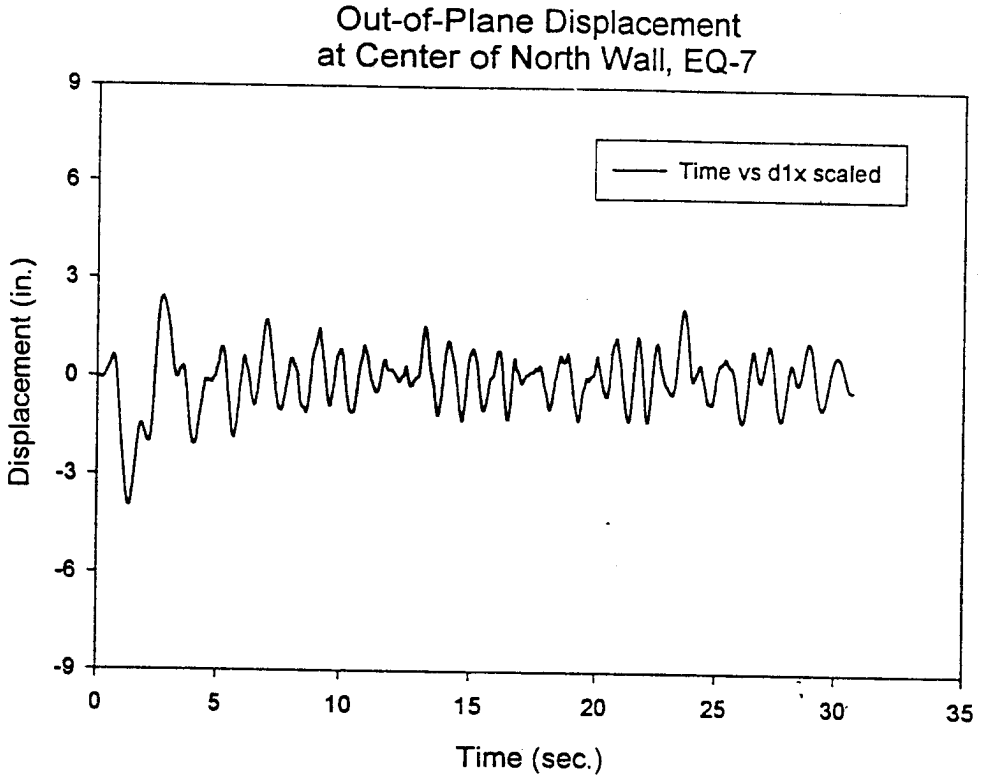
Out-of-Plane Displacement
at Center of North Wall, EQ-7
Time vs d1x scaled
Displacement (in.)
9
6
3
0
-3
-6
-9
0
5
10
15
20
25
30
35
Time (sec.)

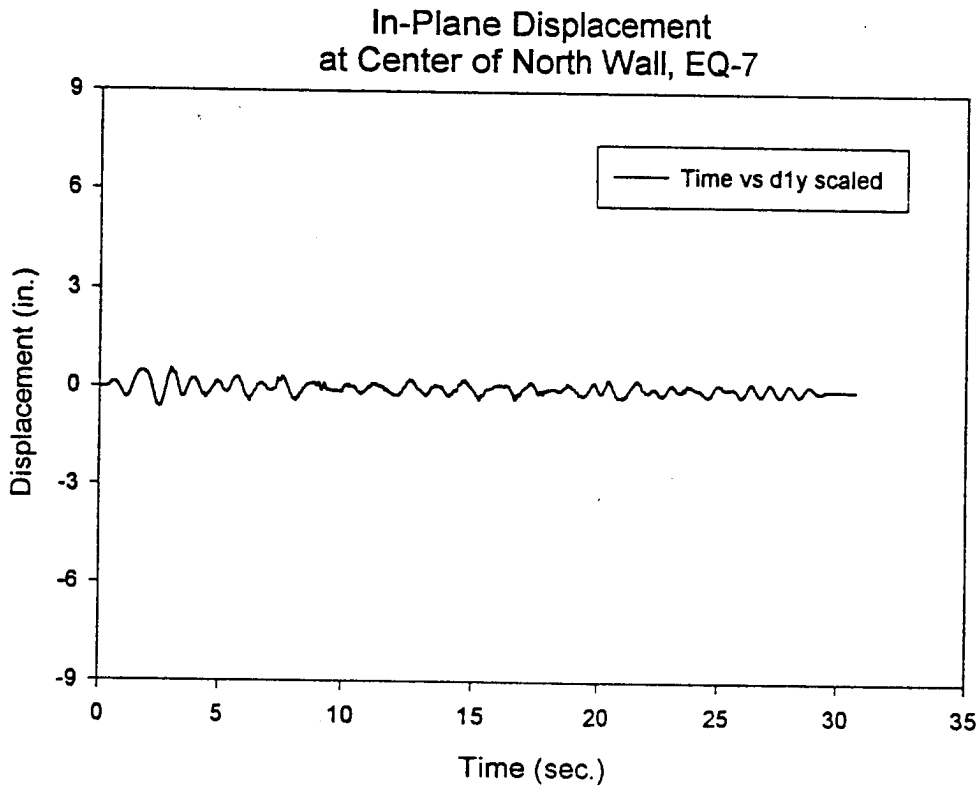
In-Plane Displacement
at Center of North Wall, EQ-7
Time vs d1y scaled
Displacement (in.)
9
6
3
0
-3
-6
-9
0
5
10
15
20
25
30
35
Time (sec.)

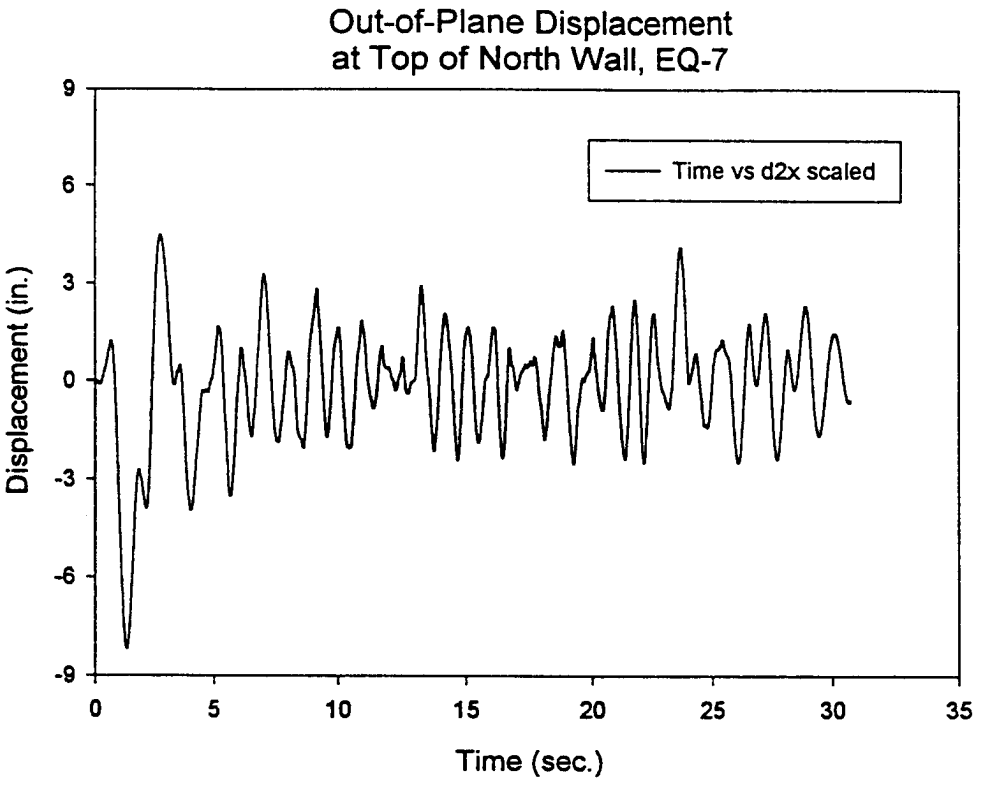
Out-of-Plane Displacement
at Top of North Wall, EQ-7
Time vs d2x scaled
Displacement (in.)
9
6
3
0
-3
-6
-9
0
5
10
15
20
25
30
35
Time (sec.)

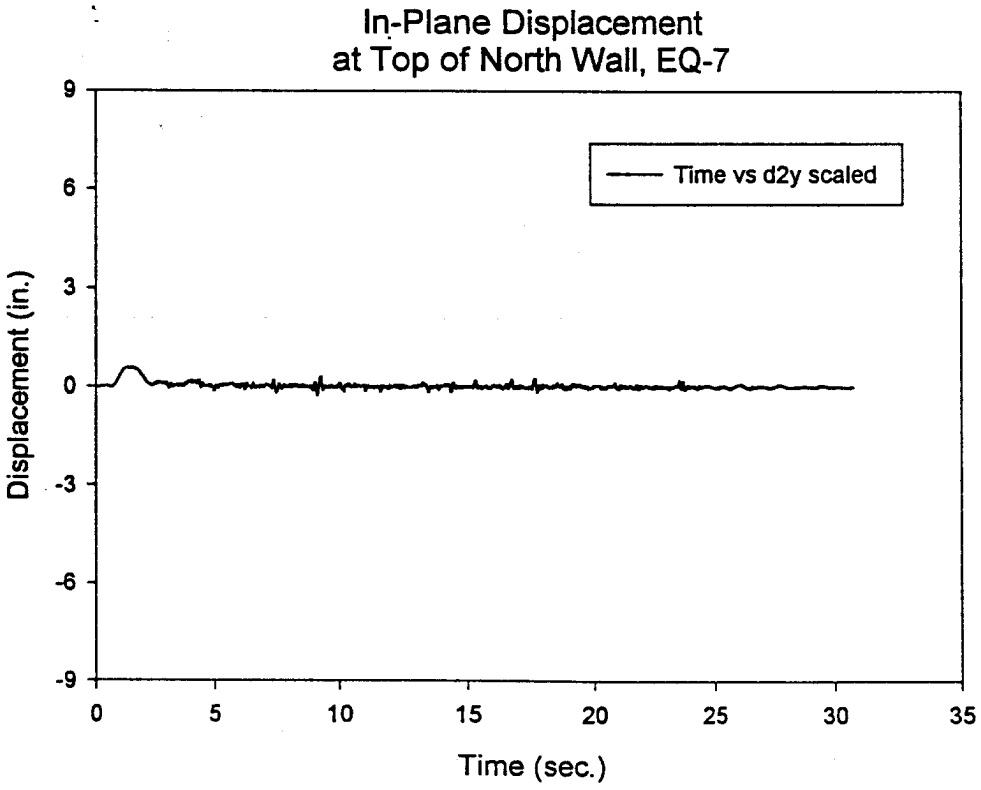
In-Plane Displacement
at Top of North Wall, EQ-7
Time vs d2y scaled
Displacement (in.)
9
6
3
0
-3
-6
-9
0
5
10
15
20
25
30
35
Time (sec.)

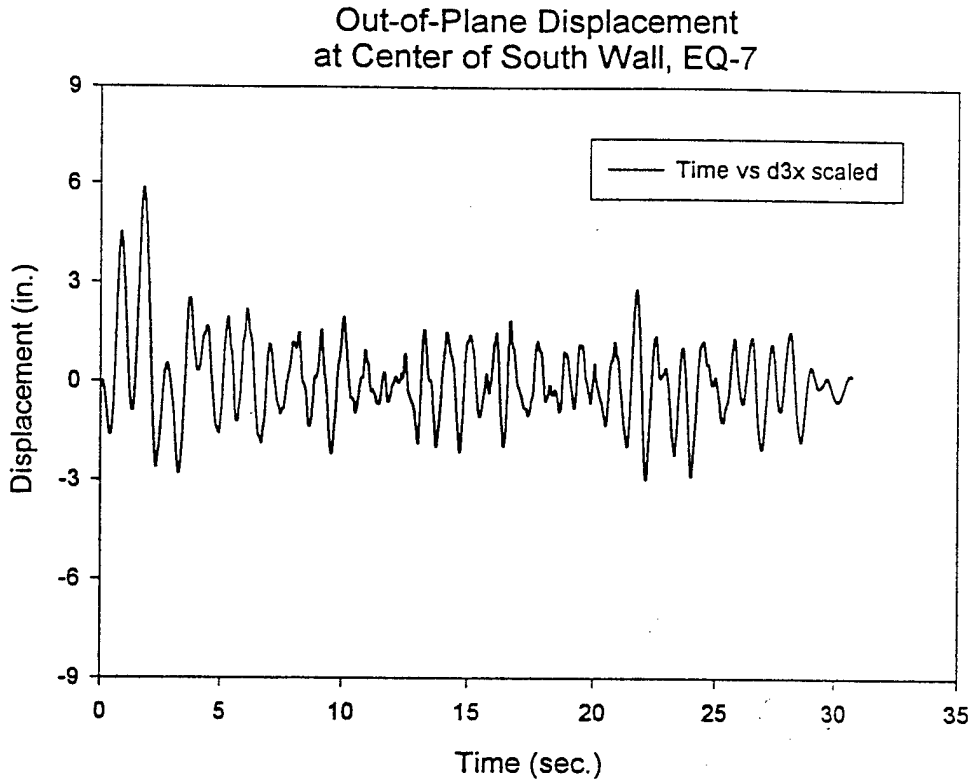
Out-of-Plane Displacement
at Center of South Wall, EQ-7
Time vs d3x scaled
Displacement (in.)
9
6
3
0
-3
-6
-9
0
5
10
15
20
25
30
35
Time (sec.)

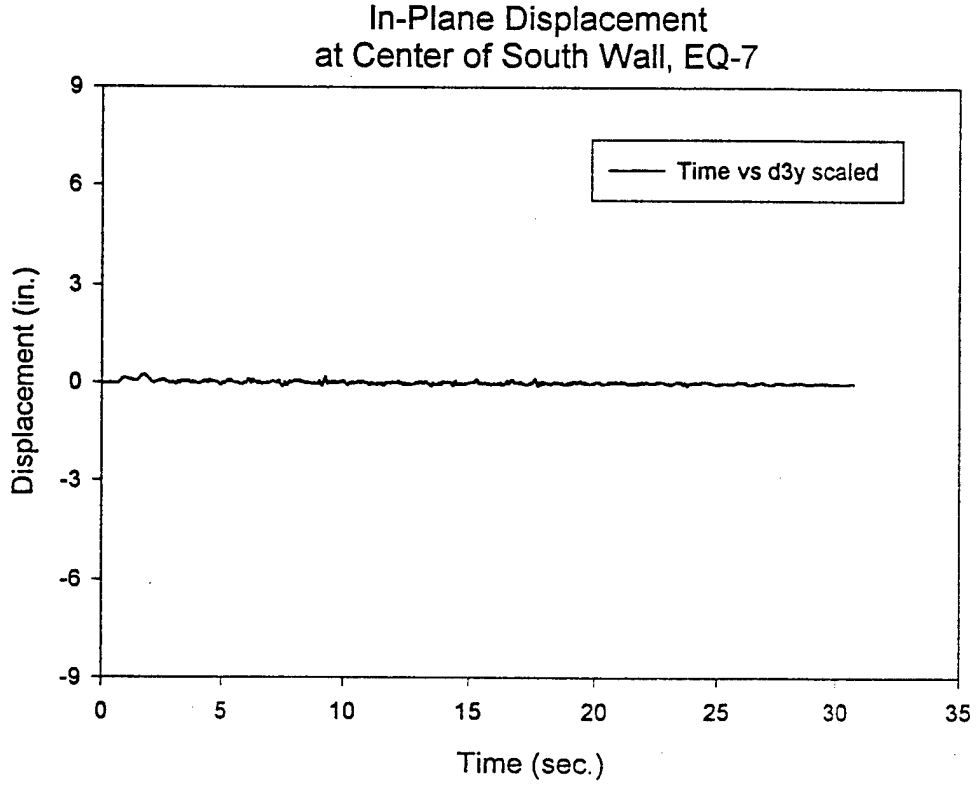
In-Plane Displacement
at Center of South Wall, EQ-7
Time vs d3y scaled
Displacement (in.)
9
6
3
0
-3
-6
-9
0
5
10
15
20
25
30
35
Time (sec.)

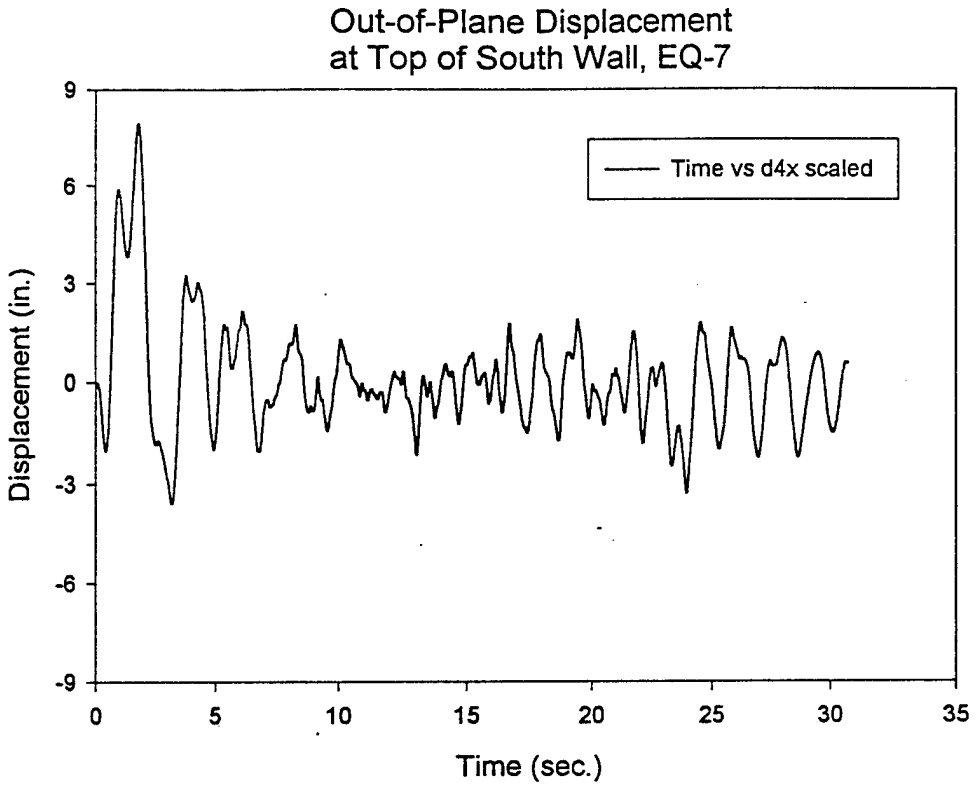
Out-of-Plane Displacement
at Top of South Wall, EQ-7
Time vs d4x scaled
Displacement (in.)
9
6
3
0
-3
-6
-9
0
5
10
15
20
25
30
35
Time (sec.)

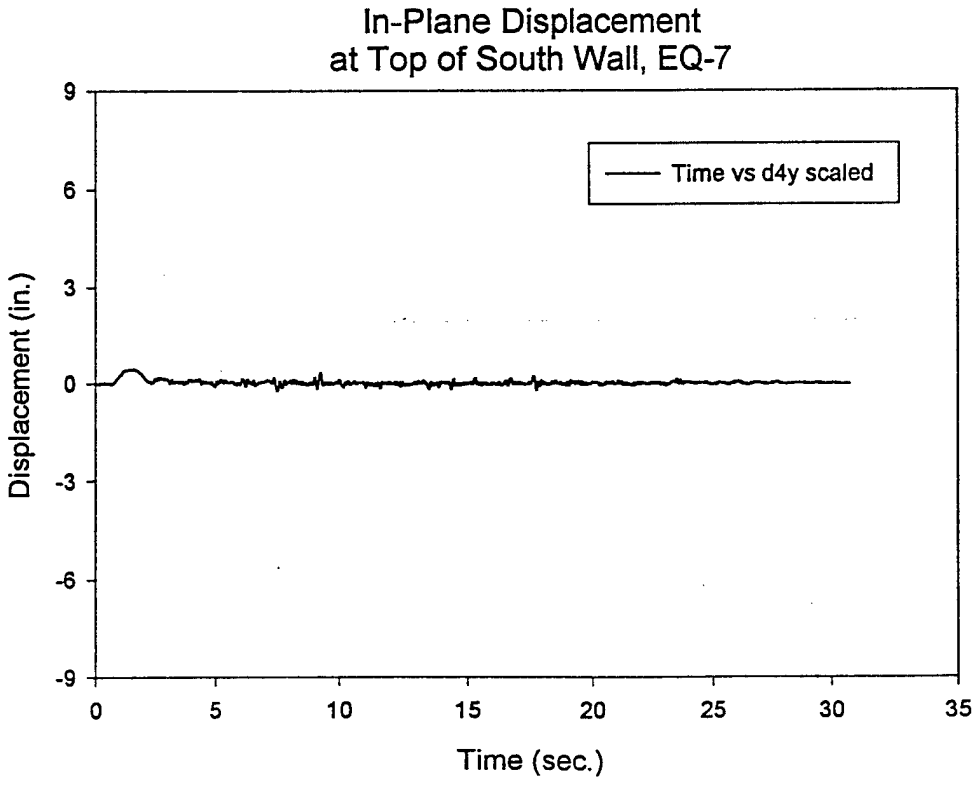
In-Plane Displacement
at Top of South Wall, EQ-7
Time vs d4y scaled
Displacement (in.)
9
6
3
0
-3
-6
-9
0
5
10
15
20
25
30
35
Time (sec.)

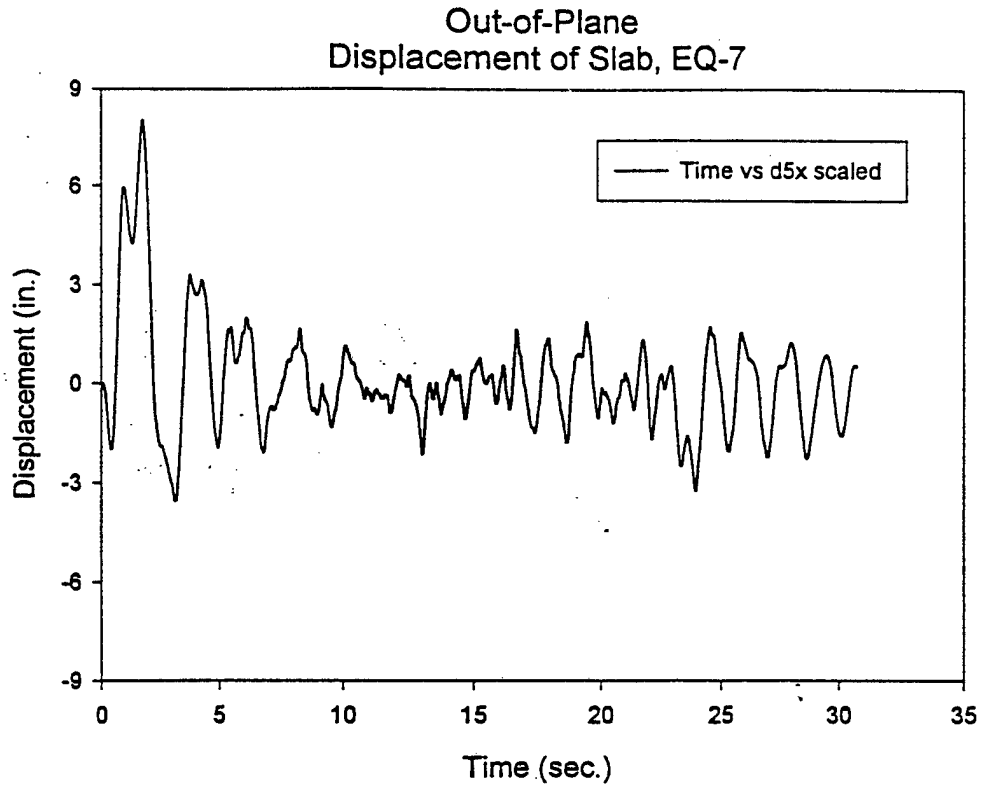
Out-of-Plane
Displacement of Slab, EQ-7
Time vs d5x scaled
Displacement (in.)
9
6
3
0
-3
-6
-9
0
5
10
15
20
25
30
35
Time (sec.)

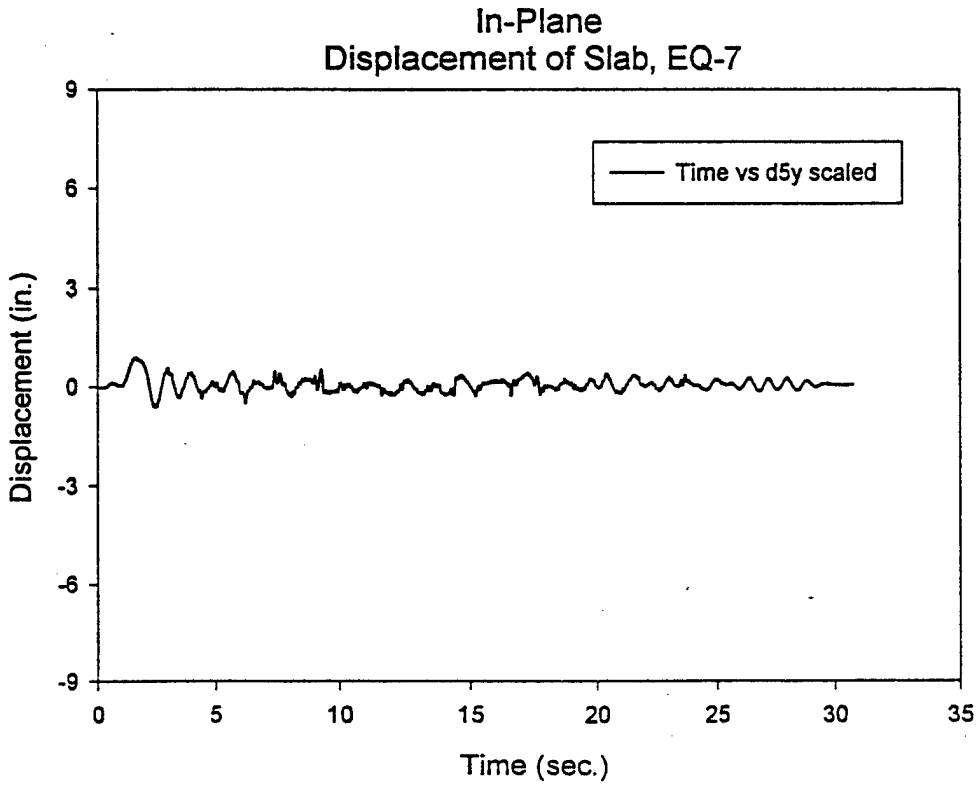
In-Plane
Displacement of Slab, EQ-7
Time vs d5y scaled
Displacement (in.)
9
6
3
0
-3
-6
-9
0
5
10
15
20
25
30
35
Time (sec.)

Appendix E: Resonant Frequency Search Tests

**OUT-OF-PLANE WHITE NOISE TEST BEFORE EQ-1
ON NORTH WALL WITHOUT SLAB ON TOP**

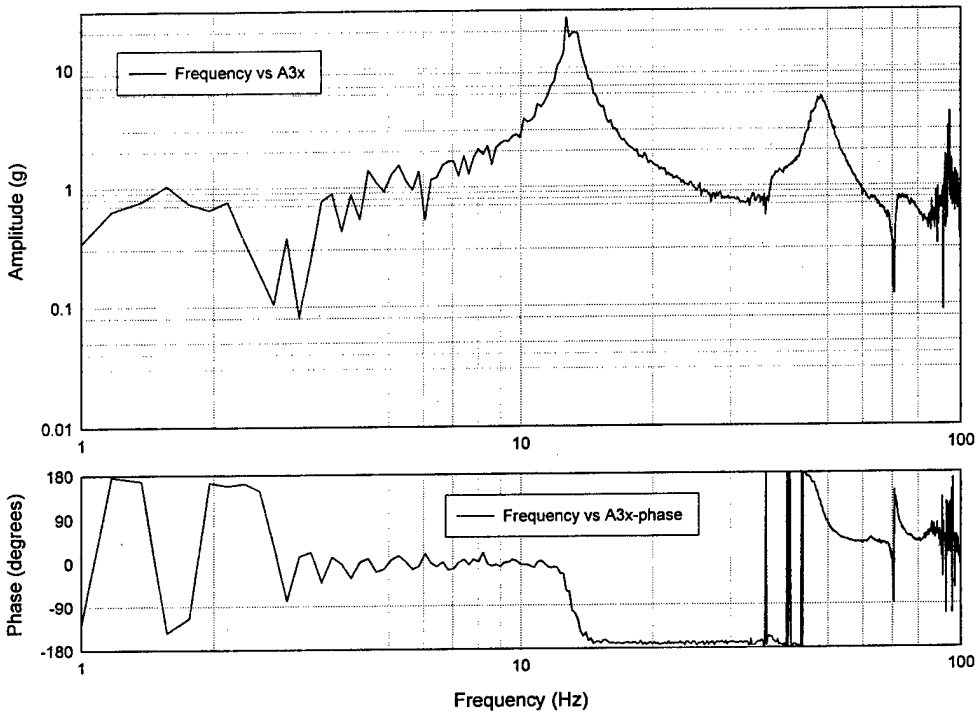

**IN-PLANE WHITE NOISE TEST BEFORE EQ-1
ON NORTH WALL WITHOUT SLAB ON TOP**

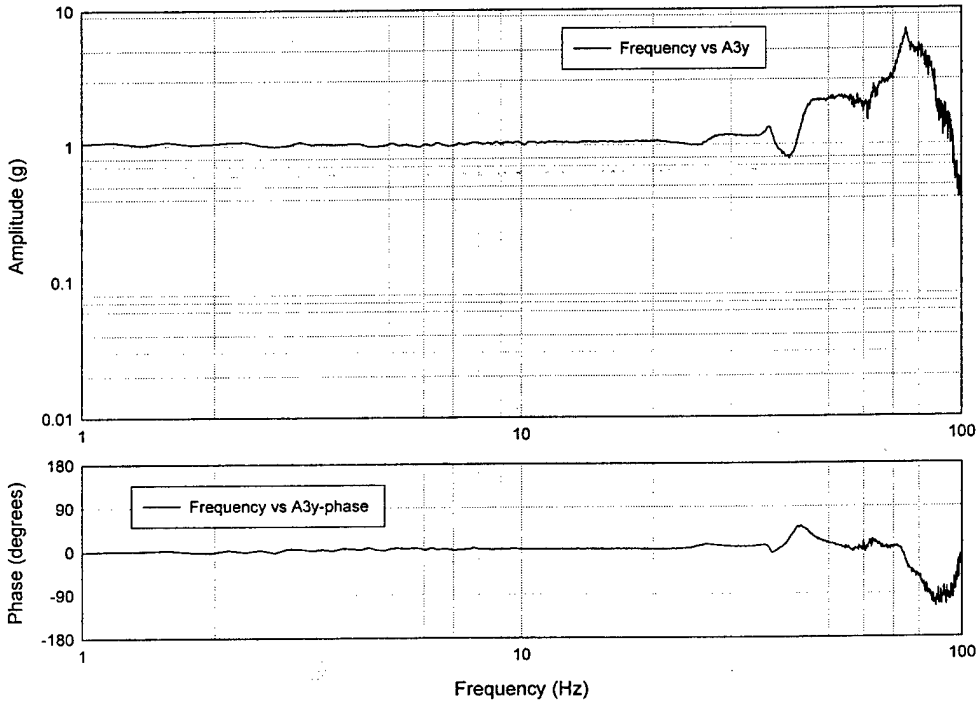

VERTICAL WHITE NOISE TEST BEFORE EQ-1 ON NORTH WALL WITHOUT SLAB ON TOP

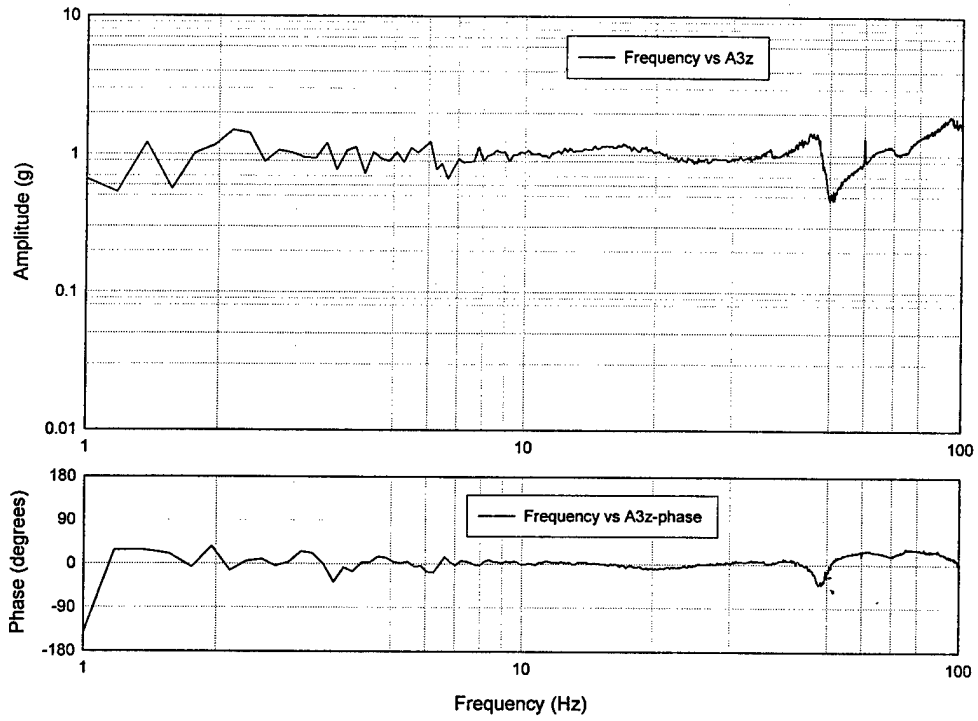

OUT-OF-PLANE WHITE NOISE TEST BEFORE EQ-1 ON SOUTH WALL WITHOUT SLAB ON TOP

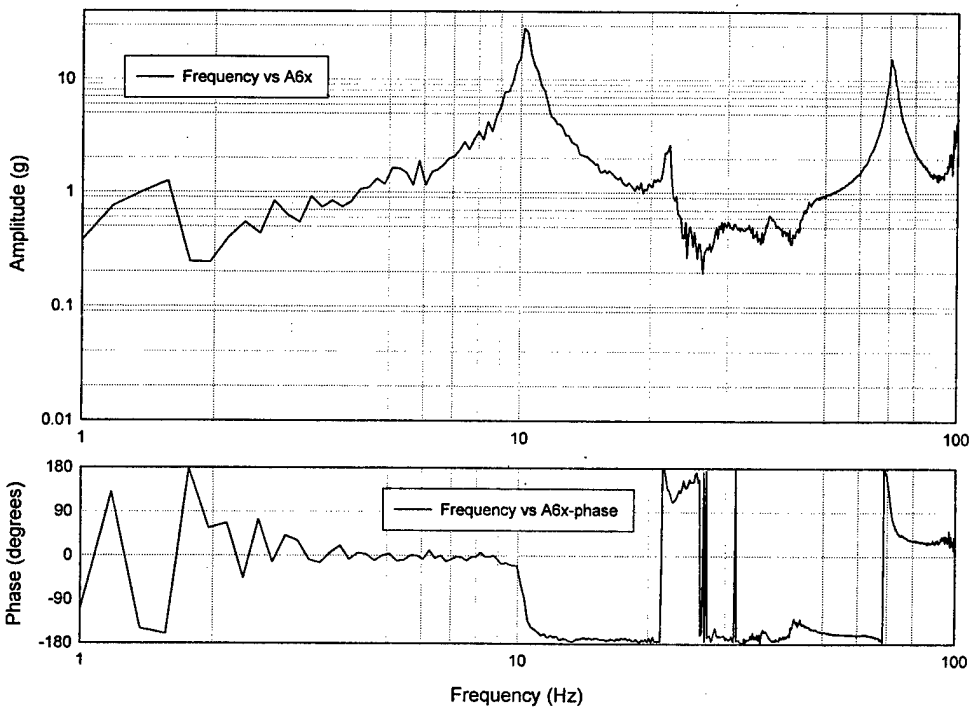

**IN-PLANE WHITE NOISE TEST BEFORE EQ-1
ON SOUTH WALL WITHOUT SLAB ON TOP**

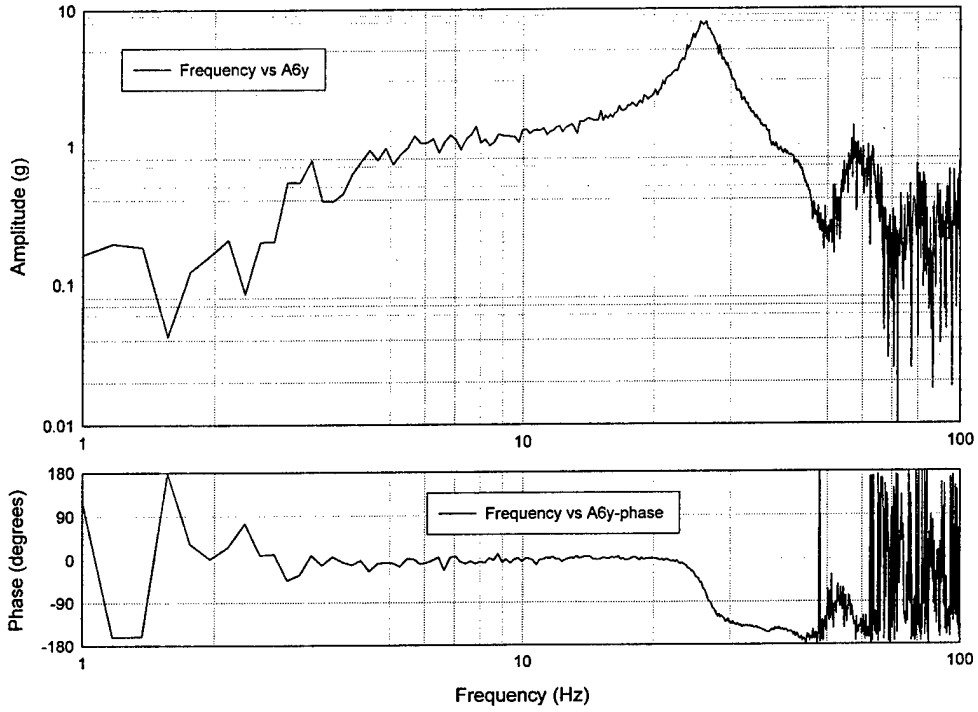

**VERTICAL WHITE NOISE TEST BEFORE EQ-1
ON SOUTH WALL WITHOUT SLAB ON TOP**

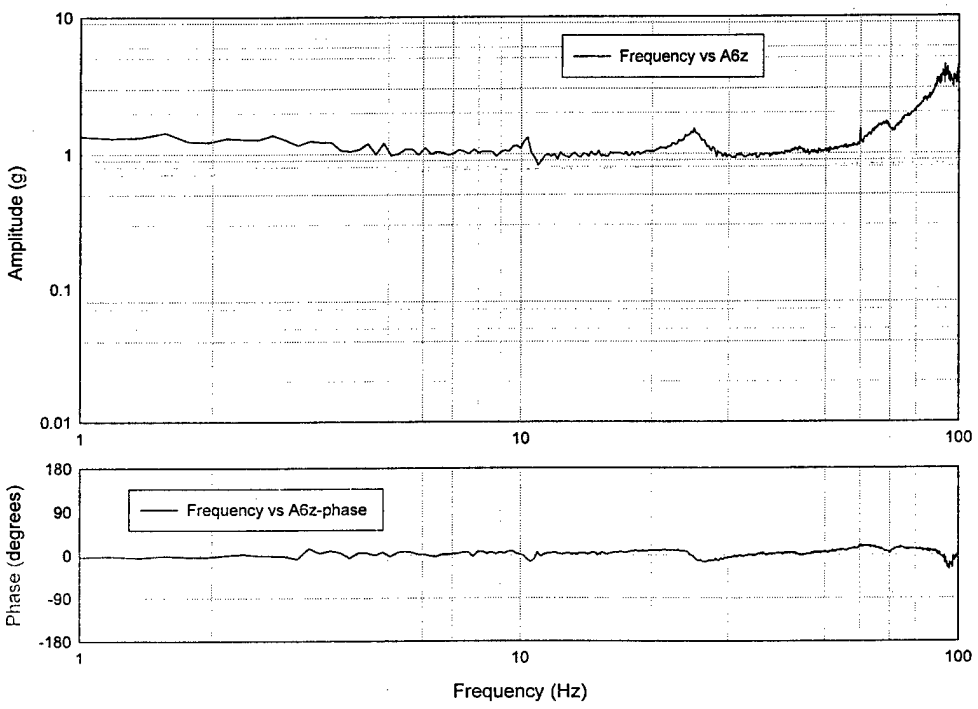

**OUT-OF-PLANE WHITE NOISE TEST BEFORE EQ-1
ON NORTH WALL WITH SLAB ON TOP**

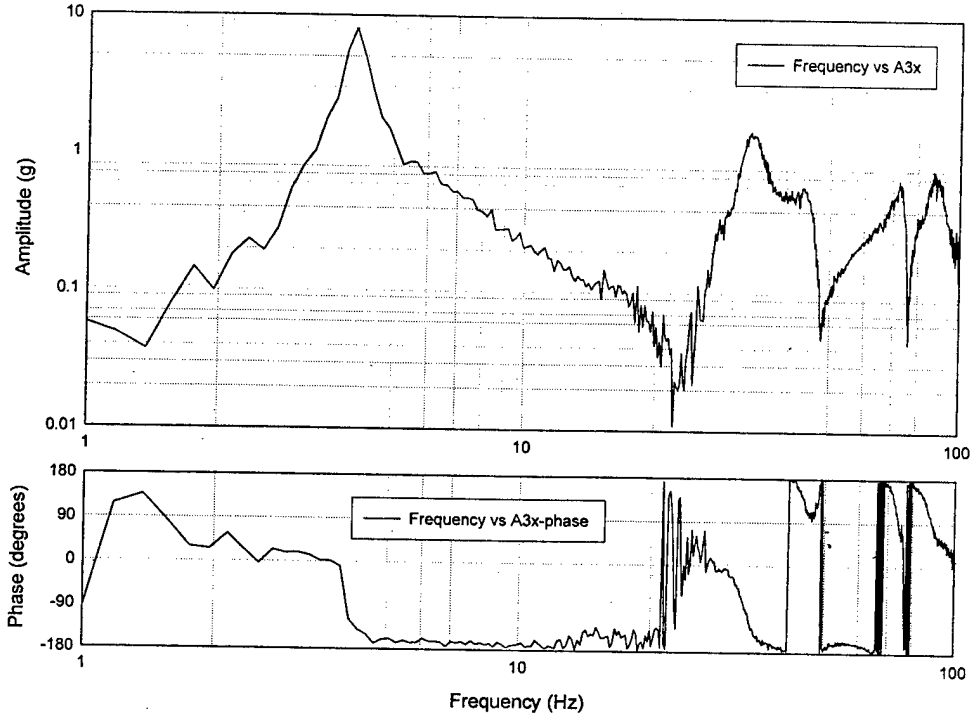

**IN-PLANE WHITE NOISE TEST BEFORE EQ-1
ON NORTH WALL WITH SLAB ON TOP**

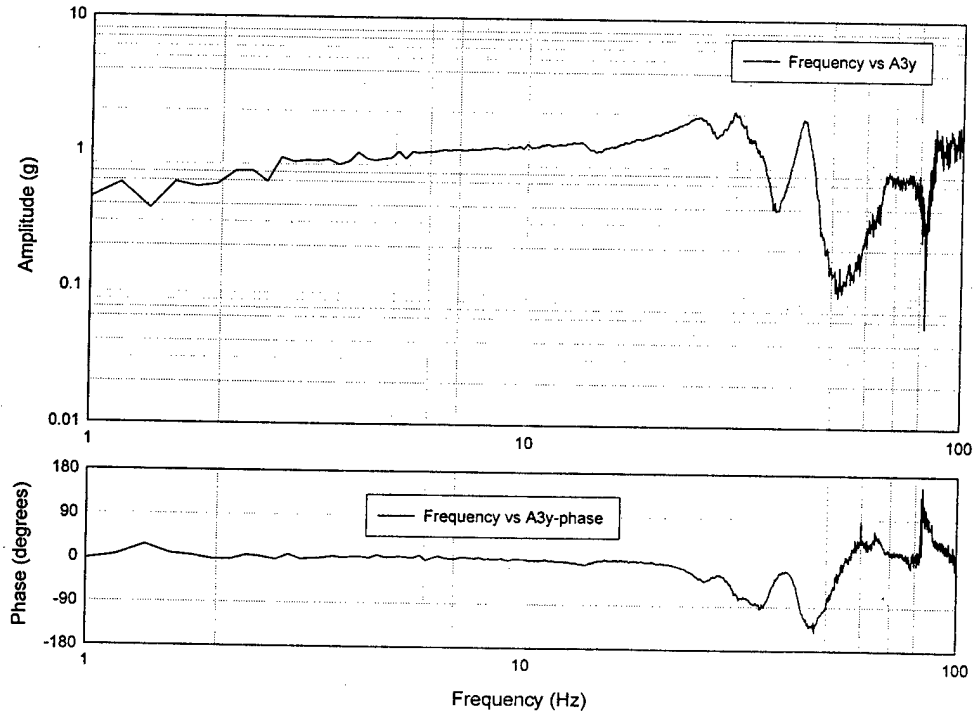

**VERTICAL WHITE NOISE TEST BEFORE EQ-1
ON NORTH WALL WITH SLAB ON TOP**

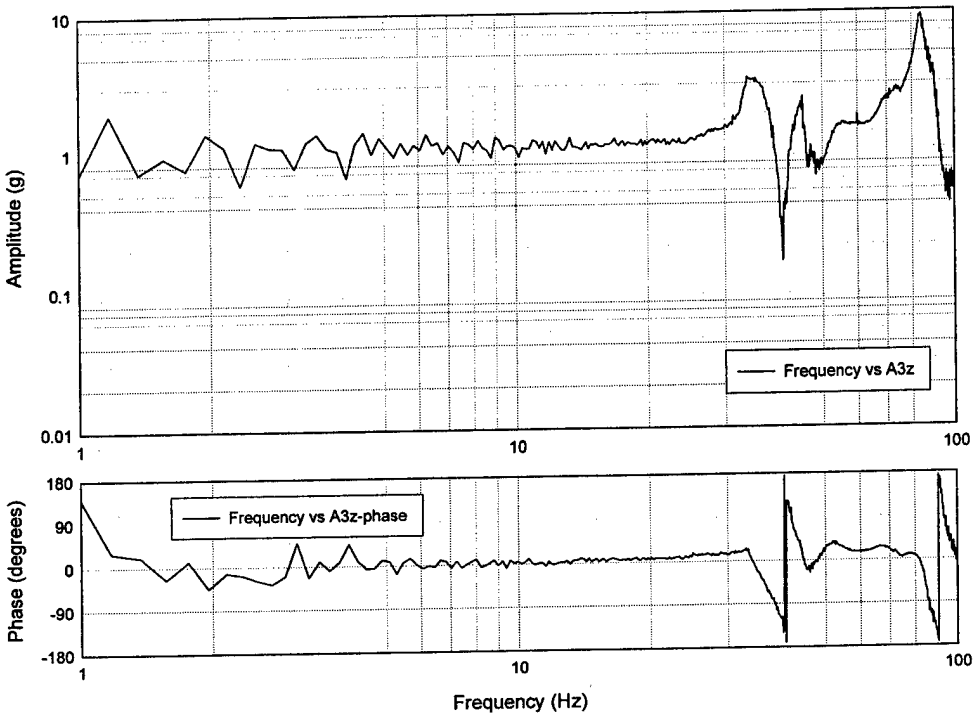

**OUT-OF-PLANE WHITE NOISE TEST BEFORE EQ-1
ON SOUTH WALL WITH SLAB ON TOP**

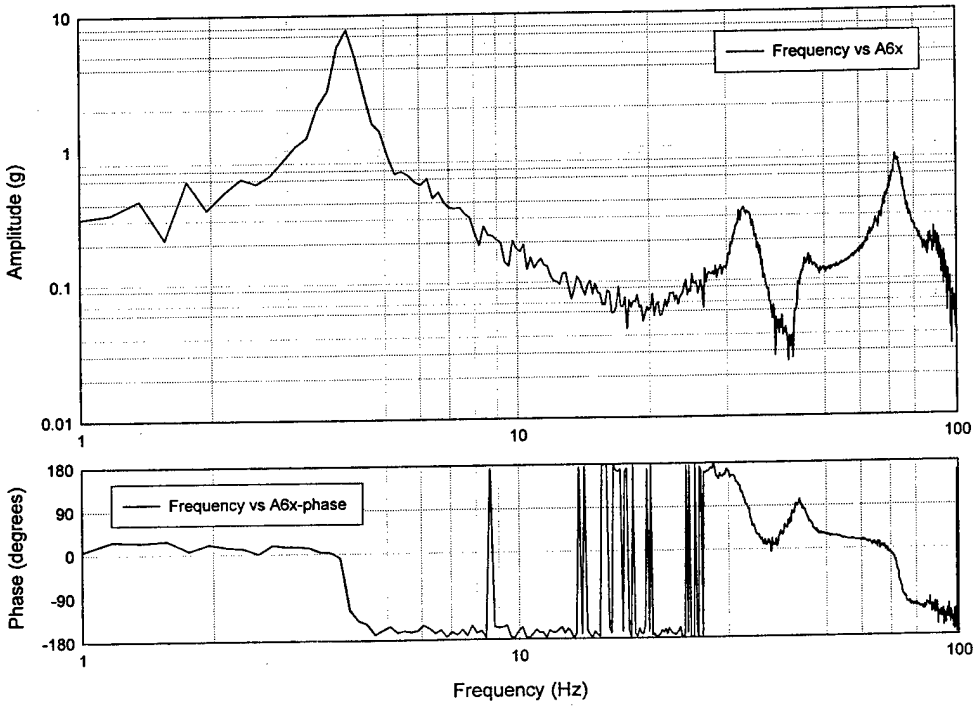

**IN-PLANE WHITE NOISE TEST BEFORE EQ-1
ON SOUTH WALL WITH SLAB ON TOP**

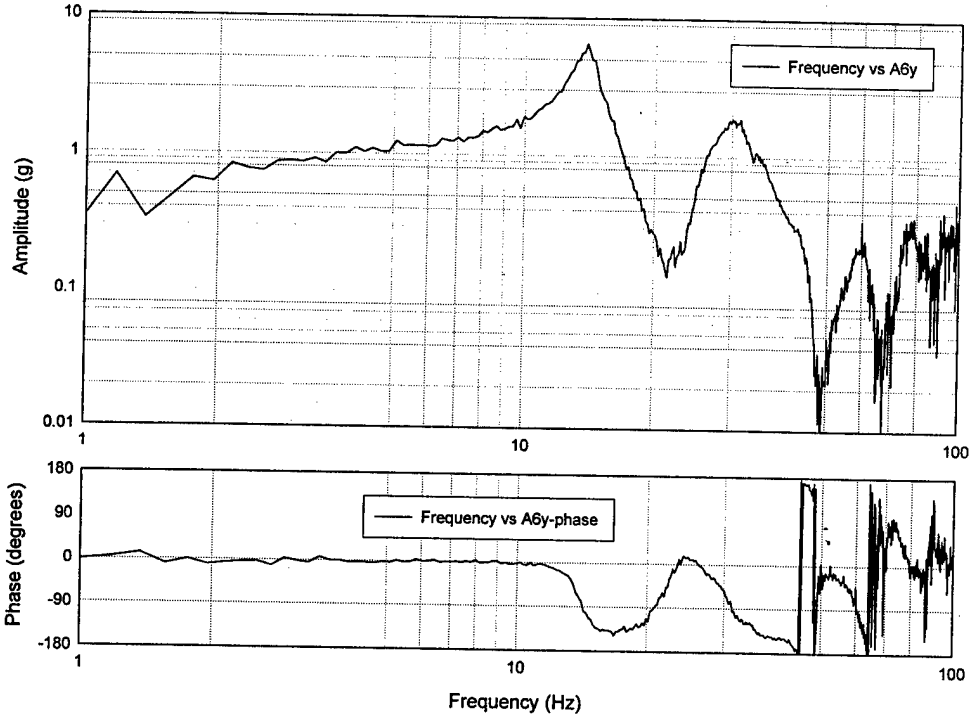

**VERTICAL WHITE NOISE TEST BEFORE EQ-1
ON SOUTH WALL WITH SLAB ON TOP**

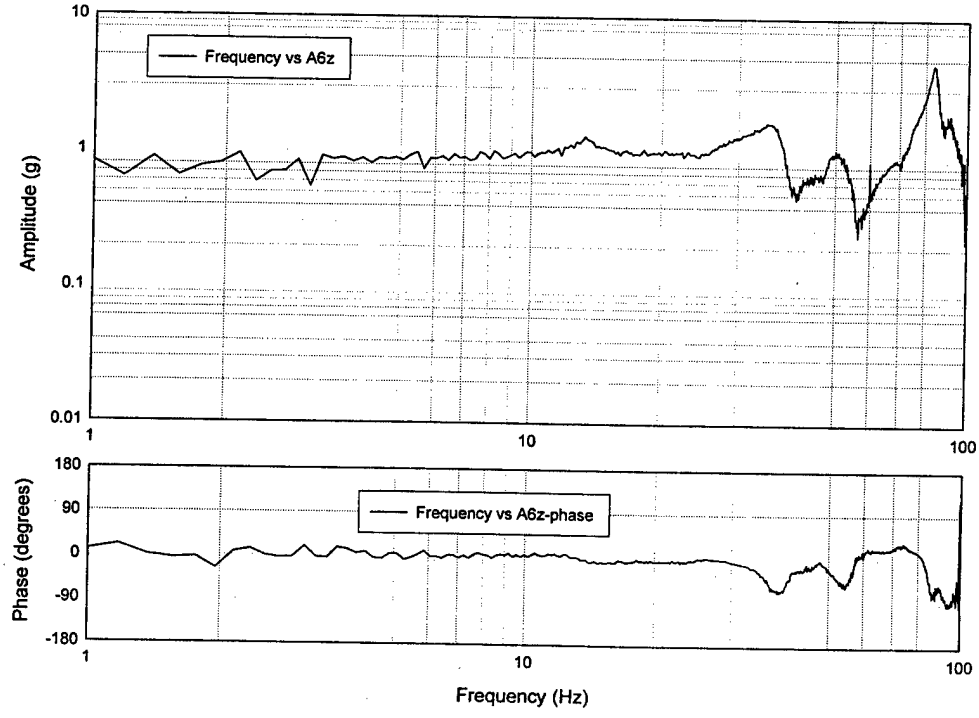

OUT-OF-PLANE WHITE NOISE TEST AFTER EQ-1 ON NORTH WALL WITH DAMAGED SOUTH WALL

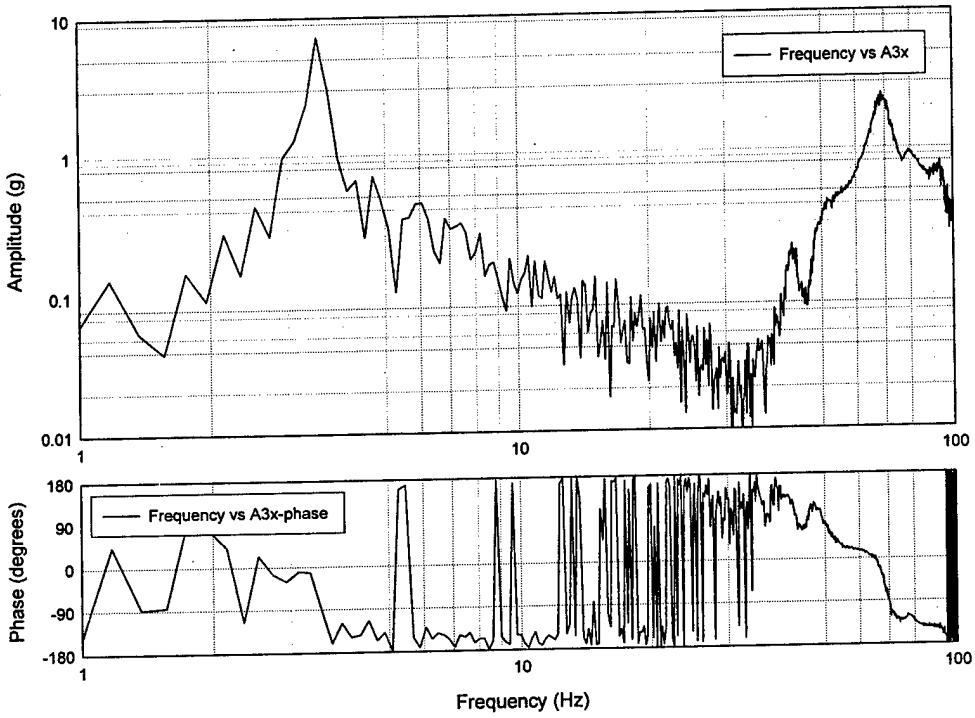

IN-PLANE WHITE NOISE TEST AFTER EQ-1 ON NORTH WALL WITH DAMAGED SOUTH WALL

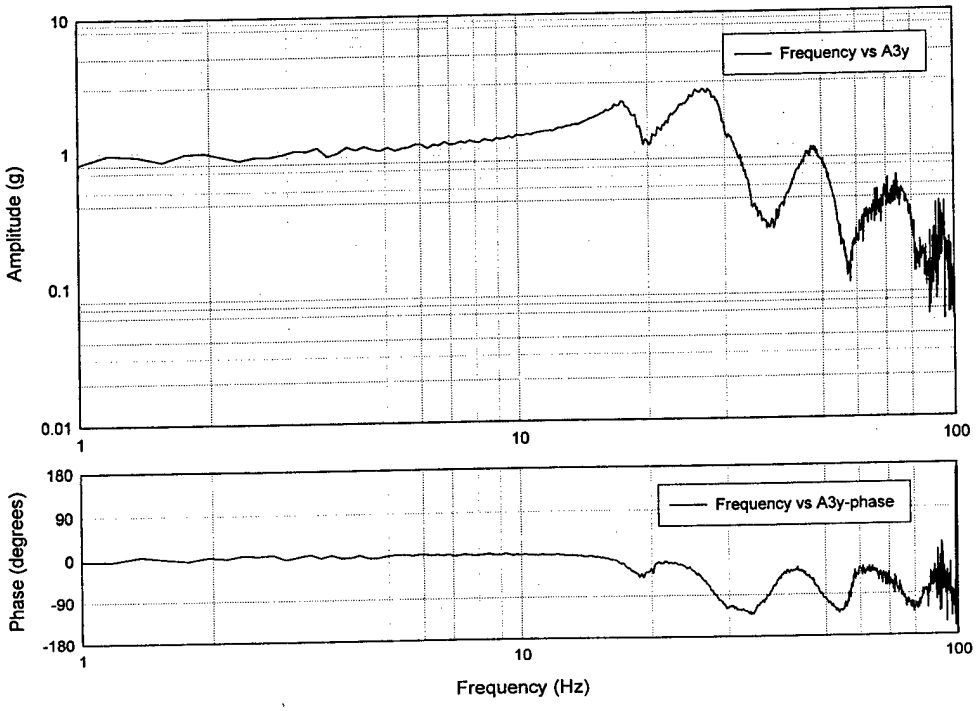

**VERTICAL WHITE NOISE TEST AFTER EQ-1
ON NORTH WALL WITH DAMAGED SOUTH WALL**

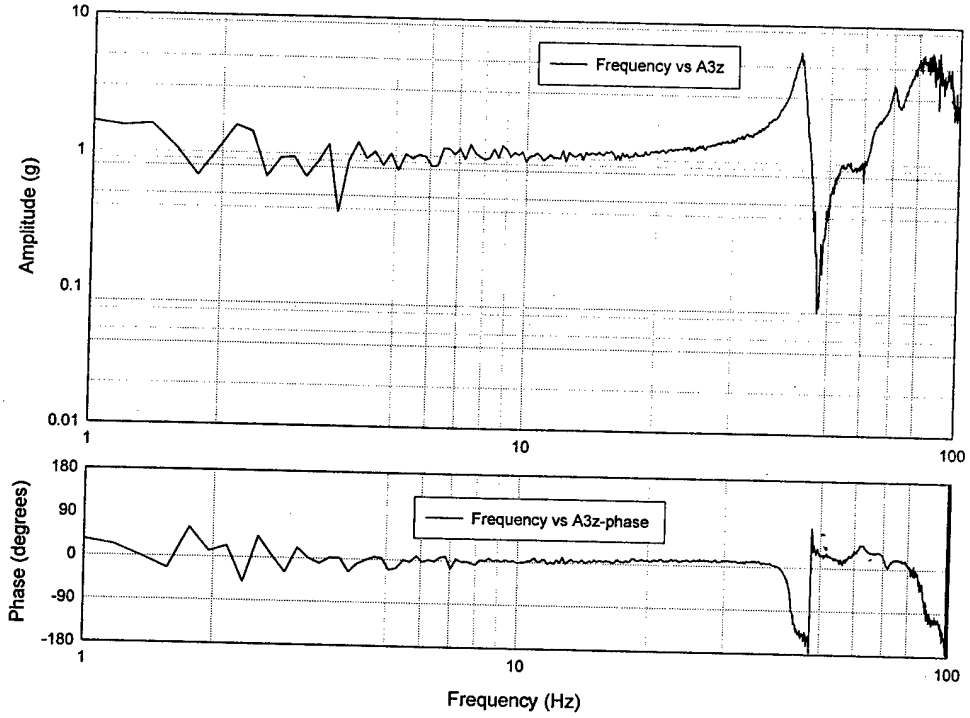

**OUT-OF-PLANE WHITE NOISE TEST AFTER EQ-1
ON SOUTH WALL WITH DAMAGED SOUTH WALL**

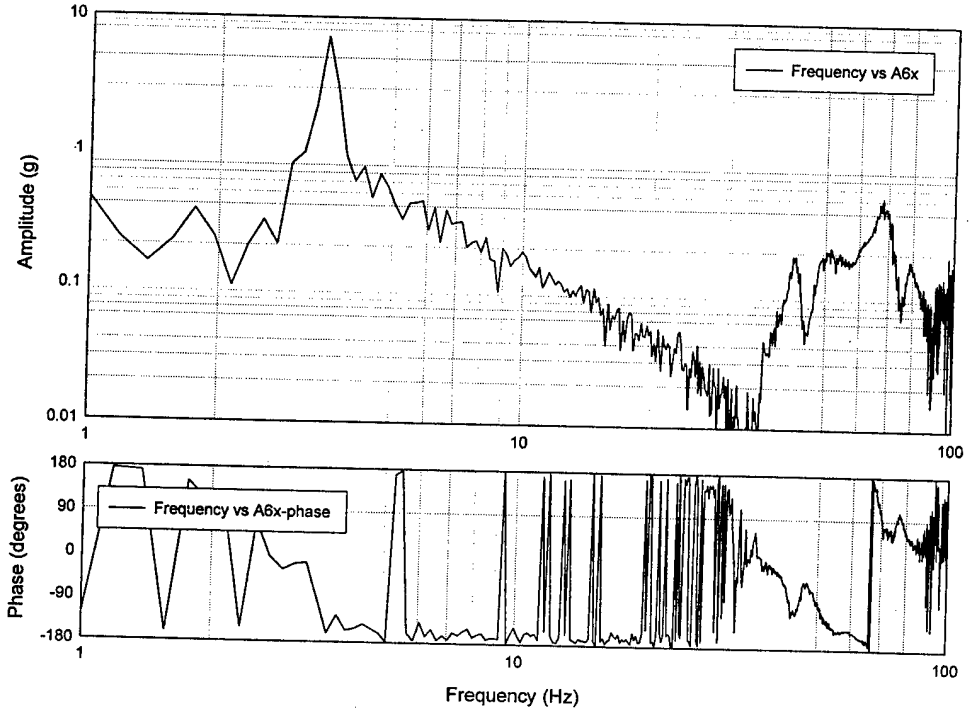

**IN-PLANE WHITE NOISE TEST AFTER EQ-1
ON SOUTH WALL WITH DAMAGED SOUTH WALL**

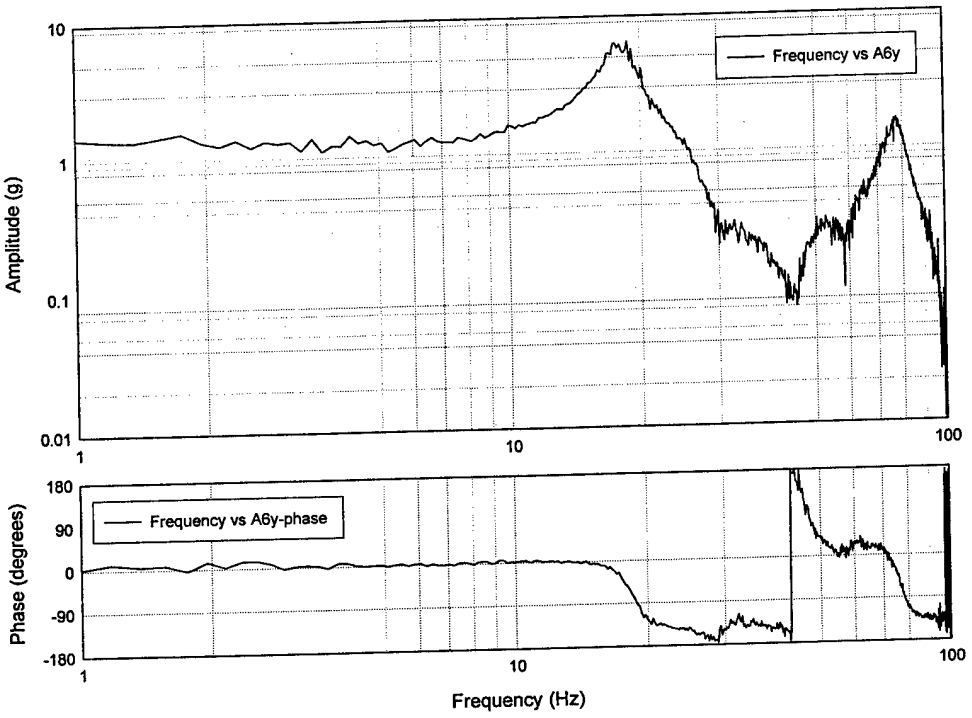

**VERTICAL WHITE NOISE TEST AFTER EQ-1
ON SOUTH WALL WITH DAMAGED SOUTH WALL**

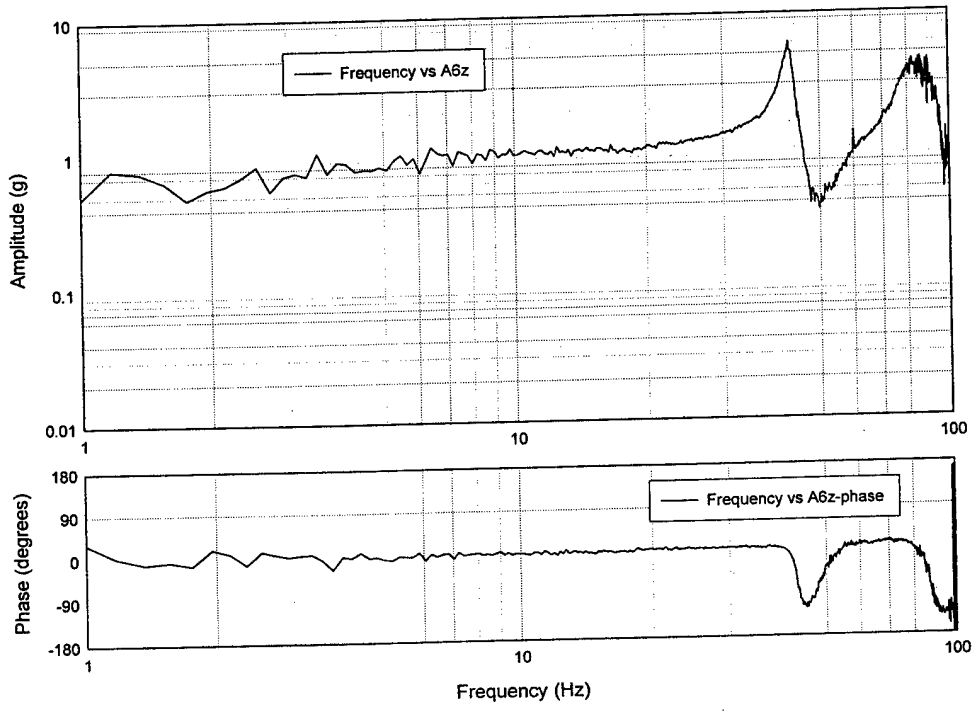

**OUT-OF-PLANE WHITE NOISE TEST AFTER EQ-1
ON NORTH WALL WITH REPAIRED SOUTH WALL**

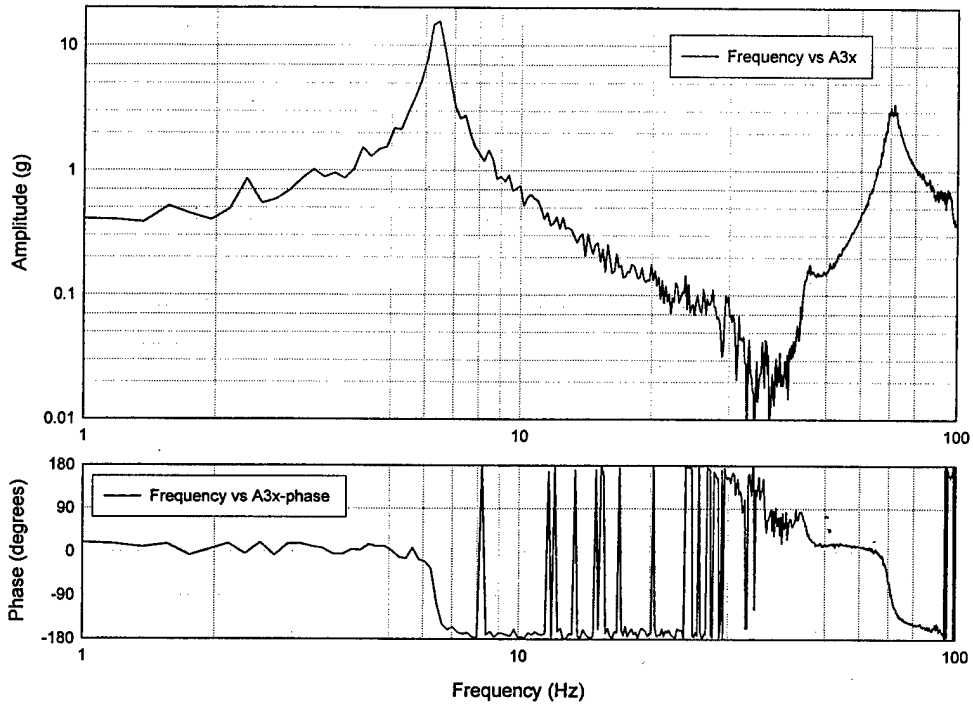

**IN-PLANE WHITE NOISE TEST AFTER EQ-1
ON NORTH WALL WITH REPAIRED SOUTH WALL**

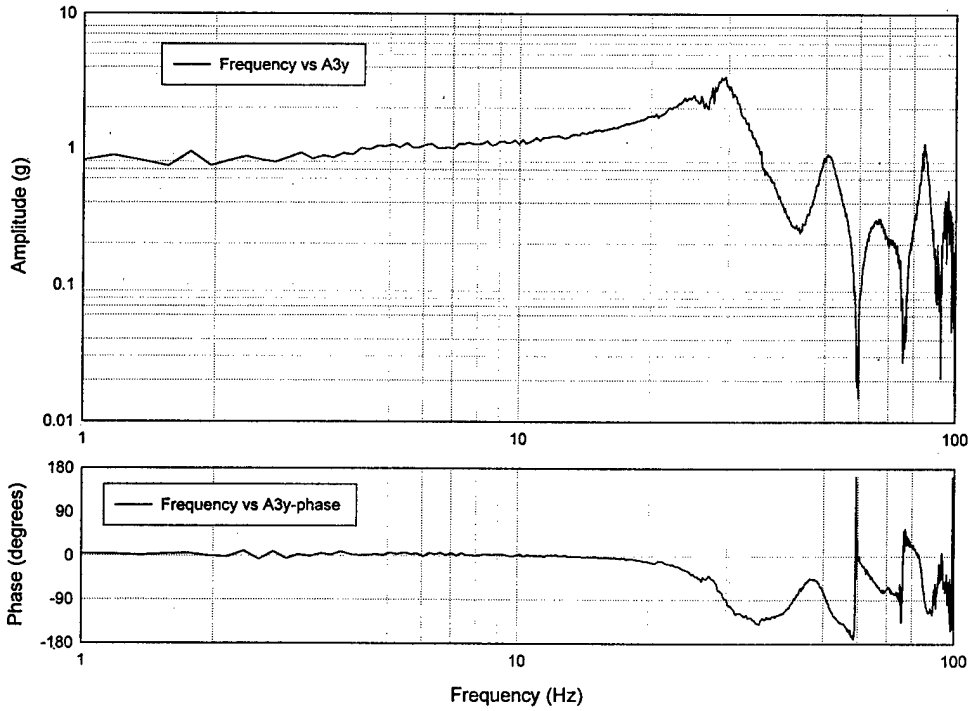

**VERTICAL WHITE NOISE TEST AFTER EQ-1
ON NORTH WALL WITH REPAIRED SOUTH WALL**

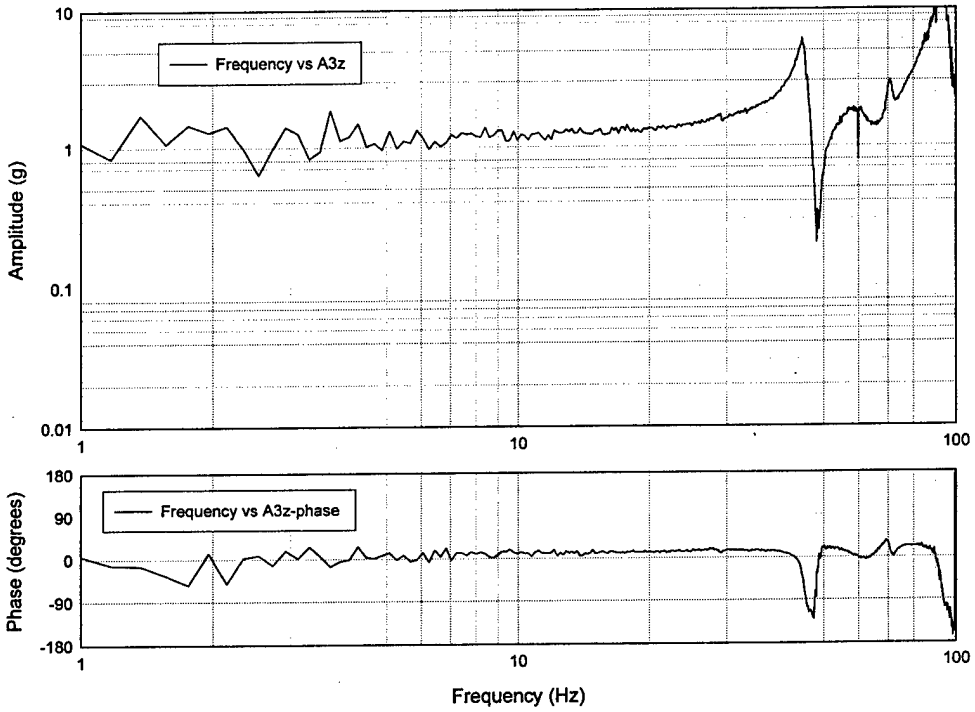

**OUT-OF-PLANE WHITE NOISE TEST AFTER EQ-1
ON SOUTH WALL WITH REPAIRED SOUTH WALL**

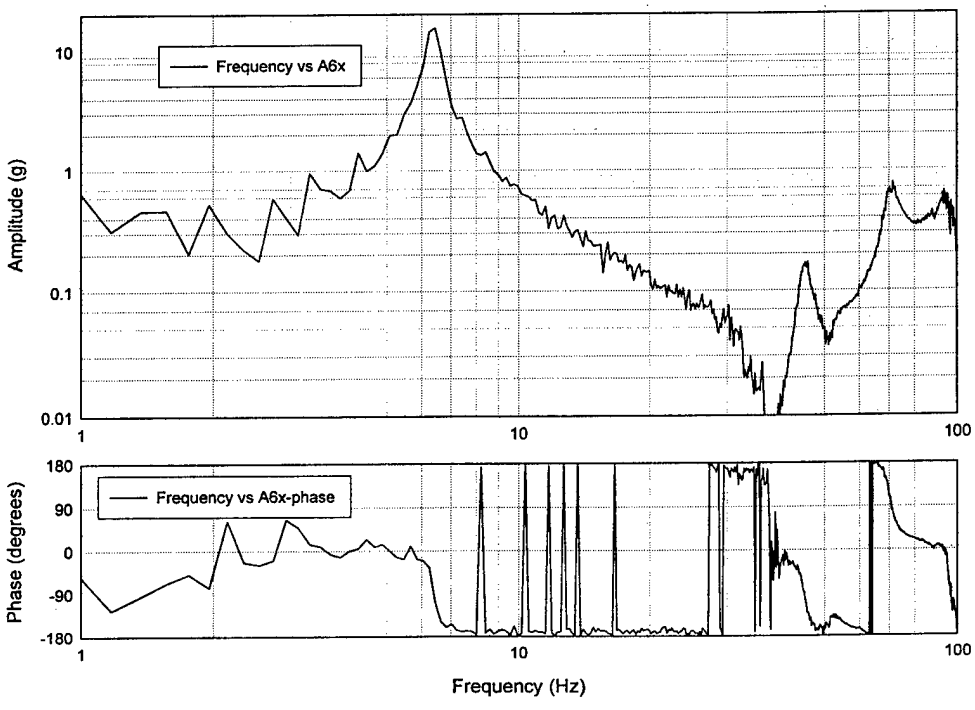

**IN-PLANE WHITE NOISE TEST AFTER EQ-1
ON SOUTH WALL WITH REPAIRED SOUTH WALL**

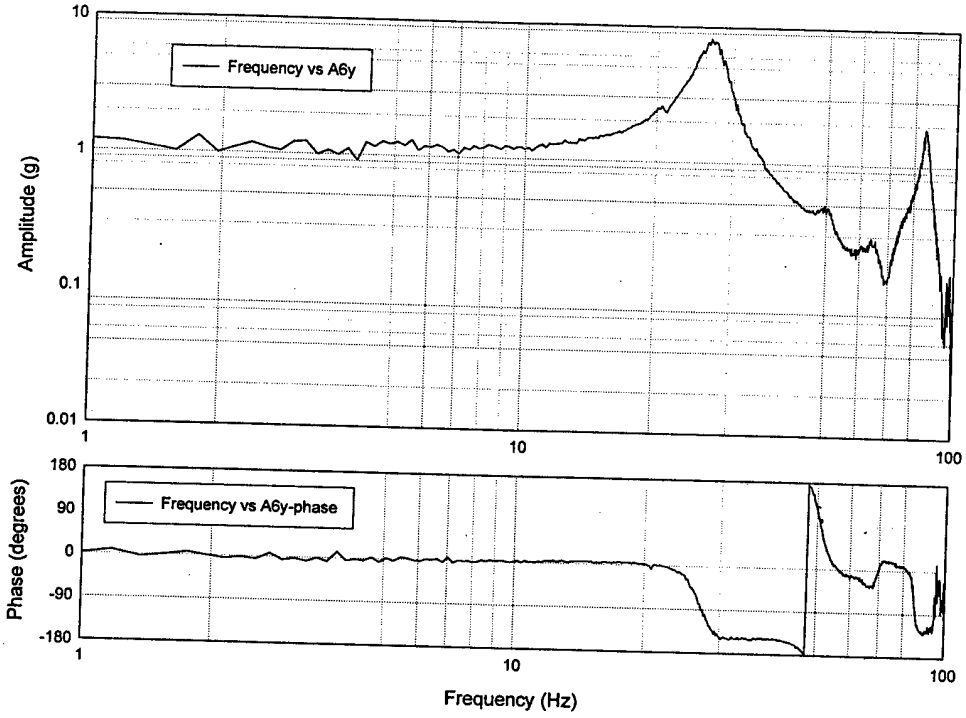

**VERTICAL WHITE NOISE TEST AFTER EQ-1
ON SOUTH WALL WITH REPAIRED SOUTH WALL**

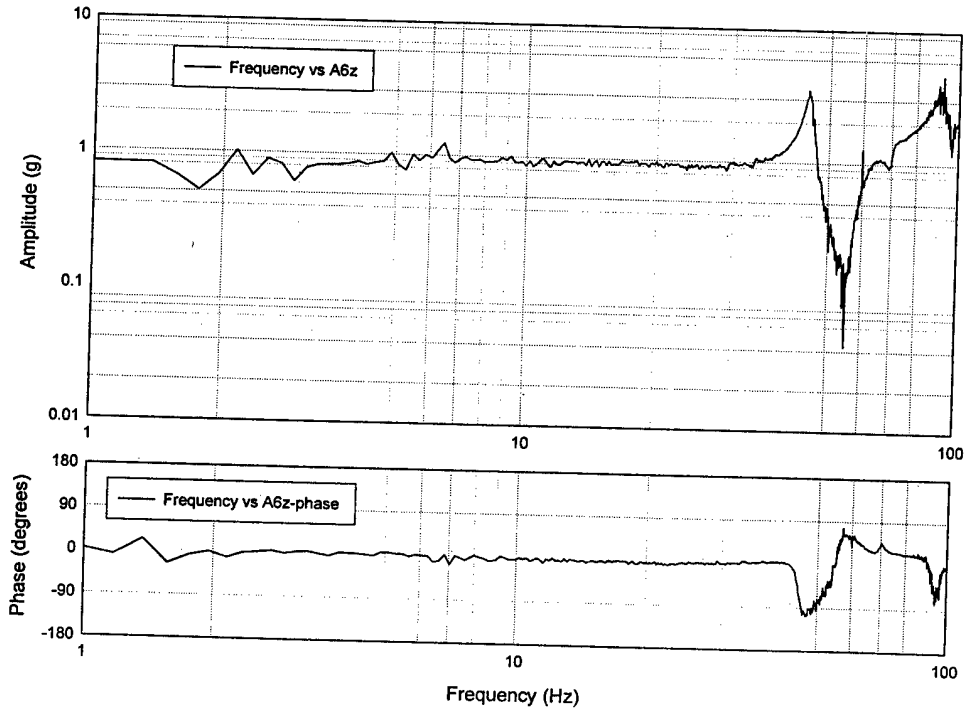

OUT-OF-PLANE WHITE NOISE TEST AFTER EQ-6 ON NORTH WALL WITHOUT SLAB

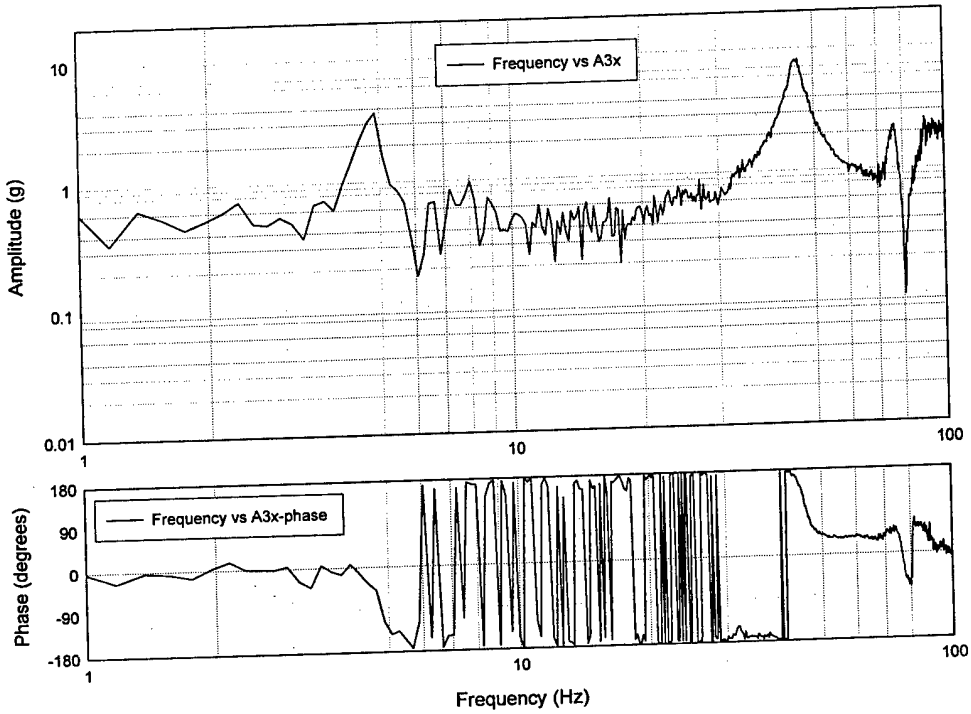

IN-PLANE WHITE NOISE TEST AFTER EQ-6 ON NORTH WALL WITHOUT SLAB

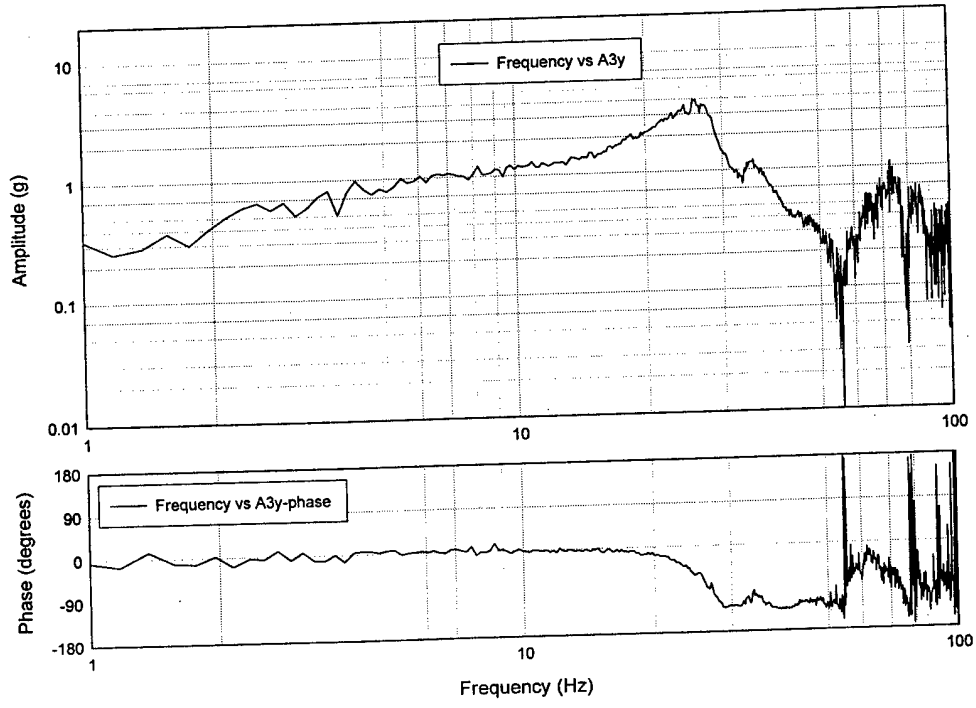

**VERICAL WHITE NOISE TEST AFTER EQ-6
ON NORTH WALL WITHOUT SLAB**

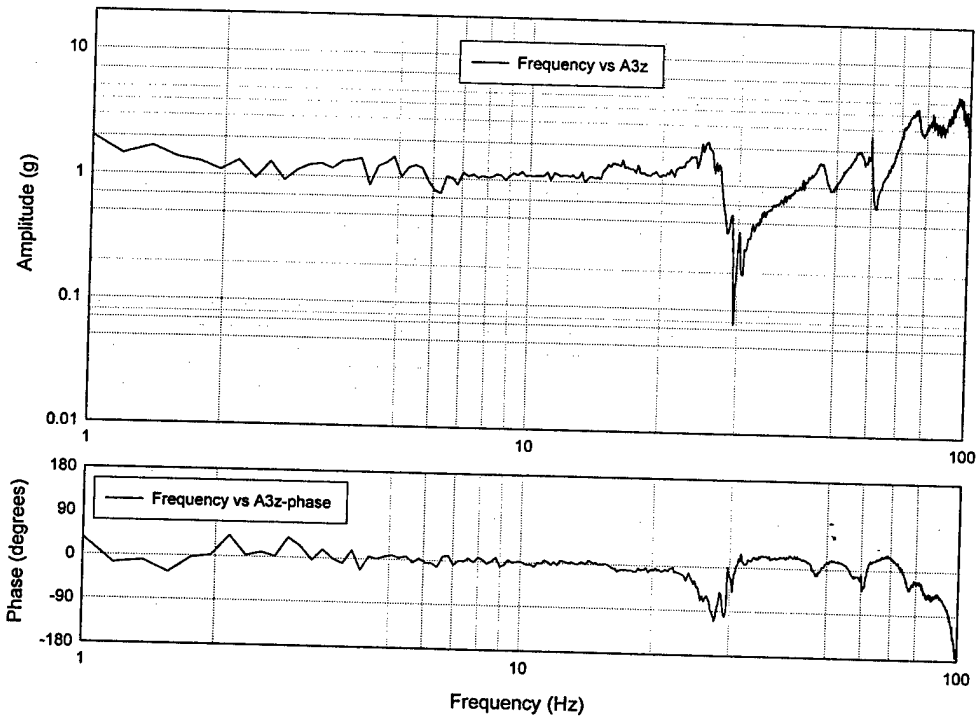

**OUT-OF-PLANE WHITE NOISE TEST AFTER EQ-6
ON SOUTH WALL WITHOUT SLAB**

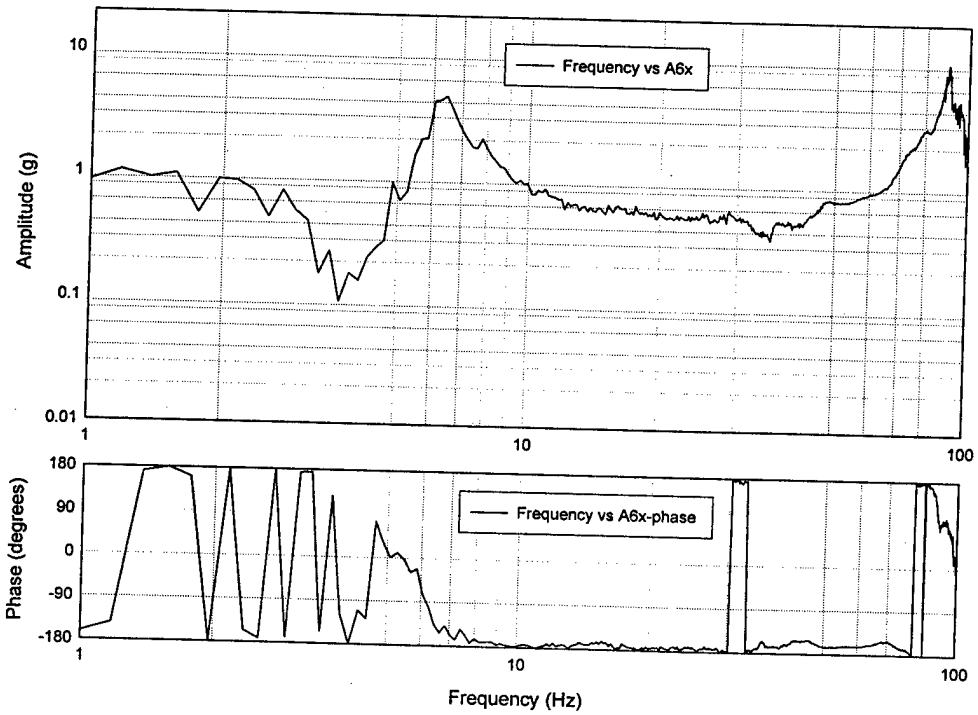

IN-PLANE WHITE NOISE TEST AFTER EQ-6 ON SOUTH WALL WITHOUT SLAB

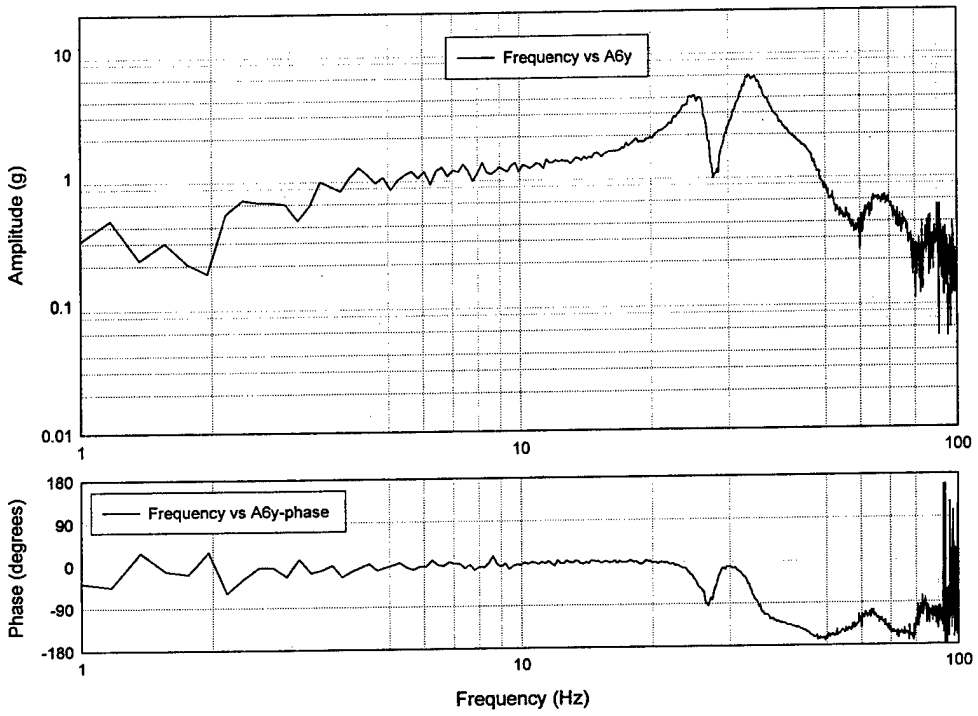

VERICAL WHITE NOISE TEST AFTER EQ-6 ON SOUTH WALL WITHOUT SLAB

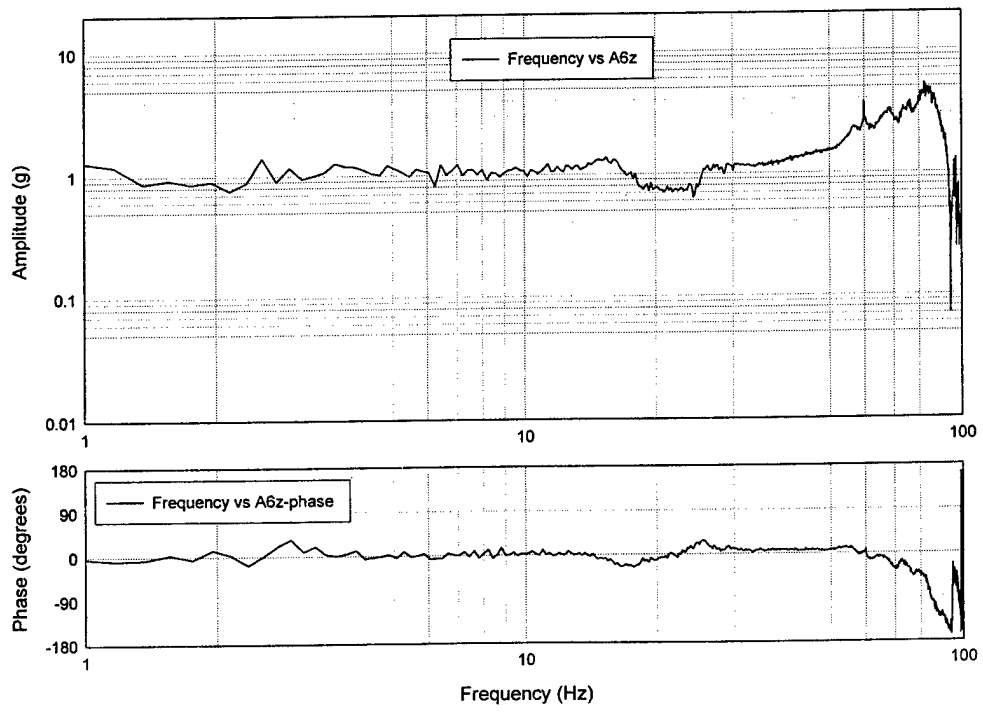

**OUT-OF-PLANE WHITE NOISE TEST AFTER EQ-6
ON NORTH WALL WITH SLAB ON TOP**

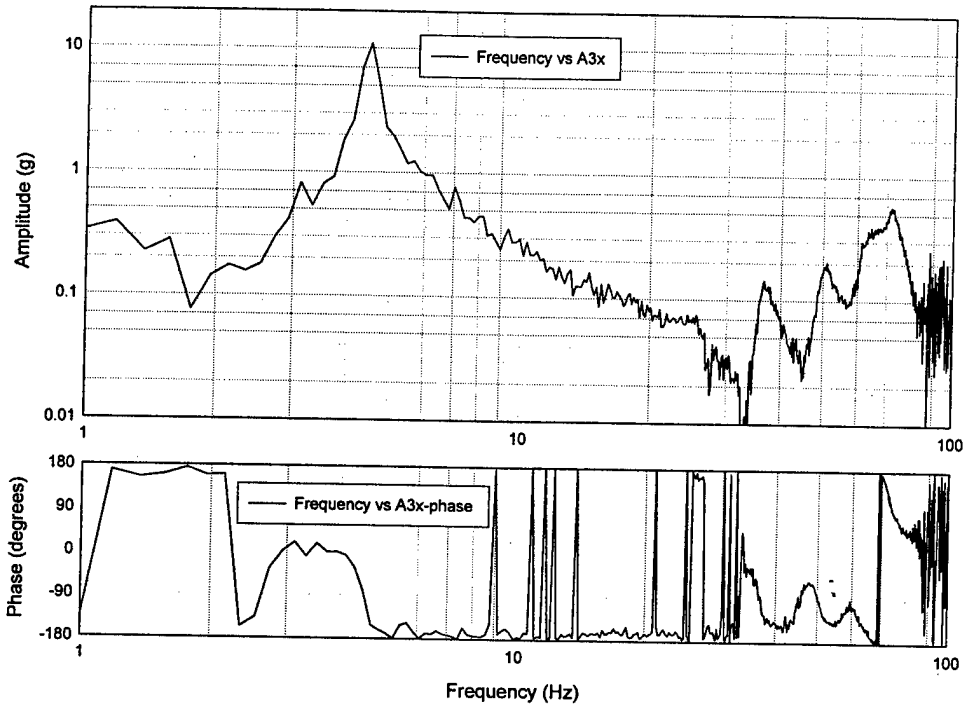

**IN-PLANE WHITE NOISE TEST AFTER EQ-6
ON NORTH WALL WITH SLAB ON TOP**

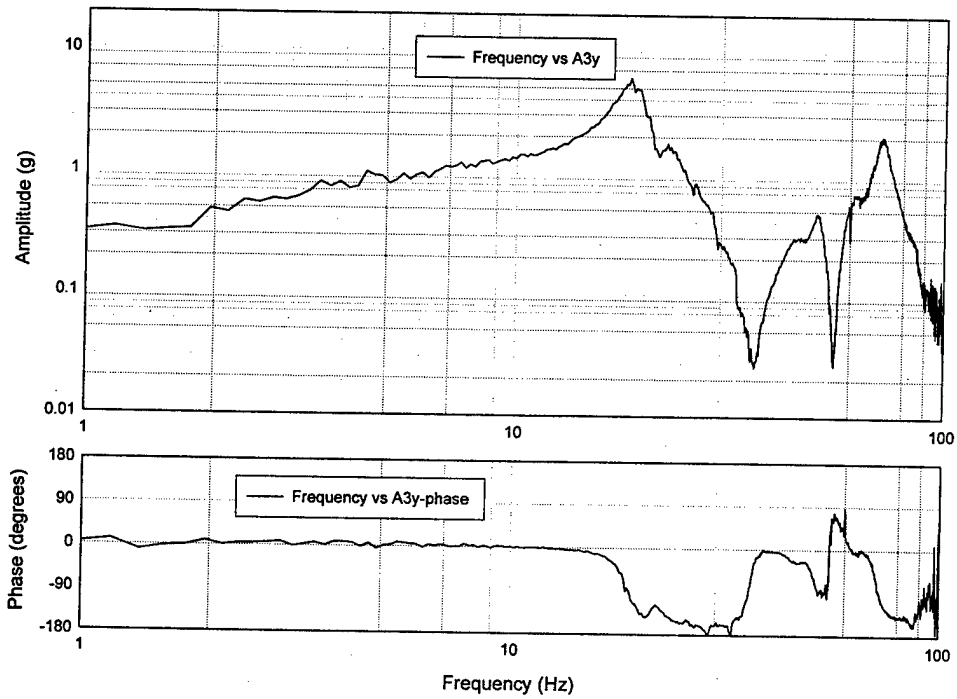

**VERTICAL WHITE NOISE TEST AFTER EQ-6
ON NORTH WALL WITH SLAB ON TOP**

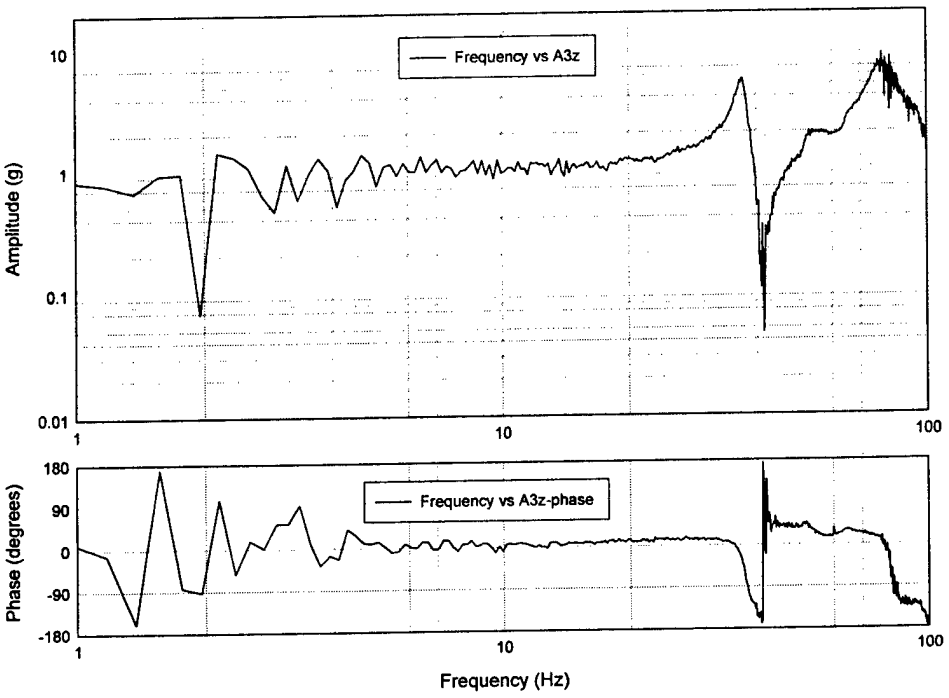

**OUT-OF-PLANE WHITE NOISE TEST AFTER EQ-6
ON SOUTH WALL WITH SLAB ON TOP**

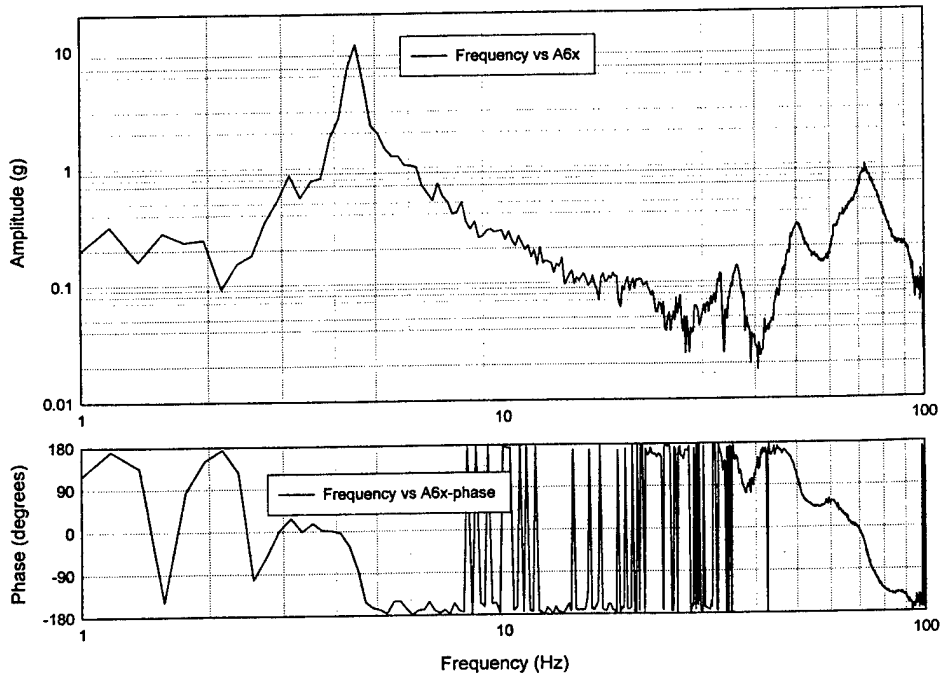

IN-PLANE WHITE NOISE TEST AFTER EQ-6 ON SOUTH WALL WITH SLAB ON TOP

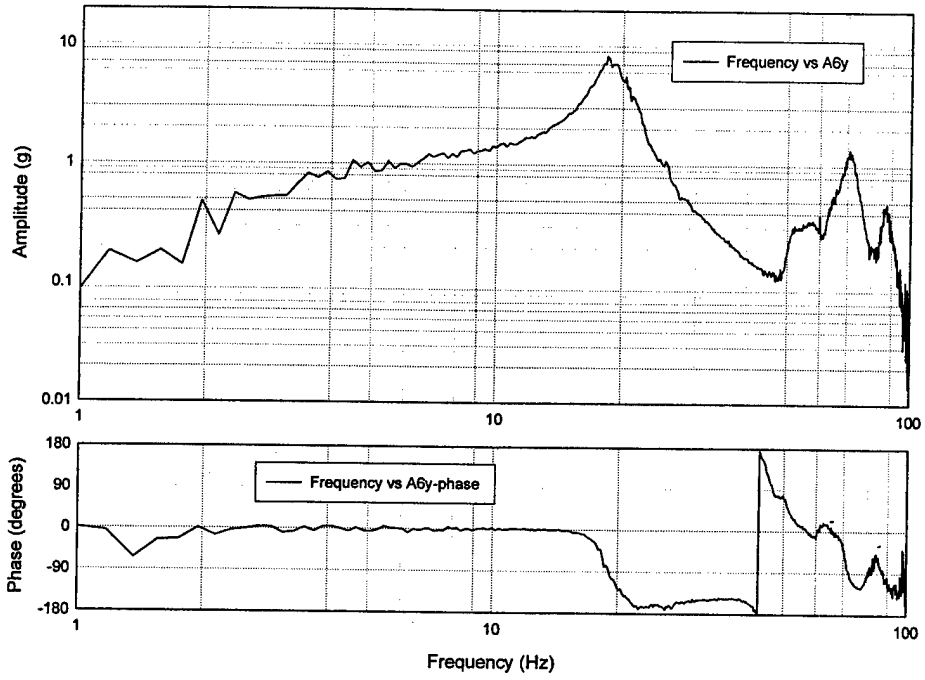

VERTICAL WHITE NOISE TEST AFTER EQ-6 ON SOUTH WALL WITH SLAB ON TOP

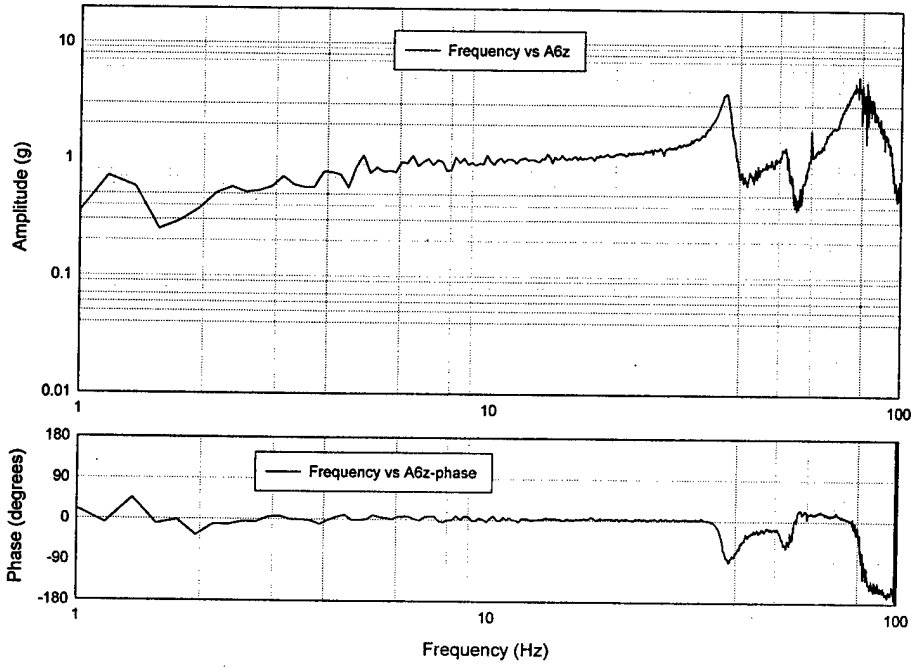

OUT-OF-PLANE WHITE NOISE TEST AFTER EQ-7
ON NORTH WALL WITH SLAB ON TOP

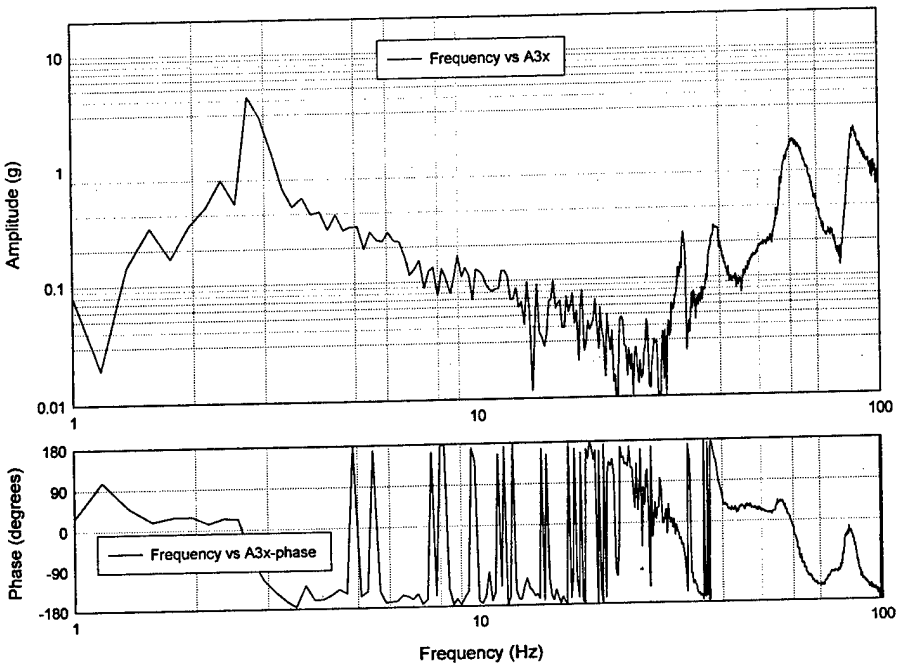

IN-PLANE WHITE NOISE TEST AFTER EQ-7
ON NORTH WALL WITH SLAB ON TOP

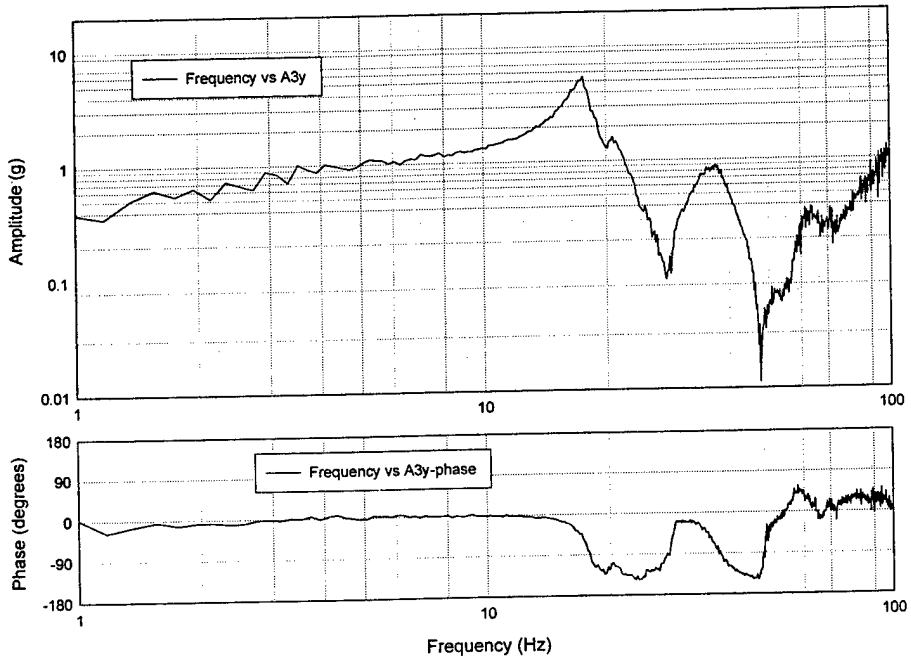

VERTICAL WHITE NOISE TEST AFTER EQ-7
ON NORTH WALL WITH SLAB ON TOP

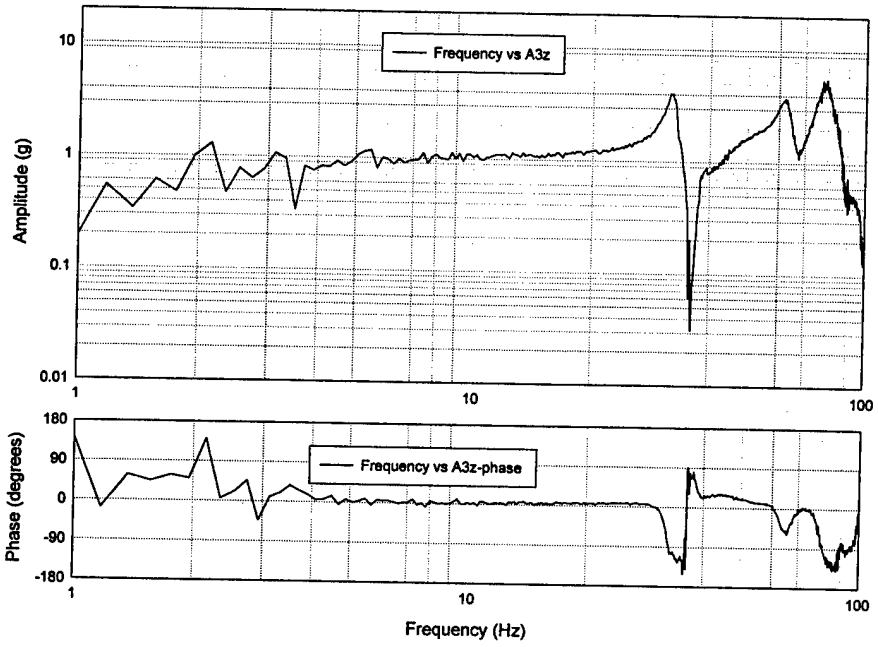

OUT-OF-PLANE WHITE NOISE TEST AFTER EQ-7
ON SOUTH WALL WITH SLAB ON TOP

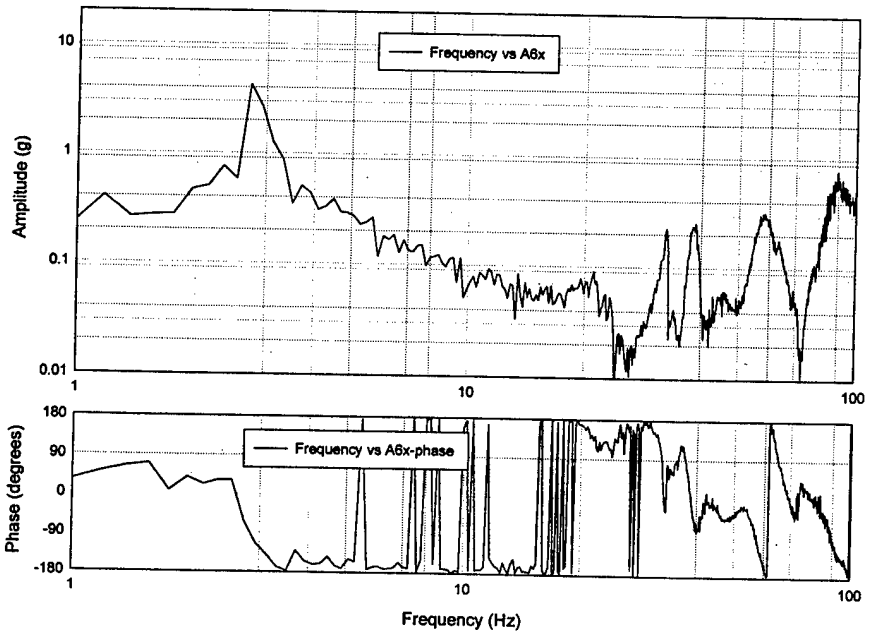

IN-PLANE WHITE NOISE TEST AFTER EQ-7
ON SOUTH WALL WITH SLAB ON TOP

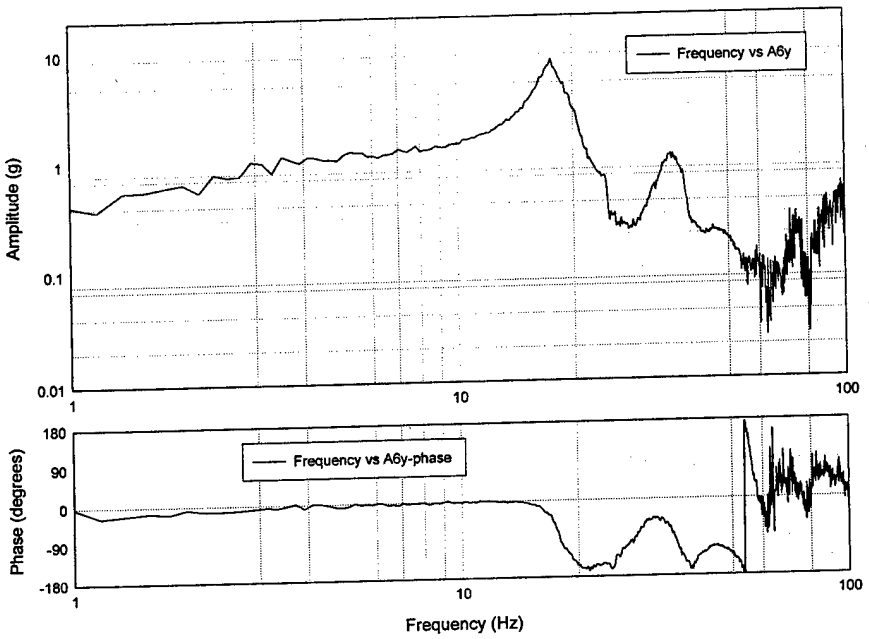

VERTICAL WHITE NOISE TEST AFTER EQ-7
ON SOUTH WALL WITH SLAB ON TOP

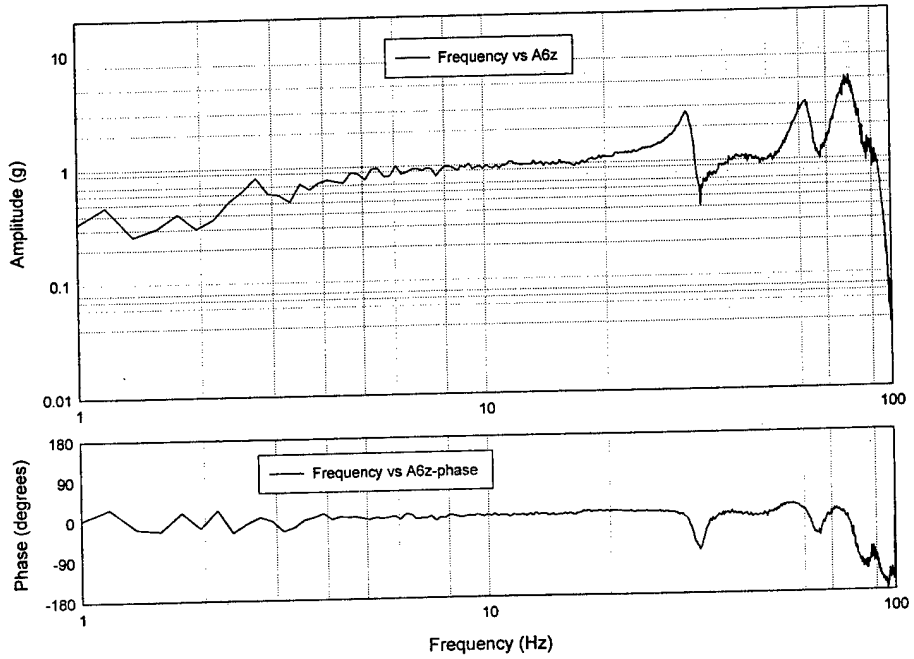

Appendix F: Acceleration Response Plots

Out-of-Plane Response Spectrum of
North Wall for EQ-1 with 5% Damping

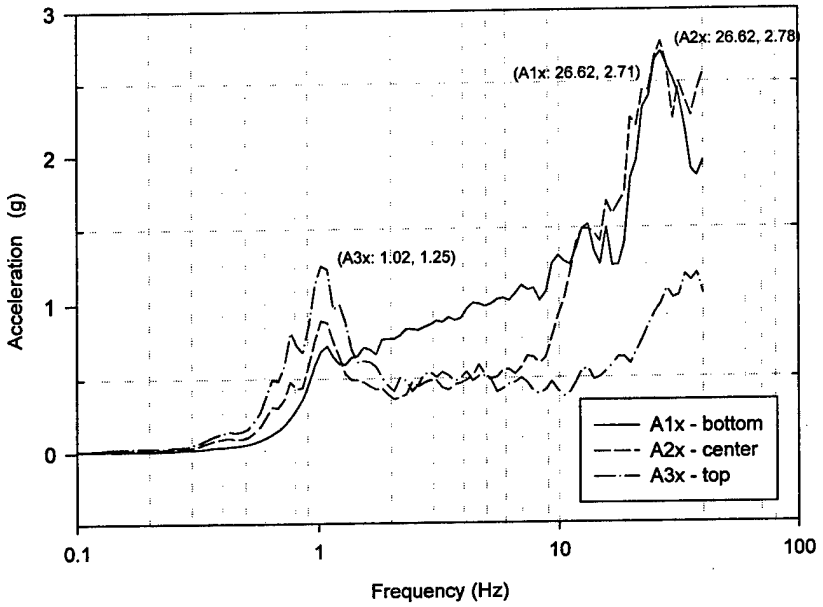

Out-of-Plane Response Spectrum of
North Wall for EQ-1 with 5% Damping

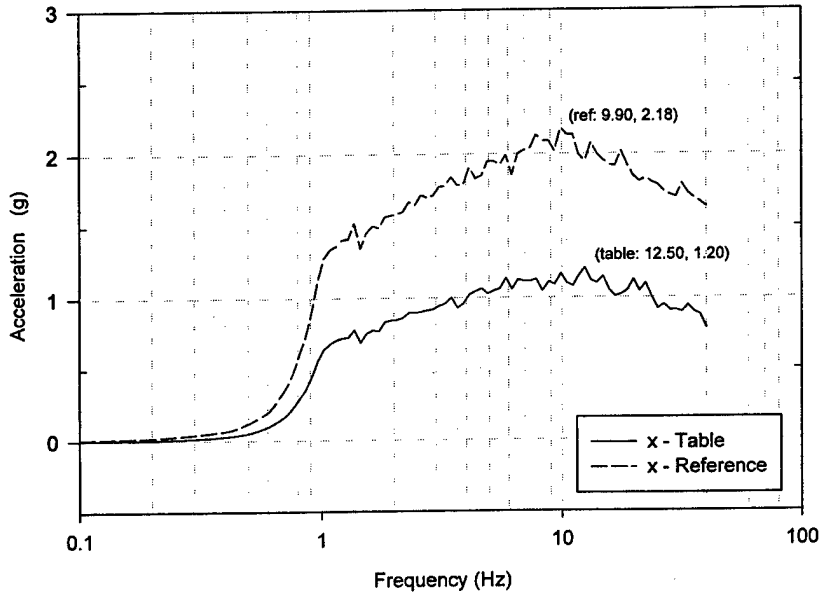

In-Plane Response Spectrum of
North Wall for EQ-1 with 5% Damping

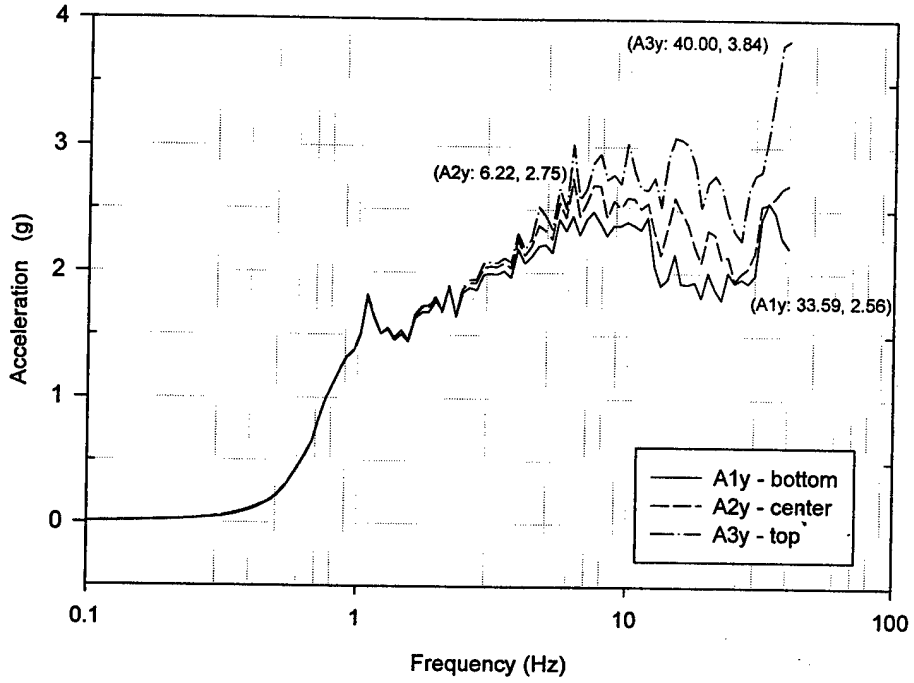

In-Plane Response Spectrum of
North Wall for EQ-1 with 5% Damping

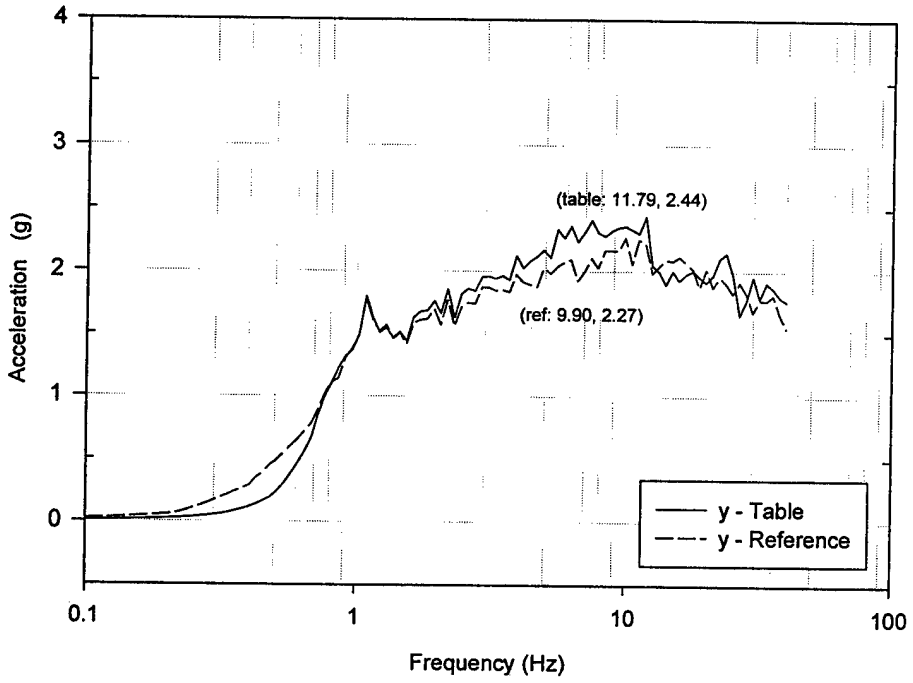

Vertical Response Spectrum of
North Wall for EQ-1 with 5% Damping

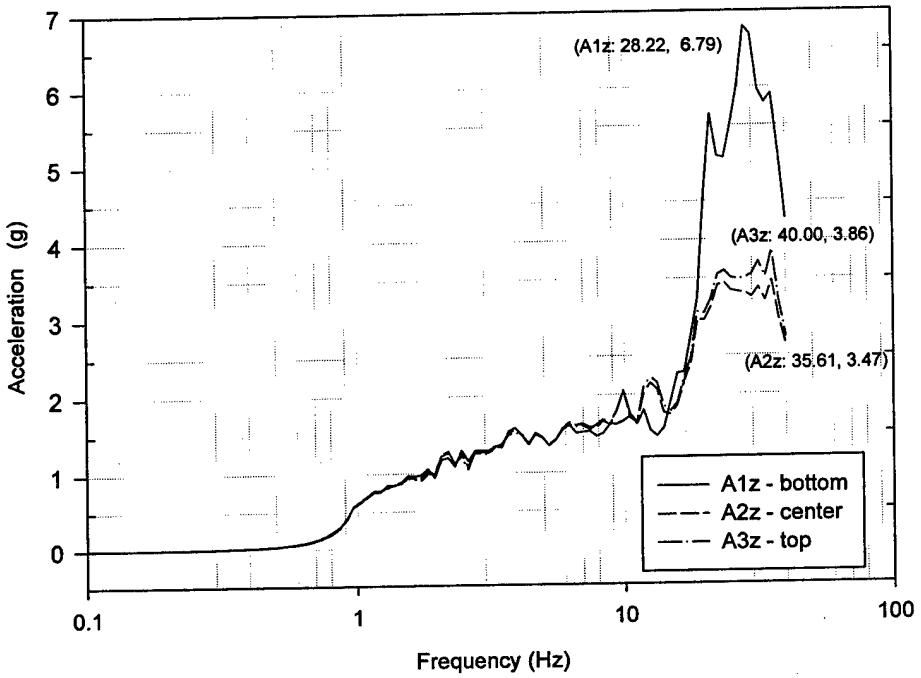

Vertical Response Spectrum of
North Wall for EQ-1 with 5% Damping

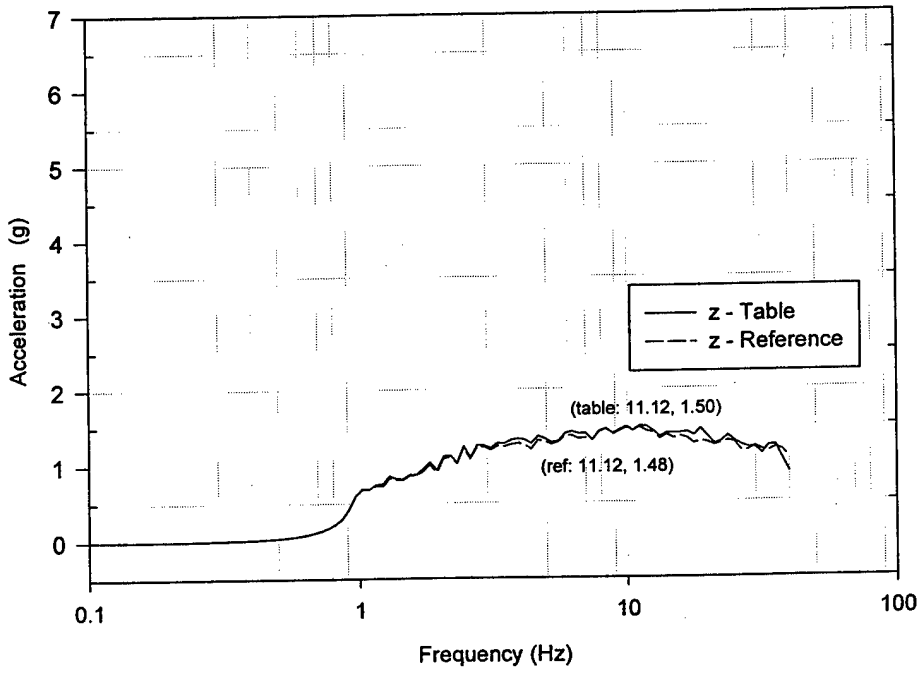

Out-of-Plane Response Spectrum of
South Wall for EQ-1 with 5% Damping

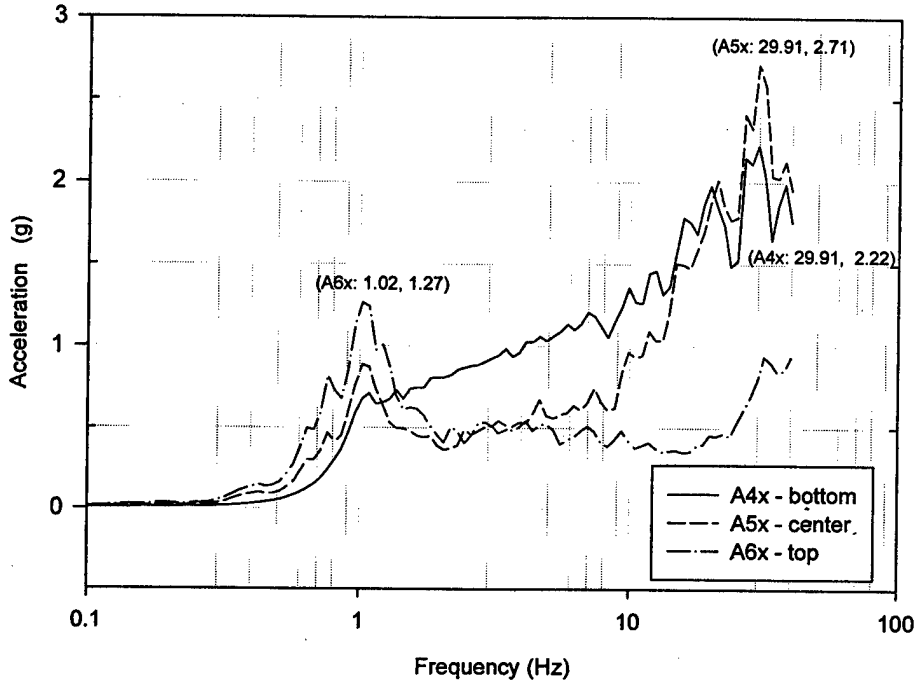

Out-of-Plane Response Spectrum of
South Wall for EQ-1 with 5% Damping

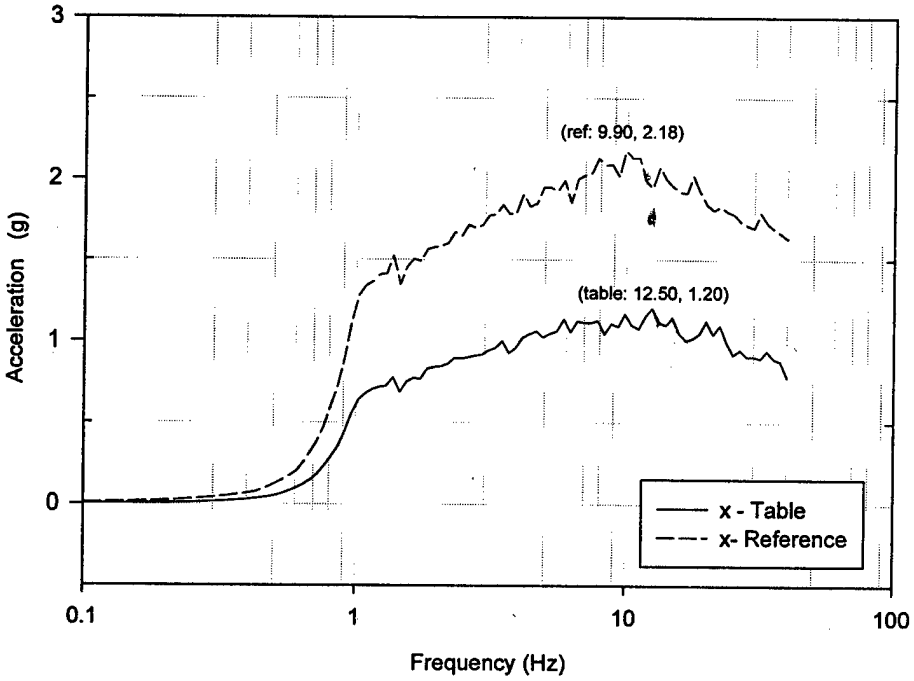

In-Plane Response Spectrum of
South Wall for EQ-1 with 5% Damping

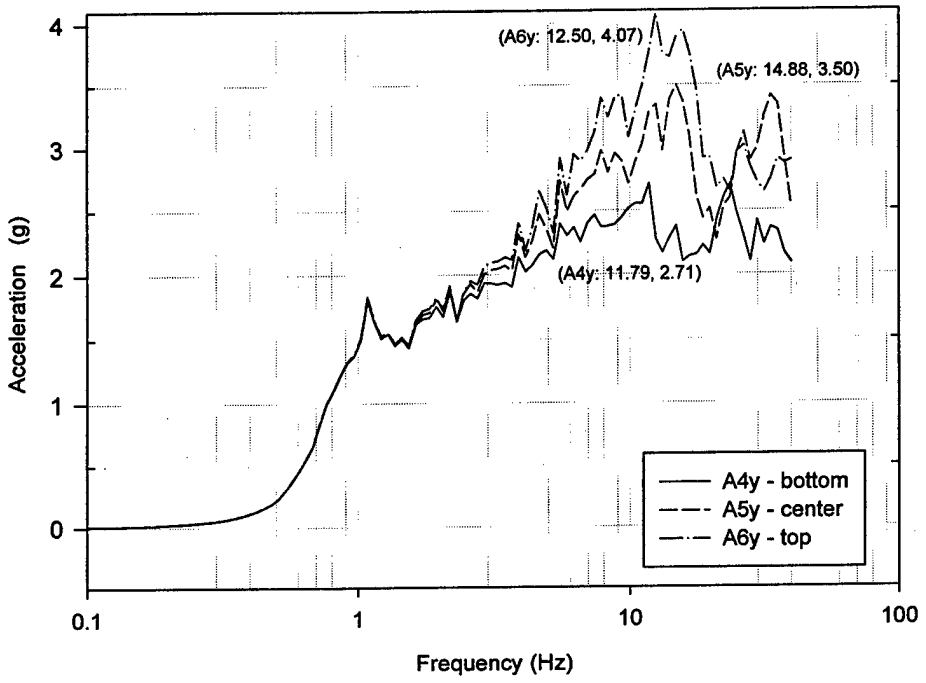

In-Plane Response Spectrum of
South Wall for EQ-1 with 5% Damping

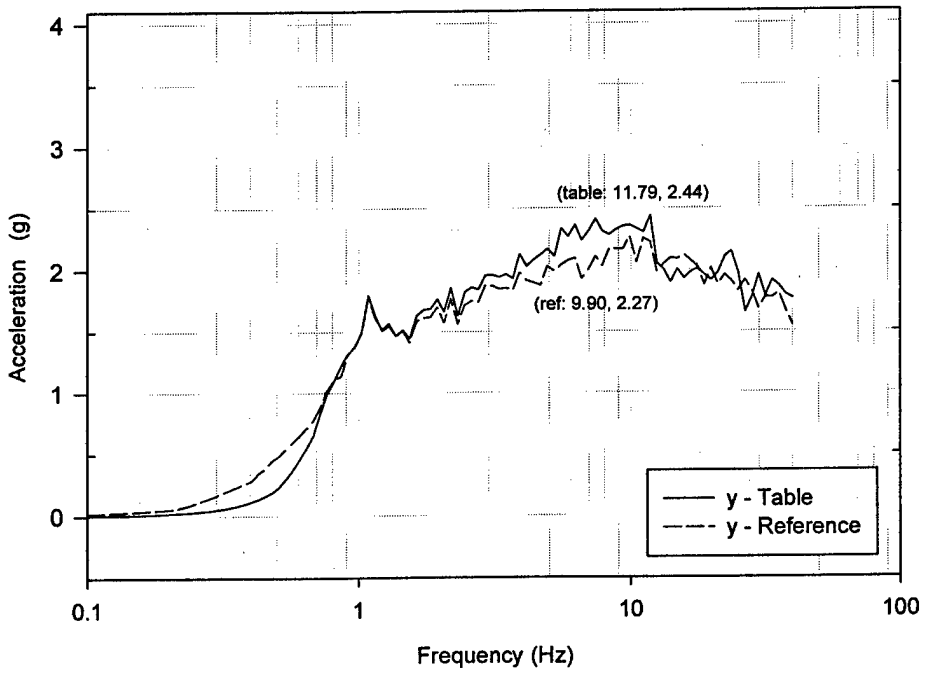

Vertical Response Spectrum of
South Wall for EQ-1 with 5% Damping

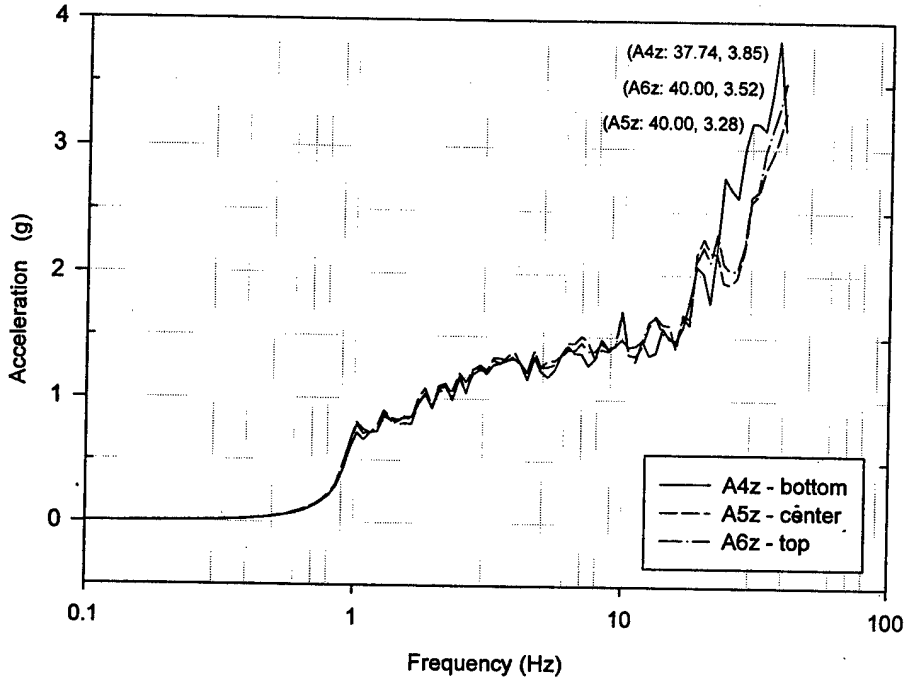

Vertical Response Spectrum of
South Wall for EQ-1 with 5% Damping

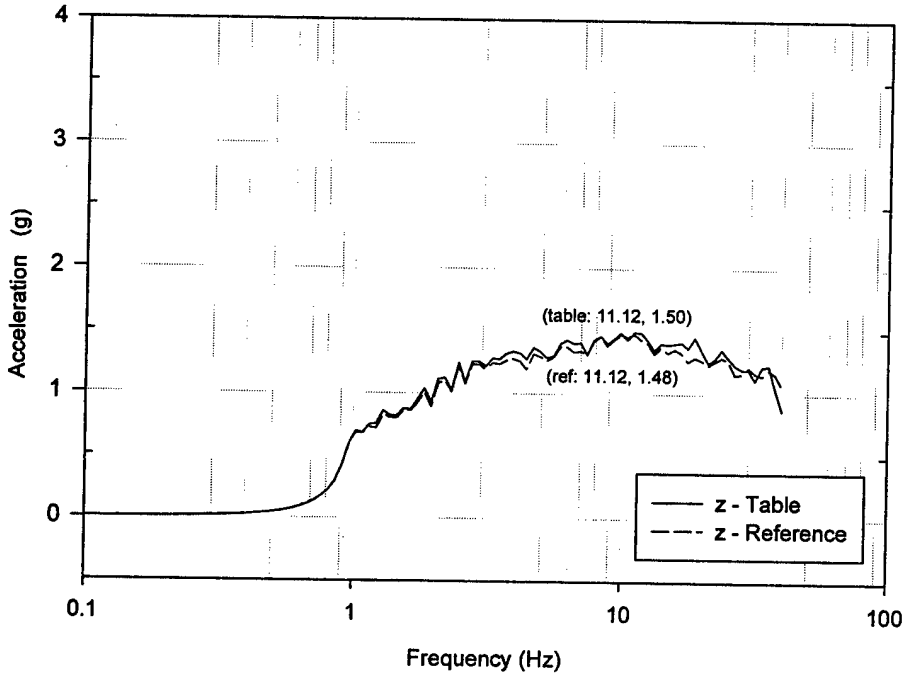

Out-of-Plane Response Spectrum of
North Wall for EQ-6 with 5% Damping

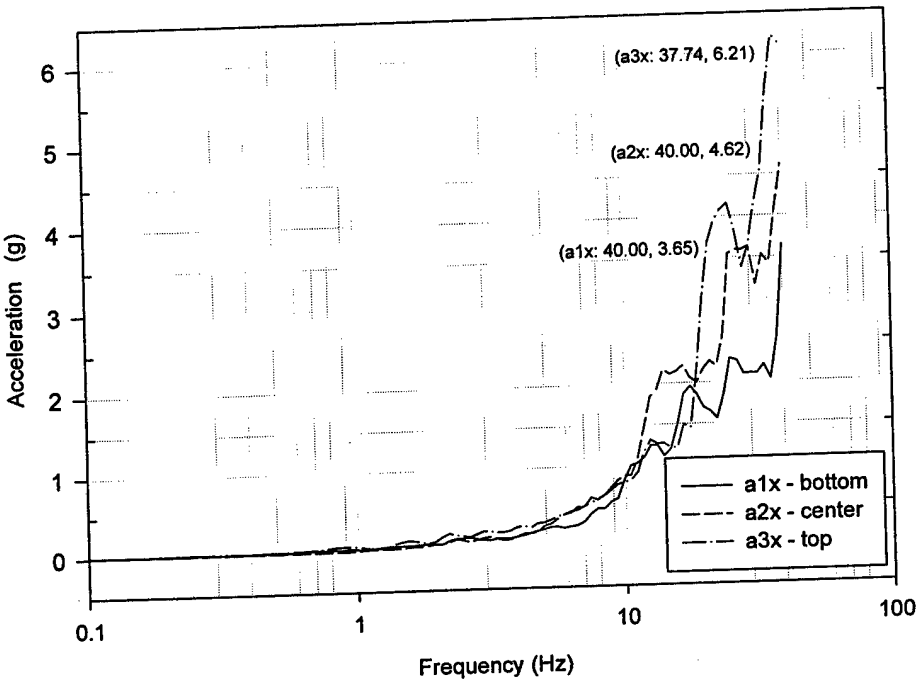

Out-of-Plane Response Spectrum of
South Wall for EQ-6 with 5% Damping

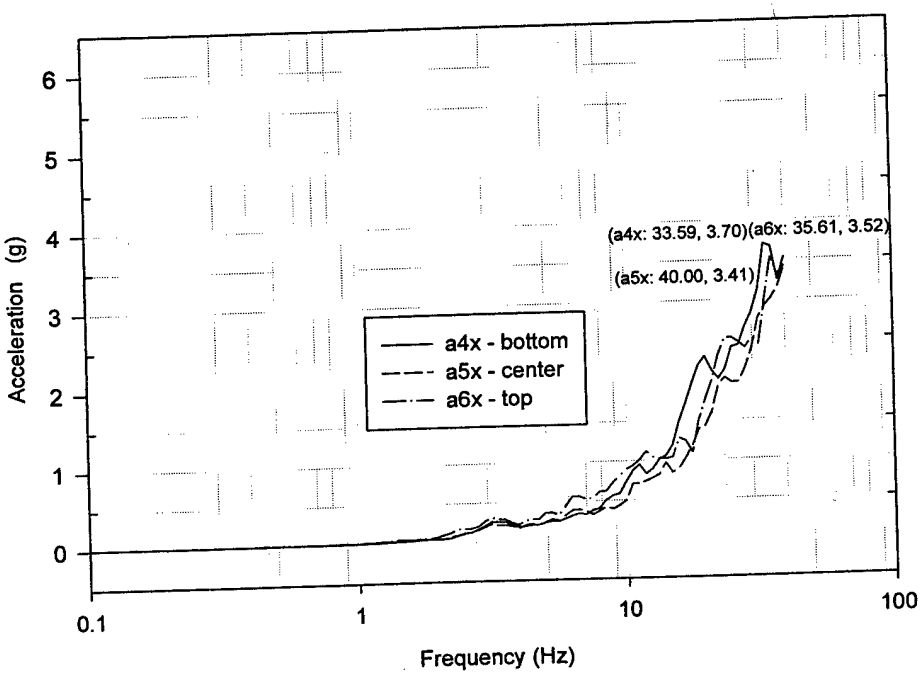

Vertical Response Spectrum of
North Wall for EQ-6 with 5% Damping

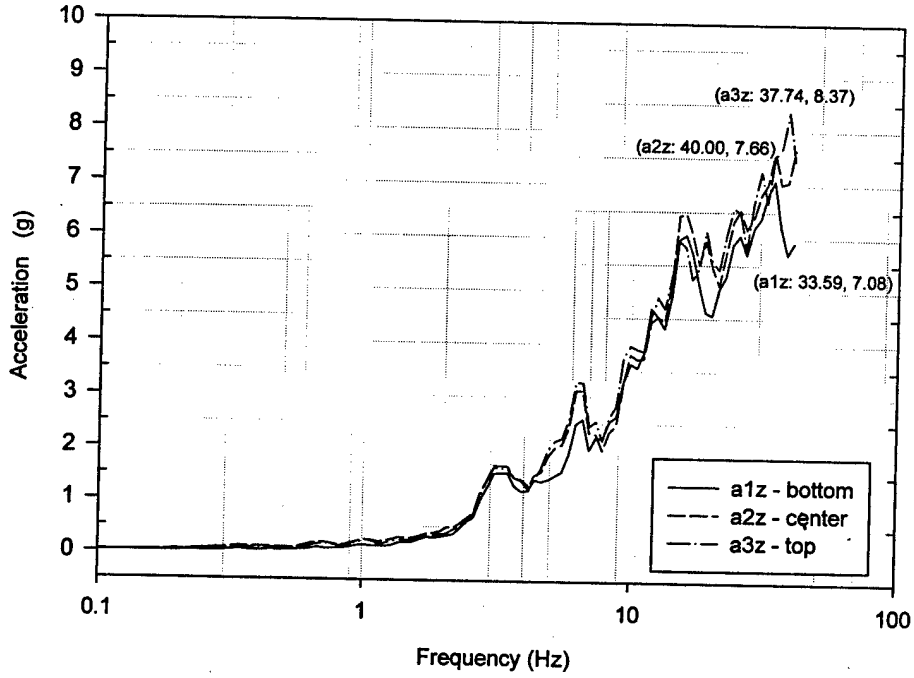

Vertical Response Spectrum of
South Wall for EQ-6 with 5% Damping

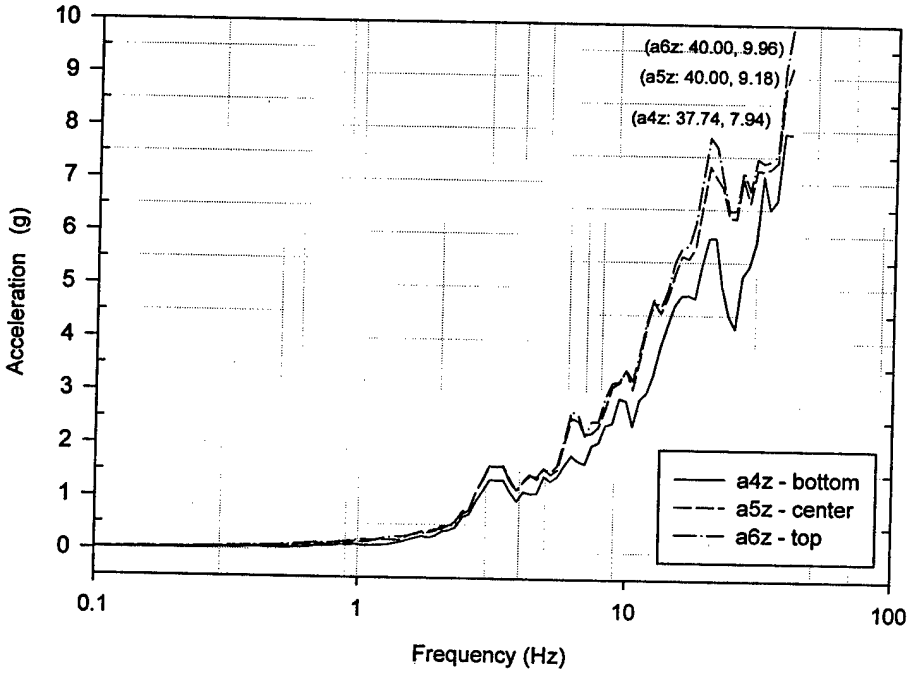

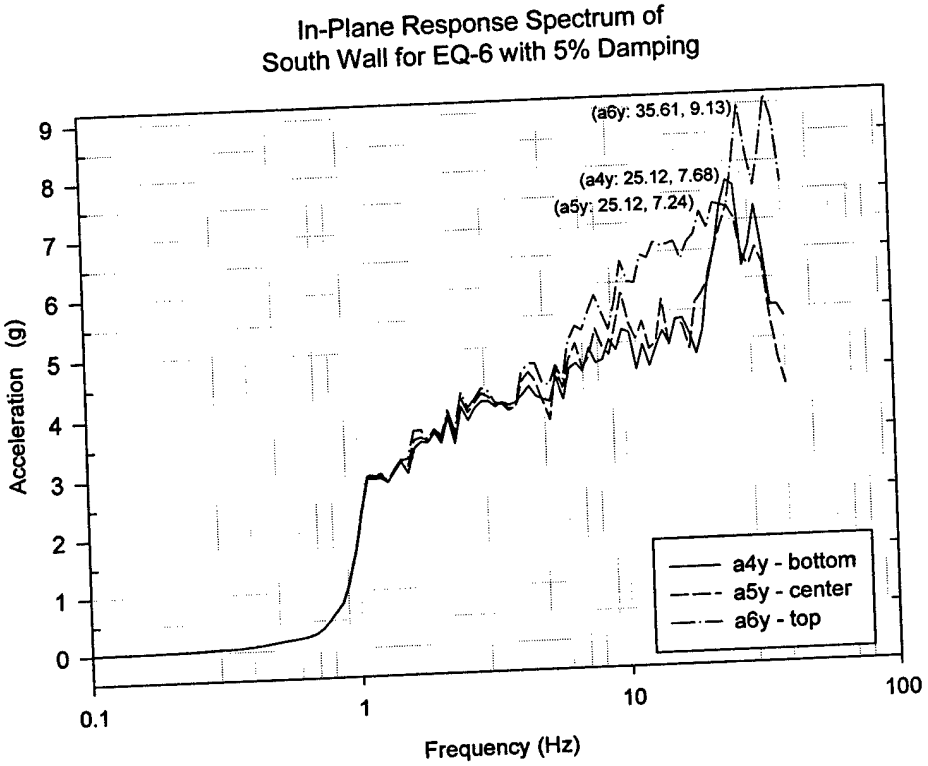
In-Plane Response Spectrum of
South Wall for EQ-6 with 5% Damping
(a6y: 35.61, 9.13)
(a4y: 25.12, 7.68)
(a5y: 25.12, 7.24)
a4y - bottom
a5y - center
a6y - top
Acceleration (g)
Frequency (Hz)
0
1
2
3
4
5
6
7
8
9
0.1
1
10
100

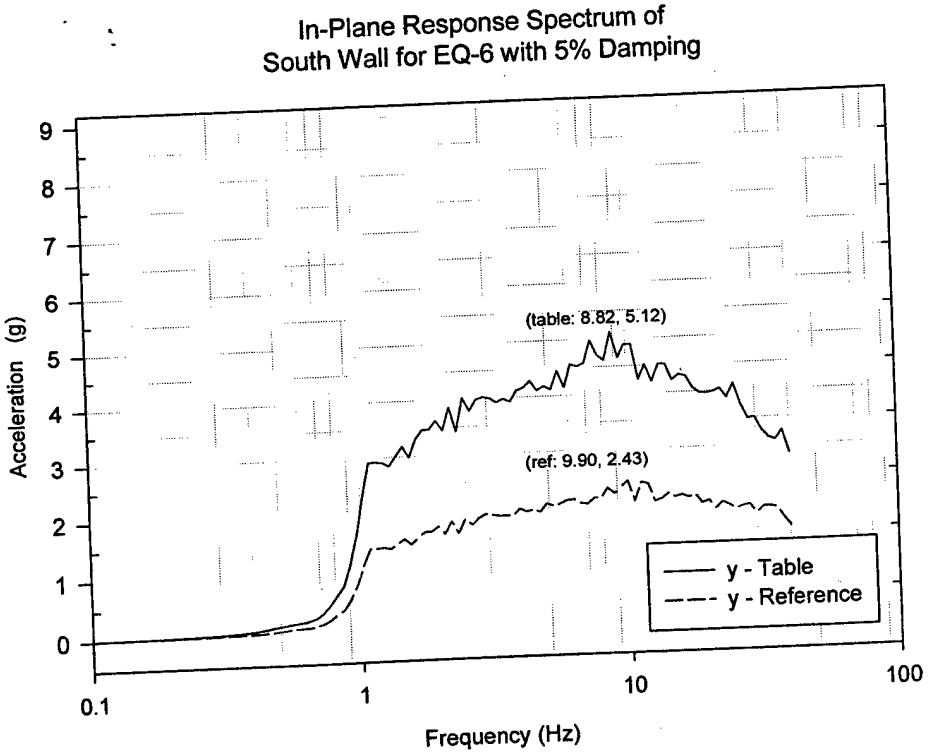
In-Plane Response Spectrum of
South Wall for EQ-6 with 5% Damping
(table: 8.82, 5.12)
(ref: 9.90, 2.43)
y - Table
y - Reference
Acceleration (g)
Frequency (Hz)
0
1
2
3
4
5
6
7
8
9
0.1
1
10
100

In-Plane Response Spectrum of
North Wall for EQ-6 with 5% Damping

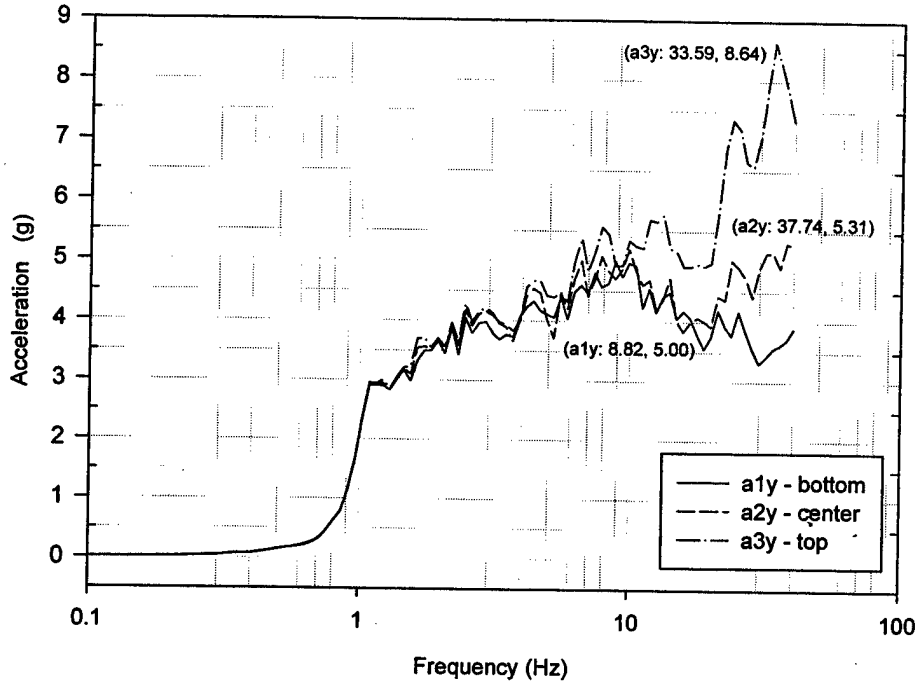

In-Plane Response Spectrum of
North Wall for EQ-6 with 5% Damping

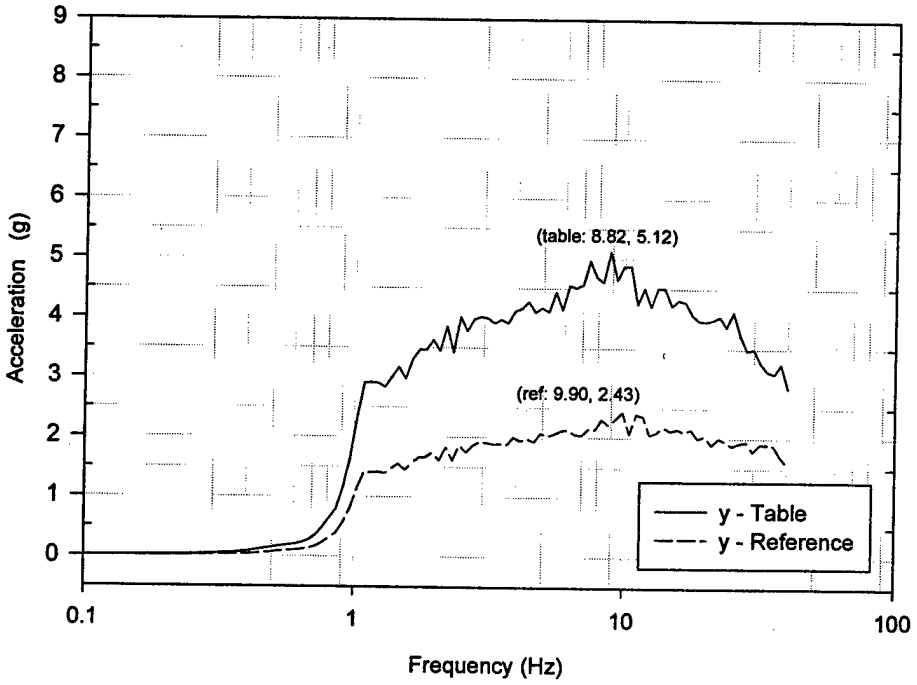

Out-of-Plane Response Spectrum of
North Wall for EQ-7 with 5% Damping

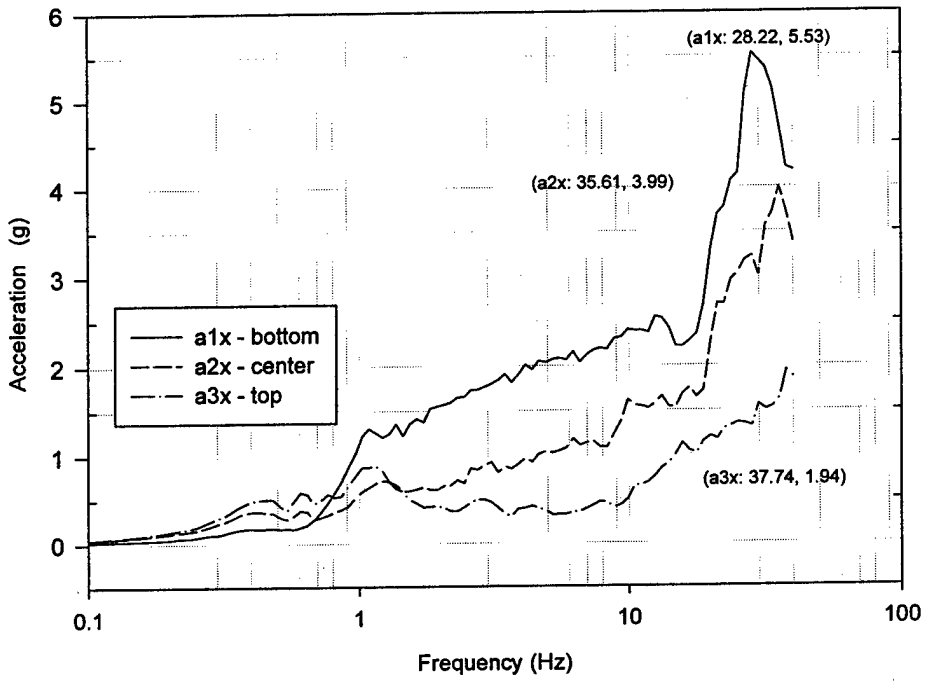

Out-of-Plane Response Spectrum of
North Wall for EQ-7 with 5% Damping

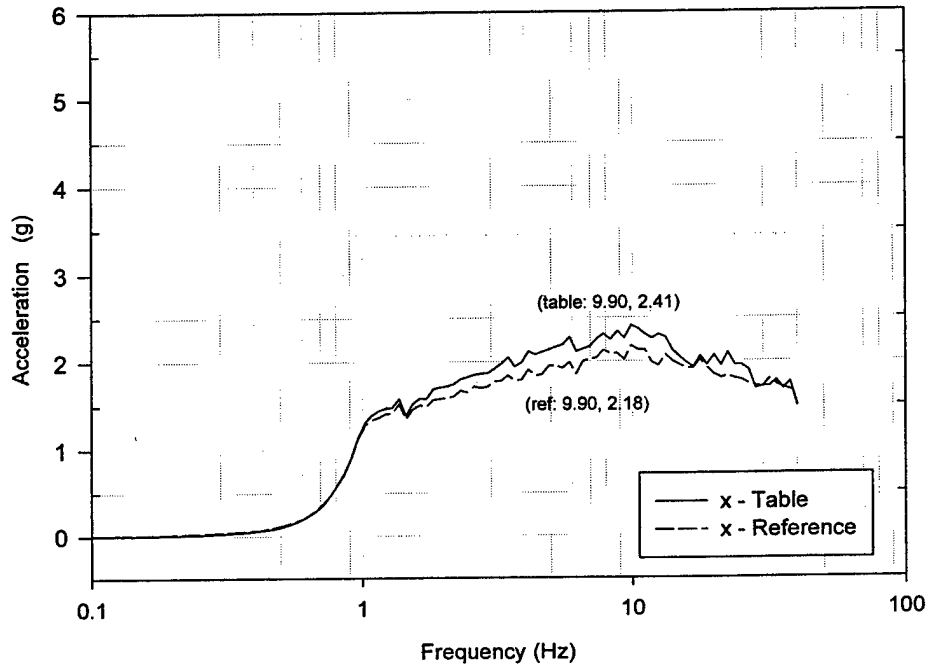

In-Plane Response Spectrum of
North Wall for EQ-7 with 5% Damping

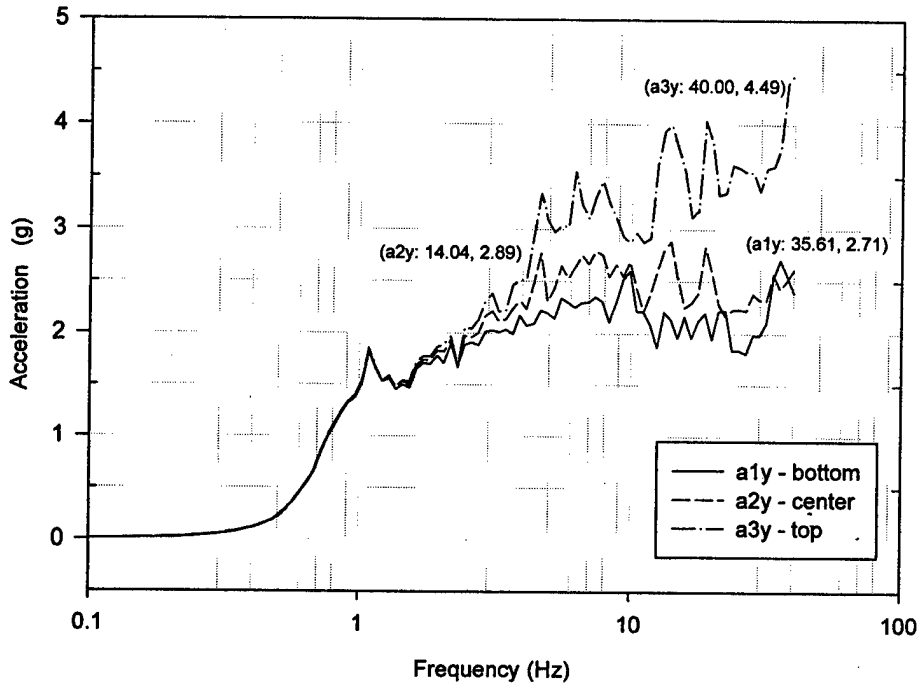

In-Plane Response Spectrum of
North Wall for EQ-7 with 5% Damping

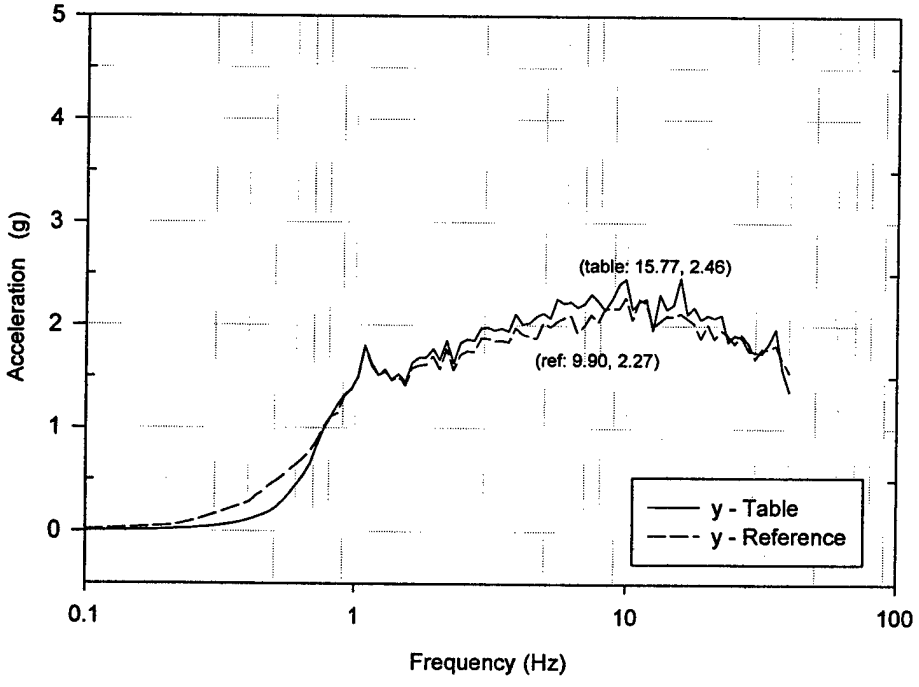

Vertical Response Spectrum of
North Wall for EQ-7 with 5% Damping

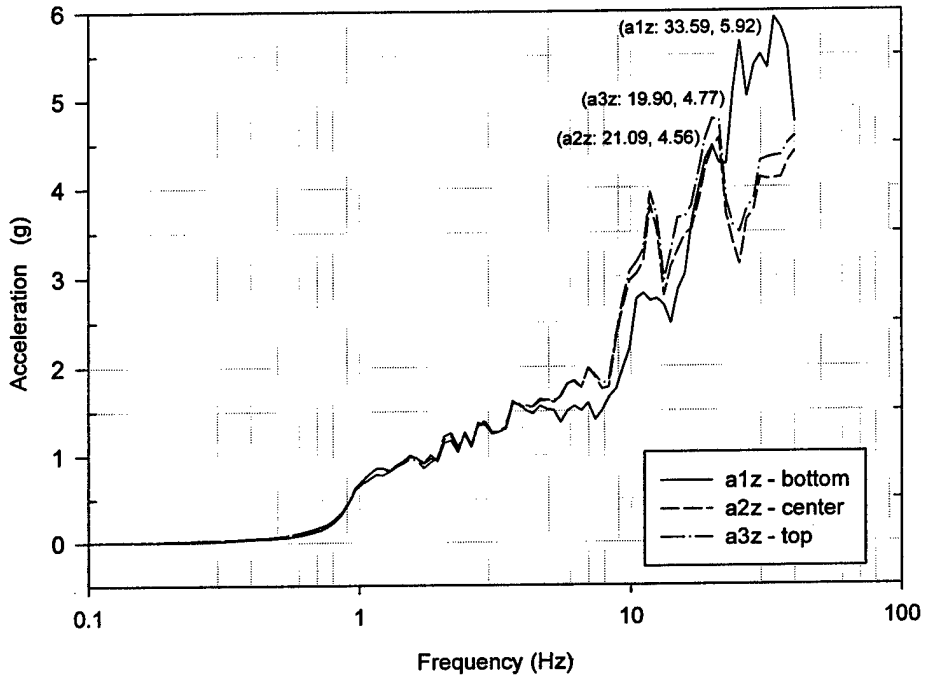

Vertical Response Spectrum of
North Wall for EQ-7 with 5% Damping

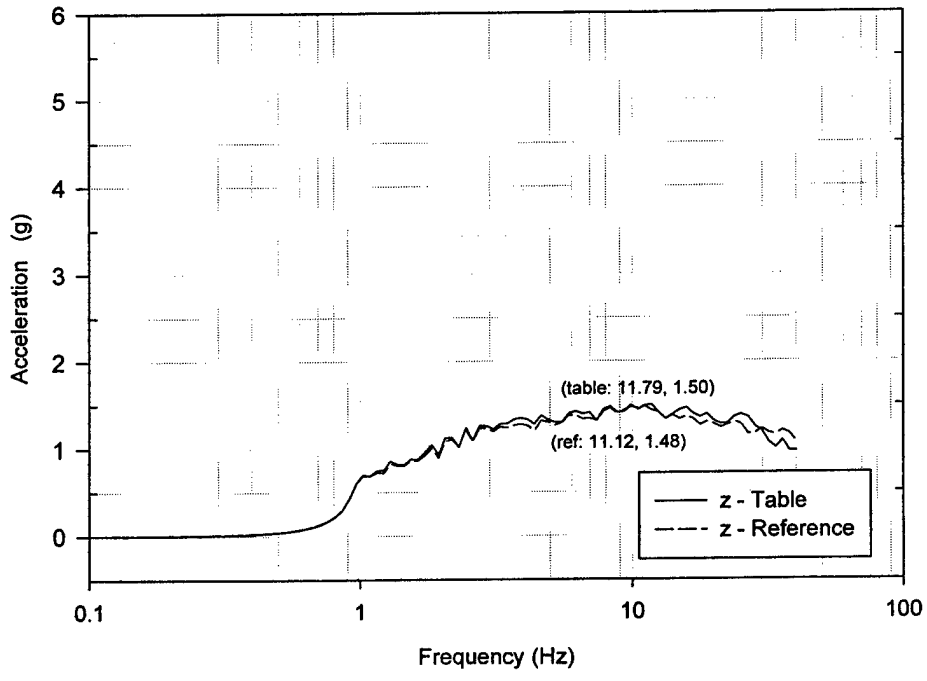

Out-of-Plane Response Spectrum of
South Wall for EQ-7 with 5% Damping

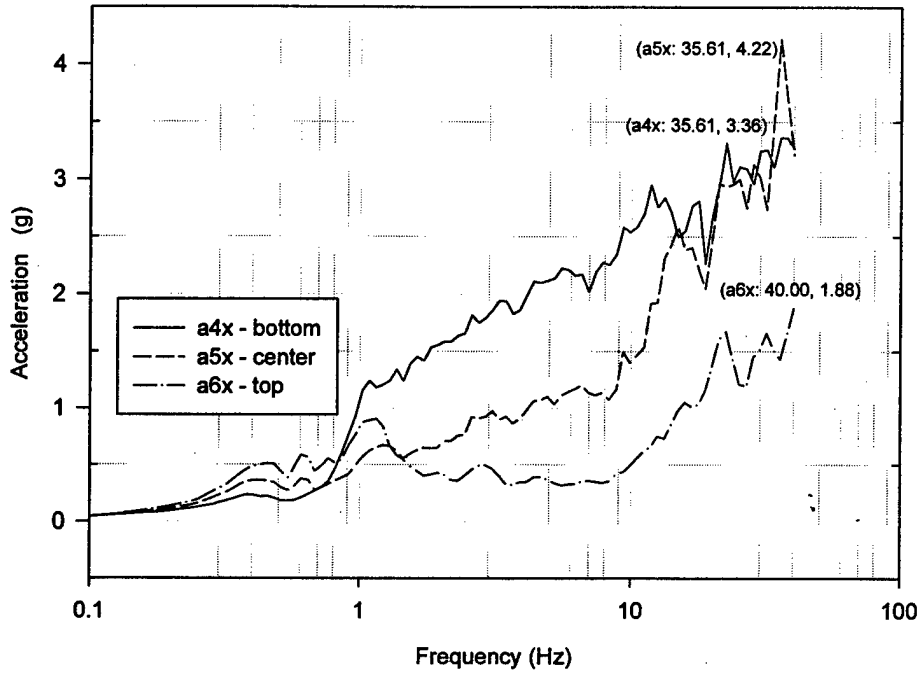

Out-of-Plane Response Spectrum of
South Wall for EQ-7 with 5% Damping

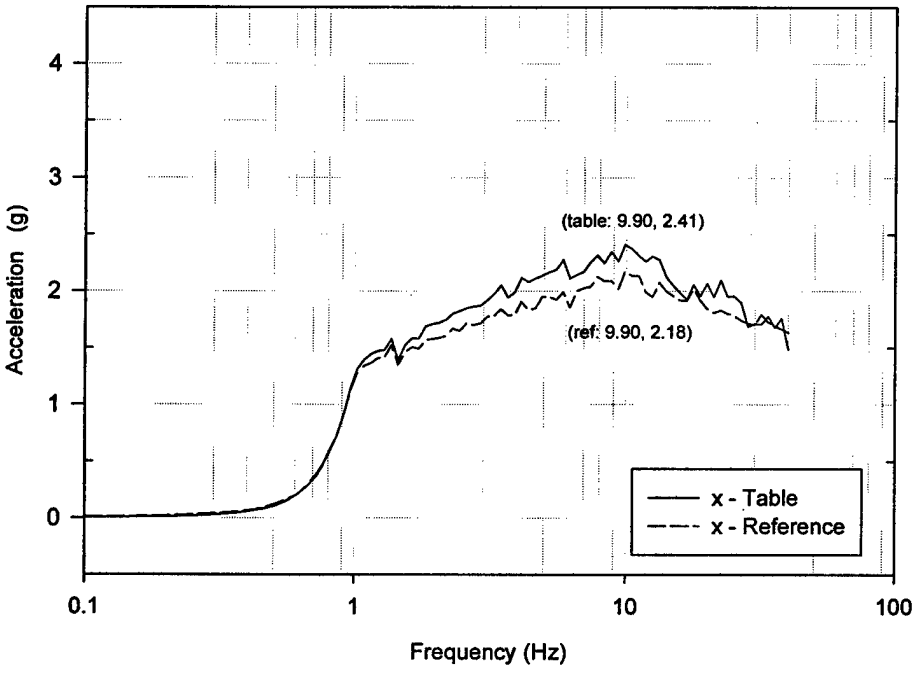

In-Plane Response Spectrum of
South Wall for EQ-7 with 5% Damping

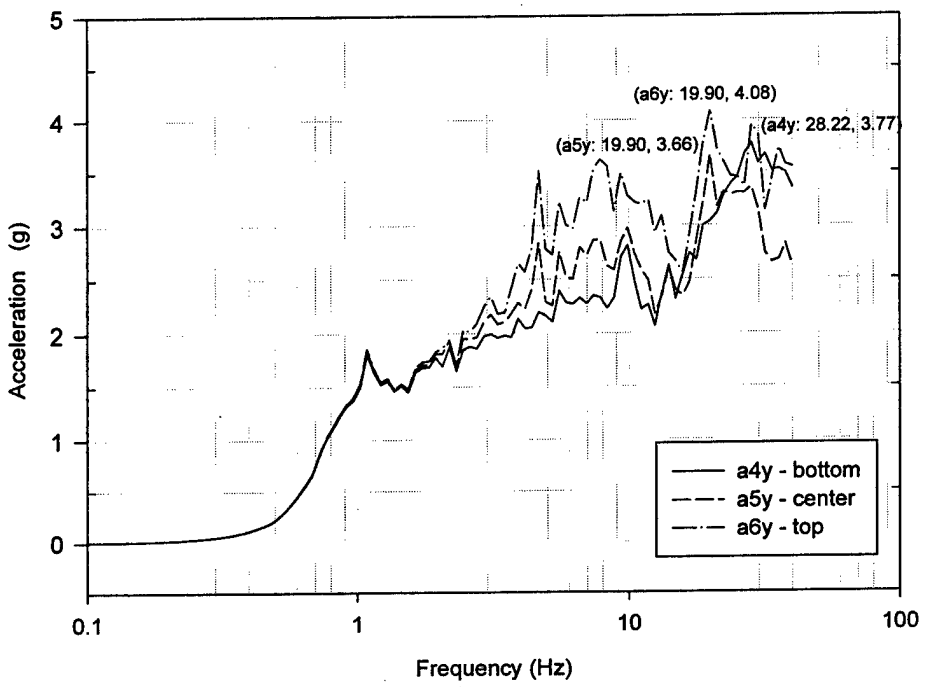

In-Plane Response Spectrum of
South Wall for EQ-7 with 5% Damping

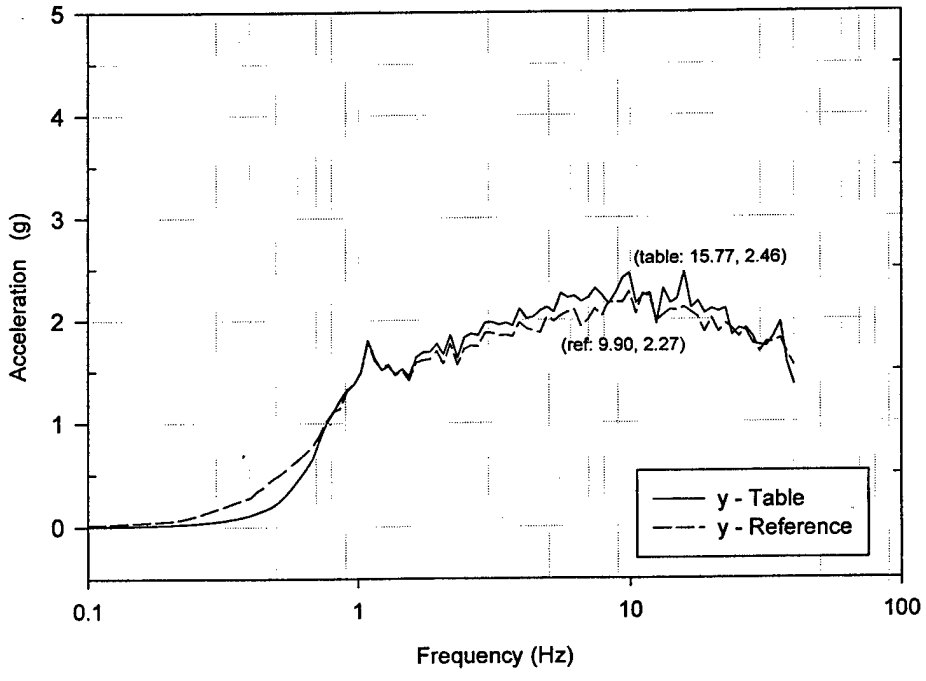

Vertical Response Spectrum of
South Wall for EQ-7 with 5% Damping

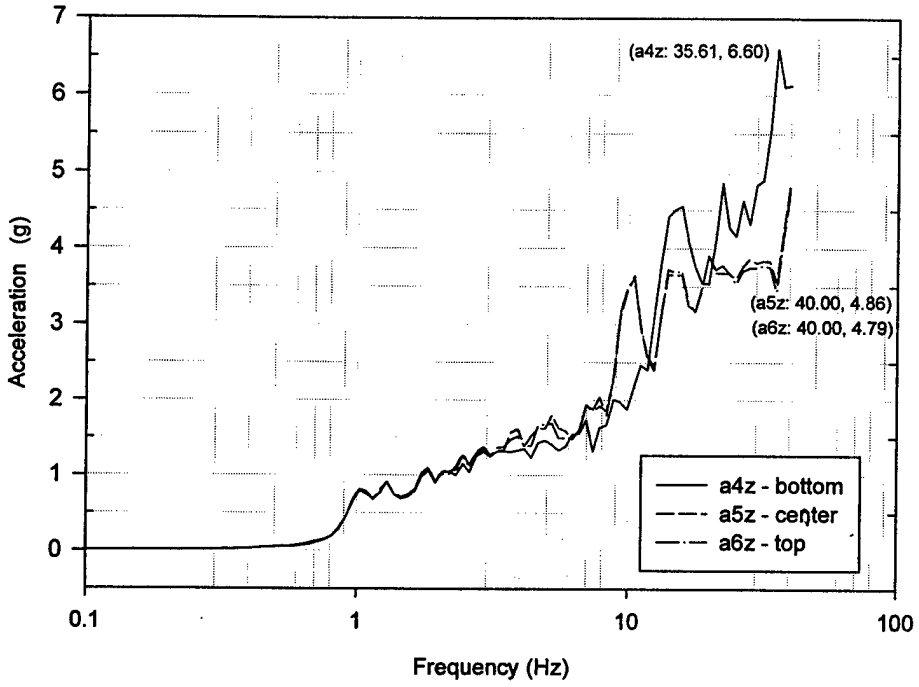

Vertical Response Spectrum of
South Wall for EQ-7 with 5% Damping

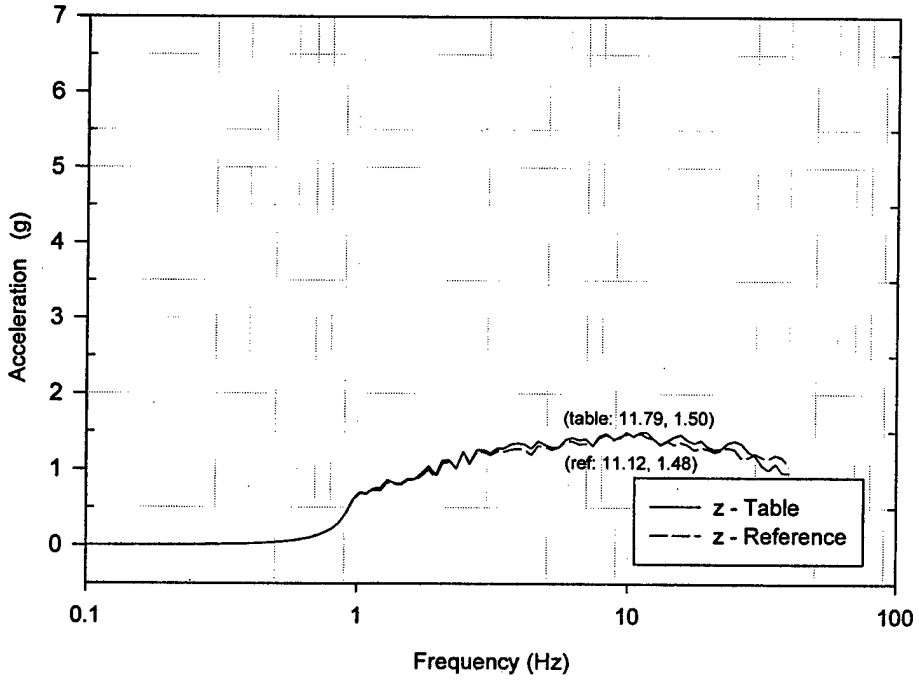

Appendix G: Plots of Stress-Displacement Response

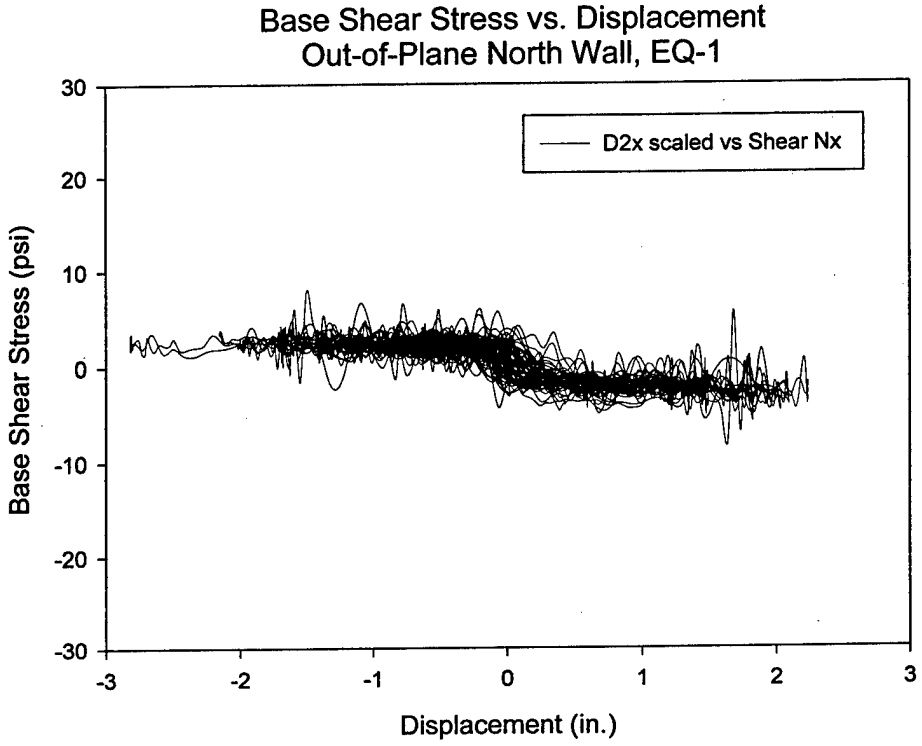
Base Shear Stress vs. Displacement
Out-of-Plane North Wall, EQ-1
D2x scaled vs Shear Nx
Base Shear Stress (psi)
30
20
10
0
-10
-20
-30
-3
-2
-1
0
1
2
3
Displacement (in.)

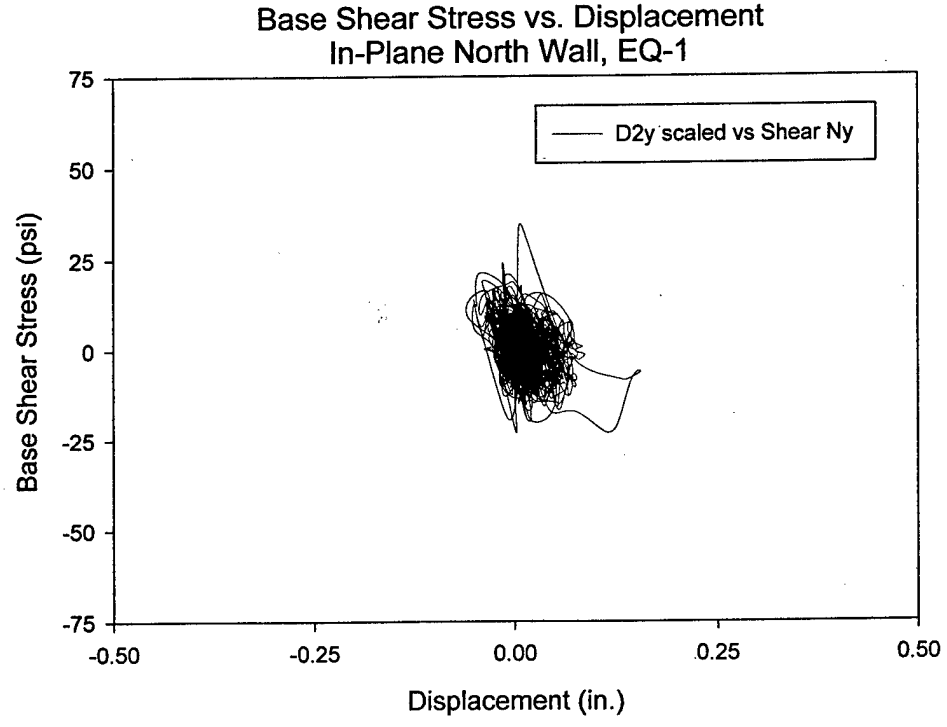
Base Shear Stress vs. Displacement
In-Plane North Wall, EQ-1
D2y scaled vs Shear Ny
Base Shear Stress (psi)
75
50
25
0
-25
-50
-75
-0.50
-0.25
0.00
0.25
0.50
Displacement (in.)

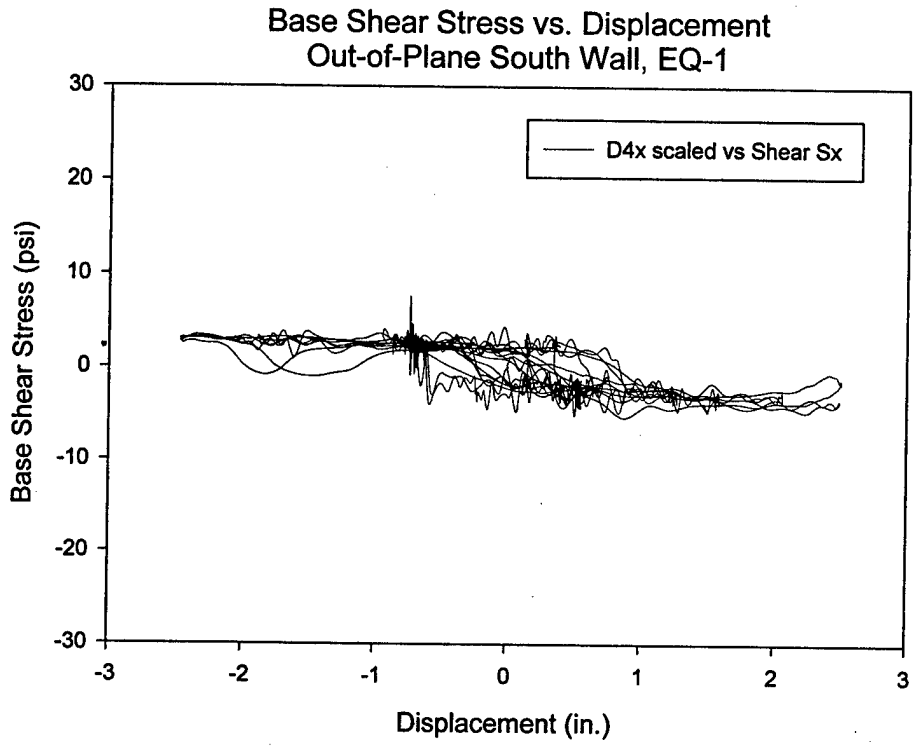
Base Shear Stress vs. Displacement
Out-of-Plane South Wall, EQ-1
D4x scaled vs Shear Sx
Base Shear Stress (psi)
30
20
10
0
-10
-20
-30
-3
-2
-1
0
1
2
3
Displacement (in.)

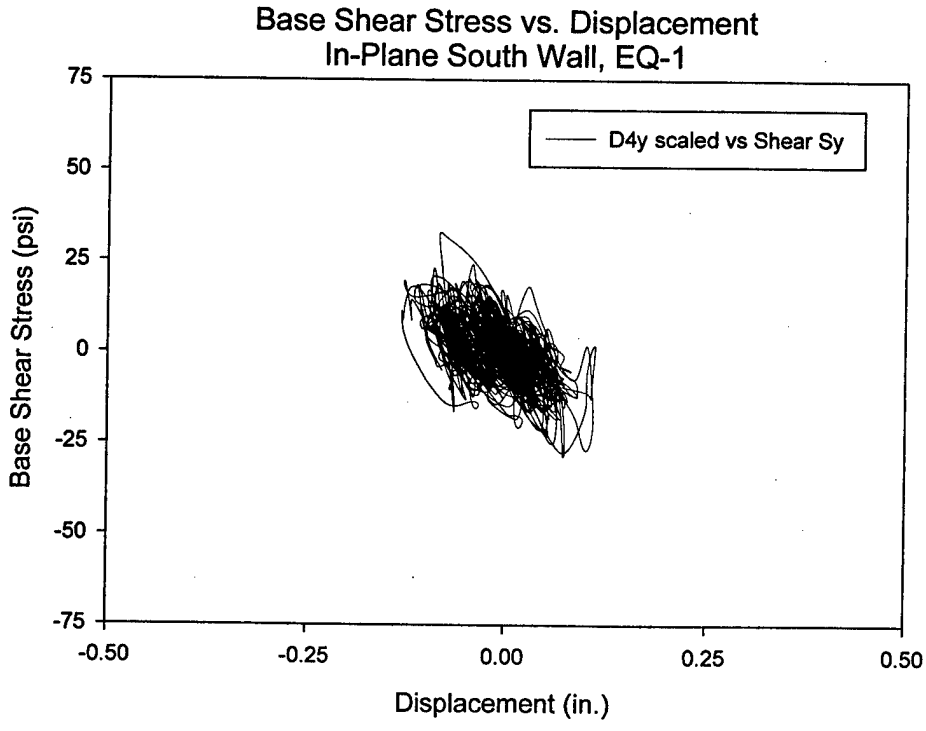
Base Shear Stress vs. Displacement
In-Plane South Wall, EQ-1
D4y scaled vs Shear Sy
Base Shear Stress (psi)
75
50
25
0
-25
-50
-75
-0.50
-0.25
0.00
0.25
0.50
Displacement (in.)

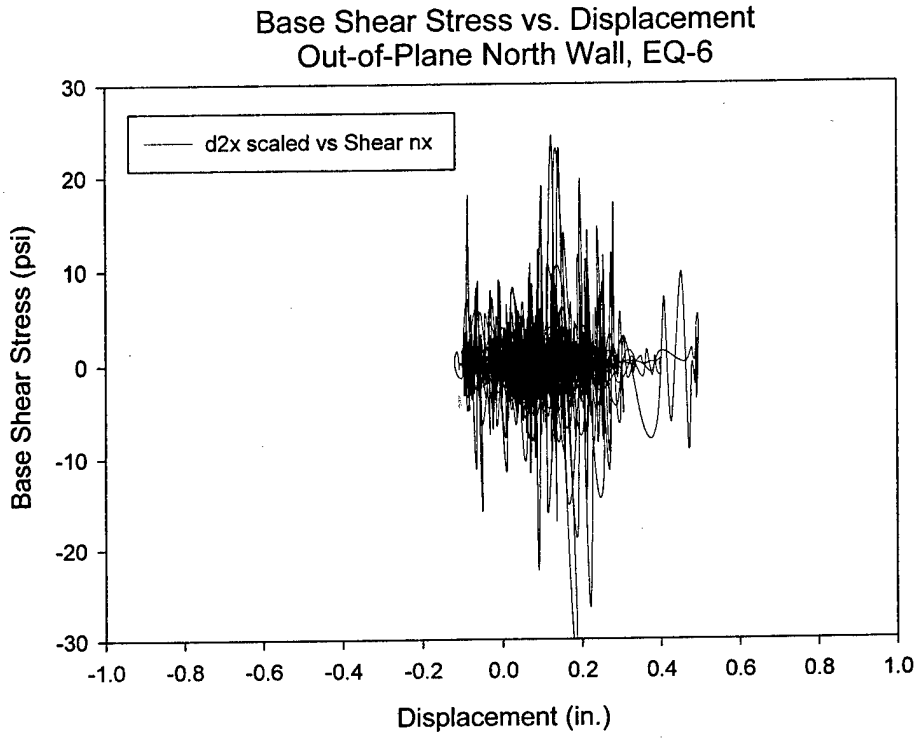
Base Shear Stress vs. Displacement
Out-of-Plane North Wall, EQ-6
d2x scaled vs Shear nx
Base Shear Stress (psi)
30
20
10
0
-10
-20
-30
-1.0
-0.8
-0.6
-0.4
-0.2
0.0
0.2
0.4
0.6
0.8
1.0
Displacement (in.)

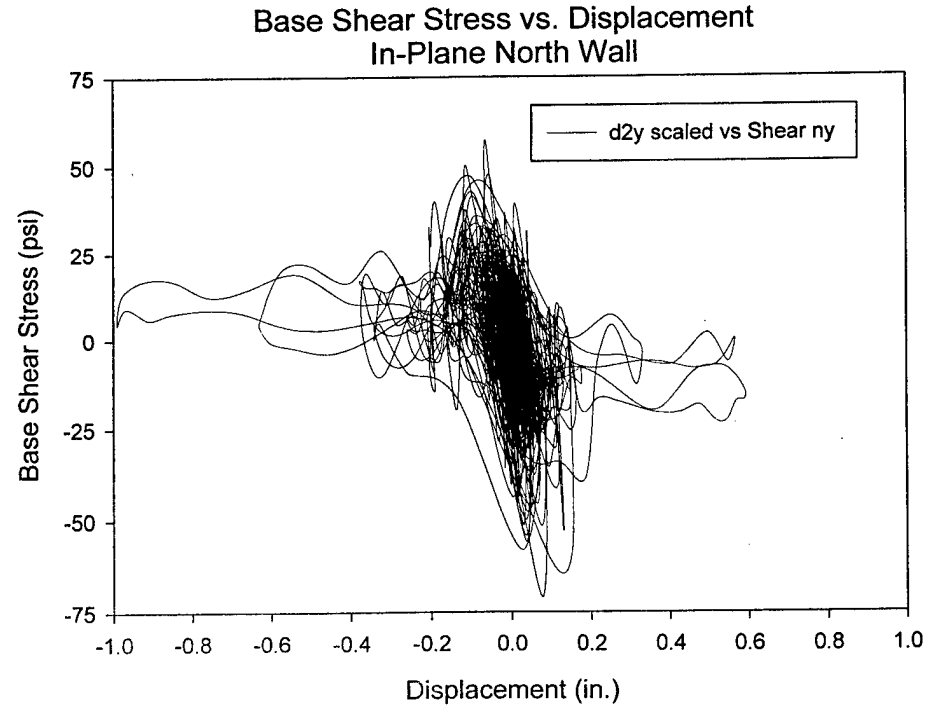
Base Shear Stress vs. Displacement
In-Plane North Wall
d2y scaled vs Shear ny
Base Shear Stress (psi)
75
50
25
0
-25
-50
-75
-1.0
-0.8
-0.6
-0.4
-0.2
0.0
0.2
0.4
0.6
0.8
1.0
Displacement (in.)

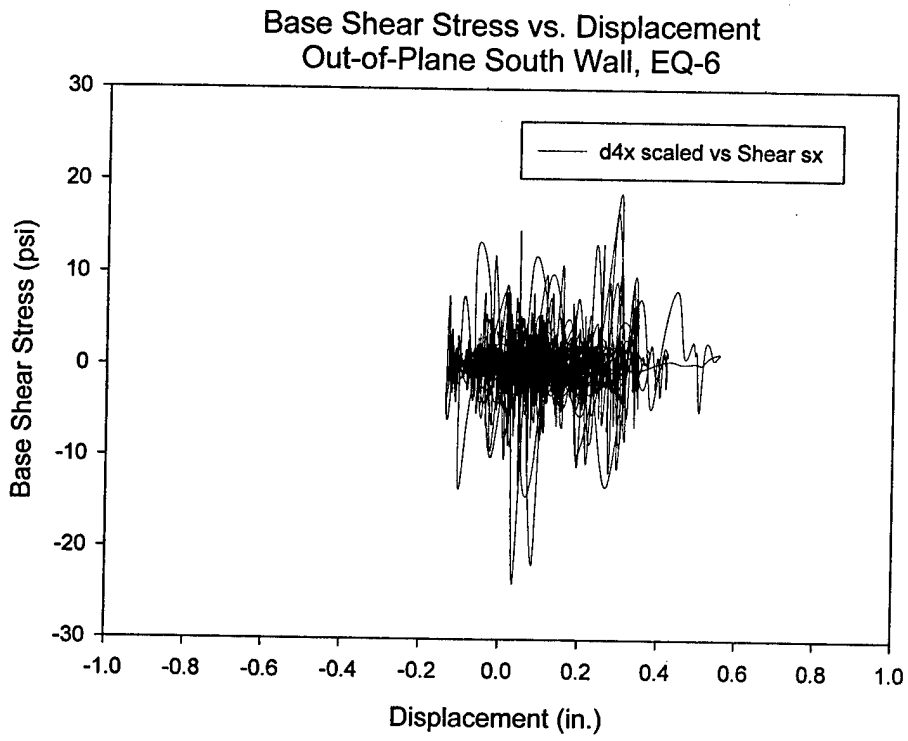
Base Shear Stress vs. Displacement
Out-of-Plane South Wall, EQ-6
d4x scaled vs Shear sx
Base Shear Stress (psi)
30
20
10
0
-10
-20
-30
-1.0
-0.8
-0.6
-0.4
-0.2
0.0
0.2
0.4
0.6
0.8
1.0
Displacement (in.)

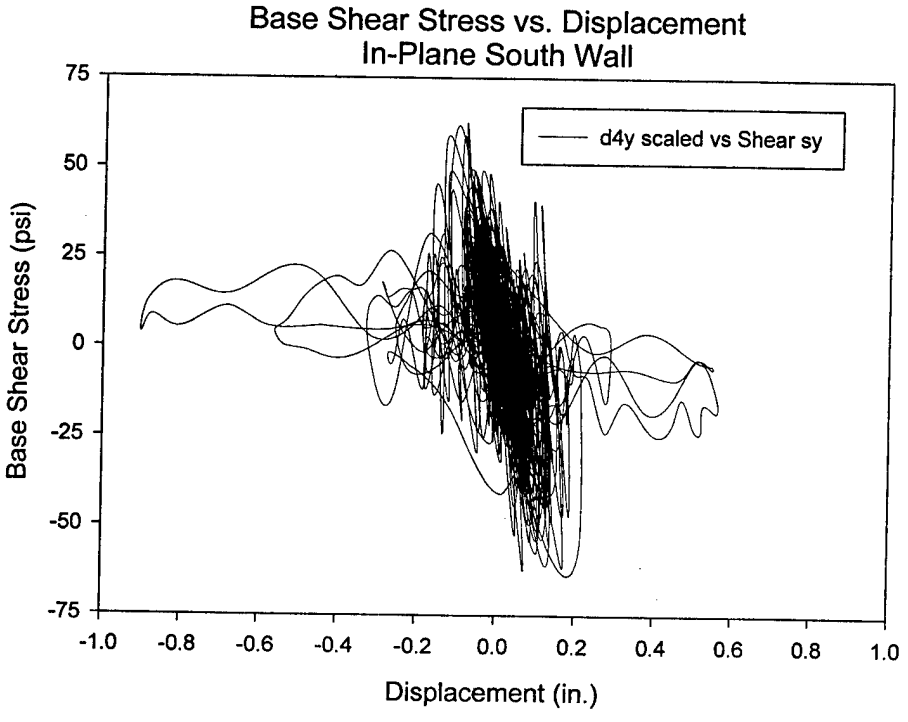
Base Shear Stress vs. Displacement
In-Plane South Wall
d4y scaled vs Shear sy
Base Shear Stress (psi)
75
50
25
0
-25
-50
-75
-1.0
-0.8
-0.6
-0.4
-0.2
0.0
0.2
0.4
0.6
0.8
1.0
Displacement (in.)

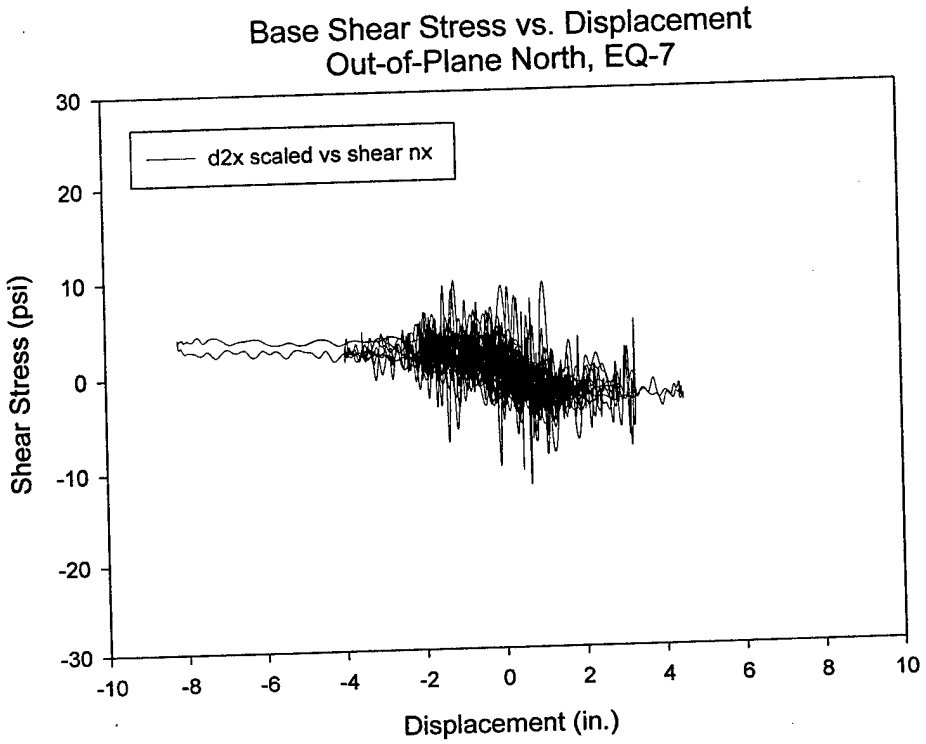
Base Shear Stress vs. Displacement
Out-of-Plane North, EQ-7
d2x scaled vs shear nx
Shear Stress (psi)
30
20
10
0
-10
-20
-30
-10
-8
-6
-4
-2
0
2
4
6
8
10
Displacement (in.)

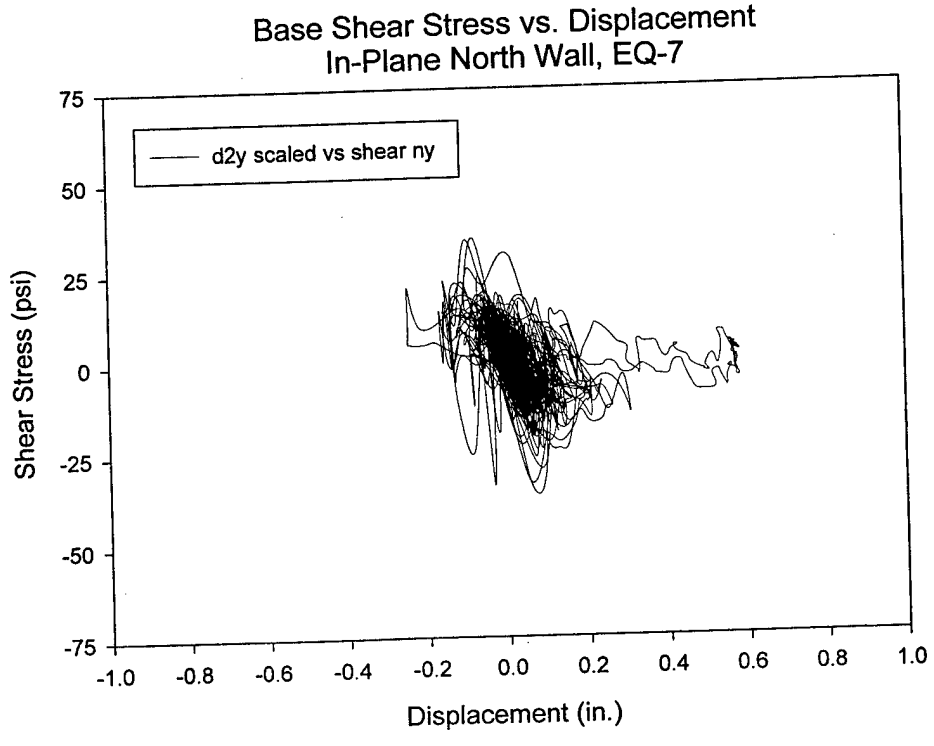
Base Shear Stress vs. Displacement
In-Plane North Wall, EQ-7
d2y scaled vs shear ny
Shear Stress (psi)
75
50
25
0
-25
-50
-75
-1.0
-0.8
-0.6
-0.4
-0.2
0.0
0.2
0.4
0.6
0.8
1.0
Displacement (in.)

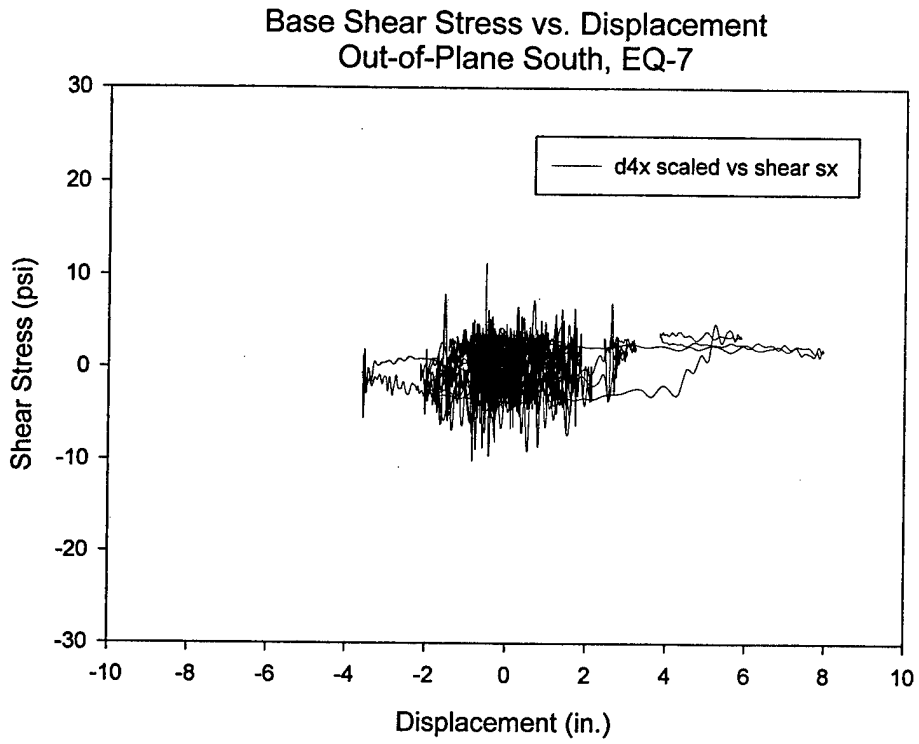
Base Shear Stress vs. Displacement
Out-of-Plane South, EQ-7
d4x scaled vs shear sx
Shear Stress (psi)
30
20
10
0
-10
-20
-30
-10
-8
-6
-4
-2
0
2
4
6
8
10
Displacement (in.)

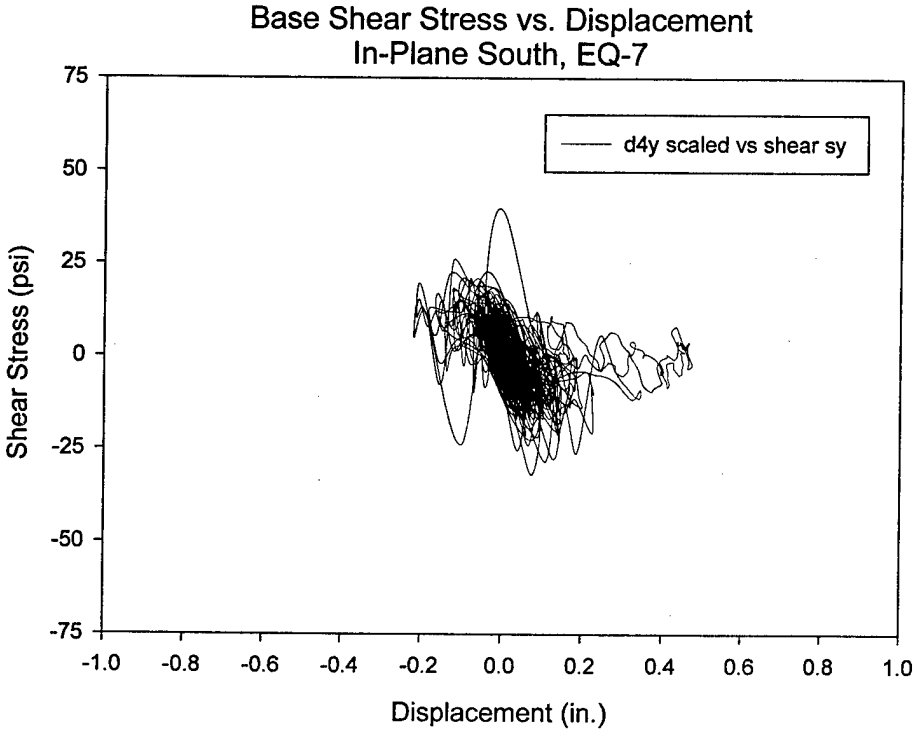
Base Shear Stress vs. Displacement
In-Plane South, EQ-7
d4y scaled vs shear sy
Shear Stress (psi)
75
50
25
0
-25
-50
-75
-1.0
-0.8
-0.6
-0.4
-0.2
0.0
0.2
0.4
0.6
0.8
1.0
Displacement (in.)

Appendix H: Maximum Shear Stress Response Per Rosette Strain Gages

Maximum Stress at Lower East Corner of
Outside Face of North Wall, EQ-1

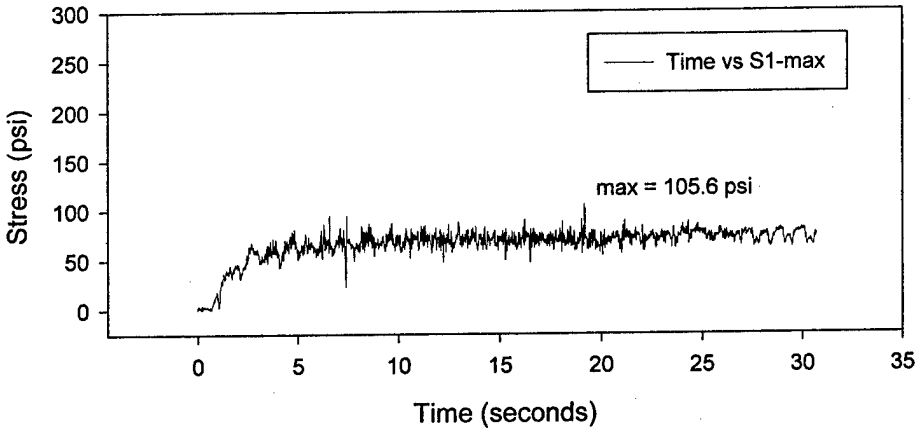

Maximum Stress at Lower West Corner of
Outside Face of North Wall, EQ-1

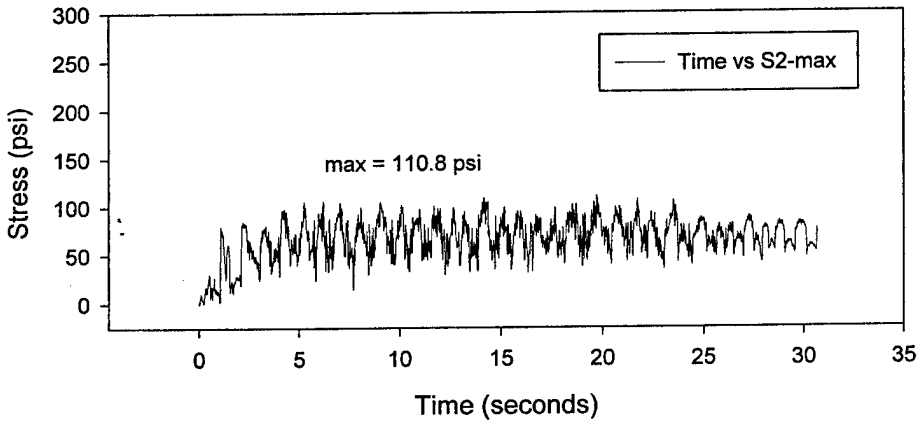

Maximum Stress at Center of
Outside Face of North Wall, EQ-1

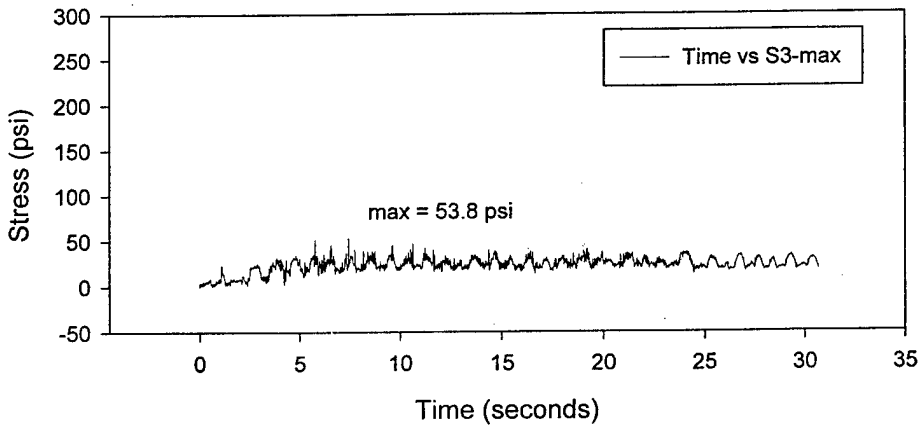

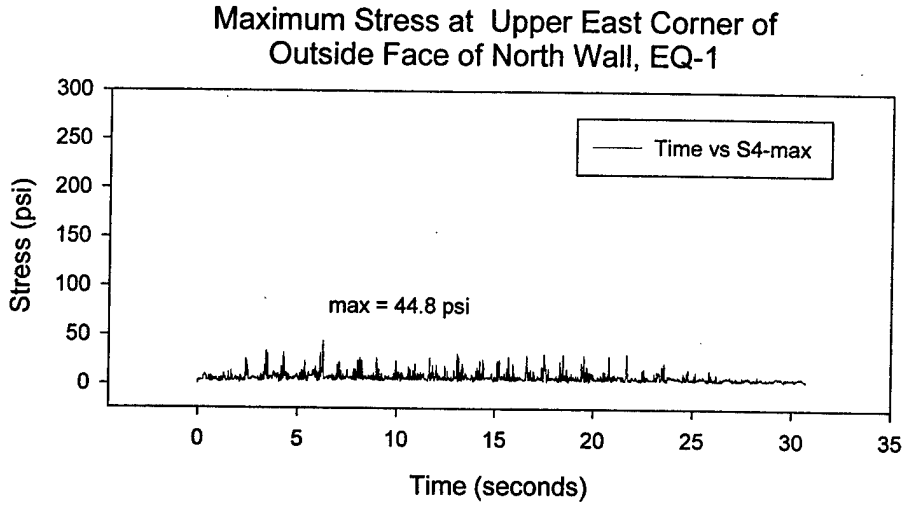
Maximum Stress at Upper East Corner of
Outside Face of North Wall, EQ-1
Stress (psi)
300
250
200
150
100
50
0
Time vs S4-max
max = 44.8 psi
0
5
10
15
20
25
30
35
Time (seconds)

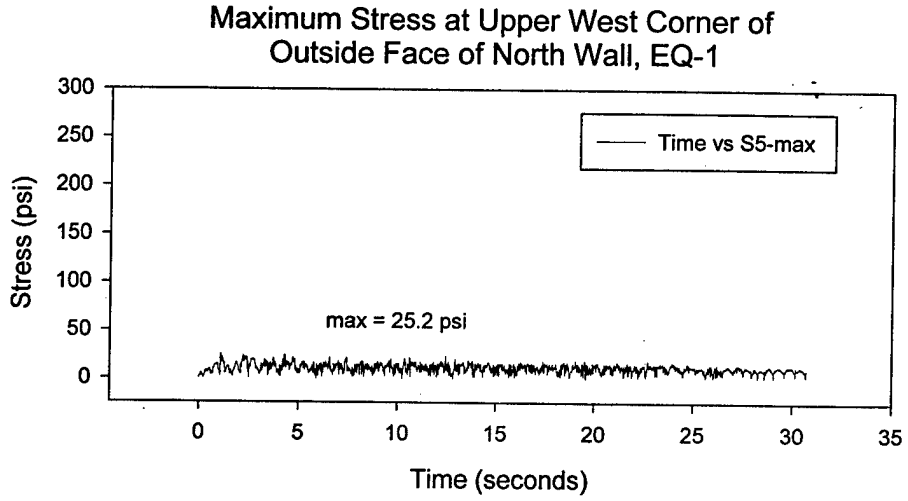
Maximum Stress at Upper West Corner of
Outside Face of North Wall, EQ-1
Stress (psi)
300
250
200
150
100
50
0
Time vs S5-max
max = 25.2 psi
0
5
10
15
20
25
30
35
Time (seconds)

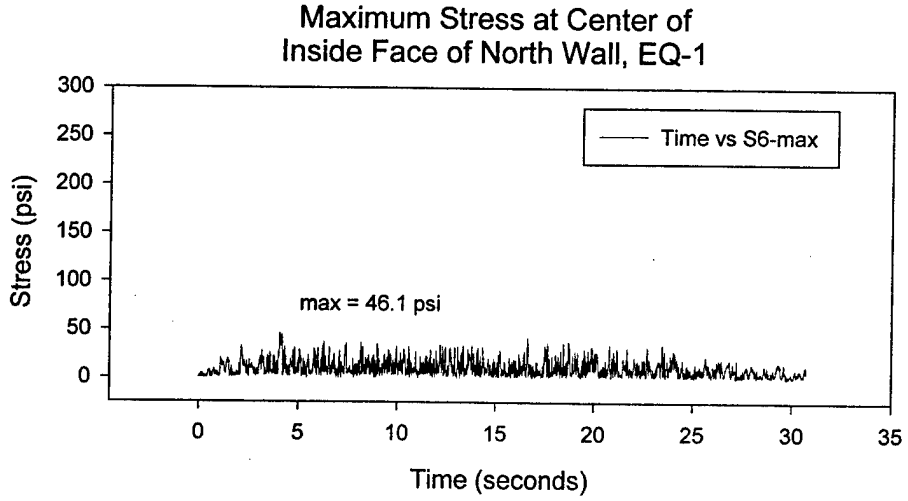
Maximum Stress at Center of
Inside Face of North Wall, EQ-1
Stress (psi)
300
250
200
150
100
50
0
Time vs S6-max
max = 46.1 psi
0
5
10
15
20
25
30
35
Time (seconds)

Maximum Stress at Lower West Corner of
Inside Face of South Wall, EQ-1

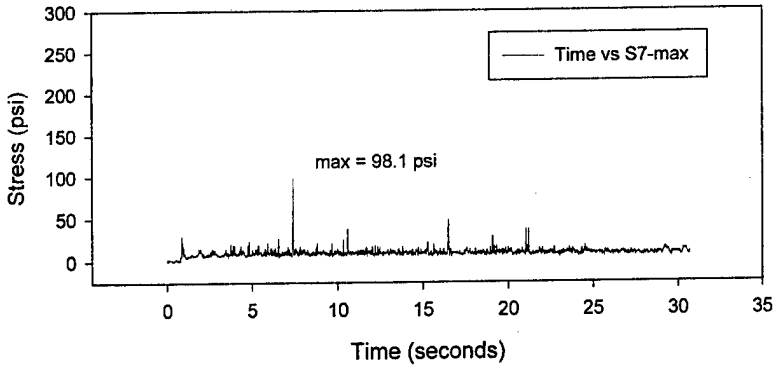

Maximum Stress at Center of
Inside Face of South Wall, EQ-1

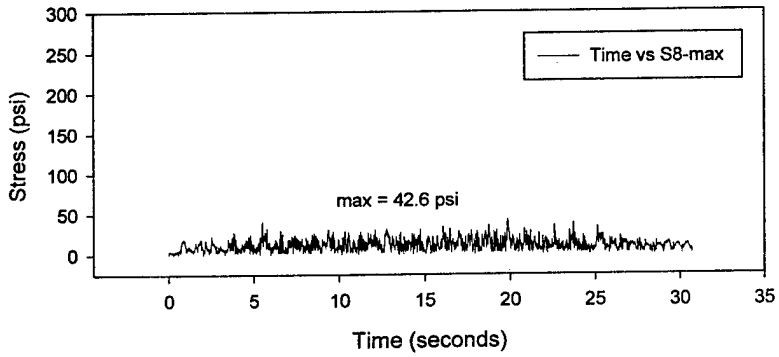

Maximum Stress at Upper West Corner of
Inside Face of South Wall, EQ-1

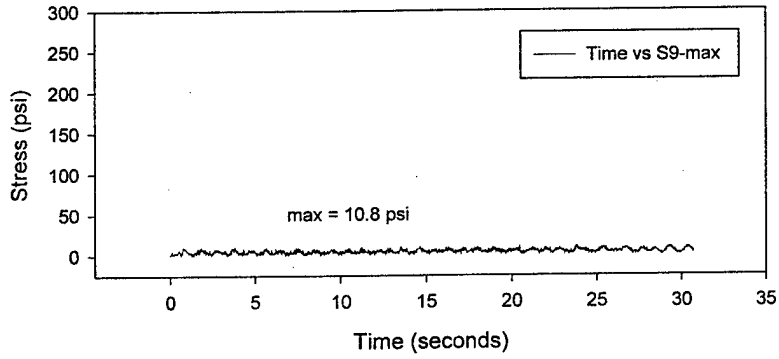

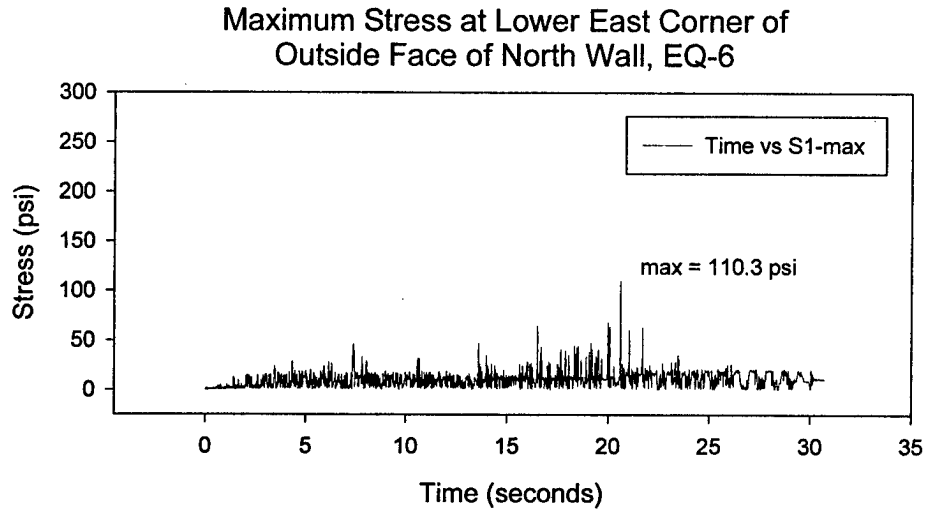
Maximum Stress at Lower East Corner of
Outside Face of North Wall, EQ-6
Stress (psi)
300
250
200
150
100
50
0
Time vs S1-max
max = 110.3 psi
0
5
10
15
20
25
30
35
Time (seconds)

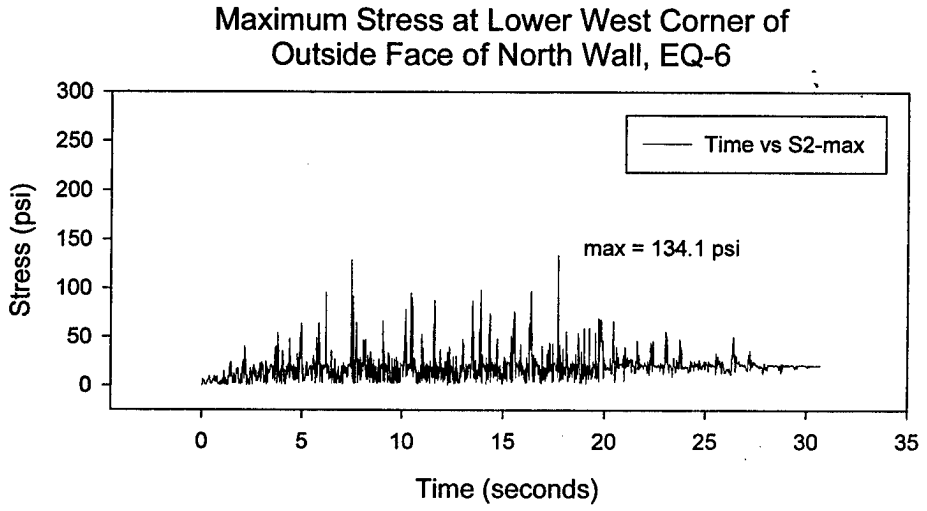
Maximum Stress at Lower West Corner of
Outside Face of North Wall, EQ-6
Stress (psi)
300
250
200
150
100
50
0
Time vs S2-max
max = 134.1 psi
0
5
10
15
20
25
30
35
Time (seconds)

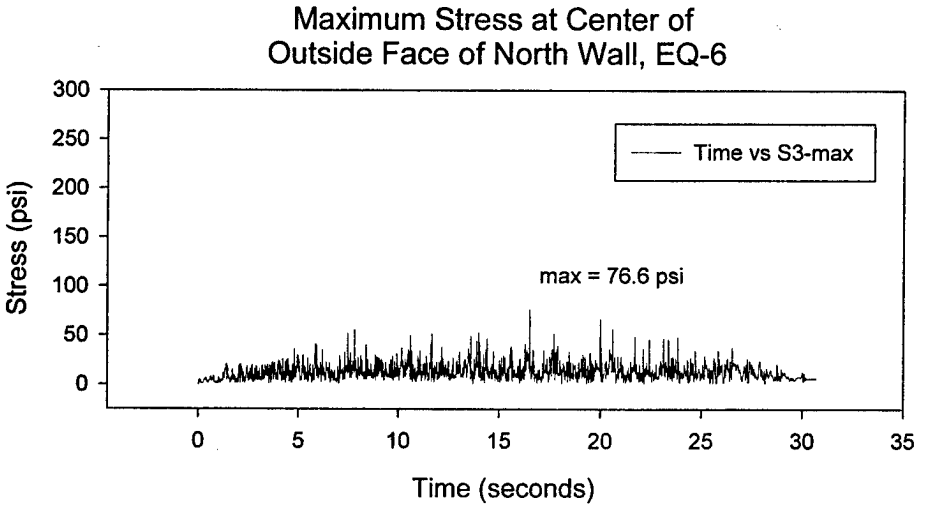
Maximum Stress at Center of
Outside Face of North Wall, EQ-6
Stress (psi)
300
250
200
150
100
50
0
Time vs S3-max
max = 76.6 psi
0
5
10
15
20
25
30
35
Time (seconds)

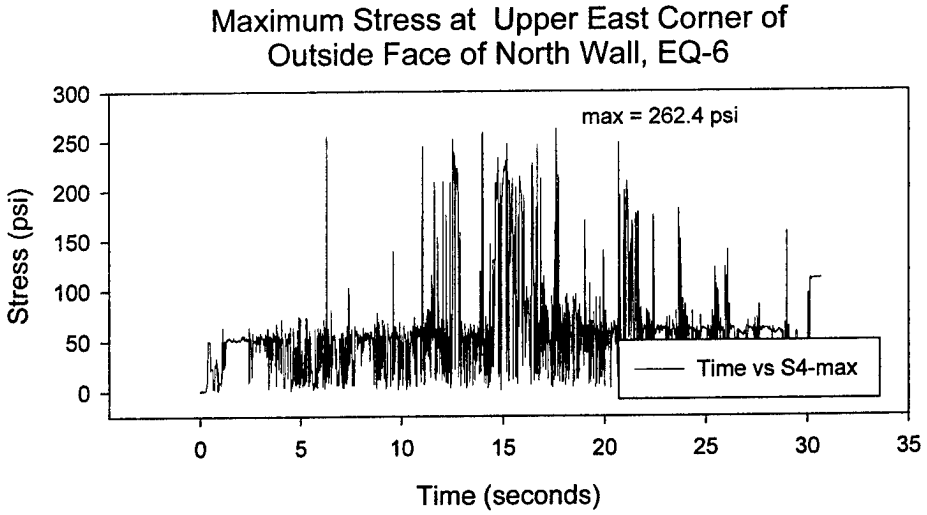
Maximum Stress at Upper East Corner of
Outside Face of North Wall, EQ-6
max = 262.4 psi
Time vs S4-max
Stress (psi)
Time (seconds)
0
50
100
150
200
250
300
0
5
10
15
20
25
30
35

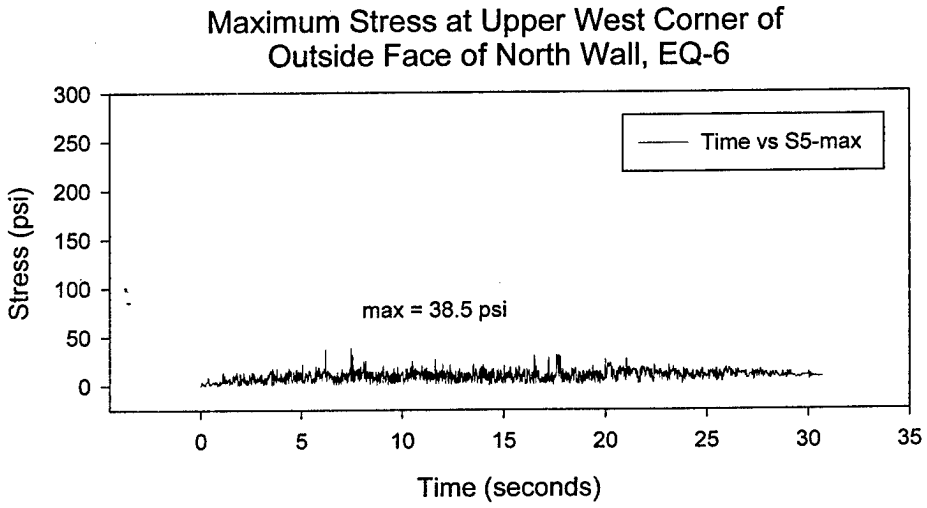
Maximum Stress at Upper West Corner of
Outside Face of North Wall, EQ-6
Time vs S5-max
max = 38.5 psi
Stress (psi)
Time (seconds)
0
50
100
150
200
250
300
0
5
10
15
20
25
30
35

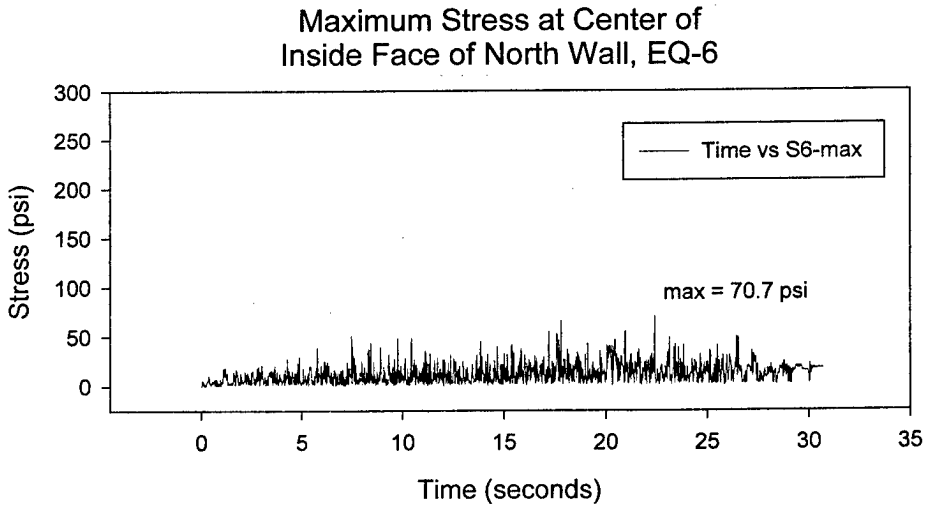
Maximum Stress at Center of
Inside Face of North Wall, EQ-6
Time vs S6-max
max = 70.7 psi
Stress (psi)
Time (seconds)
0
50
100
150
200
250
300
0
5
10
15
20
25
30
35

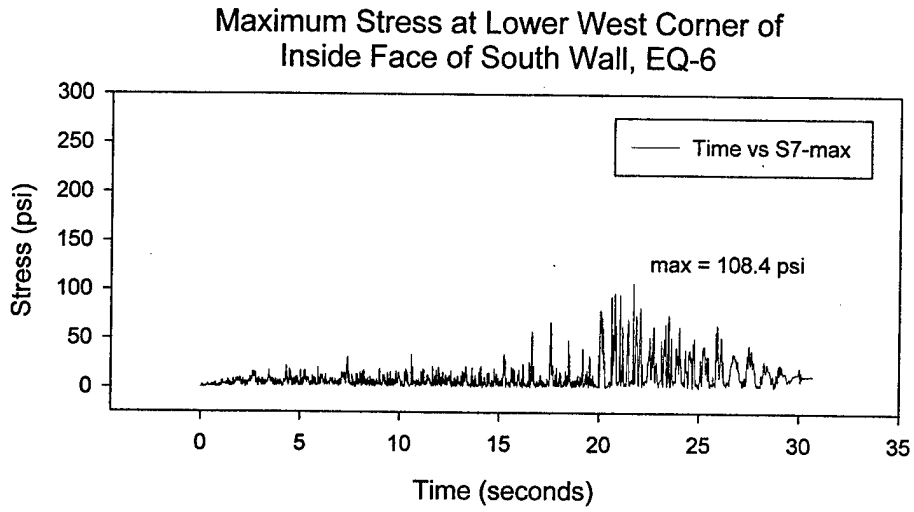
Maximum Stress at Lower West Corner of
Inside Face of South Wall, EQ-6
Time vs S7-max
max = 108.4 psi
Stress (psi)
Time (seconds)
300
250
200
150
100
50
0
0
5
10
15
20
25
30
35

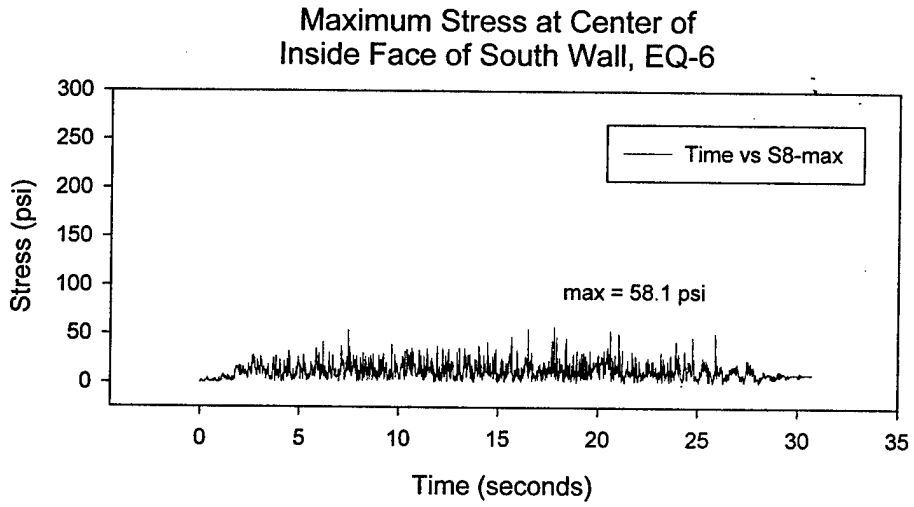
Maximum Stress at Center of
Inside Face of South Wall, EQ-6
Time vs S8-max
max = 58.1 psi
Stress (psi)
Time (seconds)
300
250
200
150
100
50
0
0
5
10
15
20
25
30
35

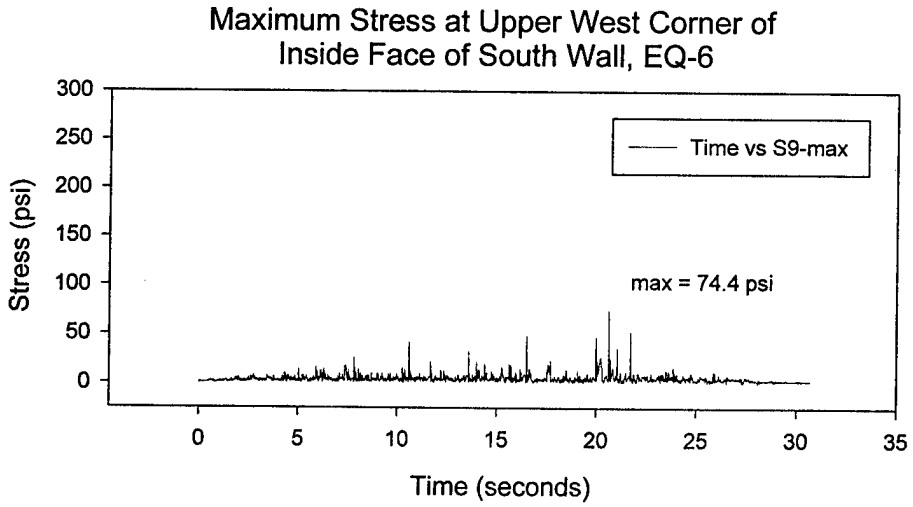
Maximum Stress at Upper West Corner of
Inside Face of South Wall, EQ-6
Time vs S9-max
max = 74.4 psi
Stress (psi)
Time (seconds)
300
250
200
150
100
50
0
0
5
10
15
20
25
30
35

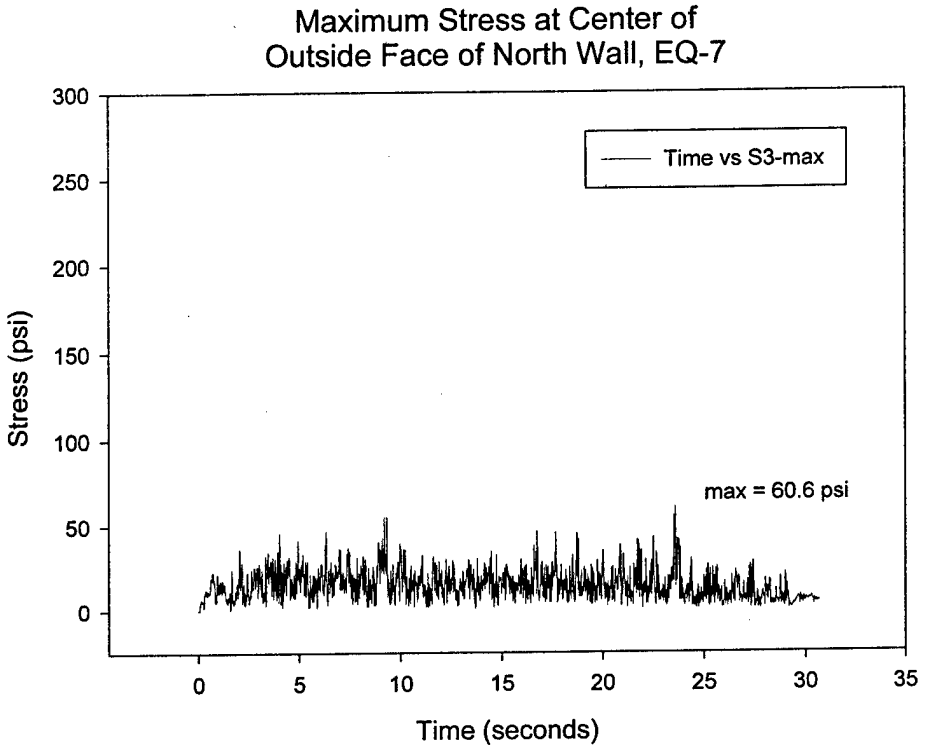
Maximum Stress at Center of
Outside Face of North Wall, EQ-7
Time vs S3-max
max = 60.6 psi
Stress (psi)
300
250
200
150
100
50
0
0
5
10
15
20
25
30
35
Time (seconds)

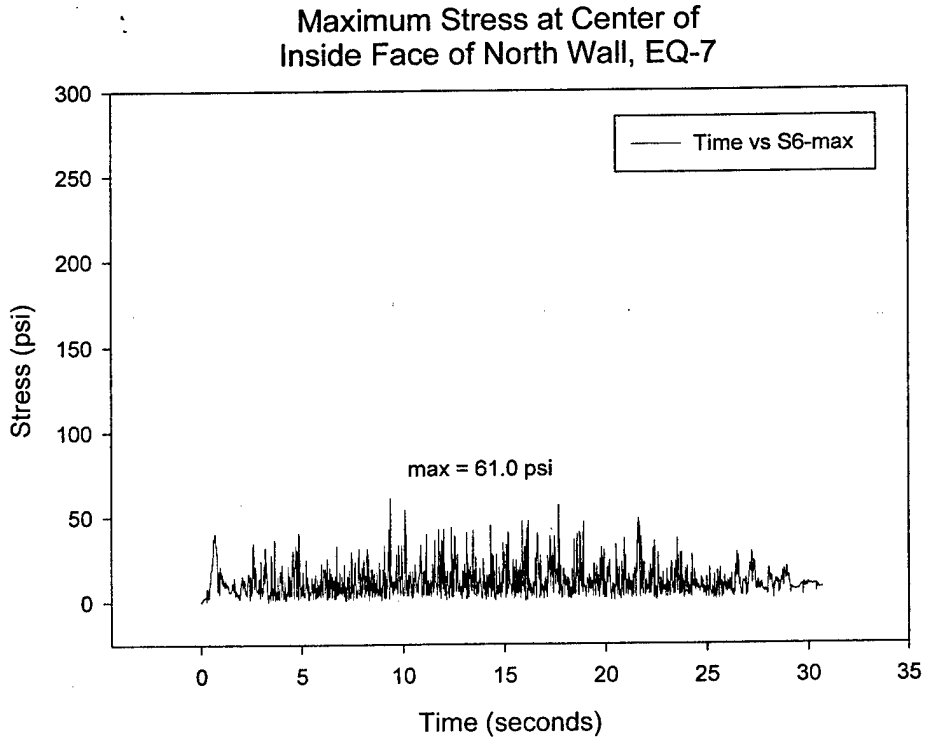
Maximum Stress at Center of
Inside Face of North Wall, EQ-7
Time vs S6-max
max = 61.0 psi
Stress (psi)
300
250
200
150
100
50
0
0
5
10
15
20
25
30
35
Time (seconds)

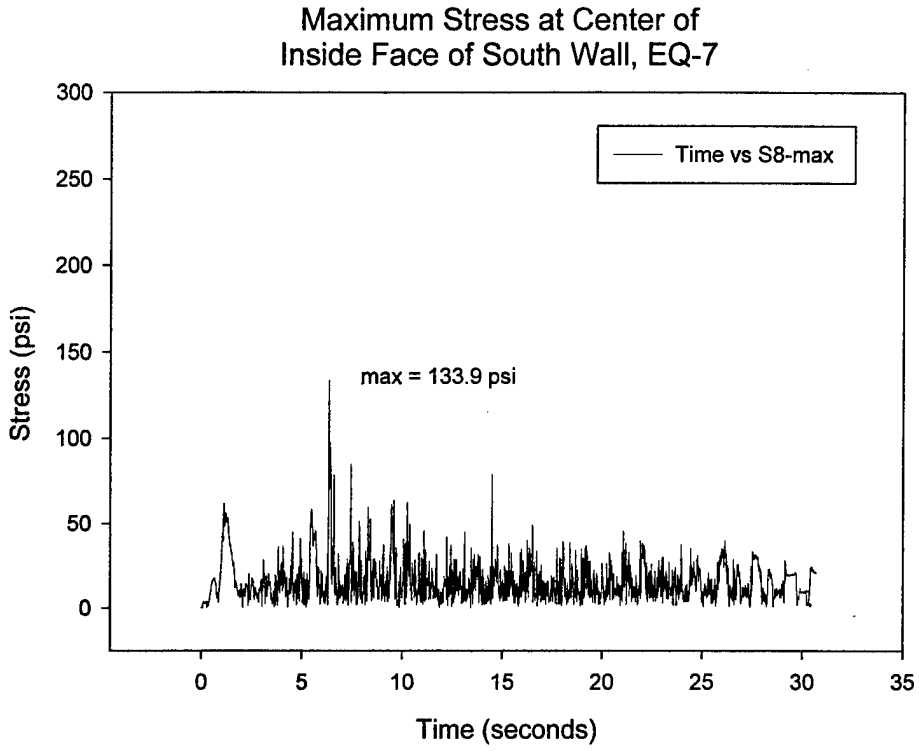
Maximum Stress at Center of
Inside Face of South Wall, EQ-7
Time vs S8-max
max = 133.9 psi
Stress (psi)
300
250
200
150
100
50
0
0
5
10
15
20
25
30
35
Time (seconds)

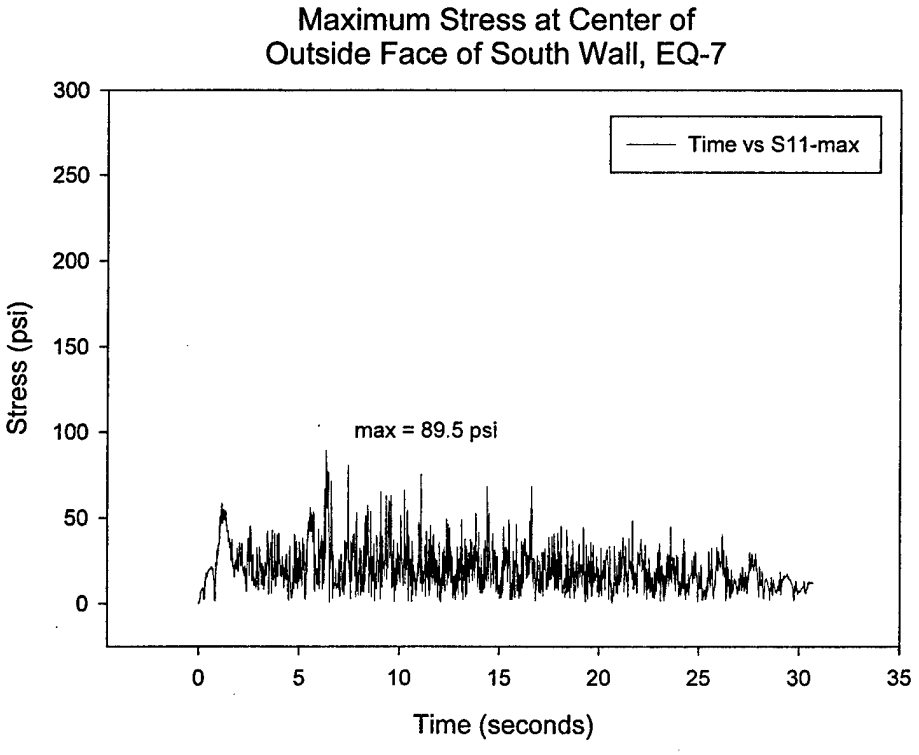
Maximum Stress at Center of
Outside Face of South Wall, EQ-7
Time vs S11-max
max = 89.5 psi
Stress (psi)
300
250
200
150
100
50
0
0
5
10
15
20
25
30
35
Time (seconds)

USACERL DISTRIBUTION

Chief of Engineers
ATTN: CEHEC-IM-LH (2)
ATTN: CEHEC-IM-LP (2)
ATTN: CECG
ATTN: CECC-P
ATTN: CECC-R
ATTN: CECW
ATTN: CECW-O
ATTN: CECW-P
ATTN: CECW-PR
ATTN: CEMP
ATTN: CEMP-ET
ATTN: CEMP-C
ATTN: CEMP-M
ATTN: CEMP-R
ATTN: CERD-C
ATTN: CERD-ZA
ATTN: CERD-L
ATTN: CERD-M (2)

ACS(IM) 22060
ATTN: DAIM-FDP

Tennessee Valley Authority
ATTN: ET P-K (2)
ATTN: SP 1A-K (2)
ATTN: WT 9D-K (10)

CECPW 22310-3862
ATTN: CECPW-E
ATTN: CECPW-FT
ATTN: CECPW-ZC

US Army Engr District
ATTN: Library (42)

US Army Engr Division
ATTN: Library (8)

US Army Engineering and Support Center
ATTN: CEHND 35807-4301

US Army Europe
ATTN: AEAEN-EH 09014
ATTN: AEAEN-ODCS 09014

US Army Materiel Command (AMC)
Alexandria, VA 22333-0001
ATTN: AMCEN-F

FORSCOM
Forts Gillem & McPherson 30330
ATTN: FCEN

TRADOC
Fort Monroe 23651
ATTN: ATBO-G

Fort Belvoir 22060
ATTN: CETEC-IM-T
ATTN: Water Resources Support Ctr

USA Natick RD&E Center 01760
ATTN: STRNC-DT
ATTN: AMSSC-S-IMI

CEWES 39180
ATTN: Library
CECRL 03755
ATTN: Library

Defense Nuclear Agency
ATTN: NADS 20305

Defense Logistics Agency
ATTN: MMBIR 22060-6221

National Guard Bureau 20310
ATTN: NGB-ARI

Naval Facilities Engr Command
ATTN: Facilities Engr Command (8)
ATTN: Engrg Field Divisions (10)
ATTN: Engrg Field Activities (4)
ATTN: Public Works Center (8)
ATTN: Naval Constr Battalion Ctr 93043
ATTN: Naval Facil. Engr. Service Ctr 93043-4328

8th US Army Korea
ATTN: DPW (11)

US Army MEDCOM
ATTN: MCFA 78234-6000

American Public Works Assoc. 64104-1806

US Army CHPPM
ATTN: MCHB-DE 21010

US Gov't Printing Office 20401
ATTN: Rec Sec/Deposit Sec (2)

Nat'l Institute of Standards & Tech
ATTN: Library 20899

Defense General Supply Center
ATTN: DGSC-WI 23297-5000

Defense Supply Center Columbus
ATTN: DSCC-WI 43216-5000

Defense Tech Info Center 22060-6218
ATTN: DTIC-O (2)

154
06/98

☆U.S. GOVERNMENT PRINTING OFFICE: 1998 -646-081/80013